Transcriptional regulation of cardiac extracellular matrix gene expression and fibroblast phenotype by Scleraxis

by

Rushita Adhikari Bagchi

A Thesis submitted to the Faculty of Graduate Studies

of The University of Manitoba

in partial fulfillment of the requirements of the degree of

DOCTOR OF PHILOSOPHY

Department of Physiology and Pathophysiology

College of Medicine, Faculty of Health Sciences

University of Manitoba

Winnipeg

ABSTRACT

Cardiac fibrosis contributes to heart failure by dramatically impairing cardiac function, increasing patient morbidity and mortality. The primary fibrillar collagen expressed in the heart is type I, and increased collagen synthesis is the hallmark of cardiac fibrosis. Our laboratory has shown that the transcription factor scleraxis is sufficient to regulate the gene encoding collagen Iα2. The present thesis identifies and focuses on three key functions of scleraxis in the heart. First, we show that scleraxis is required for production of the cardiac extracellular matrix. Using *in vitro* and *in vivo* models, we observed a significant upregulation/reduction of matrix genes in response to induction/loss of scleraxis gene function respectively. In fact, scleraxis overexpression was sufficient to rescue matrix synthesis in scleraxis-null cells. In a murine model of cardiac pressure overload, scleraxis gene deletion blunted the induction of fibrotic collagen gene expression. Second, we provide evidence that scleraxis governs fibroblast-myofibroblast phenotype transition and fibroblast number. Scleraxis gene induction promoted cardiac myofibroblast phenoconversion while knockdown reduced myofibroblast marker gene expression. Scleraxis exerts direct transcriptional control on the α-smooth muscle actin gene-an established marker of myofibroblasts. Scleraxis null mice exhibited a dramatic reduction in cardiac fibroblast numbers- this is attributed to impairment of the epithelial-to-mesenchymal transition program which was marked by a corresponding loss of mesenchymal markers and increased epithelial markers. Loss-of-function experiments using primary cardiac proto-myofibroblasts recapitulated this paradigm, whereas scleraxis gene induction showed a reciprocal effect on mesenchymal markers. Third, data from this study supports the required role

of scleraxis in the TGFβ/Smad signaling pathway. Scleraxis is strongly upregulated by the potent pro-fibrotic cytokine TGFβ, and works synergistically with the canonical Smad signaling pathway to increase *Col1α2* expression by cardiac fibroblasts and myofibroblasts. Smad3 induced expression of the fibrillar collagens – an effect that was significantly attenuated following scleraxis knockdown. Smad3 binding to the *Col1α2* gene promoter was significantly reduced in scleraxis null hearts. This study involved a comprehensive series of *in vitro* and *in vivo* experiments, and is the first to identify scleraxis as a key regulator of multiple fibroblast functions and a potential future target for therapeutic intervention in cardiac fibrosis.

ACKNOWLEDGEMENTS

This work is in its present form due to the contribution of many individuals. Foremost, I would like to express my sincere gratitude to my supervisor and mentor **Dr. Michael Czubryt** for his wisdom, guidance, motivation, (lot of) patience and encouragement throughout my PhD program. He has taught me valuable life lessons of work ethic, integrity, perseverance, and teamwork. He has been and will continue to be a role model for me.

I also sincerely thank the members of my advisory committee- **Drs. Elissavet Kardami, Ian Dixon, Lorrie Kirshenbaum and Jeffrey Wigle** for their generous support, insightful feedback and mentorship throughout my graduate program. I am grateful to their labs for their collaboration, reagents and technical expertise that were provided for this study.

This work would not have been possible without the tremendous support and technical assistance of **past and present members of the Czubryt lab**: Dr. Nina Aroutiounova, Viktoriya Mozolevska, Patricia Roche, Angela Ramjiawan, Kristin Swan-Holt, Bernard Abrenica, Leon Espira, Laura Albak, Sari Yakubovich, Ryan Wang and Shreyas Devalapurkar- thank you all for your help and friendship.

I also thank the following individuals for providing technical assistance, animal models or reagents: Drs. Eric N. Olson (UT Southwestern, Dallas), Ronen Schweitzer (Shriner's Hospital for Children, Portland), Jean-Jacques Lebrun (McGill University), Etty Benveniste (University of Alabama at Birmingham), Christine Gilles

(University of Liège), Sem Phan (University of Michigan), Christine Zhang, Davinder Jassal, Paul Fernyhough and Mr. Stephen Jones (University of Manitoba).

I am grateful to: Gail McIndless, Judith Olfert, Mary Brown and Shweta Sharma for their administrative support; staff at R.O. Burrell animal facility for animal maintenance and surgeries; Rob Blaich and Joseph Pilapil for always finding a way to print my research posters at the eleventh hour; and Deb Fowler and Shirley Mager for making sure that I always had the cleanest labware to work with.

Pursuing a PhD program is like a marathon - scholarship support from Canadian Institutes of Health Research, Research Manitoba, University of Manitoba and St. Boniface Hospital Foundation, made the run gratifying. This research was supported at various stages by research grants from Canadian Institutes of Health Research, Heart and Stroke Foundation of Canada, Research Manitoba, and a generous donation from Mr. John Loewen through the St. Boniface Hospital Foundation.

Lastly, but not the least, I thank my parents for their unconditional love and support throughout my life. And, I thank my loving husband Ashim, for his love, patience, understanding and encouragement, and for being my best friend in life. I thank the Almighty for all the wonderful things in my life.

DEDICATION

I dedicate this thesis

to

my parents, Samir and Ruma,

for being the most inspirational teachers in my life.

"The teacher who is indeed wise does not bid you to enter the house of his wisdom but rather leads you to the threshold of your mind."

- Khalil Gibran

TABLE OF CONTENTS

List of Abbreviations

ACE	Angiotensin converting enzyme
ADAMTS2	A disintegrin and metalloproteinase with thrombospondin motifs 2
ALK5	Anaplastic lymphoma kinase 5
Ang II	Angiotensin II
cAMP	Cyclic adenosine monophosphate
ANP	Atrial natriuretic peptide
AT_1	Angiotensin II receptor 1
ATF4	Activating transcription factor 4
BNP	Brain natriuretic peptide
Bop1	Block of proliferation 1
CD	Cluster Differentiation
ChIP	Chromatin immunoprecipitation
Col1	Collagen Type 1
ColIα2	Collagen Iα2 gene
CREB2	Cyclic AMP-Response Element Binding Protein
CTGF	Connective tissue growth factor
CVD	Cardiovascular disease
DAVID	Database for annotation, visualization and integrated discovery
DDR2	Discoidin Domain Receptor 2
DT	Deceleration time
ECM	Extracellular matrix
E/A	Ratio of the mitral E to A waves
EDA-Fn	Extra Domain A-containing cellular fibronectin
EMSA	Electrophoretic mobility shift assays
EMT	Epithelial-mesenchymal transition
EndMT	Endothelial-mesenchymal transition
EPDCs	Epicardium-derived cells
ERK	Extracellular signal-regulated kinase
Erm	E26 transformation-specific (Ets)-related molecule
ET-1	Endothelin1
FA	Focal adhesions
FAK	Focal adhesion kinase
FGF	Fibroblast growth factor
bFGF	Basic fibroblast growth factor (or FGF-2)
flp/frt	Flippase recognition target (*FRT*) sites by the recombinase(Flp)
FS	Fractional shortening
FSP1	Fibroblast specific protein 1

hGF	Human gingival fibroblasts
GAPDH	Glyceraldehyde 3-phosphate dehydrogenase
GFP	Green fluorescent protein
cGMP	Cyclic GMP
GSL 1	Griffonia Simplicifolia Lectin 1
HA	Hyaluronic acid
Has	Hyaluronan synthase
HDAC	Histone deacetylase
bHLH	Basic-helix-loop-helix
HSPG	Heparan sulfate proteoglycan
HR	Heart rate
Hu	Human
IL-1β	Interleukin 1β
IVS	Interventricular septal thickness
JNK	c-Jun N-terminal kinase
KEGG	Kyoto Encyclopedia of Genes and Genomes
KLF5	Kruppel-like factor 5
KO	Knock out
LAP	Latency-associated protein
LLC	Large latent complex
LTBP	Latent TGF-binding protein
LVEDD	Left ventricular end diastolic diameter
LVEF	Left ventricular ejection fraction
LVESD	Left ventricular end systolic diameter
MAPK	Mitogen- activated protein kinase
p38 MAPK	p38 mitogen- activated protein kinase
MEK	MAPK/ERK kinase
Meox 2	Mesenchyme homeobox 2
MHC	Myosin heavy chain
MI	Myocardial infarction
MMP	Matrix metalloproteinase
mPa	Millipascal
MRTFs	myocardin-related transcription factors
MT-1	Membrane-type 1
NCBI	National Center for Biotechnology Information
NFAT	Nuclear factor of activated T cells
NF-κB	Nuclear factor- κB
PDGF	Platelet-derived growth factor
hPDLC	Human periodontal ligament cells
Pea3	Polyomavirus enhancer activator 3
qPCR	Quantitative polymerase chain reaction

PI3K	Phosphatidylinositol 3-kinase
PKG	Phospholipase C
PLC	Protein kinase G (PKG)
PRP 3	Polarity-related protein 3
PWT	Posterior wall thickness
RAAS	Renin-Angiotensin-Aldosterone System
Rho-GTPase	Rho family of guanosine triphosphatase
ROCK	Rho-associated protein kinase
RNA	Ribo nucleic acid
mRNA	Messenger RNA
miRNA	microRNAs
RPEL	Arginine R, proline P, glutamate E and leucine L
RT-PCR	Real time polymerase chain reaction
SBE	Smad binding element
Scx	Scleraxis
ScxΔBD	Scleraxis mutant lacking the DNA-binding basic domain
ScxΔΔ	Scleraxis double-deletion mutant
SFs	Stress fibers
SLC	Small latent complex
SM_{emb}	Embryonic smooth muscle myosin heavy chain, Myh10
α-SMA	Alpha-smooth muscle actin
Smad2	Sma and Mad (mothers against decapentaplegic) related protein 2
SF	Stress fibers
SR	Strain rate
SRF	Serum response factor
Syn4	Syndecan-4
TAC	Transverse aortic constriction
TAK	TGFβ-activated kinase 1
TCF21	Transcription factor 21
TGF-β/TGFβ	Transforming growth factor-β
TGFβR1	TGFβ receptor 1
TIMPs	Tissue inhibitors of MMP
TL	Tibia length
TNFα	Tumor necrosis factor α
TRPM7	Transient receptor potential cation channel, subfamily M, member 7
TRPC 6	Transient receptor potential channel 6
V_{endo}	Endocardial velocity
VEGF	Vascular endothelial growth factor
WHO	World Health Organization
WT	Wild type

Zeb2	Zinc finger E-box binding homeobox 2

List of Tables

List of Figures

List of Copyrighted Material for which Permission was Obtained

1. PL Roche, KL Filomeno, RA Bagchi and MP Czubryt. Intracellular Signaling of Cardiac Fibroblasts, *Comprehensive Physiology*, 5(2): 721-760, © 2015, John Wiley and Sons, Inc. http://onlinelibrary.wiley.com/doi/10.1002/cphy.c140044/full
2. RA Bagchi and MP Czubryt. Synergistic roles of scleraxis and Smads in the regulation of collagen 1α2 gene expression, *Biochimica et Biophysica Acta-Molecular Cell Research*, 1823: 1936-1944, © 2012, Elsevier. http://www.sciencedirect.com/science/article/pii/S016748891200198X
3. RA Bagchi and MP Czubryt. Scleraxis: A New Regulator of Extracellular Matrix Formation, In: *Genes and Cardiovascular Function*, 57-65, © 2011, Springer. http://link.springer.com/chapter/10.1007/978-1-4419-7207-1_6/fulltext.html
4. Mewton N, Liu C, Croisille P, Bluemke D and Lima JC, Assessment of Myocardial Fibrosis With Cardiovascular Magnetic Resonance, *Journal of the American College of Cardiology*, 57(8): 891-903, © 2011, Elsevier. (Figure 1)

CHAPTER I: INTRODUCTION

1. Cardiovascular Disease

1.1: Incidence/ prevalence

Cardiovascular disease (CVD) is the leading cause of mortality worldwide [1]. In 2012 alone, about 17.5 million patients suffering from CVD died contributing to 31% of deaths on a global scale. The World Health Organization (WHO) has estimated that more than 23 million lives will be lost annually to heart disease by 2030 [2]. In Canada alone, CVD is the second leading cause of mortality responsible for approximately 20 percent of all deaths in the country in 2011 [3]. This non-communicable disease costs the Canadian economy more than 20 billion dollars every year in patient care services [4]. Cardiovascular disease is a broad-spectrum disease that includes numerous underlying causes like atherosclerosis, diabetes, hypertension, valve stenosis and myocardial infarction (MI, ischemic heart disease). On occurrence of an injury such as a heart attack (MI), there is an elevated risk of developing heart failure within a period of five years in patients who have survived the event [5].

1.2: Cardiac remodeling

In the presence of prolonged stress such as hypertension, the cardiac tissue undergoes dramatic morphological changes that affect the functioning of the heart. The muscularity of the heart increases resulting from a phenomenon called cardiac hypertrophy - enlargement of the heart muscle cell, which represents an attempt of the heart tissue to normalize the increased workload [6]. These adaptive changes are also seen after an acute event like MI. This adaptive phase of remodeling is followed by a decompensatory phase where loss of cardiomyocytes and ventricular wall thinning

occurs. This phase also marks the initiation of generalized fibrosis, which leads to stiffening of the myocardium, interferes with cardiac contractility and electrical activity, eventually leading to heart failure and mortality [6].

1.2.1: Cardiac hypertrophy

Cardiac hypertrophy is associated with almost all forms of heart failure and can be broadly defined as an increase in cardiac ventricular mass. Increase in cardiac workload causes enlargement of the heart muscle in an attempt to meet the demand for increased blood flow. If this increased demand is caused by activities such as chronic exercise training (athletes) or pregnancy, it is referred to as "*physiological*" hypertrophy. This is only an adaptive remodeling of the heart, is reversible, and associated with preserved or improved function of the heart. This process lacks the phenomena of fetal gene activation and fibrosis. Increased pressure or volume overload associated with a cardiac injury results in "*pathological*" hypertrophy. This compensatory process occurs due to chronic hypertension, diabetes or valve disease, leads to depressed cardiac function which is non-reversible and ultimately causes heart failure and mortality. Ischemic injury or genetic mutations can also lead to pathological hypertrophy [7]. Activation of the fetal gene expression program and subsequent fibrosis are hallmarks of pathological hypertrophy. Fatty acid oxidation is decreased and there is increased reliance on glucose as a source of fuel in pathological hypertrophy [8, 9]. This fuel source switching allows the heart to produce more ATP per molecule of oxygen consumed [10, 11]. This bears a resemblance to fetal stages of cardiac development, when there is limited supply of oxygen and impairment of fatty acid transport and metabolism [11]. It is now well-established that alterations in

cardiac contractile proteins, upregulation of fetal gene expression, and significant decrease in calcium-handling proteins are associated with pathological hypertrophy of the heart [11]. An increase in β-MHC expression and a decrease in α-MHC expression has been considered to be one of the hallmarks of cardiac hypertrophy both in *in vivo* model organisms as well as in patients [12, 13]. Found at elevated levels during development and neonatal stages are the natriuretic peptides ANP and BNP. These are almost absent in the healthy adult heart [14]. There is a dramatic increase in the expression of ANP and BNP in response to hypertrophic stimuli, and has been shown to be mediated through GATA-4 [15]. In fact, in addition to GATA4, multiple transcription factors (MEF2, c-jun, c-fos, c-myc, NFAT, Csx/Nkx2.5 and NF-κB) have also been implicated for cardiac gene activation occurring in response to hypertrophic triggers [16, 17]. It is now well-established that depressed SERCA expression is a major contributor of Ca^{2+} signaling dysregulation and impairment of calcium homeostasis in cardiac hypertrophy and heart failure [18]. In a study carried out by Kogler and colleagues, the authors showed that SERCA2 is dramatically reduced in unloaded conditions. However, this is reversed in prolonged preload conditions [18].

Thus, there are prominent structural, functional, and metabolic variations between physiological and pathological cardiac hypertrophy, and these have been reviewed in detail elsewhere [11, 19, 20]. A brief summary of these features is included at the end of this section (Table 1). Based on changes in shape, cardiac hypertrophy can be sub-divided into concentric or eccentric hypertrophy. *Concentric hypertrophy* can be distinguished from *eccentric hypertrophy* by arrangement of the sarcomeres- a parallel array of sarcomere addition leads to an increase in myocyte cell

width in the former whereas, an increased cell length is caused by addition of sarcomeres in series in the latter (eccentric hypertrophy) (Fig. 1). Concentric hypertrophy is associated with pressure overload (chronic hypertension, aortic stenosis, strength straining). The parallel pattern of sarcomere addition in concentric hypertrophy causes an increase in wall thickness. Volume overload (valve disease, endurance training) is the underlying cause of eccentric ventricular hypertrophy. The heart wall thickness in this case is mostly unaffected or thinner. *Cardiac hypotrophy*, on the other hand, is a phenomenon clinically characterized by lower left ventricular mass relative to body weight. This has been reported in patients with anorexia nervosa [21]. In mice lacking total β-adrenoreceptor, both heart weight and heart weight:body weight ratio were significantly reduced compared to their wild-type counterparts [22], suggesting the existence of cardiac hypotrophy.

Table 1: Distinct features of physiological and pathological cardiac hypertrophy

Feature	PHYSIOLOGICAL HYPERTROPHY	PATHOLOGICAL HYPERTROPHY
Stimuli	Exercise training Pregnancy	Hypertension Valve disease Cardiomyopathy
Cardiac morphology	↑ myocyte volume ↑ cardiac size	↑ myocyte volume ↑ cardiac size
Fetal gene expression	Relatively unaltered	Upregulated (ANP, BNP, α-skeletal actin, β-MHC)
Cardiac fibrosis	No	Yes
Cardiac function	Normal/ Enhanced	Depressed
Metabolism	↑ FA oxidation	↓ FA oxidation
Reversible condition	Yes	No

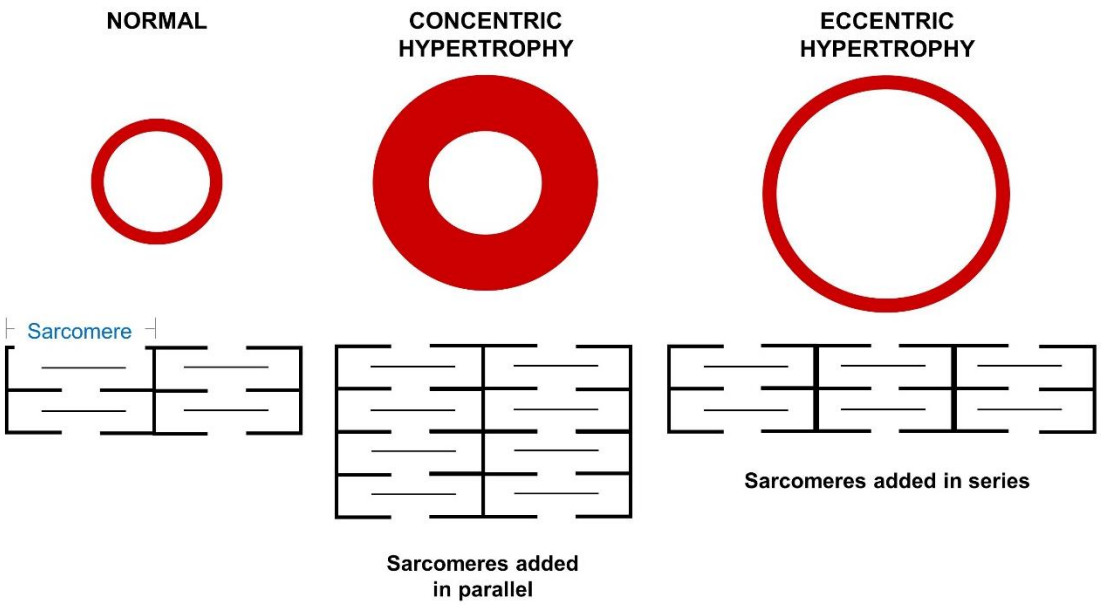

Figure 1: Patterns of ventricular hypertrophy.

Based on structure of the heart, ventricular hypertrophy can exhibit a concentric or eccentric pattern. This is due to the addition of sarcomeres in parallel or series arrangements respectively.

1.2.2: Cardiac fibrosis

Myocardial or cardiac fibrosis is a maladaptive phenomenon where there is a significant increase in the volume of collagen present in the myocardial tissue- a distinct feature of end-stage heart failure. In contrast to generalized fibrosis which occurs over time (years) in conditions such as hypertension and diabetes, there is a rapid increase (weeks) in collagen production in response to acute myocardial infarction [6, 23]. The remodeling heart after MI undergoes morphological and functional changes that can be divided into three phases [24]. Myocyte death follows rapidly after occlusion of a coronary artery stops the blood flow to the heart muscle. An inflammatory response is triggered due to the release of cellular proteins from the dying myocytes into the circulating blood. It begins with acute *inflammation* at the site of injury within a matter of hours where there is cardiomyocyte necrosis, release of pro-inflammatory cytokines, cell infiltration and ECM degradation. Infiltration of macrophages, neutrophils, monocytes and lymphocytes helps clear the cell debris. This phase usually lasts for 4-7 days [24, 25]. This is followed by a *proliferative or granulation phase* characterized by migration and proliferation of fibroblasts, phenoconversion to myofibroblasts, increased matrix turnover and also angiogenesis to revascularize the ischemic tissue. This usually happens during 1-4 weeks after MI [24, 25]. At this time, highly proliferative cardiac fibroblasts enter the site of injury and secrete ‘molecular glue’- extracellular matrix (ECM) constituents, predominantly type I collagen. This initiates the formation of a stable scar tissue that eventually replaces the dead cardiomyocytes in the infarct region, and avoids aneurysm leading to rupture of the ventricular wall. Cardiac hypertrophic pathways are activated and

dilation of the ventricles occurs in the long term. This is followed by the *maturation phase* which includes the release of anti-inflammatory cytokines and pro-fibrotic growth factors, scar stabilization and contraction, and subsequent fibrosis. This may begin as early as about a week after MI and is essential to replace the areas that are devoid of cardiomyocytes and to prevent the myocardial wall from rupturing. This is usually prominent around 3 weeks post-MI injury [24, 25]. Generalized fibrosis also occurs in regions of the heart distal to the infarcted area via unknown mechanisms.

Classification of fibrosis:

The tissue distribution of fibrotic components depends on the associated pathology. The accumulation of fibrotic tissue over time causes ventricular dysfunction affecting both systolic and diastolic functions of the heart. Depending on the cardiomyopathic process involved, cardiac fibrosis can be classified into three types: reactive interstitial fibrosis, replacement fibrosis, and infiltrative interstitial fibrosis (Fig.2).

Reactive interstitial fibrosis: Characterized by a diffuse distribution of fibrotic components in the myocardium, this type of fibrosis is closely associated with hypertension and diabetes. The major contributors in these conditions are the activation of the β-adrenergic and renin-angiotensin aldosterone systems, hyperglycemia and generation of oxidative stress [26-28]. Perivascular fibrotic deposition is prominent in this pathology [29]. Reactive fibrosis originates from areas surrounding the microvasculature and spreads throughout the myocardial tissue. Aortic valve stenosis and regurgitation have been reported to be associated with this form of fibrosis [30, 31]. Remote non-infarcted cardiac tissue also appears to exhibit reactive

interstitial fibrosis [32]. This subtype of fibrosis ultimately leads to replacement fibrosis.

Replacement fibrosis: The scarring/ replacement fibrosis occurs to replace the necrotic cardiac muscle cells after MI. The primary component involved in this form of fibrosis is type I collagen [33]. It is either diffused or restricted/ localized depending on the underlying cause of the fibrotic process. Conditions such as toxic cardiomyopathy, myocarditis, hypertrophic cardiomyopathy and ischemic heart disease are associated with this form of fibrosis [34, 35]. Replacement fibrosis is associated with loss of cardiomyocyte mass. This kind of fibrosis is consequential to infiltrative fibrosis in end-stage heart disease.

Infiltrative interstitial fibrosis: Insoluble protein deposits such as amyloids (amyloidosis) and glycosphingolipids in the myocardium over a long duration of time leads to infiltrative interstitial fibrosis [36]. This has been prominently associated with the lysosomal storage disorder known as Fabry disease [37]. The glycolipid build-up causes narrowing of the blood vessels, decreases blood flow and thus increases the risk of heart disease.

Multiple systems in the body can be affected by fibrosis. It can present as a tissue-specific condition or a multi-system disease. Tissue fibrosis affects organs such as lungs, liver, kidney, heart and skin [38-41]. Cardiac fibrosis contributes significantly to patient morbidity and mortality worldwide. In spite of its significant impact on patient outcomes, there are no publicly available drugs to treat this specific condition, partly due to an incomplete understanding of the disease pathways.

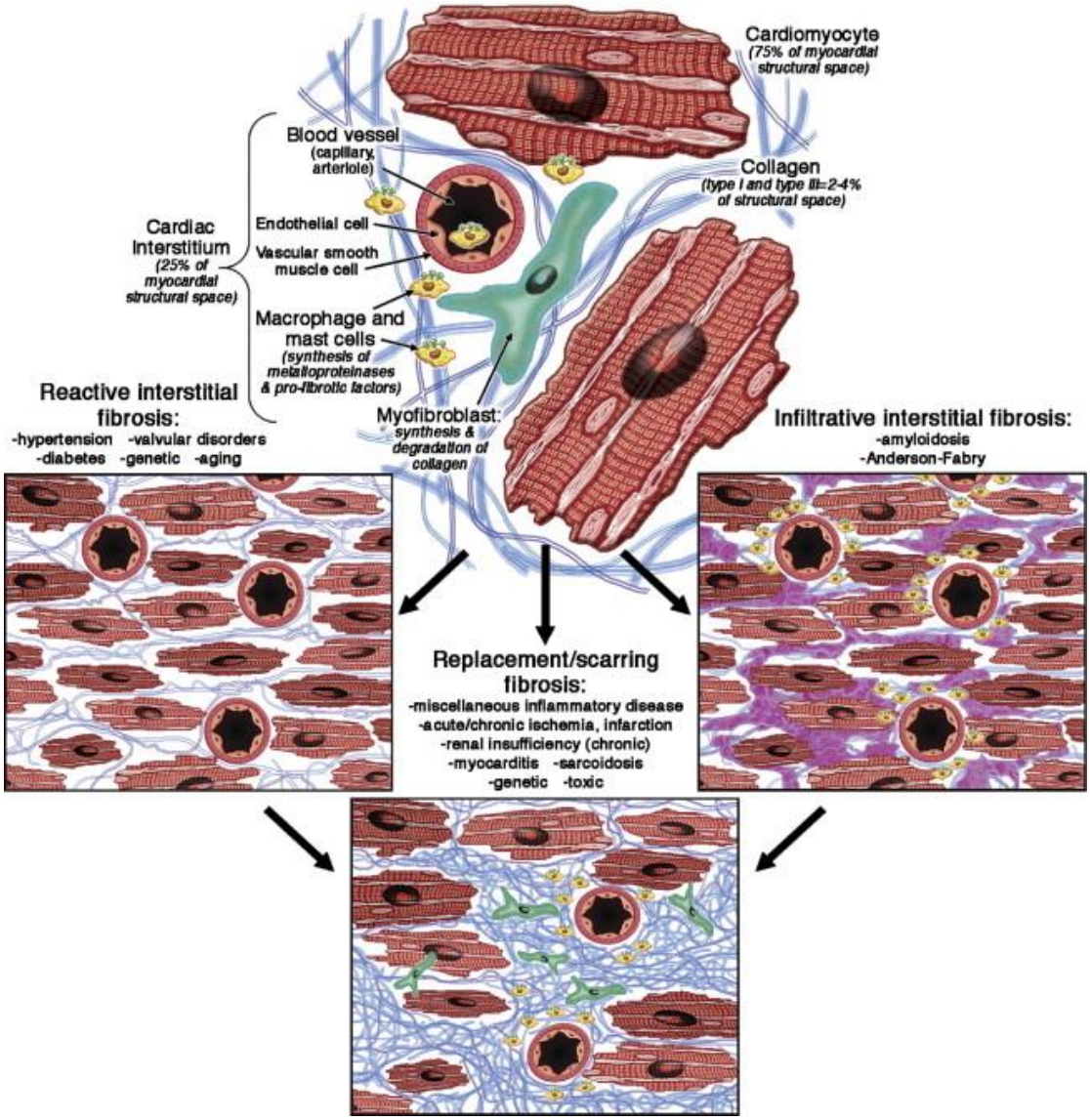

Figure 2: Etiophysiopathology of myocardial fibrosis.

Myocardial fibrosis is a complex process that involves each cellular component of the myocardial tissue. The myocardial fibroblast has a central position in this process by increasing the production of collagen and other extracellular matrix components under the influence of various factors (renin-angiotensin system, myocyte apoptosis, pro-inflammatory cytokines, reactive oxygen species). Reprinted from Journal of the American College of Cardiology, 57(8), Mewton N, Liu C, Croisille P, Bluemke D and Lima JC, Assessment of Myocardial Fibrosis With Cardiovascular Magnetic Resonance, *891-903*, © 2011, by American College of Cardiology reproduced with permission of ELSEVIER INC.
http://content.onlinejacc.org/article.aspx?articleid=1144219

Clinical diagnosis and treatments for cardiac fibrosis:

The diagnosis of cardiac fibrosis has been successful only in recent years. Previously, histological assessment of collagen content from patient biopsies was the primary mode of detecting fibrosis. The diffuse distribution of fibrotic deposits in the myocardium and requirement of invasive techniques for characterization have posed problems in diagnosis of this disease. In the present day scenario, clinicians are equipped with better tools to evaluate characteristics related to cardiac fibrosis-associated dysfunction. Patients with cardiac fibrosis present with abnormal functional parameters. These include reduced cardiac output, ejection fraction and coronary flow- all detectable by echocardiography [42]. Aberrations in the cardiac conduction system are detectable by electrocardiogram (ECG/EKG). Late-enhancement magnetic resonance imaging (MRI) is currently the gold standard for assessing fibrotic lesions. This is mostly carried out in conjunction with blood work for key cardiac protein and enzyme levels. T1 mapping techniques, such as modified Look-Locker inversion recovery (MOLLI), is a recent advancement in MRI technology [43, 44]. Chronic injury in the cardiac tissue is assessed using late gadolinium enhancement (LGE). The fibrotic interstitium expands due to an increase in collagen deposition over time. This results in increased gadolinium accumulation in injured areas [45]. Novel nanoparticle-enhanced MRI probes have been tested in *in vivo* models. These are targeted specifically for angiotensin II-converting enzyme (ACE) overexpression or fibrillar collagen [46, 47].

Current treatment approaches for cardiac fibrosis focus on improving symptoms of the causative pathology (hypertension, heart failure) rather than treating

fibrosis itself. The treatment strategies used most commonly include diuretics, vasodilators, and beta blockers. ACE inhibitors are frequently used in delaying the progression to heart failure in patients with chronic hypertension. Both lisinopril and enalapril have shown success in reducing fibrosis in patients with hypertensive heart disease [48, 49]. AT1 receptor blockers/antagonists (ARBs) have also been shown to interfere with the progression of fibrotic heart disease. They induce vasodilation, reduce secretion of vasopressin, and decrease the downstream production and secretion of aldosterone [50]. Losartan decreased collagen volume fraction (CVF) significantly in patients with hypertensive heart disease- an effect that was independent of changes in blood pressure or LV mass [51]. Another ARB, candesartan, was also effective in reducing cardiac fibrosis in a clinical trial of hypertensive patients [49]. Aldosterone antagonists function by blocking aldosterone binding to its mineralocorticoid receptors in the kidney [50]. Spironolactone reduced the serum levels of pro-collagen type III N-terminal peptide (PIIINP) and improved ejection fraction in patients with heart failure or MI [52, 53]. Carvedilol is most frequently used beta-blocker for patients with chronic heart failure. Although non-selective in its mode of action, there is some evidence that suggests this drug has anti-fibrotic properties [54]. Calcium channel blockers and statins also help in reducing fibrosis. A detailed account of current treatment strategies for cardiac fibrosis has been published recently [50].

2. Cardiac Fibroblasts

The myocardium comprises of different cell types which include cardiomyocytes, fibroblasts, endothelial cells and smooth muscle cells. The heart is also populated by immune cells, progenitor/ stem cells as well as neuronal cells. Fibroblasts, the major cellular component of the connective tissue, are cells of mesenchymal origin capable of synthesizing a wide variety of matrix proteins and biochemical constituents including growth factors [55]. They constitute the largest cell population in the heart numerically [56]. The actual number of fibroblasts in the cardiac tissue is not known. Fibroblasts morphologically are flat spindle-shaped cells with multiple projecting processes. Cardiac fibroblasts are the only cell type in the heart that lack a basement membrane. These cells were originally believed to be a homogenous cell population. It has become evident over the past few years that they are a heterogeneous cell population and not static as believed previously [55, 57]. Fibroblasts were until a few years ago considered to only being responsible for the synthesis and turnover of the ECM. The cardiac ECM provides a physical scaffold for all cells, and fibroblasts maintain the homeostasis of this dynamic matrix. Fibroblasts contribute to the structural, mechanical, biochemical, and electrical properties of the myocardium [55]. Cardiac fibroblasts are now considered to be at the interface of multiple interactions due to their involvement in multiple functions, and thereby playing a critical role in maintaining cardiac tissue homeostasis.

2.1: Origin and function of cardiac fibroblasts

Cardiac fibroblasts are mesenchymal cells. Resident cardiac fibroblasts have distinct cellular origins developmentally, and this paradigm is recapitulated in fibrotic disease of the heart as well (Fig. 3).

2.1.1: Emergence of cardiac fibroblasts during development

During cardiac development, epicardial cells from the proepicardial organ undergo epithelial-to-mesenchymal transformation and subsequently differentiate into fibroblasts. The fibroblasts of the cardiac interstitium and the annulus fibrosis derive principally from mesenchymal cells in the embryonic proepicardium [58]. The annulus of the heart is an electrically inert barrier between the atrial and ventricular tissues that is necessary for normal sequential activation of the heart. These proepicardial cells then migrate over the surface of the embryonic heart and form the epicardium. This epicardium gives rise to the epicardium-derived cells (EPDCs) [59]. These cells then undergo morphological and functional changes through the process of epithelial-mesenchymal transition (EMT) and mature into fibroblasts [60]. This differentiation occurs under the influence of growth factors like transforming growth factor beta (TGFβ) and fibroblast growth factor (FGF) among others [61]. Gittenberger-de Groot and colleagues used quail– chicken chimeras and demonstrated that these EPDCs are present in the annulus fibrosis and express periostin and type III collagen [60, 62].

The atrioventricular valvular fibroblasts originate from the endocardium (cardiac endothelium) [63]. In the region of the developing cardiac cushion, the endothelial cells delaminate and undergo endothelial-mesenchymal transition (EndMT). Under the influence of growth factors like TGFβ and transcriptional

regulators such as Wnt, these cells invade the cardiac jelly structure and transform into a mature fibroblast [63].

2.1.2: Origins of cardiac fibroblasts in pathology

During fibrosis, collagen synthesis and deposition dramatically increases in the heart, which leads to a distortion in structure and function of the heart. Cardiac fibrosis in fact is a persistent process that progresses into heart failure and death over time.

Resident cardiac fibroblasts:

The traditional view is that activated fibroblasts in fibrotic hearts are generated by proliferation and activation of the resident fibroblasts. Cardiac fibrosis in response to pressure overload is a distinct feature of this disease and has been demonstrated to result from resident fibroblast proliferation [64]. These fibroblasts present a highly viable source of matrix-synthesizing cells during replacement fibrosis. Initial studies using proliferating cell population tracking techniques showed that these cells were only found in the perivascular region in a model of cardiac hypertrophy [65, 66]. Perhaps, the resident fibroblast activation concept needs to be explored through cell fate mapping studies in future to examine the exact distribution of these cells spatially and temporally during disease progression.

Pericytes:

Although the contribution of perivascular cells such as pericytes in cardiac fibroblast formation has not been determined, these cells have been shown to transform into collagen-producing fibroblasts in the kidney [67]. $CD73^{+}$ pericytes were shown to be the source of fibroblasts in the injured kidney in this investigation. Retinal pericytes

have also been shown to exhibit a phenotypic overlap with fibroblasts *in vitro* [68]. In models of dermal scarring also, pericytes have been shown to present as another source of fibroblasts [69].

Fibroblasts derived from circulating bone marrow-derived progenitor cells, monocytes and fibrocytes:

Bone marrow-derived progenitor cells contribute substantially to the fibroblast population in the fibrotic heart [40]. Bone marrow transplantation studies have played a key role in determining the source of these fibroblasts in the diseased myocardium. The fibrotic heart tissue of mice that had received a transplant with GFP-expressing bone marrow cells prior to myocardial infarction showed GFP^+ expressing cells [70, 71]. In sex mismatched bone marrow transplantation investigations, where female mice receive bone marrow from male donor mice, aortic banding resulted in approximately 13% of $FSP1^+$ fibroblasts and 21% of α-SMA^+ fibroblasts being derived from the bone marrow in fibrotic loci. This was determined by the presence of the Y chromosome in these cells [72]. Bone-marrow-derived cells have also been found to contribute more than 60% of the cardiac fibroblast population in an experimental model of autoimmune myocarditis [71]. *Monocytes* are also a source of cardiac fibroblasts in a pathological setting. In an acute MI model, invading activated fibroblasts in the infarct region co-expressed monocytic (CD45, CD11b) and myofibroblast (S100A4, α-SMA) proteins [73]. Inhibition of monocyte recruitment reduced the number of cardiac fibroblasts and fibrosis following MI [74]. *Fibrocytes* are another source of fibroblasts in the remodeling heart. These cells co-express markers of both the hematopoietic and mesenchymal lineages [75]. The first instance

of circulating fibrocytes was described in a skin wound healing model. These cells preceded fibroblasts entering the wound from adjacent skin area [76].

Endothelial-mesenchymal transition (EndMT):

The transformation of endothelial cells to mesenchymal cells (fibroblasts) is another source of fibroblasts in the diseased heart [72]. Pro-fibrotic stimuli such as TGFβ and hypoxia cause endothelial cells to acquire a fibroblast phenotype by losing their intrinsic features [77, 78]. During cardiac fibrosis, EndMT can be induced by TGFβ in a Smad-dependent manner, while bone morphogenic protein 7 (BMP-7) is capable of blocking this process and serves the role of an anti-fibrotic agent [72]. Fate mapping studies in mice have demonstrated that up to 30% of fibroblasts in cardiac fibrosis originate from endothelial cells [72]. A recent report shows that suppression of receptor kinase Tie-1 promotes EndMT in human endothelial cells [79].

Thus, cardiac fibroblasts can be derived from numerous sources during development as well as during fibrotic remodeling of the myocardium (Fig. 3). The relative contribution of each of these sources though remains to be elucidated through future investigations.

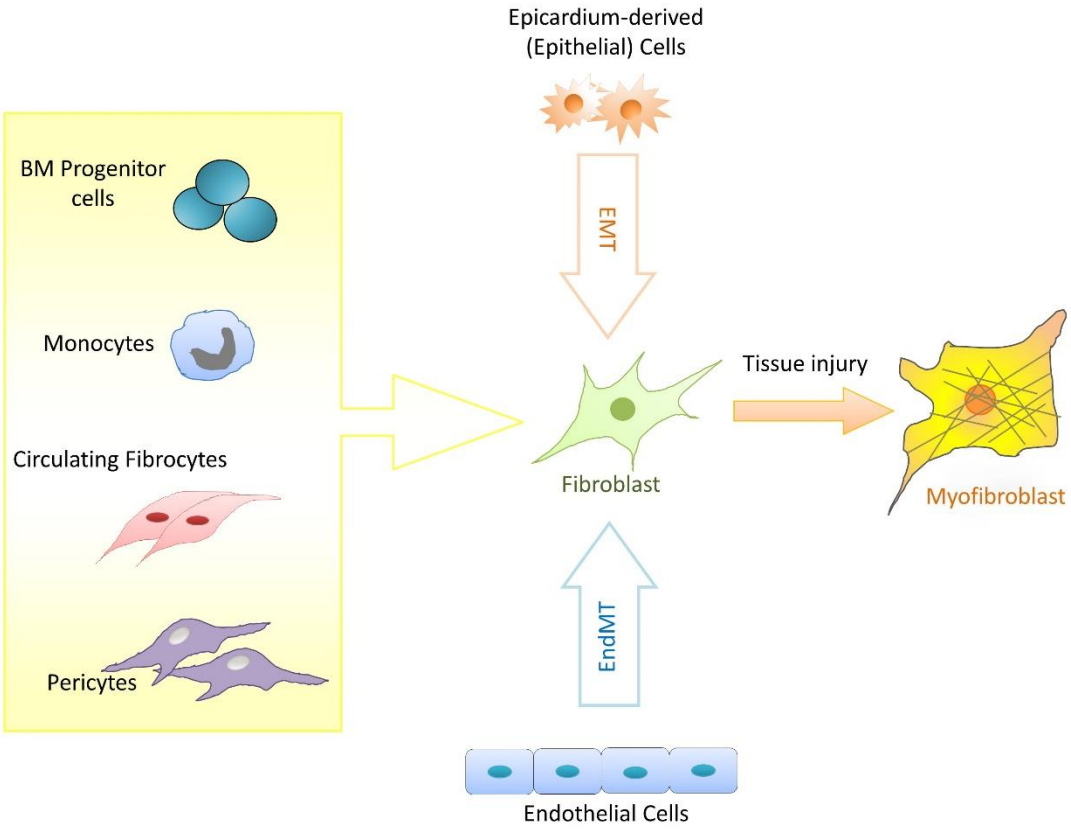

Figure 3: Origins of cardiac fibroblasts.

Epicardium-derived cells undergo epithelial–mesenchymal transition (EMT) and convert to cardiac fibroblasts during cardiac development. Endothelial cells (endocardium-derived) are also capable of undergoing an endothelial–mesenchymal transition (EndMT) to give rise to fibroblasts. In response to a cardiac injury, bone marrow (BM)-derived cells including fibrocytes and monocytes are recruited to the site of injury where they are converted to cardiac fibroblasts. These cells represent additional sources of fibroblasts in the injured myocardium other than the processes of EMT and/or EndMT. The fibroblast is activated and converts to a myofibroblastic phenotype, which is contractile, and hypersynthetic for matrix proteins, and is the causative cell type for cardiac fibrosis.

2.1.3: Role of fibroblasts in myocardial cytoarchitecture and function

Cardiac fibroblasts are involved in maintenance of tissue structure and function through homeostasis of the extracellular matrix and vasculature, production of bioactive molecules, cell–cell communication with cardiomyocytes and cardiac electrical activity (Fig. 4).

Cardiac fibroblasts are critical regulators of ECM homeostasis due to their innate ability to synthesize and degrade the matrix proteins. The cardiac ECM serves multiple roles - as a logistic network that provides a physical scaffold and interconnects cells, distributes and conveys mechanical and chemical signals, and ensures sequential cardiac conduction by creating an electrical barrier between the atria and ventricles. The cardiac ECM is primarily comprised of fibrillar collagen types I and III which constitute about 90% of the total cardiac collagen, as well as less abundant collagen types IV, V and VI. Fibronectin, laminin, elastin, proteoglycans and glycoproteins are also present in the ECM. The cardiac fibroblasts produce both fibrillar and non-fibrillar collagens, and this production is responsive to growth factors like TGFβ, cytokines such as IL-6, or even non-biochemical triggers such as mechanical stretch [80, 81]. Cardiac fibroblasts also modulate matrix degradation by producing and also regulating the activities of matrix metalloproteinases (MMPs) and their inhibitors (tissue inhibitor of MMP; TIMPs) [82]. A well-balanced function of MMPs and TIMPs is crucial in maintenance of cardiac ECM homeostasis [83]. A detailed account of the role of cardiac fibroblasts in ECM regulation follows in Section 3 of Chapter 1: Introduction.

Cardiac fibroblasts also contribute to homeostasis of cardiac vessels. The influence of the interaction between fibroblasts and endothelial cells during formation of vessels was first reported more than two decades ago [84]. Cardiac fibroblasts secrete potent inducers of angiogenesis such as vascular endothelial growth factor (VEGF), PDGF and FGFs [85, 86]. In *in vitro* studies, the pigment epithelium-derived growth factor (PEDF) has been shown to negatively regulate VEGF-induced endothelial cells [87]. Thus, depending on what they secrete, cardiac fibroblasts have the ability to have both pro- and anti-angiogenic effects on the vasculature. *Cardiac fibroblasts also influence myocyte development and proliferation* in a paracrine fashion through secretion of FGF and periostin [88, 89]. They produce mitogens that are important for myocyte proliferation.

Another important function of cardiac fibroblasts is the *production and secretion of a variety of bioactive molecules*. These include cytokines (Interleukins, TNFα), growth factors such as TGFβ, FGF, connective tissue growth factor (CTGF), vascular endothelial growth factor (VEGF), and peptides like endothelin 1 (ET-1), angiotensin II (Ang II) [90]. These biomolecules play a role in multiple cell processes such as proliferation, differentiation and apoptosis among others by exerting their effects on cells in the heart in a paracrine or autocrine manner.

Cardiac fibroblasts also contribute to the electrophysiology of the heart. Cardiac fibroblasts are capable of conducting electrical signals with a high membrane resistance [91]. Cardiac fibroblasts are also coupled to myocytes via gap junctions (connexins-43 and 45) which allows for transduction of electrical signals across these cells [91-94]. Rohr reported that the fibroblast- myocyte interconnectivity, which

could establish successful conduction over distances as long as 300 μm may provide synchronization of spontaneous activity even in distant cardiomyocytes [95]. Cardiac fibroblasts also separate the atria from the ventricles electrically for sequential contraction of these chambers. This insulation is provided by the annulus fibrosis, which is an insulating sheet of ECM produced by cardiac fibroblasts [96]. Cardiac fibroblasts also express stretch-activated ion channels, which are permeable to Na^+, K^+, and Ca^{2+} ions [97]. In fact, Kamkin and colleagues demonstrated that these ion channels open and lower fibroblast membrane potential in response to mechanical triggers [98]. These cells are therefore effective and viable electromechanical transducers.

Thus, cardiac fibroblasts constitute a dynamic cell population performing multiple functions in the healthy and diseased myocardium. Their pleiotropic functions contribute to the structural, mechanical, electrical and biochemical characteristics of the heart in development and disease.

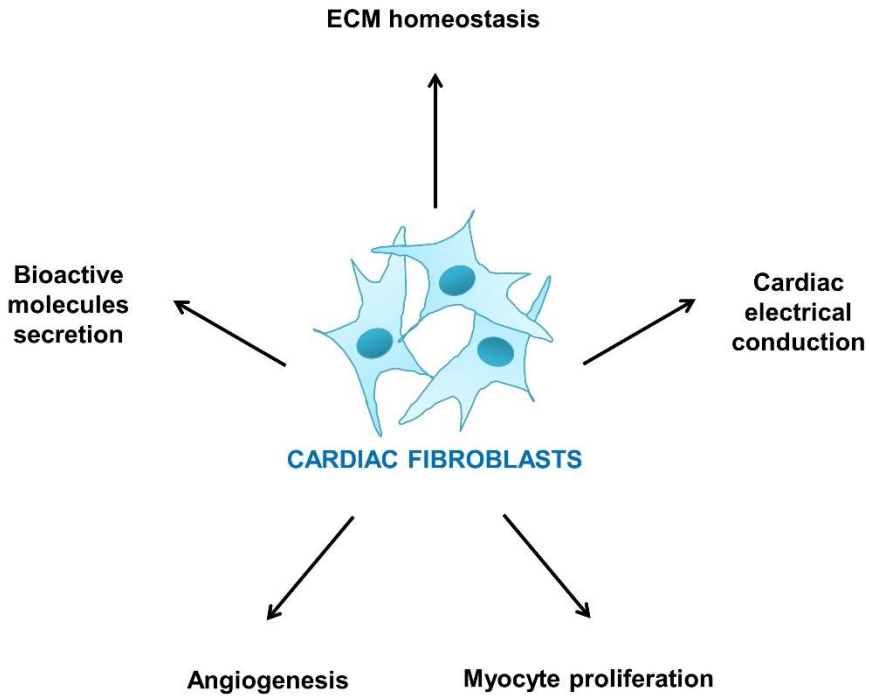

Figure 4: Functions of cardiac fibroblasts.

Cardiac fibroblasts have pleiotropic functions. They maintain ECM homeostasis by synthesis and degradation of its components. They also produce and secrete bioactive molecules, which regulate functions of other cells in the myocardium in a paracrine manner. Cardiac fibroblasts also play important roles in cardiac electrophysiology, blood vessel formation as well as proliferation of cardiomyocytes.

2.2: Fibroblast to myofibroblast phenotype conversion[1]

Fibroblasts are not only responsible for the secretion and maintenance of ECM components, but also in regulating the transmission of mechanical and electrical stimuli within the healthy working heart [99, 100]. Upon myocardial injury, in response to stress including hypoxia or cell stretch, or following stimulation by pro-fibrotic growth factors such as TGFβ, fibroblasts undergo a phenotype conversion to myofibroblasts (Fig. 5) [23]. While this conversion is frequently referred to in the literature as a differentiation process, this nomenclature is difficult to rationalize since fibroblasts already clearly exhibit signs of differentiation such as stress fibers (SFs), and it would be difficult to argue that fibroblasts are undifferentiated. Rather, this conversion may better be considered as a "fine-tuning" of the cell phenotype to meet the changing demands of the surrounding tissue. There are multiple factors and interconnecting pathways that modulate fibroblast-to-myofibroblast phenotype conversion. The dysregulation of any one of these regulatory pathways may result in either the over-accumulation of collagens or impaired healing of the injured heart, making phenotype conversion a double-edged sword. Although myofibroblasts are required to heal the injured myocardium following MI, they are also the primary drivers of tissue fibrosis. Thus, these pathways have been the subject of extensive research, and while our picture of the phenotype conversion process is more complete than ever, significant gaps in our understanding remain.

[1] Reprinted from PL Roche, KL Filomeno, RA Bagchi and MP Czubryt, Intracellular Signaling of Cardiac Fibroblasts, Comprehensive Physiology 5(2): 721-760© 2015, with permission from John Wiley and Sons, Inc.
http://onlinelibrary.wiley.com/doi/10.1002/cphy.c140044/full

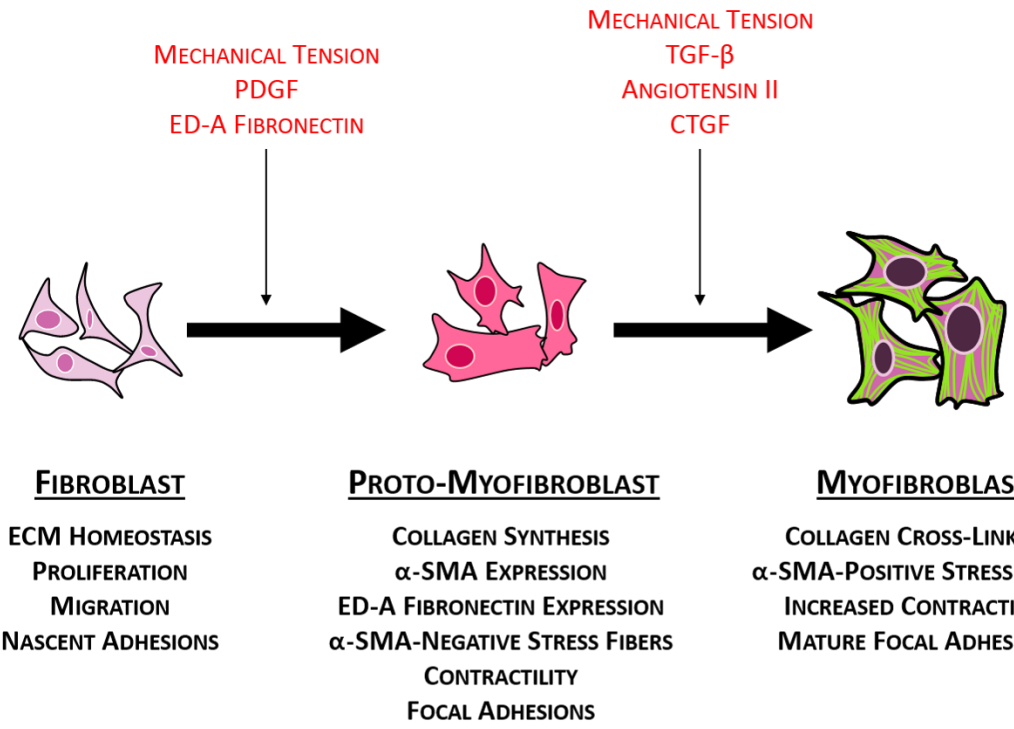

Figure 5: Cardiac fibroblast activation and phenotype conversion.
In the healthy myocardium, cardiac fibroblasts proliferate relatively slowly and maintain extracellular matrix homeostasis by continual synthesis of matrix constituents (e.g., collagens) and remodeling enzymes (e.g., matrix metalloproteinases/ MMPs) at low basal levels. In response to stressors such as myocardial infarction, related pro-inflammatory and pro-fibrotic cytokines, and/or increased matrix stiffness, cardiac fibroblasts become activated and initiate the wound healing process through matrix degradation (via increased expression of MMPs), proliferation, and migration to the site of injury, where they facilitate cardiac remodeling. *In vitro* work with fibroblasts has revealed a transient intermediate phenotype—the proto-myofibroblast, which shares features of both fibroblasts and myofibroblasts. Proto-myofibroblasts synthesize increased amounts of fibrillar collagens type I and III, and begin to express α-smooth muscle actin (αSMA) and the ED-A splice variant of fibronectin. Additionally, adhesions with the matrix are strengthened in proto-myofibroblasts as are intracellular actin filaments, imparting contractility. As of yet, it remains unclear whether proto-myofibroblasts exist as discrete entities *in vivo*. Fully phenotype converted cardiac myofibroblasts are characterized by reduced proliferation and migration, and in comparison to their precursors, are hypersynthetic for fibrillar collagens and other matrix components. Cardiac myofibroblasts also express increased levels of ED-A fibronectin and αSMA, the latter of which is also incorporated into stress fibers that are stronger and thicker than their αSMA-negative counterparts in proto-myofibroblasts. In conjunction with these fibers, the maturation and strengthening of focal adhesions imparts greater contractile ability upon cardiac myofibroblasts. Contraction of surrounding scar tissue and collagen crosslinking

performed by myofibroblasts is necessary for scar maturation, though their persistence in the healed myocardium has also been implicated in the development of cardiac fibrosis. Reprinted from PL Roche, KL Filomeno, RA Bagchi and MP Czubryt, Intracellular Signaling of Cardiac Fibroblasts, Comprehensive Physiology 5(2): 721-760© 2015, with permission from John Wiley and Sons, Inc. http://onlinelibrary.wiley.com/doi/10.1002/cphy.c140044/full

For example, there is debate as to whether an intermediate cell type, called the proto-myofibroblast, arises during fibroblast phenotype conversion *in vivo*, although a number of laboratories have reported the existence of these cells *in vitro* [101-103]. The proto-myofibroblast is characterized by increased expression of focal adhesion (FA) proteins, and the first stages of SF formation. Proto-myofibroblast SFs are composed of β- and γ-actins but specifically lack αSMA, despite the fact that αSMA expression is increased in these cells [101, 103]. Additionally, proto-myofibroblasts show TGFβ-induced activation of Rho-GTPase and ROCK, facilitating polymerization of G-actin into F-actin. However, while proto-myofibroblasts can be readily detected in vitro, the many technical challenges of studying cell adhesions in vivo leave the existence of proto-myofibroblasts during tissue pathogenesis unclear [102].

Myofibroblasts represent an activated form of fibroblast, and are the primary mediators of cardiac wound healing [23]. In contrast to fibroblasts, myofibroblasts exhibit mature SFs containing actin and myosin, which unlike proto-myofibroblast SFs, also have αSMA incorporated. These SFs exert tension on the ECM and facilitate the production of contractile force by the myofibroblast, yet at the same time oppose retractile force, aiding the physical remodeling of the ECM [99, 100, 103-105]. Phenotype conversion of fibroblasts occurs very quickly and is mainly induced by mechanical tension, deposition of the ED-A splice variant of fibronectin, and TGFβ stimulation, although many other factors have been found to affect this process both positively and negatively (see below) [106-108]. Indeed, the conversion process is easily activated *in vitro*, providing a challenge for the study of primary fibroblasts once isolated from cardiac tissue. Tissue culture plates that are most commonly used

for cell culture are highly rigid, with stiffness several orders of magnitude higher (within the MPa range) than even highly fibrotic tissue [109]. As a result, by the time isolated fibroblasts have been expanded in culture prior to experimentation, they have already begun expressing αSMA, and thus have already begun converting to proto-myofibroblasts or myofibroblasts. This can occur even before the very first cell passage, and makes studying these phenotypes challenging [100, 102].

2.2.1: Positive regulation of phenotype conversion

In cardiac fibroblasts, TGFβ_1 stimulation induces an elevation in collagen production and αSMA expression in a dose- dependent manner [81, 110, 111]. TGFβ_1 induces cardiac fibroblast phenotype conversion to myofibroblasts through canonical Smad signaling [112]. There is also evidence to suggest that TGFβ_1 signaling converges with the Ang II pathway to induce the myofibroblast phenotype. It has been shown that TGFβ_1 induces expression of the angiotensin converting enzyme (ACE) protein, which is essential for the production of Ang II [113]. Pharmacological suppression of Ang II by resveratrol or losartan results in the prevention of TGFβ_1-induced fibroblast phenotype conversion and the reduction of Smad2 and Smad4 expression, respectively [114, 115]. Ang II has also been shown to induce TGFβ_1 expression in cardiac fibroblasts [116, 117]. This cross-talk may behave as a positive feedback mechanism, in which TGFβ_1 induces more TGFβ_1 production in an autocrine fashion through mediation of ACE. Although the effects of these cytokines on cardiac fibroblasts are well characterized, the precise molecular mechanisms remain to be elucidated.

TGFβ has many origins including secretion both from resident cardiac cells and infiltrating inflammatory cells, as well as inactive stores within the tissue itself, emphasizing the importance of this cytokine in many organs including the heart. Generally, TGFβ is synthesized and secreted in a homodimeric protein pro form, consisting of a TGFβ molecule covalently linked to latency-associated protein (LAP). The resulting small latent complex (SLC) prevents TGFβ from associating with its receptor [118]. TGFβ can also be secreted as a large latent complex (LLC), composed of a SLC linked to latent TGF-binding protein (LTBP) by a disulfide bond [119]. LTBPs bind to ECM proteins such as fibrillin-1, vitronectin and fibronectin, creating a TGFβ store within the ECM [118, 120-122]. Latent TGFβ is released as an active cytokine following proteolytic cleavage by enzymes that degrade ECM, including the MMP family [118, 123-125]. Glycosidases release active TGFβ by removing carbohydrates from the SLC, resulting in a conformational change of the complex and TGFβ release [126]. Thrombospondin-1 also releases TGFβ from the SLC or LLC through the disruption of the bond between LAP and TGFβ [127]. Aside from latent TGFβ already present within the ECM and interstitium of the tissue, TGFβ may also be secreted by activated macrophages during wound healing [128]. Neonatal cardiac fibroblasts have also been shown to secrete $TGF\beta_1$ and $TGF\beta_2$ in response to norepinephrine and Ang II stimulation, working in an autocrine and paracrine fashion [129].

The endothelin family of biopeptides consists of endothelins 1-3 (ET1-3). The majority of ET1 is generated by endothelial cells and is produced in the heart, kidney, pituitary, and central nervous system [130, 131]. ET1 is a potent vasoconstrictor and is

known to increase blood pressure and vascular tone [132]. ET1 is also involved in wound healing post-myocardial injury, and leads to phenotype conversion of cardiac fibroblasts to myofibroblasts [133]. One laboratory has reported that overexpression of transient receptor potential cation channel, subfamily C, member 6 (TRPC6) or constitutively activated NFAT in cardiac fibroblasts attenuated the effect of ET1 and reduced fibroblast-to-myofibroblast conversion [134]. In sharp contrast, however, more recent studies have implicated TRPC6 as a pro-fibrotic factor: deletion of the TRPC6 gene impaired both cardiac and dermal wound healing, and TRPC6 was sufficient to increase type I collagen expression and fibroblast phenotype conversion via induction of calcineurin, the Ca^{2+}-dependent phosphatase that activates NFAT via dephosphorylation [135]. Haploinsufficiency of the TGFβ co-receptor endoglin attenuated activation of the calcineurin/TRPC6 pathway and reduced expression of αSMA [136]. Other TRP channels such as TRPC3 and TRPM7 have also been implicated in the phenotype conversion of fibroblasts to myofibroblasts and in atrial fibrosis, and the common mode of action of these channels appears to be facilitating entry of Ca^{2+} to activate calcineurin/NFAT signaling [137, 138].

The remodeled matrix itself also contributes to fibroblast phenotype conversion. As the ECM is remodeled and disrupted, fibroblast protection from mechanical stress is reduced, resulting in fibroblast phenotype conversion through the Rho/ROCK signaling cascade [103, 139]. Through this pathway, mechanical force may induce αSMA expression and ultimately induce fibroblast to myofibroblast phenotype conversion.

There is growing evidence that microRNAs can play a role in fibroblast phenotype conversion. MicroRNAs suppress protein expression by either facilitating mRNA degradation or by inhibiting translation [140, 141]. One such example is miR-145, which has been reported to induce the myofibroblast phenotype similar to TGFβ. miR-145 overexpression upregulated the myofibroblast markers fibronectin, vimentin, and αSMA as well as connexin 43, and downregulated the fibroblast marker DDR2 in cultured fibroblasts, indicative of a shift toward the myofibroblast phenotype. The cells also formed highly organized SFs and F-actin bundles, providing contractility, as well as enhanced deposition of mature collagen type I [142]. It has been shown in vascular smooth muscle cells that miR-145 regulates cellular phenotype through the negative regulation of Kruppel-like factor 5 (KLF5), which itself is a negative regulator of myocardin [143]. Wang et al. reported that this pathway exists in cardiac fibroblasts. At 3 days following MI, miR-145 was downregulated, alleviating its effect on KLF5 expression and resulting in decreased myocardin expression. At 7 days post-MI, miR-145 expression returns to basal levels, reducing KLF5 expression and in turn upregulating myocardin [142, 143]. In contrast, however, recent work has suggested that myocardin is not endogenously expressed by cardiac fibroblasts [144]. This discrepancy could be explained by the fact that myocardin and myocardin-related transcription factors (MRTFs) are very closely related and share homology in multiple functional domains as reviewed by Pipes et al. [145], thus it may be possible for MRTFs to be detected using supposedly myocardin-specific primers. Both proteins are associated with SRF [146].

Myocardin is primarily localized within the nucleus whereas MRTFs are bound to G-actin via their N-terminal RPEL domain [144, 147]. As described above, ROCK signaling reorganizes actins within the cytoplasm and releases the MRTFs, making them available to translocate into the nucleus where they enhance smooth muscle gene expression [139, 148, 149]. Small et al. found a 50% reduction in scar size within the hearts of MRTF-A null mice [144]. This was accompanied by attenuated upregulation of SM22, αSMA, Col1α1, Col1α2, Col3α1, and elastin post-MI, consistent with a diminished myofibroblast phenotype. However, the MRTF-A null mice did manage to create sufficient scar to prevent cardiac rupture. This research group also found that inhibition of ROCK signaling with Y27632 partially attenuated MRTF-A translocation and TGFβ_1-mediated collagen synthesis, providing evidence of a new potential treatment option to prevent excessive fibroblast differentiation without risking cardiac rupture.

2.2.2: Negative regulation of phenotype conversion

TGFβ signaling is negatively regulated by inhibitory I-Smad7, which both interferes with phosphorylation of receptor-Smad 2/3 (R- Smad2/3) by the TGFβ receptor and facilitates degradation of the type I TGFβ receptor subunit through the recruitment of Smurf2 [150]. The proto-oncoprotein Ski has also been shown to negatively regulate cardiac fibroblast phenotype conversion [151]. Ski inhibits Smad signaling by binding to DNA-bound R-Smad2 and repressing the transcription of Smad-activated genes [152]. Though research to date has specifically focused on R-Smad2, it has been hypothesized that Ski negatively regulates both R-Smads (Fig. 6) [151]. Through interference with Smad-mediated gene regulation, Ski downregulates

the production of Zeb2 (Smad interacting protein-1) [153]. Zeb2 acts as a negative regulator of mesenchyme homeobox 2 (Meox2), which has been shown to inhibit conversion to the myofibroblast phenotype by downregulating αSMA and ED-A fibronectin expression [153, 154]. The attenuation of Smad signaling and Zeb2 expression by Ski is alleviated following its translocation to the cytoplasm, resulting in induction of the pro-fibrotic gene expression program [151, 153]. It has been reported that Ski is upregulated within the cardiac infarct scar, but is sequestered in the cytoplasm, leaving Zeb2 to repress Meox2 and resulting in upregulation of αSMA, ED-A fibronectin, and the myofibroblast marker smooth muscle embryonic myosin heavy chain [151, 153].

Atrial natriuretic peptide (ANP)/cGMP/protein kinase G (PKG) signaling may serve a cardio-protective role by interfering with TGFβ signaling [155]. ANP induces upregulation of cGMP, which in turn activates PKG [156]. Activated PKG phosphorylates Smad3, but this occurs at different sites than those phosphorylated by the TGFβ receptor kinase, thus inhibiting the translocation of the Smad-complex to the nucleus and subsequently inhibiting collagen synthesis, fibroblast proliferation, and phenotype conversion [155]. Elevated BNP and nitric oxide levels similarly attenuate TGFβ expression through the activation of cGMP [157, 158].

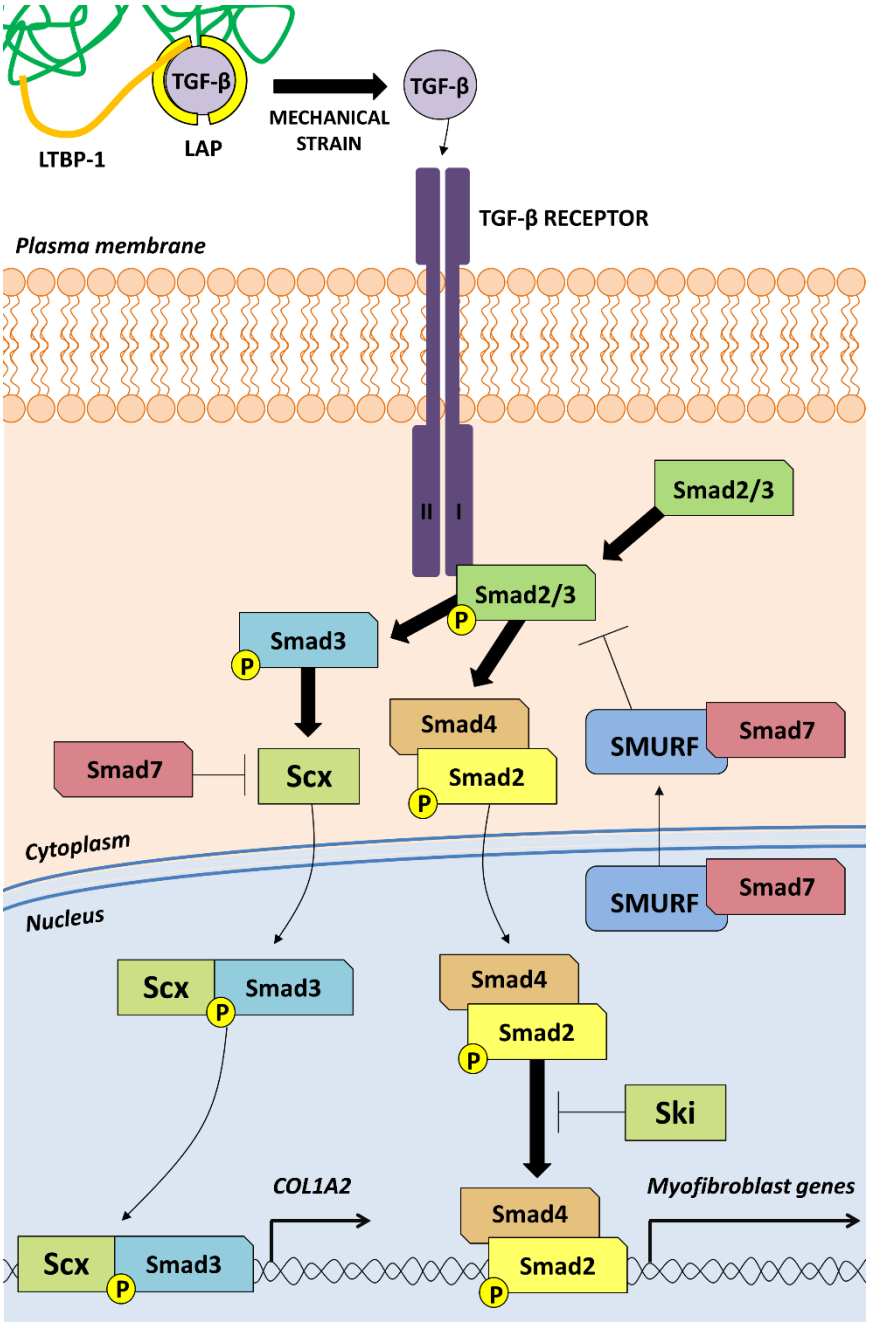

Figure 6: Canonical transforming growth factor-β (TGFβ) signaling and cardiac fibroblast gene expression.

TGFβ is secreted by cardiac fibroblasts in an inactive form, bound non-covalently to latency associated peptide (LAP). LAP binds covalently to latent-transforming growth factor-β-bound protein-1 (LTBP-1) within the normal extracellular matrix, and these three components form the large latent complex, or LLC. Increased tension within the matrix causes a conformational change in the LLC that allows rapid release and activation of TGFβ. Such forces can be transmitted to the LLC either indirectly (via

increased fibronectin fibril extension within the matrix), directly (through LLC-bound integrins on the surface of contractile myofibroblasts), or both. Active TGFβ can then bind to its receptor and induce heterotetramerization of TGFβ receptor subunits I and II. The serine/threonine kinase activity of TGFβ receptor subunit II is activated by ligand binding, in turn phosphorylating subunit I, which then phosphorylates receptor Smads 2 and 3 to allow recruitment of co-Smads such as Smad4. The Smad complex then translocates into the nucleus to activate transcription of target genes such as αSMA and fibrillar collagens. The transcription factor Ski attenuates this process in cardiac myofibroblasts, abrogating phenotype conversion. TGFβ-activated Smad3 increases expression of the transcription factor scleraxis (Scx), which acts synergistically with Smad3 to transactivate the collagen *1α2* gene. TGFβ receptor activation also activates a negative feedback loop via the expression of inhibitory Smad7, which suppresses Scx expression and forms a complex with Smurf in the nucleus that translocates to the cytoplasm to repress phosphorylation and activation of receptor Smads. Reprinted from PL Roche, KL Filomeno, RA Bagchi and MP Czubryt, Intracellular Signaling of Cardiac Fibroblasts, Comprehensive Physiology 5(2): 721-760© 2015, with permission from John Wiley and Sons, Inc. http://onlinelibrary.wiley.com/doi/10.1002/cphy.c140044/full

Another factor regulating fibroblast phenotype is bFGF (or FGF-2), which besides being a potent mitogen has been shown to prevent cardiac fibroblast phenotype conversion and to act as an anti-fibrotic factor. In cardiac fibroblasts from hypertensive rat hearts, bFGF downregulated αSMA and collagen types I and III expression [159]. It also downregulated expression of MMP2, MMP9, and TIMP2 while upregulating TIMP1. This effectively attenuated both remodeling of the ECM and collagen production. Recent evidence has shown that the high molecular weight isoform of FGF-2 possesses pro-fibrotic effects [160, 161].

2.2.3: Increased matrix production by cardiac myofibroblasts

Myofibroblasts are characterized by hyper-secretion of ECM components such as type I collagen, periostin, fibronectin, and ED-A fibronectin [103, 107]. The healthy myocardium is largely devoid of myofibroblasts; however, these cells become abundant within a few days after myocardial injury such as MI [162]. Myofibroblasts are also defined by the *de novo* expression of smooth muscle cell genes including caldesmon, SM22, and αSMA, the latter being incorporated into SFs and increasing cell contractility as noted above [102, 163-166]. Excessive production and remodeling of ECM components by myofibroblasts directly leads to cardiac fibrosis.

As mentioned previously, TGFβ plays a prime role in the phenotypic conversion of fibroblasts to myofibroblasts [167-169]. TGFβ stimulation of either cell type induces ECM gene expression and deposition of ECM components, simultaneously with alterations in expression of MMPs and TIMPs. This paradigm is not limited to the heart but extends to most tissues in the body [135, 167, 170, 171]. The canonical TGFβ-Smad2/3 signaling pathway directly transactivates ECM genes

including Col1α1 and Col1α2, as well as MMPs and TIMPs [172-174]. Hearts from Smad3 null mice exhibit attenuated collagen production and deposition, and reduced fibrotic remodeling following MI [175]. Additionally, the transcription factor scleraxis has been shown to tightly coordinate the regulation of type I collagen expression in synergy with R-Smad3 in primary isolated cardiac fibroblasts and myofibroblasts [172, 173]. The non-canonical signaling pathway initiated by TGFβ binding to TGFβ receptor subunit II induces recruitment of TAK1 and TAK1 binding protein/TAB followed by activation of MAPK signaling cascades including JNK and p38 MAPK [176]. Targeted inhibition of non-canonical TGFβ signaling using TGFβ receptor subunit II KO mice resulted in reduced fibrosis and remodeling in the pressure-overloaded myocardium [177]. Inhibition of p38 signaling can also block TGFβ-induced myofibroblast traits including expression of type I collagen, fibronectin, αSMA-positive SF formation, and collagen gel contraction [135]. Collectively, these studies identify TGFβ signaling pathways as critical drivers of myofibroblast-mediated fibrosis.

Ang II is elevated in fibrotic pressure overloaded hearts and appears to positively affect myofibroblast activity and fibrosis including increased ECM production [178, 179]. Ang II treatment of cardiac fibroblasts leads to induction of TGFβ expression through the AT1 receptor causing upregulation of down- stream fibrotic genes including type I collagen, an effect that could be blocked by the administration of losartan [116, 117]. Activation of the Smad2/3 and MAPK signaling pathways occurs in response to Ang II treatment in cardiac myofibroblasts [180, 181]. Ang II thus appears to be a crucial regulator of the myofibroblast phenotype through

multiple mechanisms. As described above, significant crosstalk also appears to exist between TGFβ and Ang II signaling pathways, resulting in reinforcing and synergistic effects on fibroblast phenotype and function.

ET1 production during cardiac injury induces myofibroblast conversion from primary cardiac fibroblasts *in vitro* [133]. ET1 also strongly induced ECM production in fibroblasts [182]. Ang II is capable of increasing ET1 expression in cardiac fibroblasts, thus driving them to a myofibroblast phenotype [183]. This effect can be blocked using losartan. TGFβ also works together with ET1 in driving the myofibroblast phenotype [184]. Thus it appears that ET1 is a downstream synergistic mediator of TGFβ and Ang II signaling, promoting fibroblast activation, maintenance of the myofibroblast phenotype and consequent tissue fibrosis [168, 185].

3. Cardiac Fibroblasts and the Extracellular Matrix[2]

Fibroblasts are the most numerous individual cell type within the heart, accounting for over 50% of the cell population (a number that may vary widely between species), yet taking up a surprisingly low volume within the myocardium owing to their small physical size in comparison to cardiomyocytes [101, 186]. During development, fibroblasts arise within the proepicardial organ from a precursor cell population dependent upon expression of the basic helix-loop-helix transcription factor TCF21: deletion of TCF21 abrogates cardiac fibroblast specification, resulting in late gestational lethality [59, 187]. Fibroblasts are recognized as having a high degree of heterogeneity between organs and tissue types, with the expression of unique protein/mRNA signatures. This heterogeneity extends to the heart as well [188]. Atrial fibroblasts have been shown to express higher levels of genes implicated in matrix formation, proliferation, cellular structure, and metabolism; however, the biological significance of these variations is not fully understood [189]. For example, platelet- derived growth factor (PDGF) and its receptor are more highly expressed in atrial fibroblasts, and it has been speculated that these chamber-specific differences may be due to unique hemodynamic, neurohumoral, and structural characteristics between these two regions of the heart, resulting in increased fibrotic responses in the atrium [189].

In the healthy adult myocardium, cardiac fibroblasts function primarily to maintain homeostasis via synthesis and secretion of ECM constituents and remodeling

[2] Reprinted from PL Roche, KL Filomeno, RA Bagchi and MP Czubryt, Intracellular Signaling of Cardiac Fibroblasts, Comprehensive Physiology 5(2): 721-760© 2015, with permission from John Wiley and Sons, Inc.
http://onlinelibrary.wiley.com/doi/10.1002/cphy.c140044/full

enzymes such as matrix metalloproteinases (MMPs; Fig. 5) [100, 190]. Fibroblasts are characterized by an interior volume extensively occupied by endoplasmic reticulum and Golgi apparatus- features indicative of the elaborate synthetic and secretory machinery required for the key role these cells play in producing and depositing ECM components.

The cardiac ECM provides a dynamic physical scaffold for the heart and plays a crucial role in initiating biochemical and mechanical cues for cell growth, development and differentiation. It is comprised of a myriad of constituents including fibrillar collagens, elastins, fibronectin, laminin, thrombospondin, proteoglycans, periostin, hyaluronan, and MMPs [80, 191-193]. Synthesis of these ECM components by cardiac fibroblasts is regulated by a complex network of signaling pathways downstream of various effector molecules such as transforming growth factor β (TGFβ), PDGF, basic fibroblast growth factor (bFGF or FGF-2), and others, in both healthy and diseased states of the heart [81, 194]. Cardiac fibroblasts also synthesize and secrete many bioactive molecules including interleukins, tumor necrosis factor α (TNFα), TGFβ, angiotensin II (Ang II), endothelin 1 (ET1), natriuretic peptides, and vascular endothelial growth factor (VEGF) [90].

3.1: Fibrillar collagen production

Fibrillar collagens are the major component of the cardiac ECM architecture and play a central role in maintaining the structural integrity of the heart [195]. The collagen fibrils provide a scaffold for cell attachment, as well as sequestration of signaling molecules such as TGFβ, thereby contributing to biomechanical homeostasis

of the myocardium. Of the more than 25 documented types of collagen, two are predominant in the heart: type I fibrillar collagen, which constitutes approximately 80% of myocardial collagen, and type III fibrillar collagen, which comprises about 10% [90, 195, 196]. The remainder are a mixture of various fibrillar and non-fibrillar collagens such as type IV, V, and VI [197-199].

Fibrillar collagens are produced and secreted into the interstitial space as procollagen molecules, which are then processed into smaller, mature collagen molecules by enzyme-mediated cleavage of the terminal propeptide domains. Mature collagen molecules can then be assembled and cross-linked to form structural collagen fibers. A disintegrin and metalloproteinase with thrombospondin motifs 2 (ADAMTS2) cleaves the amino (N)-terminal propeptide, while bone morphogenetic protein 1 cleaves the carboxy (C)-terminal propeptide [200, 201]. Upon cleavage by N- and C-proteinases, these collagen propeptides are released into the circulation [202]. Serum levels of the 100 kDa C-terminal propeptide are positively correlated with diastolic dysfunction, and this is the most commonly used biomarker for quantitative determination of type I collagen synthesis [203]. Increased serum levels of the 42 kDa N-terminal propeptide of type III collagen have been positively correlated with heart failure and mortality [204]. The N-terminal propeptide is a prominent marker of type III collagen biosynthesis [205]. Although measurements of these propeptides are indicative of overall fibrillar collagen synthesis, the organization and thickness of collagen type I and III fibrils can vary between not only healthy and diseased myocardium, but also within compartments of the heart itself such as the atria and ventricles [206].

3.1.1: Canonical TGFβ signaling

Collagen synthesis in the heart is regulated primarily through the TGFβ signaling cascade, initiated by activation of the heterotetrameric TGFβ receptor composed of type I and II subunit dimers [207, 208]. There is substantial evidence demonstrating that the canonical Smad effector protein signaling pathway, downstream of TGFβ, is responsible for increased collagen deposition in the cardiac ECM following injury [209]. The binding of TGFβ to its receptor facilitates the phosphorylation of R-Smad2 and/or R-Smad3 by the receptor's intrinsic serine-threonine kinase activity. Phosphorylated R-Smads can then associate with Co-Smad4, and the resulting R- Smad2/3-Smad4 complex translocates to the nucleus to act as a transcription factor and drive the expression of target genes such as type I collagens (Fig. 6) [210, 211]. Smad3 is required for the induction of matrix gene expression. Expression of fibrosis-related genes such as type I collagen and connective tissue growth factor (CTGF/CCN2) is interrupted in fibroblasts lacking the Smad3 gene [174, 175, 212]. The inhibitory Smads, I-Smad6 and I-Smad7, prevent R-Smad activation through competitive binding for Smad2 and Smad3 to TGFβ receptor 1 (TGFβR1/ALK5) and increased receptor degradation [213, 214]. The role of canonical signaling downstream of TGFβ has been extensively demonstrated in cardiac fibroblasts.

3.1.2: Non-Canonical TGFβ signaling

Besides Smad-mediated regulation of collagen, TGFβ binding to its receptor also activates other non-canonical signaling cascades to regulate collagen synthesis, including extracellular signal-regulated kinase (ERK), c-Jun N-terminal kinase (JNK),

TGFβ-activated kinase 1 (TAK1), and p38 mitogen- activated protein kinase (p38 MAPK) pathways [185, 215]. Experimental data indicates that Ras, ERK, and JNK are rapidly activated within minutes of TGFβ treatment in several cell types, supporting the existence of additional Smad- independent TGFβ signaling pathways [216-218]. The Leask laboratory has demonstrated that JNK activation in response to TGFβ in normal fibroblasts depends on focal adhesion kinase (FAK) [219]. Recently they also reported that the absence of TAK1 impairs TGFβ-induced JNK phosphorylation: in contrast to wild-type fibroblasts, TAK1-null fibroblasts failed to exhibit JNK activation in response to TGFβ, and failed to upregulate the expression of the myofibroblast marker α-smooth muscle actin (αSMA) and CTGF [220]. Activation of the Ras/MEK/ERK non-canonical TGFβ signaling cascade involves the heparan sulfate proteoglycan (HSPG) syndecan-4 (Syn4). In Syn4-null fibroblasts, TGFβ was unable to phosphorylate ERK or induce cell contraction [221]. Syn4 can act directly as a co-receptor for TGFβ or indirectly by modulating the expression of genes required for TGFβ-induced activation of ERK. In dermal and cardiac fibroblasts, ERK activation is required for the expression of type I collagen and CTGF [222, 223]. In turn, CTGF is an effector of TGFβ-induced myofibroblast phenotype conversion and ECM synthesis. Smad-independent responses to TGFβ appear to be mediated, at least partially, by activation of p38 MAPK. A TGFβ receptor subunit I mutant defective for Smad activation has been shown to activate p38 MAPK signaling in response to TGFβ [224].

Betaglycan, another member of the HSPG family, has been shown to bind TGFβ by its core protein compartment [225]. It controls access of TGFβ to TGFβ receptor

subunit II, thereby affecting intracellular TGFβ activity [226]. This HSPG is capable of activating the p38 MAPK pathway independently of the R-Smads and TGFβ ligand, consequently affecting target gene expression [227]. These multiple and overlapping collagen synthesis pathways explain the potent pro-fibrotic effect of TGFβ. However, the mechanisms of TGFβ-mediated activation of non-canonical pathways involving ERK, JNK, or MAPK, and the functional consequences of activation of these pathways, are incompletely characterized in cardiac fibroblasts, in contrast to other cells such as dermal fibroblasts.

3.1.3: Renin-Angiotensin-Aldosterone System (RAAS) signaling

Regulation of collagen synthesis by cardiac fibroblasts has also been associated with the renin-angiotensin-aldosterone system. Adult rat cardiac fibroblasts treated with Ang II or aldosterone demonstrated a significant increase in collagen synthesis, which is abolished by pharmacological blockade of angiotensin receptors [228]. Ang II acts via two receptors (AT_1 and AT_2) that belong to the G protein-coupled receptor superfamily [229]. The majority of the known physiological effects of Ang II occur following binding to the AT1 receptor, inducing well-defined G protein-linked signaling pathways including phospholipase C (PLC) activation, which in turn causes the release of Ca^{2+} and subsequent activation of calmodulin kinase and protein kinase C (PKC) [230].

Ang II induces upregulation of $TGF\beta_1$ expression in cardiac fibroblasts through AT1, as well as increased collagen expression via TGFβ and ERK signaling [116, 180, 181]. It was recently reported that Ang II-induced ERK activation in cardiac fibroblasts occurs via a pathway which includes the Gβγ subunit of Gi and tyrosine

kinases (e.g., Src, Ras, and Raf) [231]. Ang II also causes Smad2 phosphorylation, nuclear translocation of phospho-Smad2/4 and increased binding of the Smad complex to DNA, an effect blocked by the AT1 blocker losartan [232]. Ang II-treated cardiac fibroblasts exhibit αSMA-positive stress fibers (SFs) and contractile function in the presence or absence of TGFβ receptor subunit 1, suggesting that Ang II can also stimulate myofibroblast phenotype conversion independently of TGFβ [135]. Downregulation of the transcription factor serum response factor (SRF) in cardiac fibroblasts via RNA interference attenuates Ang II-mediated myofibroblast phenotype conversion [135].

In turn, $TGF\beta_1$ stimulates AT_1 receptor expression directly via Smads 2/3 and TGFβ receptor subunit I/ALK5, providing evidence of autocrine regulatory cross-talk between the TGFβ and Ang II signaling pathways [233]. The stimulatory effect of TGFβ on AT_1 receptor expression involves p38 MAPK, JNK, and phosphatidylinositol 3-kinase (PI3K) signaling [233]. The renin-angiotensin-aldosterone system is arguably the second most characterized mechanism of ECM regulation by cardiac fibroblasts after the TGFβ signaling pathway.

3.2: Non-collagen matrix components

The ECM protein fibronectin plays key roles in the developing heart and in the injured myocardium. Neonatal hearts synthesize more fibronectin than adult hearts [234, 235]. More specifically, the ED-A splice variant of fibronectin is implicated in phenotype conversion of fibroblasts, as well as the inflammatory response to cardiac injury. The insertion of the ED-A module into fibronectin causes a conformational

change which increases its cell adhesive properties [236]. ED-A fibronectin regulates cell adhesion and proliferation by binding integrin α4/CD49d [107, 237]. The accumulation of other ECM components, including type I collagen, depends upon polymerization of fibronectin within the ECM [238]. In a model of myocardial infarction (MI) in mice lacking ED-A fibronectin, there was reduced synthesis and deposition of collagen in cardiac tissue during the remodeling process [239]. ED-A fibronectin polymerization is required for TGFβ_1-induced fibroblast activation and phenotype conversion to myofibroblasts, preceding αSMA expression following TGFβ_1 treatment of cultured cells, as well as during granulation tissue development *in vivo* [107]. ED-A fibronectin induces pro-inflammatory gene expression by nuclear factor- κB (NF-κB) activation and acts as an endogenous ligand for TLR2 and TLR4 [240, 241]. Fibronectin has also been identified as an in vivo substrate of MMP9 using proteomic analysis as demonstrated by Zamilpa *et al*. [242]. ED-A fibronectin has been investigated primarily in fibroblasts of non-cardiac origin, but has recently been recognized as an important marker of phenotype switching in cardiac myofibroblasts [100].

Hyaluronan (hyaluronic acid, HA) is a critical component of the cardiac ECM due to its contribution to several functions such as providing a hydrated environment for cell migration and proliferation, interaction with ECM proteoglycans such as versican and aggrecan, and its association with surface receptors like CD44 to regulate cell behavior [243]. Early studies showed that a HA-rich environment was necessary for proper development of cardiac valve precursor cushions [244]. Hyaluronan

synthase (Has) enzymes appear to play a critical role in the cardiac ECM, since mice with genetic disruption of Has2 exhibit deleterious cardiovascular defects [245].

However, investigation into the role of HA and its regulation by cardiac fibroblasts is presently very limited, though HA secretion has been closely associated with maintenance of the non-cardiac myofibroblast phenotype [246, 247]. Blockade of HA synthesis inhibits the up-regulation of αSMA expression that occurs during myofibroblast phenotype conversion induced by TGFβ [248]. Interaction of HA with its receptor CD44 triggers intracellular signaling via Ras, Rac, and PI3K [249-251]. It may be through these pathways that HA contributes to myofibroblast development and maintenance.

3.3: Matrix metalloproteinases (MMPs) and matrix remodeling

The cardiac ECM is a dynamic structure requiring a precise balance between synthesis and degradation of its components, particularly the collagens. Interference with this equilibrium can lead to significant disruption of matrix organization in the myocardium. This is evident in the failing heart, when collagen synthesis outpaces degradation, leading to excessive deposition of collagen, myocardial stiffness, and fibrosis. Conversely, excessive degradation may weaken the ECM and contribute to chamber dilatation. ECM degradation may occur as a result of physical damage, but is also dynamically regulated by the activity of a family of proteolytic enzymes, the MMPs (Table 2).

Secreted by various cardiac cell types including fibroblasts, myocytes, and endothelial cells, as well as inflammatory cells such as macrophages, the MMPs are zinc-dependent remodeling endopeptidases capable of collectively degrading the

majority of the ECM components [80, 252-254]. These enzymes are synthesized as relatively inactive zymogens or pro-MMPs, which are activated by cleavage of an amino-terminal pro-peptide, exposing the enzyme's catalytic domain. More than 25 MMPs have been cloned and characterized to date. Of these, MMP1, MMP2, MMP3, MMP8, MMP9, MMP12, MMP13, MMP28, and membrane-type MMPs (MT1-MMP/MMP14) are involved in myocardial remodeling [255-258].

MMP1 (collagenase I) targets collagen types I, II, and III, as well as basement membrane proteins. MMP2 and MMP9, also known as gelatinases, can process collagen types I, IV, and V, while MMP2 can also degrade collagen type III [259]. Furthermore, MMP2 and MMP9 play an active role in the development of fibrosis-both MMPs can release ECM-bound latent TGFβ, thereby inducing collagen synthesis via the canonical Smad and non-canonical MAPK signaling pathways [125]. Cardiac fibroblasts constitutively secrete MMP2 and its expression is significantly upregulated by TGFβ, TNFα, IL-1β, BNP, mechanical stress, and oxidative stress [260-269]. IL-1 and BNP are also capable of inducing MMP3 (stromelysin-1) secretion by cardiac fibroblasts [266, 269]. Under basal conditions, cardiac fibroblasts express very low amounts of MMP9. However, this increases dramatically when these cells are exposed to pro-inflammatory cytokines and oxidative stress [266, 267, 270]. Ang II appears to elicit variable, species-dependent responses in MMP9 secretion from cardiac fibroblasts [271, 272]. MMP8 and MMP13 also degrade type I, II, and III collagen, whereas MMP12 specifically tar- gets elastin. The membrane-type MT1-MMP, which is likely associated with the cell surface (rather than being secreted into the matrix), is

capable of cleaving ECM proteins such as fibronectin, laminin, and type I collagen [273-275].

Overall, the activity of most MMPs is generally upregulated by oxidative stress, mechanical stretch, BNP, and proinflammatory cytokines with varying effects caused by Ang II. These modulators have also been shown to induce transcription of tissue inhibitors of metalloproteinases (TIMPs) in the myocardium, which oppose and control the proteolytic activity of MMPs. TIMPs are the principal inhibitors of MMPs in the heart, and are produced primarily by cardiac fibroblasts [83, 276]. Of the four TIMPs that have been cloned and characterized to date, TIMP2, TIMP3, and TIMP4 are expressed in the healthy myocardium [254]. The expression of TIMP1 in the healthy heart is quite low but it is significantly upregulated in diseased cardiac tissue [277-279]. TIMP1 expression is regulated by TNFα and IL-1β, and TIMP2 expression is similarly regulated by these cytokines as well as BNP [269, 280].

In the healthy myocardium, MMPs and TIMPs are co-expressed and strictly controlled to maintain homeostasis of the cardiac matrix, while dysregulation of this balanced system resulting in net changes in proteolytic activity contributes to myocardial remodeling and development of heart failure [281, 282]. A number of clinical studies have revealed that the activity of MMPs is increased while TIMPs are decreased in the failing heart [283-285].

Table 2: Matrix metalloproteinases secreted by cardiac fibroblasts and their target molecules[3]

Group	MMP	Name	Substrates
Collagenase	1	Interstitial collagenase	Fibrillar collagens, aggrecan, versican, proteoglycans
	8	Neutrophil collagenase	
	13	Collagenase 3	
Gelatinase	2	Gelatinase A	Denatured fibrillar collagens, collagen type IV, fibronectin, laminin, proteoglycans
	9	Gelatinase B	
Stromelysins	3	Stromelysin 1	Collagens I, III, IV, fibronectin, proteoglycans
	7	Matrilysin	
Membrane-type MMP	14	MT1-MMP	Fibrillar collagens, perlican, versican

[3] Reprinted from PL Roche, KL Filomeno, RA Bagchi and MP Czubryt, Intracellular Signaling of Cardiac Fibroblasts, Comprehensive Physiology 5(2): 721-760© 2015, with permission from John Wiley and Sons, Inc. http://onlinelibrary.wiley.com/doi/10.1002/cphy.c140044/full

4. Scleraxis: A new regulator of extracellular matrix formation[4]

By regulating the expression of a multitude of target genes, transcriptional regulators have the potential to play dramatic roles in cell, tissue, and organ physiology and pathophysiology. Understanding how these regulators function, and identifying their target genes, is thus critical for better understanding disease and developing new treatments. Scleraxis is a member of the basic-helix-loop-helix (bHLH) superfamily of transcription factors, and was originally considered to be a highly specific marker for progenitor cells destined to form tendons, ligaments, and bronchial cartilage [286-288]. Recent studies, however, suggest that scleraxis is expressed in a much wider variety of tissues, such as cardiac fibroblasts, and thus may have a broader range of activity than originally believed [173].

To date, the target genes regulated by scleraxis are largely unknown. Studies carried out over the past several years by our laboratory and others suggest that scleraxis regulates expression of a variety of connective tissue genes, including those encoding fibrillar collagens [173]. Our data indicate that scleraxis is involved in cardiac fibrosis, and the expression of scleraxis in other tissues suggests the intriguing possibility that it may play a regulatory role in other forms of organ fibrosis. Additional work is needed to further our understanding of the mechanisms by which scleraxis works, to identify its target genes, and to better understand how expression and activity of scleraxis itself is controlled. Indeed, despite the fact that it was cloned

[4] Reprinted from RA Bagchi and MP Czubryt, Scleraxis: A New Regulator of Extracellular Matrix Formation, Genes and Cardiovascular Function, 57-65, © 2011, with permission from Springer. http://link.springer.com/chapter/10.1007/978-1-4419-7207-1_6/fulltext.html

well over a decade ago, at the time of this writing there are fewer than 120 papers referencing scleraxis in the literature[5] [288]. The need for additional research on this intriguing protein is thus significant.

4.1: Structure and function

The various members of the bHLH transcription factor superfamily play critical roles in such varied processes as cell proliferation, differentiation, and regulation of oncogenesis [289-291]. Structurally, these proteins contain a bHLH moiety consisting of a short stretch of hydrophilic residues followed by a set of mainly hydrophobic residues located in two short helices separated by a non-conserved sequence of variable length which constitutes the loop [292, 293]. The basic domain of bHLH proteins constitutes the actual interface for DNA interaction. One helix is slightly smaller than the other to provide additional flexibility to facilitate dimerization by folding and packing against the other helix. Typically the larger helix contributes to the DNA interaction interface [294]. The bHLH proteins bind to signature motifs consisting of a core hexanucleotide sequence, CA*NN*TG (*N* represents any nucleotide), referred to as an e-box [288, 295, 296]. A transactivation domain, typically located in the C-terminal region, is responsible for the activity of these factors.

Small (~22 kDa), scleraxis is structurally very similar to other bHLH factors, including possession of an N-terminal bHLH motif and a C-terminal transactivation domain [288]. Scleraxis was first cloned in a yeast two-hybrid screen to identify interacting partners of E12 [3]. E12 is an ubiquitous Class A bHLH protein, also

[5] This was at the time of publication of the book chapter (2011). In 2015, there were 238 papers referencing scleraxis on PubMed (http://www.ncbi.nlm.nih.gov/pubmed), April 20, 2015.

known as an E-protein [297]. Conversely, scleraxis is a Class B bHLH protein exhibiting a tissue-restricted expression pattern. Like other bHLH proteins, it binds specifically to E-boxes, and its ability to bind to oligonucleotides containing E-boxes from the muscle creatine kinase gene promoter is augmented by E12, suggesting that scleraxis heterodimerizes with E-proteins for full activity [288]. Using artificial promoter constructs, it has been shown that another E-protein, E47, also augments the ability of scleraxis to bind to E-boxes [298]. At present it is unclear how scleraxis "recognizes" specific E-boxes in target gene promoters. The identities of the two central nucleotides of the E-box hexamer are likely to be important, and it is possible that other nearby nucleotides also play a role in selectivity. Regardless of mechanism, it is clear that Class B E-box-binding bHLH proteins like scleraxis are not typically promiscuous for example, while we noted that scleraxis strongly transactivated the human collagen Iα2 gene proximal promoter, which contains three E-boxes, the bHLH transcription factor MyoD had no effect on this promoter [173].

The Noda laboratory identified *aggrecan* as the first gene to be directly regulated by scleraxis, and noted that scleraxis was able to transactivate an aggrecan promoter reporter construct even without the addition of exogenous E-proteins E12 or E47 [299]. Deletion studies from our laboratory have shown that removal of the HLH domain, which mediates protein–protein interaction, resulted in an approximately 50% reduction in scleraxis activity [173]. This indicates that heterodimerization augments transactivation by scleraxis, but is not specifically required. This augmentation is likely to be context-specific governed by the individual cell- type involved, the specific E-box sequence and the availability and identity of potential binding partners

[299]. In contrast to the HLH domain, deletion of the basic DNA-binding domain completely attenuated transactivation by scleraxis, demonstrating an absolute requirement for DNA contact [173].

It is unclear whether scleraxis can interact with other proteins besides E12 and E47. However, specific experiments indicate that scleraxis does not appear to interact with the HLH inhibitory protein Id2 [298]. In our experiments, Id2 was able to inhibit scleraxis-mediated transactivation of the collagen Iα2 promoter, thus we hypothesized that Id2 may act by sequestering required scleraxis-binding partners [173]. Similarly, we have generated a mutant form of scleraxis lacking the basic DNA-binding domain and found that this mutant appears to act in a dominant negative fashion – also possibly by sequestration of binding partners. Nonetheless, it remains unclear whether these partners are E-proteins such as E12, or whether other critical partners exist. It is also unclear whether scleraxis is capable of forming homodimers to regulate gene expression. One novel binding partner for scleraxis is cAMP response element binding protein CREB2/ATF4, which represses scleraxis function in Sertoli cells [300].

Although the primary structure of scleraxis reveals a number of potential sites for post-translational modification (e.g. phosphorylation), information is currently lacking as to whether such modifications may impact the transactivation activity, stability, or dimerization capabilities of scleraxis. It is thus difficult to theorize at this time exactly which intracellular signaling pathways may be important in mediating scleraxis function, although several such pathways have been demonstrated to be important. We have shown that scleraxis expression is up-regulated in response to TGF-β signaling, but it is not yet known whether this effect is mediated by the

canonical TGF-β-Smad pathway or some other mechanism [173]. Furthermore, it is unclear whether scleraxis-mediated transactivation of gene promoters is modulated by this pathway independently of its expression level, although a study in ROS17/2.8 osteoblastic osteosarcoma cells suggested that TGF-β stimulated the DNA-binding activity of scleraxis [301]. Scleraxis expression is also up-regulated by cAMP or follicle stimulating hormone in Sertoli cells, although the mechanism is unclear [302]. Smith et al. have reported that scleraxis expression is regulated by ERK1/2 signaling [303]. FGFs also appear to be important regulators of scleraxis expression. The transcription factors Pea3 and Erm, which function downstream of FGF signaling, regulate scleraxis somite expression, and FGF4 was sufficient to increase scleraxis expression in developing avian heart valves downstream of ERK and in chick limb tendons [304-306].

4.2: Gene expression

The human scleraxis gene is currently identified in the NCBI sequence database as two variants *SCXA* and *SCXB*; however, these sequences represent a single gene located on chromosome 8 in the region of 8q24.3. The scleraxis protein itself is highly conserved, with nearly 100% identity between rats and mice, and approximately 90% identity between humans and lower mammals (Fig. 7). This high degree of identity suggests that the biological function of scleraxis may be critical for proper development. Supporting this idea, knockout of scleraxis is associated with a significant decrease in the number of viable pups at birth, with greatly reduced survival at 2 months [307]. Scleraxis gene homologs have been identified in a variety of other organisms, including chicken, frog, cow, horse, and zebra fish. During murine

embryonic development, scleraxis is widely expressed at the time of gastrulation around embryonic day (E) 6.0, but its expression pattern becomes restricted soon thereafter [308]. Its expression can be detected as early as E9.5 in the sclerotome compartment of somites from which the ribs and vertebrae arise [288, 308]. Scleraxis is highly expressed in a number of pre-skeletal mesenchymal cells prior to chondrogenesis, but a decrease in its expression has been noted during ossification. There is abundant expression of scleraxis in progenitor cells destined to form ligaments, tendons, and bronchial cartilage [288]. High levels of this gene have also been noted throughout the pericardium [288]. It has been shown to be expressed during valvulogenesis in the developing *chordae tendinae* proximal to the papillary muscles of the embryonic chick heart as well as in semilunar valve precursor cells [309].

Scleraxis is highly expressed in the syndetome compartment of developing somites, a region that is spatially situated between future muscle- and bone-forming regions, and that is destined to generate tendons [287, 310]. This gene is highly expressed at the interface between muscles and skeletal primordial in E13.5 mouse embryos, but then becomes largely restricted to tendons by E15.5 [311]. One striking aspect of this expression pattern is that scleraxis tends to be expressed in precursors of tissues with significant extracellular matrix (ECM) composition.

Research to date has largely focused on the developmental expression pattern of scleraxis, and its expression in neonatal and adult tissues is only beginning to be explored. One of the barriers to this work has been the lack of an effective scleraxis antibody for use in tissue sections. An RT-PCR analysis of scleraxis expression in

adult tissues showed expression in brain, heart, kidney, lung, muscle, spleen, and testis, but not in liver, prostate, or ovary [302]. Data from our laboratory show that scleraxis is expressed in adult rat cardiac fibroblasts and myofibroblasts as well as in cardiomyocytes, i.e. it is expressed throughout the myocardium [173]. It remains unclear whether the various embryonic tissues that express scleraxis continue to do so in the adult, and whether new regions of scleraxis arise during maturation.

```
Mouse     MSFAMLRSAPPPGRYLYPEVSPLSEDEDRGSESSGSDEKPCRVHAARCGL 50
Rat       MSFAMLRSAPPPGRYLYPEVSPLSEDEDRGSESSGSDEKPCRVHAARCGL 50
Human     MSFATLRPAPP-GRYLYPEVSPLSEDEDRGSDSSGSDEKPCRVHAARCGL 49
          **** **.*** ******************:******************

Mouse     QGARRRAGGRRAAGSGPGPGGRPGREPRQRHTANARERDRTNSVNTAFTA 100
Rat       QGARRRAGGRRAAGSGPGPGGRPGREPRQRHTANARERDRTNSVNTAFTA 100
Human     QGARRRAGGRRAGGGGPG--GRPGREPRQRHTANARERDRTNSVNTAFTA 97
          ************.*.***  ******************************

Mouse     LRTLIPTEPADRKLSKIETLRLASSYISHLGNVLLVGEACGDGQPCHSGP 150
Rat       LRTLIPTEPADRKLSKIETLRLASSYISHLGNVLLVGEACGDGQPCHSGP 150
Human     LRTLIPTEPADRKLSKIETLRLASSYISHLGNVLLAGEACGDGQPCHSGP 147
          ********************************.**************

Mouse     AFFHSGRAGSPLPPPPPPP--PLARDGGENTQPKQICTFCLSNQRKLSKD 198
Rat       AFFHSGRAGSPLPPPPPPPPLPLARDGGENTQPKQICTFCLSNQRKLSKD 200
Human     AFFHAARAGSPPPPPPPPP----ARDG-ENTQPKQICTFCLSNQRKLSKD 192
          ****:.***** *******    **** **********************

Mouse     RDRKTAIRS 207
Rat       RDRKTAIRS 209
Human     RDRKTAIRS 201
          *********
```

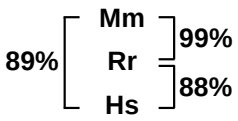

Figure 7: Protein sequence alignment of scleraxis from mouse, rat and human. NCBI protein sequences from mouse (accession NP_942588), rat (accession NP_001123980), and human (accession NP_001008272) were aligned using ClustalW2 (www.ebi.ac.uk). Asterisks denote amino acids conserved across all three species; colons denote conserved substitutions; periods denote semi- conserved substitutions. *Inset:* BLAST sequence alignment identity between mouse (Mm), rat (Rr), and human (Hs) scleraxis protein sequences. Reprinted from Genes and Cardiovascular Function, RA Bagchi and MP Czubryt, Scleraxis: A New Regulator of Extracellular Matrix Formation, 57-65, © 2011, with permission from Springer. http://link.springer.com/chapter/10.1007/978-1-4419-7207-1_6/fulltext.html

4.3: Physiological role

Since scleraxis is expressed in a variety of tissues, its specific physiological role may vary according to tissue type. However, insight into its role may be obtained by identifying genes that are regulated by scleraxis, of which several have been identified to date. Collectively, these data suggest that scleraxis may be a general regulator of ECM formation, although the specific gene targets appear to vary by tissue type. Indeed, in some cases scleraxis appears to have opposing effects on gene expression depending on cell type.

In a number of studies, scleraxis expression has been associated with putative target gene expression, although a direct causal regulatory mechanism has not yet been demonstrated. For example, several lines of evidence suggest that scleraxis may regulate type II collagen production in a variety of cell types. Scleraxis overexpression in ROS17/2.8 cells resulted in increased expression of collagen II and the cartilage marker osteopontin, while at the same time leading to a decrease in expression of osteoblast markers collagen I and alkaline phosphatase [299, 312]. The coordinated up-regulation of scleraxis, collagen IIb, and aggrecan marks the differentiation of embryonic stem cells to a chondrocyte phenotype [313]. Scleraxis expression also correlates with expression of collagen II and tenascin during development of heart valves, and addition of FGF4 to developing avian heart valves resulted in increased expression of both scleraxis and tenascin [305, 309]. It was recently shown that scleraxis and E47 appear to work synergistically with Sox9 to regulate collagen 2α1 gene expression, which is interesting since the expression patterns of scleraxis and Sox9 overlap in early tendon development [311, 314]. The expression of the tendon

differentiation marker, tenomodulin, increases in cultured tendon-generating tenocytes in response to retroviral delivery of scleraxis, but whether scleraxis directly transactivates the tenomodulin gene or affects expression indirectly by acting on differentiation pathways is unknown. Both scleraxis and tenomodulin were concomitantly down- regulated in myostatin-null mice, suggesting they are co-regulated [315].

Scleraxis has also been demonstrated to directly regulate a number of target genes. Aggrecan 1, a major proteoglycan component of cartilage, is directly upregulated by scleraxis in ROS17/2.8 cells, due to interaction of scleraxis with the aggrecan 1 promoter [299, 316]. In Sertoli cells, scleraxis has been shown to upregulate the expression of transferrin and androgen-binding protein, which may contribute to regulation of Sertoli cell function [302].

Recently, evidence from our laboratory and others has demonstrated that scleraxis directly regulates expression of type I collagen. Both scleraxis and collagen I genes were concomitantly expressed in pluripotent tendon-derived cell lines [317]. Type I collagen comprises two subunits, each expressed from its own gene – collagen Iα1 and Iα2. Scleraxis appears to directly regulate expression of both of these genes. Rossert's group recently demonstrated that the collagen Iα1 gene is directly regulated by scleraxis via a short promoter element that was required for expression in rat tendon fibroblasts, in conjunction with NFATc [318]. Our laboratory has reported that scleraxis is expressed by fibroblasts and myofibroblasts, the primary collagen synthesizing cells of the heart, and that scleraxis expression increases more than four-fold during the phenoconversion of fibroblasts to myofibroblasts [173]. We found that

scleraxis directly transactivates the human collagen Iα2 gene promoter in both NIH 3T3 fibroblasts and primary rat cardiac fibroblasts. We also noted that cardiac fibroblast expression of scleraxis itself was strongly up-regulated by TGF-β, a potent pro-fibrotic factor implicated in fibrosis of multiple tissues including the heart, which was previously shown to up-regulate scleraxis expression in ROS17/2.8 cells [301]. It thus appears that a major role for scleraxis is as a master regulator of collagen synthesis. Experiments to examine how scleraxis interacts with the canonical collagen synthetic pathways, including Smad transcription factors, are under way in our laboratory. While there is this clear evidence that scleraxis regulates type I collagen gene expression, the finding that scleraxis over-expression in ROS17/2.8 cells leads to a down-regulation of type I collagen expression indicates that cell context is critical [299].

Additional insight into the role of scleraxis has come from mouse knockout studies. The initial study reporting the generation of scleraxis knockout animals suggested that it was essential for early embryonic development, since embryos homozygous for a targeted scleraxis knockout allele suffered mortality in the early stages of embryogenesis [308]. Recently however, Schweitzer's group produced a novel line of scleraxis-null animals, and found that the initial attempt had generated a hypomorph of an overlapping gene due to a neomycin-resistance selection cassette inserted into the scleraxis locus during generation of the mice. The scleraxis gene is located in the third intron of *Bop1*, a housekeeping gene essential for biogenesis of ribosomes; thus the presence of a Neo minigene may alter Bop1 splicing [319]. Schweitzer's laboratory performed elegant conditional recombination experiments in

which they selectively excised the scleraxis coding region using a Cre/loxp approach, and excised the Neo cassette with flp/frt [320]. Leaving the Neo cassette intact resulted in embryonic lethality similar to the previous knockout line but excision of the selection marker permitted the production of full-term pups.

Scleraxis knockout mice, though viable, had significant defects in load-bearing tendon formation [320]. These animals exhibited a dramatic disruption of tendon differentiation that was manifested in dorsal flexure of the forelimb paw, limited use of all paws, reduced functionality of the back muscles, and complete loss of ability to move the tail. Tendon defects were first noticed close to E13.5 in all tendons. Based on the phenotype observed in the scleraxis-null mice, it appears that scleraxis function is related to the incorporation of tendon progenitors into discrete tendons [320]. This is an important finding since there is little information on the molecular mechanisms that enable tenocytes to coordinate the secretion and organization of matrix structures during tendon genesis [321]. Scleraxis-null mice also showed alterations in their ability to produce tendon matrix, manifested in a dramatic decrease in the number of collagen fibers and their organization within the tendon matrix [320]. Significantly, there was a reduction or loss of collagen I expression in affected tendons, suggesting that scleraxis is required for normal collagen gene expression in agreement with our data in primary cardiac fibroblasts. However, since not all tendons were affected, and since type I collagen expression was relatively normal in some tissues, it is clear that scleraxis is not absolutely required for all such synthesis, and again suggests that cell context is likely to be critical. This study by Schweitzer's group presented the first demonstration of a tendon differentiation phenotype and provided significant insight

into the role of scleraxis. Mice in which the myostatin gene has been knocked out appear with a milder phenotype of scleraxis-null mice: tendons are smaller and have reduced fibroblast density [315]. Furthermore, myostatin-null mice have reductions in tendon expression of type I collagen, scleraxis, and tenomodulin.

Recent work has also highlighted a potential role for scleraxis in periodontal ligament formation. Scleraxis is expressed in human periodontal ligament cells (hPDLC) and gingival fibroblasts (hGF), with highest expression in hPDLC and lowest in hGF [322, 323]. Indeed, scleraxis is frequently used as a marker for periodontal ligament cells or cell lines committed to a PDL fate [324-326]. Notably, there was a decrease in hPDLC scleraxis expression with increasing passage number in culture [322]. Another study investigated the role of scleraxis in modulating the effect of high glucose concentration on differentiation of hPDLC [327]. Scleraxis expression was upregulated in hPDLC cultured in high glucose medium *in vitro*, concomitant with inhibition of osteogenetic differentiation in these cells [327]. These studies suggest that scleraxis expression persists in PDL cells, but is lost if these cells undergo osteogenetic differentiation. However, in contrast to these results it was recently reported that scleraxis expression in a PDL-derived cell line did not decrease with passage number, and appeared to only diminish minimally with osteogenetic induction [328]. The expression of tenomodulin decreased with passaging or osteogenesis induction, even though scleraxis did not appear to change. This is surprising, since an earlier study had identified scleraxis as a regulator of tenomodulin expression [312]. It should be noted, however, that most of these studies were performed in immortalized cultured cell lines derived from PDLs; thus the specific

conditions employed may alter cell phenotype and make broad conclusions difficult. Further research into the potential role of scleraxis in inhibiting PDL differentiation is warranted.

4.4: Pathological role

With such limited information to date on the normal roles and mechanism of function of scleraxis, it is perhaps not surprising that little is known about its role in disease and pathological processes. A number of diseases of connective tissue have been described, such as various classifications of Ehlers–Danlos syndrome in which various connective tissue components (particularly fibrillar collagens such as type III, V, and I) are mutated or otherwise incorrectly synthesized [329]. However, the possibility that scleraxis functionally affects initiation or progression of these diseases is completely unexplored to date. It was also previously reported that scleraxis expression is down-regulated in the brains of Down syndrome and Alzheimer disease patients, but this study reported only correlative data [330]. Nonetheless, potential roles for scleraxis in several pathologies are starting to be identified.

A recent study found concomitant increases in scleraxis and collagen Iα1 expression over several weeks in a mouse model of pathological patellar tendon injury [331]. Since scleraxis is expressed at much higher levels in cell cultures derived from patellar compared to Achilles tendons, it is possible that scleraxis plays a role specifically in the healing process of patellar tendons [332]. The possibility that scleraxis plays distinct roles in only a subset of tendons is further supported by the finding that scleraxis knockout largely affected only force-transmitting or inter-muscular tendons [320].

The primary collagen constituent of the heart is type I fibrillar collagen, and this collagen is significantly up-regulated in cardiac fibrosis and in the formation of scar tissue following myocardial infarction [333]. We found a significant increase in scleraxis expression in the region of the infarct scar 4 weeks after surgically induced infarction in parallel with up-regulation of collagen Iα2 gene expression [173]. In contrast, these increases were not observed in distal non-infarcted myocardium or in sham-operated animals. We previously generated an acute heart failure model in transgenic mice by specifically expressing a constitutively active HDAC5 mutant in the heart [334]. Microarray analysis of these animals revealed a significant up-regulation of scleraxis expression several days prior to up-regulation of fibrillar collagens. Our data suggest that scleraxis may play a causal role in the induction of cardiac fibrosis. At this time, however, it is unclear whether scleraxis regulates type I collagen expression under basal conditions, in pathological conditions (e.g. post-infarct or during hypertension), or both.

Keloids are dermal thickenings or scars characterized by rampant over-expression of fibrillar type I or III collagen. Intriguingly, scleraxis expression is strongly induced in fibroblasts isolated from samples of dermal keloids [335]. In contrast, scleraxis is not expressed in normal dermal fibroblasts. Since our data indicate that scleraxis is sufficient to drive collagen Iα2 expression, it is intriguing to speculate that aberrant expression of scleraxis in dermal fibroblasts may contribute to the pathology of keloids. Since keloids represent a form of fibrosis, this finding in conjunction with our cardiac data suggests that scleraxis may be involved in the general induction of fibrosis, regardless of tissue type. If scleraxis is in fact a central

player in multiple forms of fibrosis, then it may represent a convenient target for the development of novel anti-fibrotic therapies. The need for such therapies is significant, since pharmaceuticals specifically directed at reducing fibrosis are currently lacking [333].

The regulation of ECM formation plays a key role in mediating the function of many tissues. The association of scleraxis expression with that of a number of ECM genes suggests that it plays a central role in ECM synthesis, and thereby impacts ECM function through direct or indirect regulation of target genes. A clear role for scleraxis regulation of tendon development, structure, and function has been shown with the creation of scleraxis-null mice [320]. Data from our laboratory and others showing that scleraxis regulates type I collagen gene expression, that it is expressed in cardiac fibroblasts, and that its expression is associated with post-infarct cardiac remodeling indicate that scleraxis has other critical functions that are only beginning to be explored [173, 318]. Scleraxis may thus represent a candidate target for treatment of fibrosis in the heart and other tissues, but more work remains to be done before the promise of anti-fibrotic treatments based on interference with scleraxis function can be exploited.

CHAPTER II: HYPOTHESIS & SPECIFIC OBJECTIVES

Our laboratory has demonstrated that the transcription factor scleraxis is sufficient to regulate gene expression of collagen Iα2 (*ColIα2*) [173], a component of the primary collagen (type I) expressed in the heart. Increased collagen synthesis and deposition is the hallmark of cardiac fibrosis [336]. It is not known if scleraxis function is required for basal or pathological collagen gene expression and whether it interacts with other known transcriptional regulators of fibrosis such as Smads.

HYPOTHESIS:

Scleraxis is required for cardiac extracellular matrix synthesis and potentiates cardiac fibrosis.

SPECIFIC OBJECTIVES:

Objective 1: To determine whether scleraxis and Smads cooperatively regulate the human collagen Iα2 gene.

Objective 2: To determine the role of scleraxis in regulation of cardiac fibroblast ECM gene expression and phenotype modulation.

Objective 3: To assay expression of cardiac ECM genes in wild-type and Scx-null mice under basal conditions.

Objective 4: To compare the expression of fibrillar collagens and ECM genes in wild type and scleraxis conditional null mice in which cardiac fibrosis has been induced by aortic banding.

CHAPTER III: MATERIALS & METHODS

Reagents

Product	Source
Acrylamide (37.5:1)	Fisher Scientific
Bouin's solution	Sigma
ChIP Kit	Millipore
Collagenase type II	Worthington Biochemicals
Coomassie protein assay kit	Pierce Technologies
DAPI	Life Technologies
DME/F12	Hyclone
DMEM High Glucose	Hyclone
DNaseI	Roche
Dual Luciferase Assay Kit	Promega
ECL Chemiluminiscence kit	Santa Cruz Biotechnology
FBS	Gibco/Hyclone
Hematoxylin	Vector Laboratories
HEPES	Life Technologies
Herring sperm DNA	Promega
L-Ascorbic Acid	Sigma
Liberase Blendzyme TH	Roche
OCT	VWR
Paraformaldehyde	Alfa Aesar
Penicillin/Streptomycin	Hyclone
Picrosirius red	Sigma
Ponceau S	Sigma
Prolong Gold/Diamond antifade agent	Life Technologies

Protease inhibitor cocktail	Roche/ Thermo Scientific
qScript One-Step SYBR Green qRT-PCR Kit for iQ	Quanta Biosciences Inc.
QuikChange II Site-Directed Mutagenesis kit	Agilent Technologies (previously Stratagene)
SMEM	Life Technologies
Sodium Chloride	Fisher Scientific
Sodium dodecyl sulphate (SDS)	Fisher Scientific
TEMED	Fisher Scientific
Trichrome Kit	Sigma
Tris-OH	Fisher Scientific/VWR Canada
Triton X100	Fisher Scientific
TrypLE Express	Life Technologies
Tween20	Fisher Scientific
Zymogram gels	Life Technologies

Antibodies

Protein target	Source
CD31 (PE/Cy7)	BD Biosciences
Collagen type I	Cedarlane
Collagen type III	Developmental Studies Hybridoma Bank, Iowa
Collagen type IV	Developmental Studies Hybridoma Bank, Iowa
DDR2	Sigma
FITC-αSMA	Abcam
GAPDH	Sigma
Scleraxis	QED Biosciences (custom)
Smad3 (ChIP grade)	Abcam
αMHC	Abcam
αSMA	Sigma
α-Tubulin	Developmental Studies Hybridoma Bank, Iowa

Methods for Scleraxis-Smad interaction study[6]

1: Cell culture

NIH-3T3 mouse embryonic fibroblasts were cultured in DMEM supplemented with 10% FBS, 1% penicillin/streptomycin and 1% L-glutamine, and were seeded 24 h prior to transfection in 6-well culture plates to reach ~ 70% confluence. Adult human cardiac fibroblasts were obtained commercially (Cell Applications Inc., USA). Primary cardiac fibroblasts were isolated from adult rats by Langendorff perfusion of 0.1% collagenase type II (Worthington Biochemicals, USA). Cells were collected after gentle centrifugation as previously described [337] and maintained in DMEM-F12 supplemented with 10% FBS, 1% penicillin/streptomycin and 1 mM L-ascorbic acid. Preparations of fibroblasts obtained through this method are typically ≥ 95% as confirmed by cell-specific marker analysis [338]. Animals were cared for in accordance with the guidelines of the Canadian Council on Animal Care and the University of Manitoba Animal Protocol Management and Review Committee.

2: Chromatin immunoprecipitation assay (ChIP)

Adult human cardiac fibroblasts (~8×10^6 cells) were grown in 100 mm dishes and fixed by addition of 280 µl 37% formaldehyde to 10 ml of culture media for 10 min at 37 °C. The cells were then washed with ice-cold PBS and harvested in SDS lysis buffer. Cell lysates were sonicated to shear DNA to 200–500 bp fragments. A 1% aliquot of this cell lysate was used as an input control. Samples were pre-cleared with

[6] Reprinted from RA Bagchi and MP Czubryt, Synergistic roles of scleraxis and Smads in the regulation of collagen 1α2 gene expression, *Biochimica et Biophysica Acta-Molecular Cell Research*, 1823:1936–1944, © 2012, with permission from ELSEVIER INC. http://www.sciencedirect.com/science/article/pii/S016748891200198X

75 µl bovine serum albumin (0.5 mg/ml)/herring sperm DNA (200 µg/ml)/protein A-agarose mixture for 1 hour with rotation at 4 °C to reduce non-specific background. Lysates with soluble chromatin collected after brief centrifugation were incubated at 4°C overnight with 10 µg anti-scleraxis antibody or 10 µg pre-immune serum as a negative control. The production of this antibody by our laboratory was previously described [9]. The DNA-protein immune complexes were precipitated, washed, eluted and subsequently reverse cross-linked, then purified by phenol/chloroform extraction. DNA samples were subjected to PCR amplification using primers specific to the scleraxis-binding E box sequences (Table 7) in the human COL1A2 gene proximal promoter. Primers encompassing a region of the human GAPDH promoter were used as a negative control (Table 7; Upstate Cell Signaling Solutions EZ ChIP kit).

3: Luciferase reporter assays

NIH-3T3 fibroblasts were seeded in 6-well dishes 24 h prior to transfection to reach ~80% confluency. Samples were co-transfected (Lipofectamine 2000; Invitrogen, USA) with 500 ng reporter plasmid (COL1A2 full-length 3.7 kb or 0.7 kb proximal promoters, or empty pGL3 Basic as a control) plus 500 ng expression vectors as needed (pECE-HA-FLAG-Scx, pECE-ScxΔBD, pCMV tag3C-Myc-Smad3, pCMV tag3C-Myc-Smad2, pcDNA3.1(+)-FLAG-Smad7). Mutation of the E boxes and SBE within the COL1A2 0.7 kb promoter was performed using a QuikChange II Site-Directed Mutagenesis kit (Stratagene) and nested PCR using primers listed in Table 4. Renilla luciferase expression vector (pRL) was used as a transfection control. The luciferase activity of each sample was assayed using the Dual Luciferase Reporter

Assay System (Promega, USA) on a TD20/20 luminometer (Turner BioSystems, USA).

4: Treatment of cells

NIH-3T3 fibroblasts were grown to ~70% confluency, then co-transfected with COL1A2 0.7 kb reporter plasmid and pECE-HA-FLAG-Scx expression vector for luciferase assays, or with pECE-HA-FLAG-Scx or pECE-ScxΔBD expression vectors alone for mRNA analysis. Cells were treated with 10 ng/ml TGF-β_1 or vehicle for 24 h post-transfection where required. Cell lysates were collected for luciferase assay or qRT-PCR. Primary rat cardiac myofibroblasts (passage 2) were grown in 6-well tissue culture dishes to ~70% confluence in complete medium followed by equilibration for 24 h in serum-free medium. Cells were infected with adenoviruses encoding LacZ (AdLacZ), FLAGSmad3 (AdSmad3), FLAG-Smad7 (AdSmad7), FLAG-scleraxis, FLAG-ScxΔBD or LacZ (control) for 24 h. Serum-free medium was replaced and cells were then treated with 10 ng/ml TGF-β_1 or vehicle as required, and were harvested for protein or RNA 24 h later. Total protein and total RNA was used for western blotting and qPCR analysis respectively. The scleraxis adenovirus was described previously [173]. To generate the ScxΔBD adenovirus, we used PCR to amplify and sub-clone the ScxΔBD coding region into pSHUTTLE-CMV transfer vector from the AdEasy Vector System (Qbiogene, Canada). The shuttle vector was then cloned into BJ5183 bacterial cells to generate replication-deficient adenoviruses.

5: Quantitative real-time-PCR (qRT-PCR)

Total RNA was isolated from cells using commercial kits (Sigma, USA) according to manufacturer's instructions. 25 ng RNA was used for each of the

reactions performed using the qScript One-Step SYBR Green qRT-PCR Kit for iQ (Quanta Biosciences, USA) on an iQ5 multicolor real-time PCR thermocycler (Bio-Rad, USA). mRNA abundance was calculated using the $2^{-\Delta\Delta CT}$ method and was normalized to GAPDH. Specific primers used to amplify sequences of interest are listed in Table 3.

6: Western blotting

Total cell protein was isolated using RIPA buffer (50 mMTris pH 7.4, 150 mM NaCl, 1 mM EDTA, 1 mM EGTA, 0.5% Na-deoxycholate, 1% Triton-X 100 and 0.1% SDS) containing complete mini protease inhibitor cocktail (Roche, Canada). Proteins were separated by SDS-PAGE and then transferred to PVDF membranes (Pall, USA). Primary antibodies used for western blotting were rabbit anti-scleraxis antibody [173], mouse anti-α-tubulin antibody (DSHB, USA) or rabbit anti-collagen type I antibody (Cedarlane, Canada). Antibodies were detected using Western Blotting Luminol Reagent (Santa Cruz Biotechnology, USA) and CL-Xposure blue X-ray film (Thermo Scientific, Canada). Quantity One software (Bio-Rad, USA) was used to measure relative band intensity. The intensity of the scleraxis bands was normalized to those of α-tubulin to control for loading.

7: Electrophoretic mobility shift assay (EMSA)

COS7 cells were transfected with 1 μg scleraxis expression vector, and 48 h later nuclear proteins were isolated using NE-PER nuclear and cytoplasmic extraction reagents (Pierce Biotechnology, USA). 5 μl nuclear extract was used in binding reactions as required. Assays were performed using a Lightshift Chemiluminescent EMSA kit (Pierce Biotechnology, USA) as per manufacturer's instructions. Binding

reactions were incubated at room temperature for 30 min in buffer containing 10 mM Tris pH 7.5, 100 mM KCl, 0.5 mM EDTA, 5% glycerol, 50 ng poly (dI-dC), 5 μg bovine serum albumin and 20 fmol biotin endlabeled probe. For competition experiments, a 250-fold molar excess (5 pmol) of unlabeled probe was included in the binding reactions and incubated for 15 min before addition of the labeled probes. For supershift reactions, 1 μg anti-scleraxis antibody was incubated overnight at 4 °C prior to addition of the biotin-labeled probes to the reaction [173]. DNA-protein complexes were then fractionated on a non-denaturing 6% native polyacrylamide gel at 100 V for 1 h. Chemiluminescent complexes were detected using CL-XPosure clear blue film (Thermo Scientific, Canada).

8: Statistical analysis

Statistical significance of data was determined using Student t-test or one-way analysis of variance (ANOVA) with Student-Newman–Keuls post-hoc analysis. Results with $p<0.05$ were considered statistically significant.

Methods for Scleraxis regulation of cardiac ECM gene expression, fibroblast phenotype and cardiac fibrosis studies

1: Animal studies

The generation of scleraxis null mice has been described previously [320]. Mice were on a C57BL/6 background, and wild type littermates were used as controls. The Schweitzer lab developed the original null mice as a floxed line [320]. These mice were bred to $TCF21^{iCre}$ [339] or B6.Cg-Tg(CAG-cre/Esr1*)5Amc/J [340] mice to generate $Scx^{flox/flox}$-$TCF21^{iCre}$ and $Scx^{flox/flox}$-panCre lines respectively (Appendix 3). Genotype of all transgenic mice were confirmed by PCR using specific primers. Animals were provided with food and water ad libitum and maintained on a 12/12 day/night cycle. Thoracic aortic constriction/ banding (TAC/TAB) model of pressure overload is a well-established physiologically relevant model for studying cardiac disease. In brief, the mice were anesthetized, thoracic cavity was opened by snipping the first two ribs, exposing the transverse aorta, and a 7-0 silk suture was placed using a 27 gauge guide, followed by wound closure and recovery. The use of the 27 gauge guide ensures that a similar degree of overload is induced in each animal, and results in compensated hypertrophy and fibrosis [341]. $Scx^{flox/flox}$-$TCF21^{iCre}$ or $Scx^{flox/flox}$-panCre animals were gavaged with corn oil (vehicle; Sigma Aldrich) or tamoxifen (0.2 mg/g body weight; Sigma Aldrich [187]) (Fig. 8). These mice along with WT mice were subjected to the TAC procedure. Heart and body weights, and tibia lengths were recorded at the time of tissue harvest four weeks post-surgery. WT sham-operated animals were used as controls. For analyses of gene expression in all hearts, ventricular myocardium was dissected clear of the atria and valves. All animals were

cared for as prescribed by the guidelines of the Canadian Council on Animal Care and the University of Manitoba Animal Care Committee.

2: Murine echocardiography

Non-invasive murine transthoracic echocardiography was performed on 6 week old, non-sedated animals using a GE Vivid 7 machine equipped with a 13 MHz linear probe [342, 343]. Cardiac dimensions and function were evaluated using 2D and M mode data collected in long and short parasternal axis views, as well as tissue Doppler Imaging. Data collection and analysis was performed separately by observers blinded to the genotype of the animals.

3: Ventricular ECM mass determination

Cardiac ventricles from WT or scleraxis KO animals were removed and fragmented. Tissue fragments were processed for decellularization using a conventional cell maceration technique with modifications [344, 345]. Briefly, tissues were fixed in 10% neutral buffered formalin. After 4-5 thorough rinses in distilled water, the tissue fragments were immersed in a 10% sodium hydroxide solution for 4-5 days to remove the cellular elements. The decellularized tissue was rinsed with water until it became transparent, then dehydrated in 100% methanol followed by freeze drying to yield dry ECM, and the dry mass recorded.

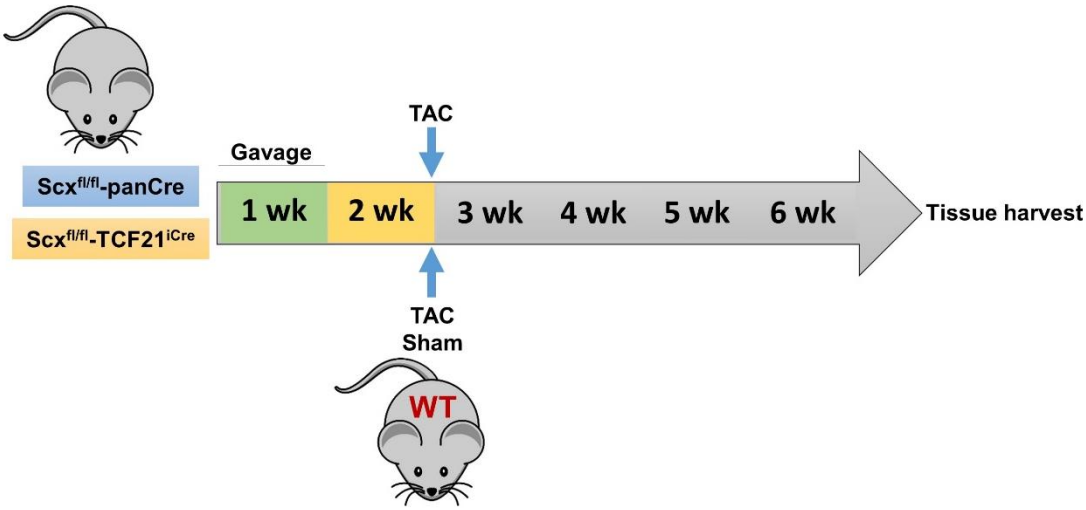

Figure 8: Experimental regimen of induction of pressure overload in scleraxis conditional knockout mice.

$Scx^{fl/fl}$/Cre mice were gavaged with corn oil or tamoxifen once a day for 5 days. TAC surgeries were performed a week after the last day of gavage. WT mice also underwent the procedure or were treated as sham controls. Tissues were harvested for analysis 4 weeks post-TAC.

4: Cell culture and treatments

Primary cardiac fibroblasts were isolated from adult male Sprague-Dawley rats and were maintained in DME/F12 media as mentioned previously. Cells were then passaged once to P1 (passage 1) proto-myofibroblasts 48h after isolation (Fig. 9), and plated appropriately for downstream assays [173]. Equilibration of cells for 24 h in serum-free medium was carried out prior to all treatments. For over-expression studies, cells were infected with adenoviruses encoding LacZ (AdLacZ), GFP (AdGFP) or Scleraxis (AdScx) for 24 h [172, 173]. For experiments requiring treatment of cells with TGF-β_1, media was replenished and cells treated for an additional 24 h with recombinant TGF-β_1 or vehicle (control). Cell treatments with Ang II (1 μM) or CTGF (100ng/mL) were also performed for 24h. The ScxΔΔ mutant was generated using nested PCR based on our previous mutant [173]. Primary rat cardiac proto-myofibroblasts ($5x10^5$ cells) were transfected by electroporation (BioRad Gene Pulser II) at 220V and 500 μF in 0.5 mL serum-supplemented DME/F12 media with 2 μg pECE (control) or ScxΔΔ. Total RNA was isolated from these cells 24 hours post-transfection and analyzed for target gene expression. For some studies, cardiac fibroblasts were isolated from 6 week old WT and scleraxis KO mice using Liberase TH Research Grade (Roche) [73]. Cells from the first passage were used for adenovirus-mediated gene rescue experiments.

5: Generation of shRNA- encoding adenovirus

The BLOCK-iT RNAi Advisor program (Life Technologies) was used to design shRNA sequences for rat scleraxis gene knockdown. The two pairs of oligonucleotides were annealed and cloned into the pENTR/U6 RNAi Entry Vector

following the manufacturer's instructions (Life Technologies), then subcloned into pAd/BLOCK-iT-DEST vector to generate pAd-shScleraxis. The vectors were finally packaged to produce Ad-shScleraxis adenovirus (AdshScx) in 293A cells. Viral titer was determined using a commercial kit (Adeno-X Rapid Titer Kit) following manufacturer's instructions (Clontech Laboratories, Inc.). P1 rat cardiac proto-myofibroblasts were infected at various multiplicities of infection (MOI; 50, 100, 200) for 48h to determine optimal MOI for further experiments (Appendix 1). All experiments were carried out using MOI 200 for 72h. Infection control groups received adenovirus encoding shLacZ (AdshLacZ) [346]. The following oligonucleotides were used for scleraxis knockdown: 5'- CACCGCCTCAGCA ACCAGAGAAAGTCGAAACTTTCTCTGGTTGCTGAGGC-3' (forward) and 5'- AAGCCTCAGCAACCAGAGAAAGTTTCGACTTTCTCTGGTTGCTGAGGC-3' (reverse).

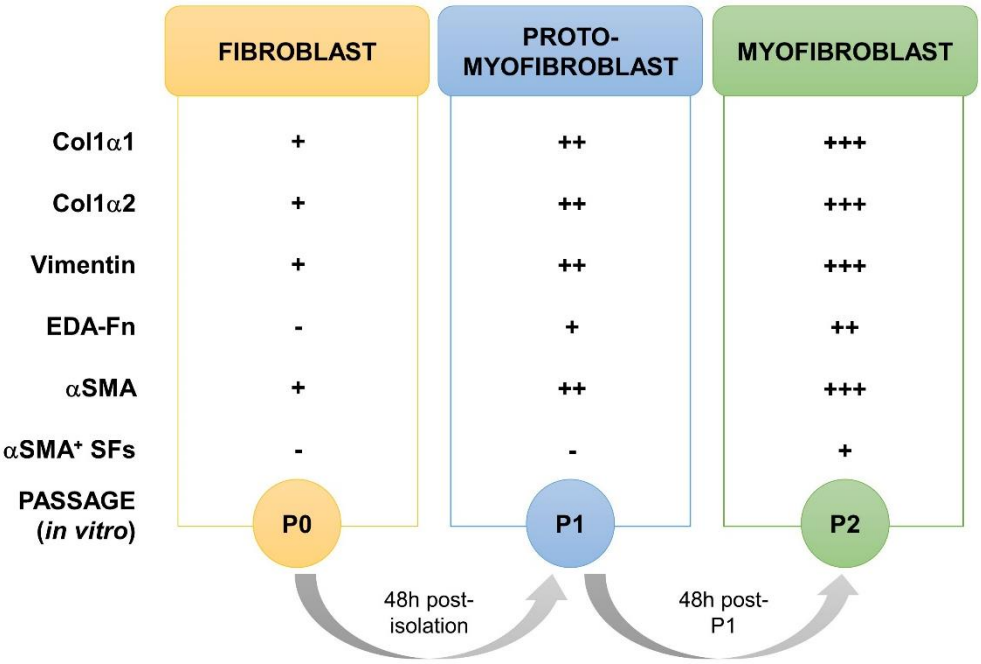

Figure 9: Cell culture workflow of primary cardiac fibroblasts.

Freshly isolated cardiac fibroblasts (P0) were passaged once after 48h of incubation in serum-supplemented (10% FBS) media in culture dishes, and referred to as P1 proto-myofibroblasts. When these P1 cells were passaged once again and plated for experiments- these were labeled as P2 myofibroblasts. This workflow was maintained for all experiments using primary cultured cells throughout the study.

6: Cell viability assay

Primary adult rat cardiac fibroblasts were grown in Permanox plastic chamber slides (Thermo Scientific Nunc) in DME/F12 medium (Hyclone) supplemented with 0.5% FBS and 500µM ascorbic acid. Cells were infected with AdshLacZ (control) or AdshScx adenovirus at MOI 200 for 48 hours. Cell viability was assayed using the Live/Dead viability/cytotoxicity kit as per manufacturer's instructions (Life Technologies Inc.). Vital dyes calcein acetoxymethylester (calcein-AM) and ethidium homodimer-1 were used to visualize live (green) and dead (red) cells respectively using a Zeiss Axiovision epifluorescence microscope. Data was recorded as percent cell death compared to control from three independent experiments (minimum total cell count of 400). 200 µmol/L H_2O_2-treated cells were used as dead cell control.

7: Quantitative real-time PCR (qPCR)

Total RNA was collected from isolated cells using a commercial kit as per manufacturer's directions (Thermo Scientific). Cardiac tissue RNA was isolated using TRIzol reagent (Ambion, Life Technologies) as per manufacturer's instructions. Equal amounts of RNA (25 ng for cells, 50 ng for tissue) were assayed using an iQ5 multicolor real-time PCR thermocycler (Bio-Rad) using the qScript One-Step SYBR Green qRT-PCR kit for iQ (Quanta Biosciences). Amplicon abundance was quantified using the $2^{-\Delta\Delta CT}$ method, and normalized to GAPDH. Primers used for these reactions have been used previously or are listed in Table 3 [172, 173].

8: Immunoblotting

Total protein was isolated from cells using radioimmunoprecipitation assay buffer (RIPA) comprised of 50 mmol/L Tris pH 7.4, 150 mmol/L NaCl, 1 mmol/L

EDTA, 1 mmol/L EGTA, 0.5% Na-deoxycholate, 1% Triton-X 100 and 0.1% sodium dodecyl sulfate (SDS). Protease inhibitor cocktail (Thermo Scientific), 1 mmol/L DTT and 1 mmol/L PMSF were added to the RIPA buffer prior to use. Mouse tissue lysates were prepared by homogenizing cardiac tissue in protein extraction reagent type 4 (Sigma-Aldrich). Proteins were separated under reducing conditions using SDS polyacrylamide gel electrophoresis and transferred onto polyvinylidene difluoride membranes (Pall Corporation). Blots were probed with specific primary antibodies for scleraxis [172, 173]; collagen type I (Cedarlane); collagen type III, type IV or α-tubulin (Developmental Studies Hybridoma Bank, University of Iowa); GAPDH, DDR2 or αSMA (Sigma-Aldrich); β-actin (Cell Signaling). Blots were then incubated with appropriate HRP-conjugated mouse or rabbit secondary antibodies. Protein bands were visualized using Western Blotting Luminol Reagent (SantaCruz Biotechnology) on CL-Xposure blue X-ray film (Thermo Scientific). Band intensities were quantified using Quantity One (Bio-Rad) or ImageJ (NIH) applications. Target band intensity was normalized to GAPDH, β-actin or α-tubulin.

9: Gelatin zymography

Serum-free conditioned cell culture medium from P1 proto-myofibroblasts was collected at 24h or 48h post-infection with AdGFP or AdScx and concentrated using centrifugal filter devices (Millipore). Cardiac tissue extracts from WT and KO mice were prepared using lysis buffer (25 mmol/L Tris-HCl pH 7.5, 100 mmol/L NaCl, 1% NP-40) supplemented with protease inhibitors [347]. 20 µg concentrated proteins (culture media or tissue lysate) was electrophoresed under denaturing conditions using commercial pre-cast 10% acrylamide gels containing 0.1% gelatin (Novex, Life

Technologies). Gels were then renatured in 2.5% Triton-X100 for 30 min at room temperature followed by incubation in developing buffer (50 mmol/L Tris base, 40 mmol/L HCl, 200 mmol/L NaCl, 5 mmol/L $CaCl_2$ and 0.02% Brij 35) at 37ºC for 16 h in a closed tray. Gelatinolytic activity was then visualized by staining with Coomassie Brilliant blue R250 dye (0.5% in 5% methanol and 10% acetic acid) followed by destaining (10% methanol, 5% acetic acid) to reveal clear bands over the blue background of the dye. Gels were dried and scanned on a densitometer, and band intensities were quantified using Image J software (NIH) [348].

10: Flow cytometry

Whole hearts below the atria were isolated from WT and scleraxis KO mice and were immediately flushed with ice-cold HBSS. The method described by Banerjee et al. was used with modifications [349]. Briefly, hearts were immersed in HBSS supplemented with 1 mg/ml bovine serum albumin (BSA), minced and repeatedly passed through a 19-gauge needle, then incubated for 5 min with shaking at 100 rpm at 37ºC. The supernatant was collected, and the rest of the tissue was subjected to enzymatic digestion using 140 U/ml collagenase supplemented with 10 mg/ml BSA. This process was repeated six times at 37ºC. The supernatant was pooled from all steps and centrifuged at 1000xg for 5 m at 4ºC. The supernatant was discarded and cells resuspended in Gey's solution for 5 min on ice to lyse red blood cells. After centrifugation cells were resuspended in 1 ml staining buffer (phosphate-buffered saline with 1% FBS). Cells were then counted and resuspended at 0.5 million cells/100 µL for flow cytometry analysis. Cells were processed using the BD Cytofix/ Cytoperm kit (BD Bioscience Pharmingen) per manufacturer's instructions. Single cell

suspensions from both WT and KO groups (n=3) were stained with FITC-conjugated-αSMA (Abcam), R-PE-conjugated-DDR2, APC/Cy7- conjugated αMHC or PE/Cy7-conjugated-CD31 (BD Biosciences) antibodies. Fluorochrome conjugation for DDR2 and αMHC was performed using EasyLink Kits (Abcam). Acquisition of cell samples was performed on a FACSCantoII cytometer using FACSDiva software (Becton Dickinson). Data were analyzed with FlowJo software (Treestar).

11: Cardiac tissue histology

Cardiac tissues from KO mice or WT littermates were formaldehyde-fixed, embedded in OCT or paraffin and processed for assessment of histological features. Five-µm sections were subjected to Masson's trichrome staining using commercial reagents (Sigma-Aldrich). Briefly, tissue sections were mordant in pre-heated Bouin's solution (Sigma-Aldrich) for 15 min at 56^{o}C, then rinsed with tap water to remove excess reagent. Sections were stained with Weigert's Hematoxylin solution (Sigma-Aldrich), rinsed sequentially in tap and deionized water, and then stained with the trichrome kit. Slides were treated with 1% acetic acid, dehydrated through alcohol, cleared in xylene and mounted using Permount (Fisher Scientific). For discrete visualization of collagen deposits in the myocardium, tissue sections were stained with picrosirius red (PSR). Slides were incubated in Bouin's solution as above, followed by staining in picrosirius red (0.1%) for 60 min at room temperature. Sections were then washed with 1% acetic acid twice, dehydrated, cleared and mounted using Permount. Both trichrome and PSR- stained sections were examined using a Zeiss Axioskop 2 mot plus microscope equipped with an AxioCam digital camera and AxioVision 4.6 software (Zeiss). For enhanced visualization of blue staining in Masson's trichrome

sections, images were processed with Adobe Photoshop CS6 to remove the red color channel, followed by selection and extraction of the blue channel.

12: Luciferase gene reporter assay

NIH-3T3 cells were plated in 6-well dishes and transfected at ~70% confluence. After equilibration in Opti-MEM (Gibco Life Technologies) for thirty minutes, cells were co-transfected (Lipofectamine 2000; Life Technologies) with one of the following luciferase reporter vectors: rat pGL3-αSMA [350] (courtesy Dr. Sem H. Phan, University of Michigan), human pGL2-MMP2 [351] (courtesy Dr. Etty Benveniste, University of Alabama) or human pGL3-Vimentin [352, 353] (courtesy Dr. Christine Gilles, University of Liege), and pECE (control) or Scleraxis expression vectors [172, 173] for 24 hours. Renilla luciferase expression vector (pRL) was used for normalization of luciferase reporter activity. Luciferase activity in the samples was analyzed using the Dual Luciferase Reporter Assay System (Promega) on a Glomax-Multi+ Multimode Plate Reader (Promega) equipped with Instinct software. Point mutations were introduced in the E Box sequences of the 0.7kb αSMA promoter construct using site-directed mutagenesis (Agilent Technologies) (Table 4) and verified by sequencing. A scleraxis double deletion mutant (ScxΔΔ) was generated using nested PCR (Table 5).

13: Electrophoretic mobility shift assay (EMSA)

Gel mobility shift assays were performed as described previously [172]. Biotin-labeled oligonucleotides and cold probes (Table 6) were synthesized commercially (Integrated DNA Technologies). The assays were performed using a

Lightshift Chemiluminescent EMSA kit (Pierce Biotechnology, USA) according to manufacturer's instructions.

14: Chromatin immunoprecipitation assay (ChIP)

Assays were performed as described previously [172]. Solubilized chromatin from adult rat cardiac fibroblasts and myofibroblasts was incubated overnight at 4^{o}C with 10 μg anti-scleraxis antibody or pre-immune serum (PIS). Protein-DNA complexes were isolated from scleraxis WT and KO cardiac tissues using a commercial kit (Millipore) and incubated with 5 μg anti-Smad3 antibody (Abcam) or rabbit IgG (Santa Cruz Biotechnology) overnight at 4^{o}C. The immunoprecipitates were collected and eluted DNA was subjected to qPCR using specific primers (Integrated DNA Technologies; Table 7)[354] and SYBR Green reagents (Quanta Biosciences). Fold enrichment was calculated (ΔC_t) and represents the ratio of protein-bound DNA (scleraxis or Smad3) to a negative control (pre-immune serum for cells; non-specific IgG for tissues) normalized for input DNA. A region of GAPDH promoter (rat or mouse) was amplified to represent negative control for the experiments; no differences were observed for scleraxis or Smad3 binding to the GAPDH promoter ($P>0.05$; $n=3$).

15: Immunofluorescence imaging

Cardiac P1 proto-myofibroblasts were plated onto glass coverslips infected at MOI 10 with AdLacZ or AdScx for 24 h. Cells were then fixed in 2% paraformaldehyde (Alfa Aesar), permeabilized in 0.3% Triton-X100 and 0.1% Na-citrate and blocked in 5% goat serum (Life Technologies). Cells were incubated with FITC-αSMA antibody (Abcam) at 4^{o}C overnight followed by mounting onto slides

using SlowFade Gold Antifade reagent with DAPI (Molecular Probes). For DDR2 staining, paraffin-embedded 5 μm tissue sections were deparaffinized and rehydrated to distilled water. Tissue slides were processed for antigen retrieval using a citrate-based commercial reagent (antigen unmasking solution, Vector Laboratories) at 90^{o}C for 30 minutes and then cooled at room temperature for another 30 minutes. Sections were then washed with PBS and incubated in blocking reagent (Roche Applied Science, USA) for 1h at room temperature. Slides were incubated with anti-mouse DDR2 antibody (Sigma Aldrich) at 4^{o}C overnight. Tissue sections were then washed thrice with 0.1% Triton X-100 in PBS and incubated with Alexa594-conjugated goat anti-rabbit secondary antibody (Life Technologies) for 1 h at room temperature. Slides were then rinsed in Triton/PBS and mounted with ProLong Diamond Antifade Mountant (Life Technologies). Images were acquired using a Zeiss Axio Imager M1 epifluorescence microscope using appropriate filters.

16: Measurement of cardiomyocyte cross-sectional area

Cardiomyocyte cross-sectional area (width) was measured as previously described [355, 356]. Cardiac tissue was mounted apex-down, and tissue slices were obtained from the mid-ventricular region. Six μm-thick OCT-embedded cardiac tissue sections were treated with 3.3 U/ml neuraminidase type V (Sigma Aldrich) for 1 h at room temperature. Sections were then rinsed with PBS and stained with fluorescein-labelled peanut agglutinin (Vector Laboratories) overnight at 4^{o}C. Tissue sections were rinsed with PBS thrice and mounted with ProLong Diamond Antifade Mountant (Life Technologies). The mountant was allowed to cure overnight in the dark and images were acquired on a Zeiss Axio Imager M1 epifluorescence microscope with a

Plan-Neofluar 40x objective and bounded area measured using AxioVision software. Fifty cells were analyzed from each animal.

17: Determination of cardiac capillary density

Cardiac capillary density was assayed as previously described [357, 358]. Six µm-thick left ventricle sections were treated with neuraminidase type V and stained with Rhodamine-labeled *Griffonia (Bandeiraea) simplifolica* lectin I (GSL-I, BSL-I; Vector Laboratories) overnight at 4ºC. Slides were then washed with PBS, mounted using ProLong Diamond Antifade Mountant (Life Technologies) and allowed to cure overnight. Images were acquired as per measurements of cardiomyocyte cross-sectional area. Two fields were randomly selected from left ventricular region by a blinded observer, analyzed and averaged from each animal.

18: Statistical analysis

Results are reported as mean ± standard error for at least three independent samples. Means were compared by two-sided Student's t-test, or for multiple comparisons by one-way ANOVA with Student-Newman-Keuls post-hoc analysis; results were considered significant when $P<0.05$.

Table 3: Primers used for qPCR analysis.

Amplicon	Direction	Sequence (5'→ 3')
Scleraxis (Rat/Mouse)	Fwd	AACACGGCCTTCACTGCGCTG
	Rev	CAGTAGCACGTTGCCCAGGTG
Col 1α2 (Rat/Mouse)	Fwd	GTCCCCGAGGCAGAGAT
	Rev	CCTTTGTCAGAATACTGAGCAGC
Biglycan (Rat)	Fwd	CTTCCGCTGCGTCACTGA
	Rev	GGTGGCTACCACTGCTTCTACTTC
Biglycan (Mouse)	Fwd	ATTGCCCTACCCAGAACTTGAC
	Rev	GCAGAGTATGAACCCTTTCCTG
Claudin1 (Mouse)	Fwd	TGGGGCTGATCGCAATCTTT
	Rev	ATGGGGGTCAAGGGGTCATA
Col5α1 (Rat)	Fwd	CACTCGACGATCTTCCAAAG
	Rev	TCAGGATGGAGAAGTCCTC
Col5α1 (Mouse)	Fwd	GGACTAGTCCGCTTTCCCTGTCAACTTGTCCGATGG
	Rev	GTGGTCACTGCGGCTGAGGAACTTC
Decorin (Rat/Mouse)	Fwd	CCTGACAATCCCCTGATATCTATGT
	Rev	GTCCAGACCCAGATCAGAACACT
Desmoplakin (Mouse)	Fwd	GCAGAAGGAAGACGATTCCAAGA
	Rev	TTCCGAGCCACAGGCTTTC
Fibromodulin (Rat)	Fwd	GCTCTGGGCTCCTACTCCTT
	Rev	GTCCTGCCATTCTGAGGTGT
DDR2 (Rat/Mouse)	Fwd	GATCATGTTTGAATTTGACCGA
	Rev	GCACTGGGGTTCACATC

ED-A-Fn (Rat/Mouse)	Fwd	ACTGCAGTGACCAACATTGACC
	Rev	CACCCTGTACCTGGAAACTTGC
Fibromodulin (Mouse)	Fwd	CAATGTCTACACCGTCCCTGA
	Rev	AGAAGGCTGCTGGAGTTGAAG
Lumican (Rat)	Fwd	GTTGAAAAGTGTGCCCATGGT
	Rev	TTCATCAATATGGTCGATCTGGTT
Lumican (Mouse)	Fwd	AGATGCTTGATCTTGGAGTAAGA
	Rev	CAATGAACTTGAAAAGTTTGATG
MMP2 (Rat/Mouse)	Fwd	CCCATGAAGCCTTGTTTACCA
	Rev	TGGAAGCGGAACGGAAACT
MMP3 (Rat)	Fwd	AGGTCATGAAGAGCTAGCAG
	Rev	CAGGAGTGTGTTTTCTCCTC
MMP3 (Mouse)	Fwd	CTATACGAGGGCACGAGGAG
	Rev	CCACCCTTGAGTCAACACCT
MMP9 (Rat)	Fwd	CGTGGCCTACGTGACCTATGA
	Rev	TGCACCGCTGAAGCAAAAG
MMP9 (Mouse)	Fwd	TGTCTGGAGATTCGACTTGAAGTC
	Rev	TGAGTTCCAGGGCACACCA
MMP11 (Rat)	Fwd	AAGTTTCCCTCGACCCATAGG
	Rev	AGGTGTTGTCAGCGGAAAGTG
MMP11 (Mouse)	Fwd	CCTTCCAGGATGCTGAGGGCTAT
	Rev	ATGACAGCATGGTCGTTCCTACAA
Par3 (Mouse)	Fwd	TCCTGCTGTTTGTGGTTGGT
	Rev	GTGACCTCGCCAAATACCCA
Periostin (Rat)	Fwd	TCGTGGAACCAAAAATTAAAGTC

	Rev	CTTCGTCATTGCAGGTCCTT
Periostin (Mouse)	Fwd	TGCTGCCCTGGCTATATGAG
	Rev	GTAGTGGCTCCCACAATGCC
SMemb (Rat/Mouse)	Fwd	CAATGAGGGTGGGAGTGGGTG
	Rev	CCTCTCGGGATCCTCCAGTC
Snai1 (Mouse)	Fwd	AGTTGACTACCGACCTTGCG
	Rev	TGCAGCTCGCTATAGTTGGG
Snai1 (Rat)	Fwd	GGAAGCTTGAACCCCACTCA
	Rev	CCACTTGGCCCCTAACAAGT
TCF21 (Mouse)	Fwd	CATTCACCCAGTCAACCTGA
	Rev	CCACTTCCTTCAGGTCATTCTC
Twist1 (Rat/Mouse)	Fwd	CAGCGGGTCATGGCTAACG
	Rev	ATCTTGCTCAGCTTGTCCGA
Versican (Rat/Mouse)	Fwd	CTGATAGCAGATTTGATGCCTACTGC
	Rev	GTGGTTCTTTGGATAAACTGGGTGATG
Vimentin (Rat/Mouse)	Fwd	ACATCCACCCGCACCTAC
	Rev	CAACTCCCTCATCTCCTCCTC
Zeb1 (Mouse)	Fwd	GCGGCGCAATAACGTTACAA
	Rev	GGGCGCCTCAGGATAAATGA
Zeb1 (Rat)	Fwd	GCGGCGCAATAACGTTACAA
	Rev	TCCACGTTGGGATCATGGTT

Table 4: Primers used for cloning and site-directed mutagenesis.

Amplicon	Direction	Sequence (5'→ 3')
COL1α2—0.7 kb (cloning)	Fwd	GCCCTTTCCCGAAGTCATAAGAC
	Rev	TCGAGCCCGGGCTAG
COL1α2—0.7 kb ΔE1	Fwd	GAGCCCTCCACCCTACCATGGGCCTACAGGGCACAG
	Rev	CTGTGCCCTGTAGGCCCATGGTAGGGTGGAGGGCTC
COL1α2—0.7 kb ΔE2	Fwd	GGCCTACAGGGCACTGCAGAGGCGGGACTGGA
	Rev	TCCAGTCCCGCCTCTGCAGTGCCCTGTAGGCC
COL1α2—0.7 kb ΔE3	Fwd	CGCAGGCTCCTCCCCCGGGTGGCTGCCCGGGC
	Rev	GCCCGGGCAGCCACCCGGGGGAGGAGCCTGCG
COL1α2—0.7 kb ΔSBE	Fwd	ATGCGGAGGGCGGAGGTATGCGCACAACGAGTCAGAGTTTCCCCTT
	Rev	AAGGGGAAACTCTGACTCGTTGTGCGCATACCTCCGCCCTCCGCAT
αSMA-mE box 1	Fwd	GTCTGGGCATTTGAGCCGATGTTCTGAGGGCTCAGG
	Rev	CCTGAGCCCTCAGAACATCGGCTCAAATGCCCAGAC
αSMA-mE box 2	Fwd	GTTTATCCCCATAAGCTGGTGAACTGCCTCCTGTTT
	Rev	AAACAGGAGGCAGTTCACCAGCTTATGGGGATAAAC

Table 5: Primers used for nested PCR generation of ScxΔΔ.

Amplicon	Direction	Sequence (5'→ 3')
ScxΔΔ	Forward	GGGCTCGCGGCCTGGC
	Reverse	AATGTGCTGCTGGTGGGTGAGGC

Table 6: Probes used for electrophoretic mobility shift assay.

Amplicon	Direction	Sequence (5'→ 3')
αSMA-E box 1 (E1)	Fwd	GTCTGGGCATTTGAGCAGTTGTTCTGAGGGCTCAGG
	Rev	CCTGAGCCCTCAGAACAACTGCTCAAATGCCCAGAC
αSMA-E box 2 (E2)	Fwd	GTTTATCCCCATAAGCAGCTGAACTGCCTCCTGTTT
	Rev	AAACAGGAGGCAGTTCAGCTGCTTATGGGGATAAAC
αSMA-E box 1 mutant (mE1)	Fwd	GTCTGGGCATTTGAGCCGATGTTCTGAGGGCTCAGG
	Rev	CCTGAGCCCTCAGAACATCGGCTCAAATGCCCAGAC
αSMA-E box 2 mutant (mE2)	Fwd	GTTTATCCCCATAAGCTGGTGAACTGCCTCCTGTTT
	Rev	AAACAGGAGGCAGTTCACCAGCTTATGGGGATAAAC

Table 7: Primers used for chromatin immunoprecipitation assay.

Amplicon	Direction	Sequence (5'→ 3')
COL1α2-E box 1/2	Fwd	CTTCCCTCCCTCCTTCTCTG
	Rev	ACTATGGGACACGTCGGAGT
COL1α2-E box 3	Fwd	CAAAAGTGTCCACGTCCTCA
	Rev	CCCGGATCTGCCCTATTTAT
GAPDH (Human)	Fwd	TACTAGCGGTTTTACGGGCG
	Rev	TCGAACAGGAGGAGCAGAGAGCGA
αSMA-E box 1/2	Fwd	AAAGGCTAGCCTGACAGGAAGAGC
	Rev	GGGACCTCAGCACAAAACTCTCTAATC
GAPDH (Rat)	Fwd	AAACAAGTTCACCACCATGTGAAA
	Rev	CCAGGGATTGACCAAAGGTGAGTT

CHAPTER IV: RESULTS

1. Regulation of human COL1α2 gene promoter by scleraxis and Smads[7]

1.1: Regulation of scleraxis expression by Smads

We previously reported that scleraxis expression is up-regulated in cardiac fibroblasts by TGF-β1, and in turn regulates the COL1A2 promoter [173]. Because Smads are the primary mediator of TGF-β1 signals in fibrosis, we assayed the effect of pro-fibrotic Smad3 or inhibitory Smad7 on scleraxis expression. Adenoviruses encoding Smad3 or Smad7 were used to transfect primary rat cardiac fibroblasts. Smad3 over-expression significantly up-regulated scleraxis expression, while Smad7 attenuated scleraxis expression (Fig. 10). These changes were observed at the level of both transcription and translation, and demonstrate that Smad signaling can regulate scleraxis expression.

1.2: Scleraxis transactivation of the proximal COL1α2 gene promoter

Scleraxis binds specifically to E boxes similar to other bHLH transcription factors [288, 298]. We previously noted the existence of up to 12 putative E boxes in the human 3.7 kb COL1A2 gene promoter [173]. Three of these sites are located within the proximal COL1A2 gene promoter (~700 bp), a region that is highly responsive to TGF-β_1 signaling and rich in binding sites for transcription factors that regulate collagen synthesis including Sp1, Sp3 and Smads [359, 360]. To test whether this proximal region could be transactivated by scleraxis, we amplified by high-fidelity

[7] Reprinted from RA Bagchi and MP Czubryt, Synergistic roles of scleraxis and Smads in the regulation of collagen 1α2 gene expression, *Biochimica et Biophysica Acta-Molecular Cell Research*, 1823:1936–1944, © 2012, with permission from ELSEVIER INC. http://www.sciencedirect.com/science/article/pii/S016748891200198X

PCR a sequence comprising 706 bp of the COL1A2 proximal promoter, including 54 bp of 5′ untranslated region. This sequence was sub-cloned into the luciferase reporter vector pGL3 Basic for further study. This sequence encompasses three putative E boxes, in contrast to previously reported COL1A2 proximal promoter constructs which lack the two most 5′ distal E boxes [361].

We examined the relative transactivation by scleraxis of the proximal COL1A2 promoter (COL1A2pr-0.7) compared to the full-length 3.7 kb promoter (COL1A2pr-3.7). Both promoters were strongly and significantly transactivated by scleraxis, but the proximal promoter exhibited a nearly three-fold higher level of activity compared to the full-length promoter (Fig. 11A). We also compared transactivation of the full-length and proximal promoters by scleraxis in comparison to an empty expression vector. Again we observed that both promoters were significantly transactivated by scleraxis, and that the proximal promoter was induced to a statistically significantly greater degree than the full-length promoter, also by approximately three-fold (Fig. 11B). These results suggest that the full-length promoter may contain repressor elements that negatively affect transactivation. These results also suggest that transactivation of the COL1A2 gene by scleraxis may be largely determined by sequences within the proximal promoter.

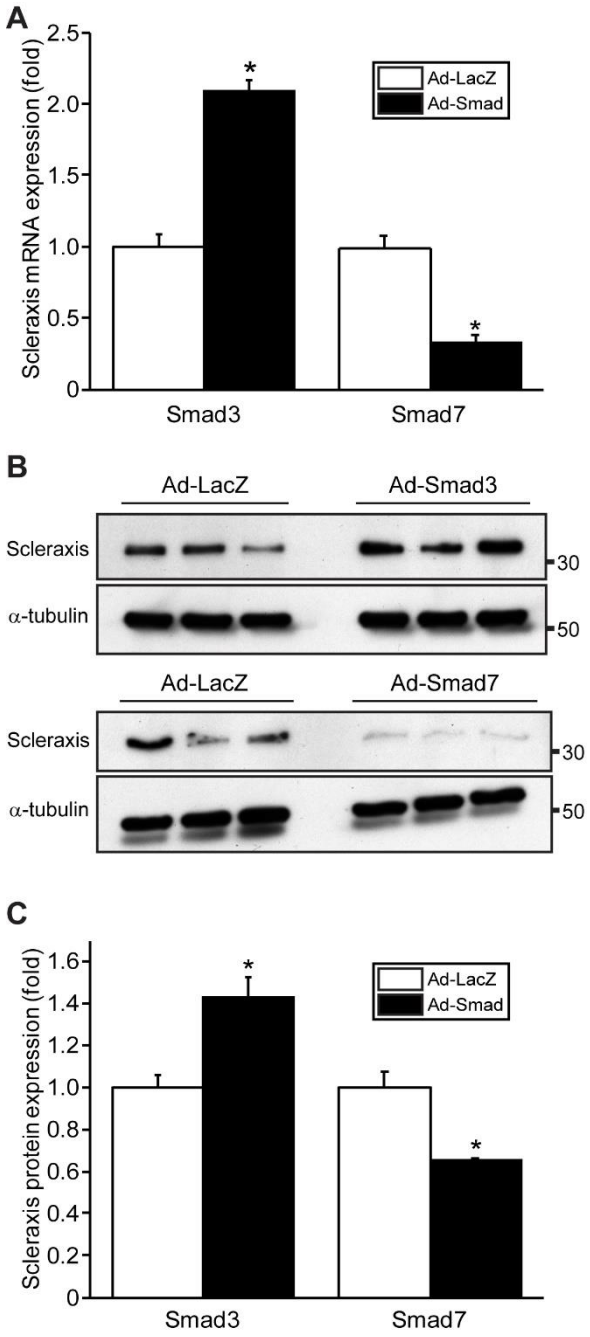

Figure 10: Regulation of scleraxis expression by Smads.

(A) Primary adult rat cardiac fibroblasts were infected with adenovirus encoding Smad3 (MOI10), Smad7 (MOI100) or LacZ (MOI10 or 100) adenoviruses. After treatment for 24 h, cells were lysed and total RNA was isolated for quantitative PCR. Scleraxis mRNA abundance was calculated using the $2^{-\Delta\Delta CT}$ method and normalized to GAPDH. Results represent three independent experiments, normalized to AdLacZ (control), and are reported as mean±standard error; *$p<0.05$ vs. AdLacZ. **(B)** Isolated adult rat cardiac fibroblasts were infected with adenoviruses encoding

LacZ or Smads as in A. Twenty-four hours later, total cell protein was isolated for western blotting with anti-scleraxis antibodies and α-tubulin as a loading control. Numbers refer to molecular weight in kilodaltons. Results are quantified in C and represent three independent experiments, normalized to α-tubulin expression, and are reported as mean±standard error; *$p<0.05$ vs. AdLacZ. Reprinted from RA Bagchi and MP Czubryt, Synergistic roles of scleraxis and Smads in the regulation of collagen 1α2 gene expression, *Biochimica et Biophysica Acta-Molecular Cell Research*, 1823:1936–1944, © 2012, with permission from ELSEVIER INC. http://www.sciencedirect.com/science/article/pii/S016748891200198X

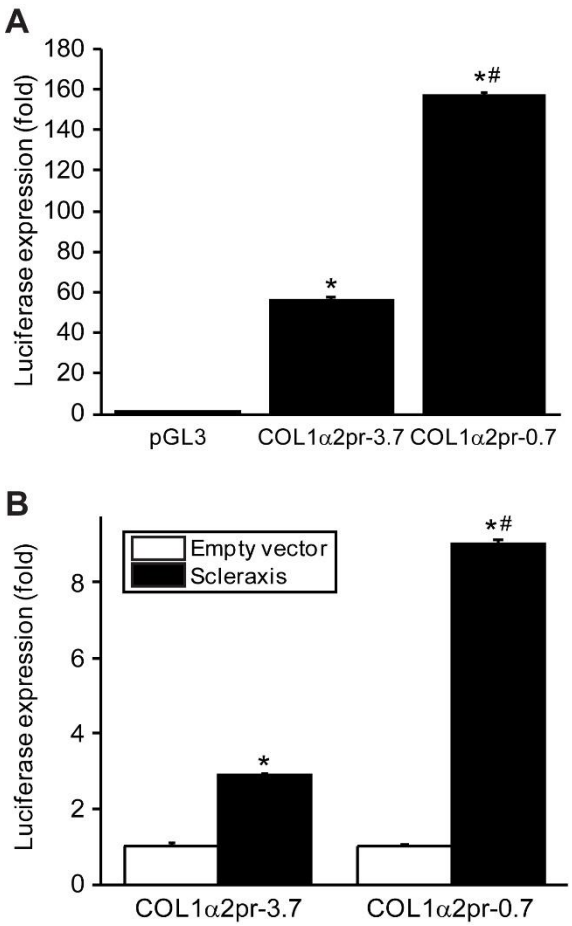

Figure 11: Transactivation of the proximal human COL1A2 promoter by scleraxis.

(A) NIH-3T3 fibroblasts at ~70% confluence were co-transfected with luciferase reporter plasmids (3.7 kb full length or 0.7 kb proximal COL1A2 promoter cloned into pGL3 Basic, or empty pGL3 Basic (pGL3) as control) plus scleraxis expression vector (pECE-HA-FLAG-Scx). Renilla luciferase expression vector pRL was co-transfected as a transfection control. The luciferase activity of each sample was assayed 24 h later. Results of three independent experiments were normalized to pGL3 and pRL, and are reported as mean±standard error; *p<0.05 vs. pGL3, #p<0.05 vs. full length promoter. **(B)** Luciferase reporter assays were performed as in A with either full length or proximal COL1A2 luciferase reporter vectors, plus empty pECE or scleraxis expression vector. Results were normalized to pECE and pRL. Results of three independent experiments are reported as mean±standard error; *p<0.05 vs. empty vector, #p<0.05 vs. full-length promoter. Reprinted from RA Bagchi and MP Czubryt, Synergistic roles of scleraxis and Smads in the regulation of collagen 1α2 gene expression, *Biochimica et Biophysica Acta-Molecular Cell Research*, 1823:1936–1944, © 2012, with permission from ELSEVIER INC. http://www.sciencedirect.com/science/article/pii/S016748891200198X

1.3: E box-mediated transactivation of the COL1A2 proximal promoter by scleraxis

As noted above, the COL1A2 proximal promoter contains three putative scleraxis-binding E boxes (designated E1 to E3; Fig. 12A), including one sequence (E2) that exactly matches a previously-defined scleraxis binding site in the aggrecan gene promoter [299]. Homologous E boxes are located in the mouse and rat Col1α2 promoters in positions closely proximal to their locations in the human promoter (Fig. 12A). Chromatin immunoprecipitation assay confirmed that scleraxis directly binds to the promoter regions encompassing the E box sequences present within the COL1A2 promoter in normal human cardiac fibroblasts *ex vivo* (Fig. 12B). However, ChIP resolution is determined by the size of the immunoprecipitated DNA fragments, typically 200 to 500 bp. The gap between E1 and E2 is only 12 bp, while E1 and E3 are separated by 310 bp, thus while it is clear that scleraxis binds to this region, it is difficult to ascertain by ChIP the importance of any single E box. To determine which of these three sites are involved in scleraxis- mediated transactivation of the COL1A2 promoter, we performed mutation analysis studies in which individual or combinations of E boxes were mutated to prevent scleraxis binding in luciferase reporter assays. Mutation of any single E box (ΔE1, ΔE2 or ΔE3; Fig. 12A) resulted in a significant attenuation of promoter transactivation by scleraxis, although transactivation was still significantly greater than control empty vector (Fig. 12C). Intriguingly, mutation of both E1 and E3 completely prevented promoter transactivation by scleraxis. Transactivation was significantly lower than control, and was significantly decreased further when all three E boxes (ΔE1/2/3) were mutated.

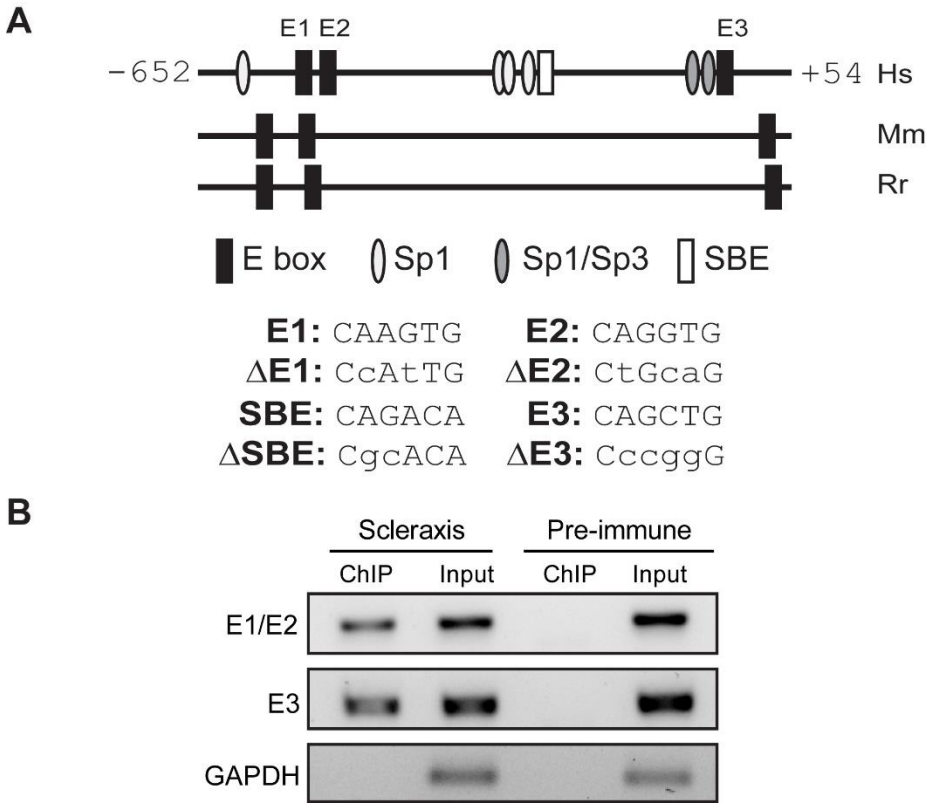

Figure 12: Interaction of scleraxis with the proximal COL1A2 promoter.

(A) The proximal human COL1A2 gene promoter, spanning a region from −652 to +54 relative to the transcription start site, contains three putative E boxes (black rectangles, denoted E1 to E3) that match the consensus CANNTG E box sequence. For comparison, the locations of homologous E boxes within the mouse (Mm) and rat (Rr) Col1α2 gene promoters are depicted in comparison to the human (Hs) promoter. Binding sites for various other regulatory transcription factors within the human promoter are indicated, including Sp1 GC boxes (light gray ovals), Sp1/Sp3 T boxes (dark gray ovals), and a Smad Binding Element (SBE; white rectangle). The E box and SBE mutations used in the study are also indicated. **(B)** Chromatin immunoprecipitation was performed on human cardiac fibroblasts using anti-scleraxis (Scx) antibody or pre-immune serum. PCR primers were used to amplify the collagen 1α2 promoter sequence flanking E boxes 1 and 2 (E1/E2) or E box 3 (E3). Genomic DNA was used as a positive input control. Scleraxis binds to both the E1/E2 and E3 sites. A region of the human GAPDH promoter was used as a negative control.

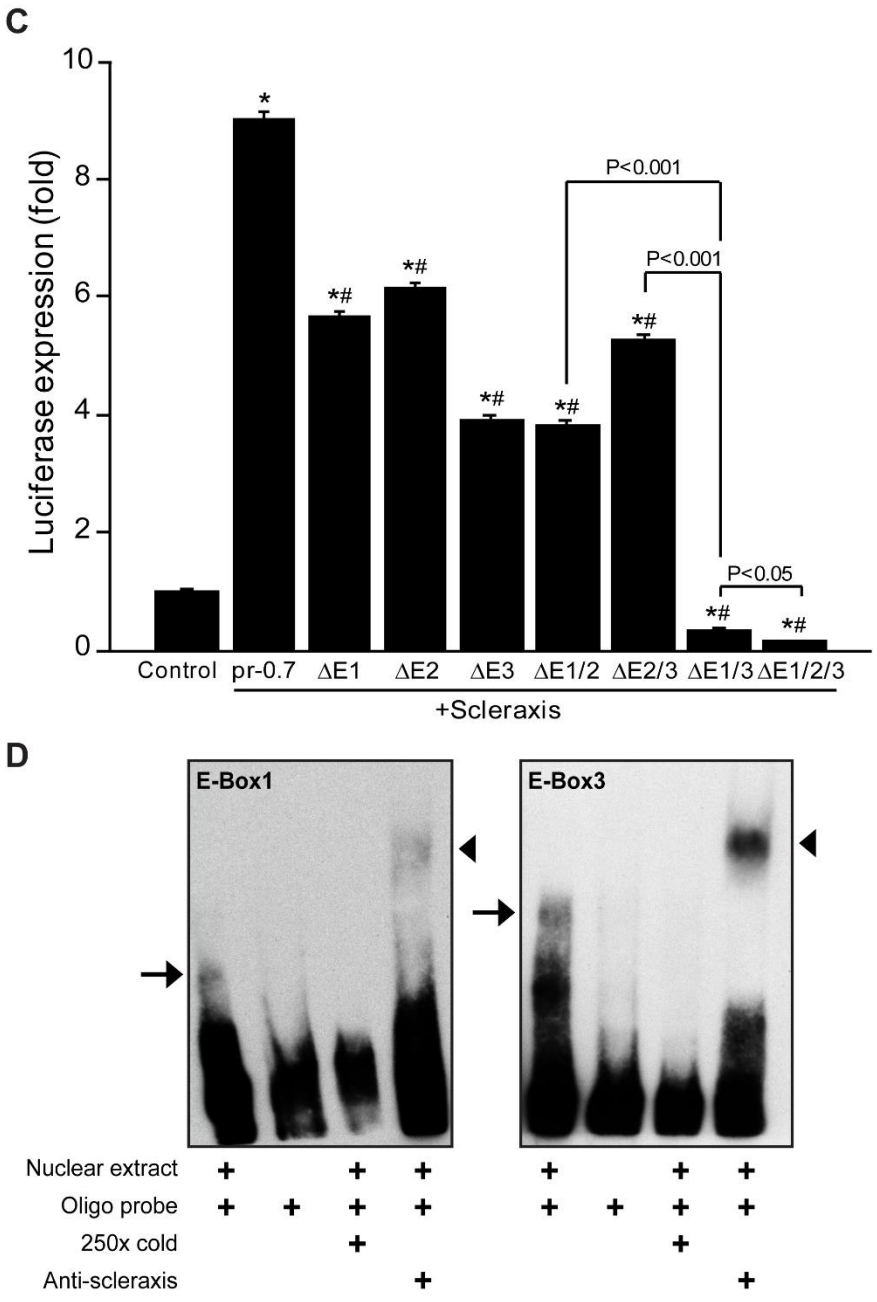

(C) Point mutations were sequentially introduced to the three E boxes of the COL1A2 proximal promoter individually or in combination as per the sequences shown in panel A. NIH-3T3 fibroblasts were transfected with intact (pr-0.7) or mutated (ΔE1, ΔE2 etc.) proximal COL1A2 promoter reporters plus scleraxis expression vector or empty pECE (Control). pRL was co-transfected as a transfection control. Twenty-four hours after transfection, luciferase assays were performed. Results of three independent experiments were normalized to Control and pRL, and are reported as mean±standard error; *p<0.001 vs. Control, #p<0.001 vs. pr-0.7. **(D)** The binding of scleraxis to E boxes 1 and 3 was confirmed by EMSA. Scleraxis-containing COS7 nuclear extracts

were incubated with biotin-labeled oligonucleotide probes corresponding to either E box. A 250-fold molar excess of unlabeled oligonucleotide (250X cold) was used to compete the scleraxis-DNA complex (arrow). Inclusion of an anti-scleraxis antibody resulted in a supershift of the complex (arrowhead). Reprinted from RA Bagchi and MP Czubryt, Synergistic roles of scleraxis and Smads in the regulation of collagen 1α2 gene expression, *Biochimica et Biophysica Acta-Molecular Cell Research*, 1823:1936–1944, © 2012, with permission from ELSEVIER INC. http://www.sciencedirect.com/science/article/pii/S016748891200198X

These results indicate that E boxes E1 and E3 are strictly required for transactivation of the COL1A2 proximal promoter by scleraxis. Conversely, E2 appears to have a contributory effect but is not absolutely required: although E2 mutation alone reduced transactivation by scleraxis, the double mutations ΔE1/2 and ΔE2/3 did not cause the dramatic attenuation observed with ΔE1/3, although the triple mutant was significantly lower than ΔE1/3 (Fig. 12C). One possibility is that E2, separated from E1 by only 12 nucleotides, may indirectly modulate transcription factor binding to E1, perhaps by affecting local DNA topography and thus access by scleraxis to E1.

The attenuation of scleraxis-mediated transactivation of the COL1A2 promoter below control in the ΔE1/3 and ΔE1/2/3 experiments may be due to endogenous scleraxis expression in the NIH-3T3 fibroblasts used in the reporter assay [173]. Thus, the intact COL1A2-pr0.7 promoter reporter may exhibit some activity even in the absence of exogenously added scleraxis. Mutation of the reporter E boxes would eliminate transactivation by endogenous scleraxis, resulting in reporter activity below control levels.

To confirm the ability of scleraxis to bind to E boxes 1 and 3, electrophoretic mobility shift assays were performed using scleraxis-containing nuclear extracts and biotin-labeled oligonucleotides corresponding to one or the other E box. A shifted band was observed for both E boxes which was lost with a 250-fold excess of unlabeled oligonucleotide competitor (Fig. 12D, arrows). Both bands were supershifted upon inclusion of anti-scleraxis antibody (Fig. 12D, arrowheads), confirming the formation of a scleraxis-DNA complex.

1.4: Synergistic regulation of the COL1A2 promoter by scleraxis and Smads

Multiple pro-fibrotic TGF-β1-responsive signaling pathways con- verge on the COL1A2 proximal promoter [359, 360]. While we have shown that TGF-β1 also induces scleraxis expression, and that scleraxis in turn up-regulates COL1A2 expression, it is unclear whether TGF-β1 and scleraxis exert independent effects on promoter activation [173]. We therefore examined whether TGF-β1 and scleraxis exert additive effects on proximal COL1A2 promoter transactivation. While scleraxis alone strongly activated the promoter, the addition of TGF-β1 induced a further statistically significant increase in promoter activation (Fig. 13A). This result suggests that scleraxis may function together with other TGF-β1-responsive signaling pathways such as Smads.

To determine whether scleraxis directly interacts with the Smad signaling pathway to regulate transcription, luciferase assays were performed with scleraxis in combination with pro-fibrotic Smad3, Smad2 or inhibitory Smad7. As expected, either scleraxis or Smad3 alone significantly transactivated the proximal COL1A2 promoter. Smad2 alone had a statistically significant but much more modest effect on COL1A2 transactivation. Intriguingly, scleraxis and Smad3 together exhibited synergistic activation of the promoter (~ 33-fold activation, compared to 10 ~ 14-fold activation for scleraxis or Smad3 alone; Fig. 13B). Conversely, Smad7 completely abrogated promoter transactivation by scleraxis. Smad2 had no effect in combination with scleraxis, and only a modest effect when transfected with Smad3 and scleraxis together, in keeping with its greatly diminished ability to regulate gene expression compared to Smad3 [362].

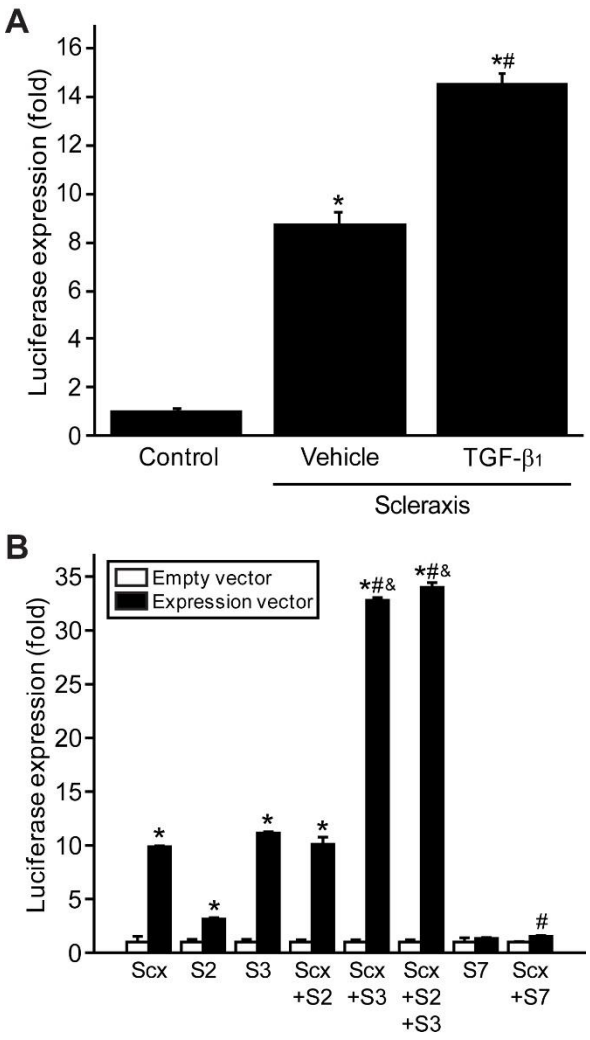

Figure 13: Cross-talk between scleraxis and Smad signaling.

(A) NIH-3T3 fibroblasts were transfected with empty pECE (Control) or scleraxis expression vectors plus the proximal COL1A2 luciferase reporter vector. Twenty-four hours later, cells were treated with vehicle or 10 ng/ml TGF-β1 as indicated for an additional 24 h prior to luciferase assay. pRL was co-transfected as a transfection control. Results of three independent experiments were normalized to Control and pRL, and are reported as mean±standard error; *p<0.05 vs. Control, #p<0.05 vs. scleraxis plus vehicle. **(B)** Luciferase reporter assays were performed using proximal COL1A2 promoter reporter vector, plus empty pECE or scleraxis expression vector; or pCMV tag3C or pCMV tag3C-Myc-Smad3 or pCMV tag3C-Myc-Smad2; or pcDNA3.1(+) or pcDNA3.1(+)-FLAG-Smad7. pRL was co-transfected as a transfection control. Results of three independent experiments were normalized to the respective empty vectors and pRL, and are reported as mean±standard error; *p<0.001 vs. empty vector, #p<0.001 vs. scleraxis alone; &p<0.001 vs. Smad3 alone.

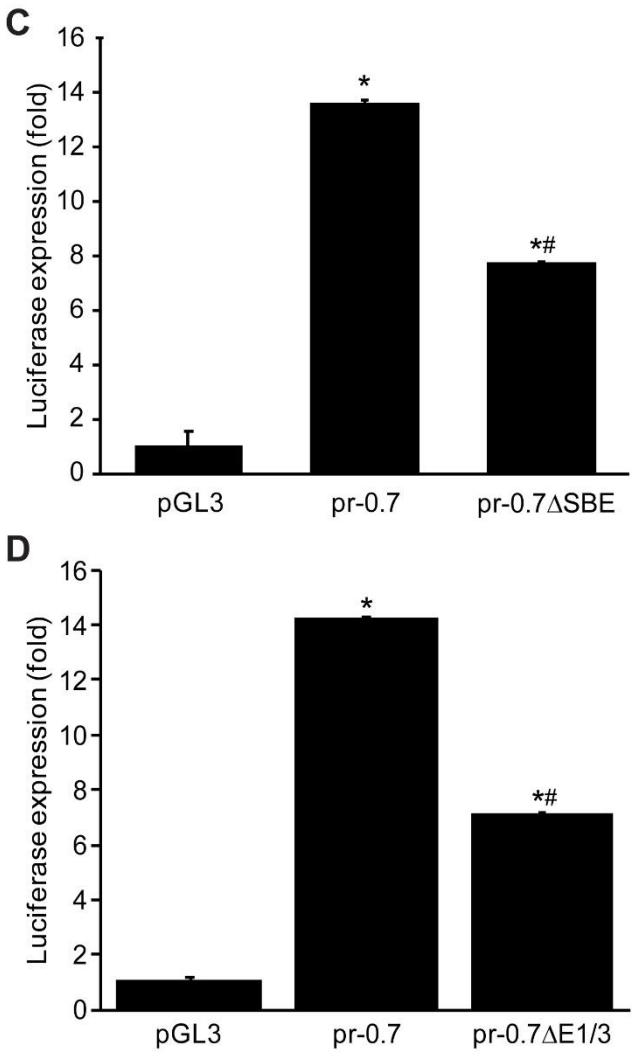

(C) NIH-3T3 fibroblasts were transfected with the intact (pr-0.7) or SBE mutant (pr-0.7ΔSBE) proximal COL1A2 promoter reporter or pGL3 (Control), plus scleraxis expression vector. pRL was co-transfected as a transfection control. Twenty-four hours after transfection, luciferase assays were performed. Results of three independent experiments were normalized to empty pGL3 vector and pRL, and are reported as mean±standard error; *p<0.05 vs. pGL3, #p<0.05 vs. pr-0.7. **(D)** NIH-3 T3 fibroblasts were transfected with the intact (pr-0.7) or double E box mutant (pr-0.7ΔE1/3) proximal COL1A2 promoter reporter or pGL3 (Control), plus scleraxis expression vector. pRL was co-transfected as a transfection control. Luciferase assays were performed 24 h after transfection. Results of three independent experiments were normalized to empty pGL3 vector and pRL, and are reported as mean±standard error; *p<0.05 vs. pGL3, #p<0.05 vs. pr-0.7. Reprinted from RA Bagchi and MP Czubryt, Synergistic roles of scleraxis and Smads in the regulation of collagen 1α2 gene expression, *Biochimica et Biophysica Acta-Molecular Cell Research*, 1823:1936–1944, © 2012, with permission from ELSEVIER INC. http://www.sciencedirect.com/science/article/pii/S016748891200198X

1.5: Cross-talk in proximal COL1A2 promoter activation by Smad3 and scleraxis

The scleraxis binding sites are in close juxtaposition with those of other fibrotic regulators: E1 and E3 are a mere 167 and 136 nucleotides, respectively, away from the SBE (Fig. 12A), suggesting the possibility that these sites contribute to the assembly of a common transcription complex. We tested whether scleraxis-mediated transactivation of the proximal COL1A2 promoter is dependent on Smad3 and vice versa. Scleraxis-mediated promoter transactivation was significantly attenuated by mutation of the SBE (Fig. 13C). Similarly, Smad3-mediated promoter activation was significantly attenuated by mutation of the two critical scleraxis binding sites, E1 and E3 (Fig. 13D). In both cases, promoter transactivation was reduced by approximately 50%, similar to the loss of activity observed when the HLH protein–protein interaction domain of scleraxis is deleted [173]. Collectively, these results suggest that scleraxis and Smad3 functionally interact to regulate COL1A2 transactivation.

1.6: Blockade of COL1A2 expression by a scleraxis dominant negative mutant

bHLH transcription factors contain a basic domain that mediates DNA binding [288, 296]. Deletion of this domain may give rise to a protein that acts in a dominant negative fashion to inhibit gene expression. For example, Inhibitor of Differentiation 2 is an HLH transcriptional repressor that functions by binding to ubiquitous bHLH factors like E12 and E47, thus preventing these factors from forming heterodimers with other bHLH proteins while at the same time interfering with binding to DNA [363]. We previously generated a scleraxis mutant lacking the DNA-binding basic domain (ScxΔBD) and demonstrated that this mutant was completely unable to transactivate the COL1α2 promoter [173].

We tested whether this mutant may act as a dominant negative regulator of COL1α2 promoter transactivation via luciferase assays in NIH-3T3 fibroblasts using ScxΔBD in combination with scleraxis. Scleraxis- mediated transactivation of the proximal COL1A2 promoter was attenuated by ScxΔBD in a dose-dependent manner, with as little as 100 ng transfected ScxΔBD vector sufficient to completely block transactivation (Fig. 14A). The three highest doses of ScxΔBD vector significantly reduced luciferase activity below the level of the empty vector control. As in Fig. 11C above, this suggests that basal transactivation of the reporter by endogenous factors was inhibited, and demonstrates that the ScxΔBD mutant does, indeed, behave as a dominant negative regulator of scleraxis-mediated gene transactivation.

We next examined whether ScxΔBD could interfere with TGF- β_1-mediated induction of collagen 1α2 gene expression. We confirmed that collagen 1α2 mRNA expression was up-regulated to similar levels in NIH-3T3 fibroblasts in response to TGF-β_1 treatment or scleraxis over-expression (Fig. 14B). Strikingly, ScxΔBD completely abrogated that effect of TGF-β_1 on collagen 1α2 expression in these cells. Indeed, ScxΔBD also resulted in a significant reduction in basal collagen 1α2 mRNA expression compared to vehicle-treated cells transfected with an empty expression vector. These results support the suggestion that scleraxis plays a critical role in mediating TGF-β1-induced COL1α2 gene expression, and demonstrate that ScxΔBD is capable of interfering with TGF-β1-mediated collagen production. We confirmed these results in primary rat passage 2 cardiac myofibroblasts at both the mRNA and protein level (Fig. 14C, D).

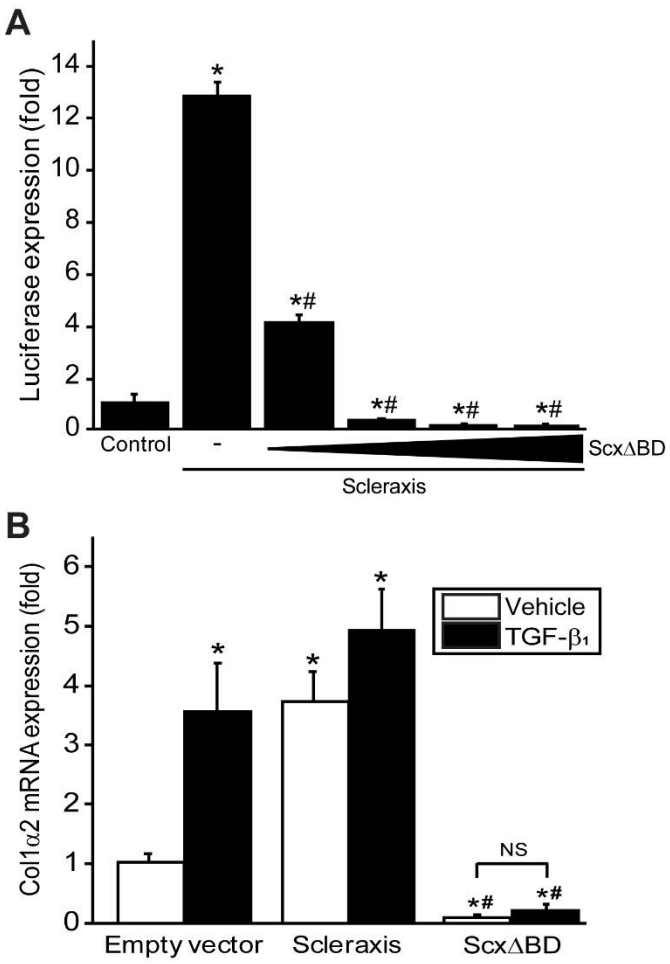

Figure 14: Inhibition of collagen 1α2 expression by a scleraxis dominant negative mutant.

A) NIH-3T3 fibroblasts were transfected with the proximal COL1A2 promoter reporter plus empty pECE (Control) or intact scleraxis expression vectors. Some samples were co-transfected with increasing amounts (20, 100, 250 or 500 ng DNA) of ScxΔBD. pRL was co-transfected as a transfection control. Twenty four hours after transfection, luciferase assays were performed. Results of three independent experiments were normalized to pECE and pRL, and are reported as mean±standard error; *p<0.05 vs. Control, #p<0.05 vs. intact scleraxis alone (−). **B)** NIH-3T3 fibroblasts were transfected with empty pECE, intact scleraxis or ScxΔBD expression vectors. Twenty four hours later, cells were treated with vehicle or 10 ng/ml TGF-β_1. After another 24 h, total RNA was isolated for quantitative RT-PCR. Col1α2 mRNA abundance was calculated using the $2^{-\Delta\Delta CT}$ method and was normalized to GAPDH. Results of three independent experiments were normalized to samples receiving empty vector plus vehicle, and are reported as mean±standard error; *p<0.05 vs. empty vector+vehicle, #p<0.05 vs. corresponding intact scleraxis-transfected samples. NS, not significant.

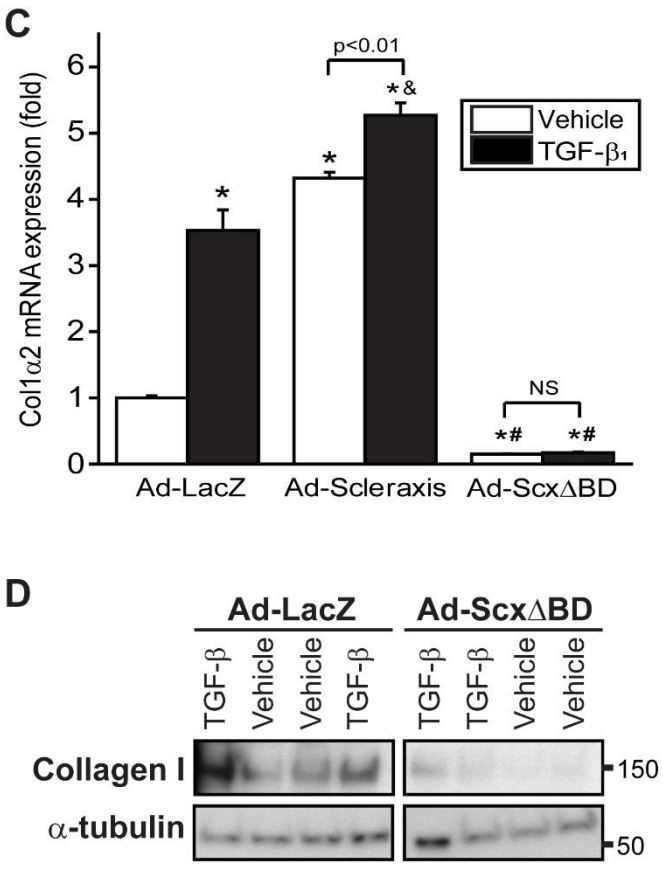

C) A similar experiment was carried out as in panel B, using primary rat passage 2 myofibroblasts and adenoviruses encoding scleraxis or ScxΔBD (MOI 10). Results of three independent experiments were normalized to samples receiving empty vector plus vehicle, and are reported as mean±standard error; *$p<0.01$ vs. empty vector+vehicle, #$p<0.001$ vs. corresponding intact scleraxis infected samples; &$p<0.01$ vs. empty vector plus TGF-β_1. NS, not significant. D) Primary rat passage 2 myofibroblasts were treated with vehicle or 10 ng/ml TGF-β_1 with or without adenovirus encoding the ScxΔBD mutant for 24 h. Total protein lysates were separated by SDS-PAGE, western blotted as in the Materials and methods and visualized using anti-collagen type I antibody. α-tubulin was used as a loading control. Reprinted from RA Bagchi and MP Czubryt, Synergistic roles of scleraxis and Smads in the regulation of collagen 1α2 gene expression, *Biochimica et Biophysica Acta-Molecular Cell Research*, 1823:1936–1944, © 2012, with permission from ELSEVIER INC.
http://www.sciencedirect.com/science/article/pii/S016748891200198X

2. Regulation of cardiac fibroblast ECM gene expression by scleraxis

2.1: Modulation of expression of fibrillar collagens in cardiac proto-myofibroblasts by scleraxis

We previously demonstrated that scleraxis directly regulates Col1α2 expression in cardiac myofibroblasts via conserved promoter E boxes [172, 173]. Lejard *et al* demonstrated that scleraxis up-regulates Col1α1 in tendon fibroblasts [318]. Scleraxis may thus play a broader role in regulation of cardiac ECM gene expression and its function may not just be limited to modulation of type I collagen expression, an avenue that had not been explored. We examined this possibility using gain and loss of function experimental approaches. Proto-myofibroblasts, an intermediate phenotype between fibroblasts and myofibroblasts, provide a viable *in vitro* system to examine features of multiple fibroblast phenotypes with or without experimental manipulation [103, 169]. In isolated primary rat proto-myofibroblasts, overexpression of scleraxis induced the expression of major cardiac fibrillar collagens namely *Col1α1*, *Col1α2*, *Col3α1*, *Col5α1*, but not of non-fibrillar *Col4α1* (Fig. 15A). This suggests that this is a specific effect on fibrillar collagens, and does not represent a general effect on collagen expression.

2.2: Changes in expression of proteoglycans and MMPs in cardiac proto-myofibroblasts by scleraxis

Several proteoglycans were up-regulated by scleraxis. This included fibromodulin, lumican and decorin (Fig. 15B). The expression of versican and biglycan did not exhibit any significant alteration. Scleraxis thus exerts varying effects on proteoglycan expression, although fibromodulin and possibly lumican may

represent true direct gene targets of scleraxis. Similar results were previously reported for proteoglycan regulation by scleraxis in cardiac valves [364].

Scleraxis over-expression in cardiac proto-myofibroblasts significantly increased the expression of *Mmp2* and *Mmp3* genes, but decreased *Mmp9* and *Mmp11* expression (Fig. 16A). In agreement with these results, scleraxis transiently increased proMMP2 activity >5-fold (concomitant with a loss of mature MMP2 activity), but decreased combined MMP9/proMMP9 activity within 24 hours (Fig. 16B). By 48 hours, proMMP2 and combined MMP9 activity returned to control levels, while MMP2 activity remained lower. These results suggest that some MMPs (e.g. MMP2, MMP3) may be under direct transcriptional control by scleraxis, however MMP activity can be altered by TIMP expression, which could potentially confound the interpretation of these results. A follow-up study investigating the role of scleraxis in regulation of expression of TIMPs would provide a better understanding of the matrix turnover process mediated by scleraxis.

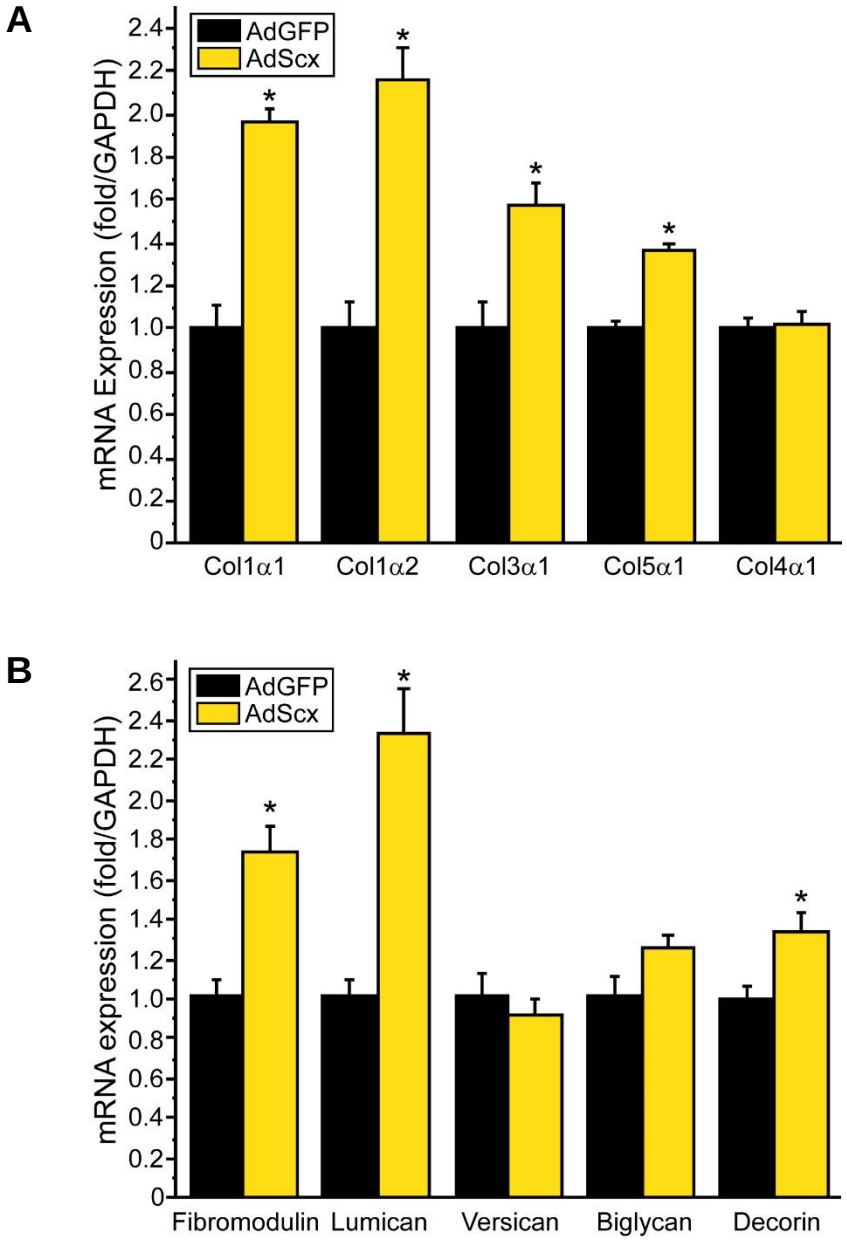

Figure 15: Upregulation of select putative ECM gene targets by scleraxis.

Primary rat cardiac proto-myofibroblasts were infected with adenovirus encoding scleraxis cDNA (AdScx) or control cDNA (AdGFP) for 24 h. mRNA expression of **(A)** collagens and **(B)** proteoglycans was assayed by qPCR. Results were calculated using the $2^{-\Delta\Delta Ct}$ method and normalized to the respective AdGFP sample; n=3, *P<0.05 vs AdGFP.

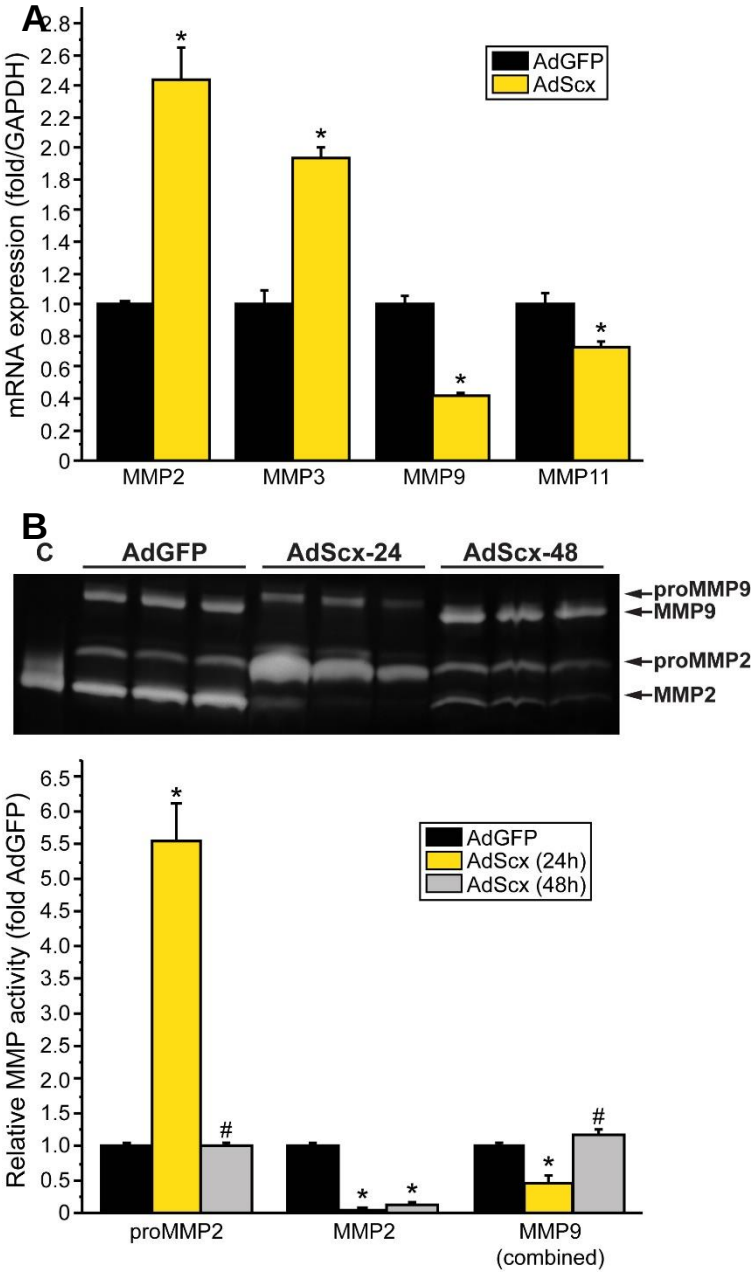

Figure 16: Regulation of MMP expression and activity by scleraxis.

(A) Assay of matrix metalloproteinase mRNA expression by qPCR following scleraxis over-expression (AdScx) in primary rat cardiac proto-myofibroblasts compared to controls (AdGFP); n=3, *P<0.05 vs AdGFP. **(B)** Conditioned media from AdGFP- or AdScx-infected primary rat cardiac proto-myofibroblasts were assayed by gel zymography. Zymograms were obtained 24 or 48 hours following infection; C, control recombinant human MMP2 protein. Results from were quantified; n=3, *P<0.05 vs AdGFP; #P<0.05 vs corresponding 24 hour time point.

2.3: Impact of loss of scleraxis function on cardiac fibroblast ECM gene expression in vitro

We confirmed that scleraxis is required for ECM gene expression via shRNA-mediated loss of function in primary rat cardiac proto-myofibroblasts. We generated a novel adenovirus encoding a scleraxis shRNA (AdshScx), which rapidly and potently attenuated scleraxis expression but had no effect on paraxis, a bHLH transcription factor with the highest homology to scleraxis (Fig. 17A) [365]. Scleraxis expression was blunted even after treatment with TGFβ, which potently induces scleraxis expression as demonstrated previously (Fig. 17B) [172, 173]. Scleraxis knockdown attenuated expression of the same fibrillar collagens induced by scleraxis over-expression, and did not affect *Col4α1* expression (Fig. 18A, B). Immunoblotting for type I collagen expression, the primary form of collagen found in the heart, also revealed a significant increase in response to scleraxis gene induction compared to control cells. Scleraxis knockdown similarly resulted in the down-regulation of several proteoglycans including fibromodulin, lumican and decorin, complementing the results obtained in response to scleraxis gene over-expression studies (Fig. 19A). Similarly, knockdown of scleraxis in cardiac proto-myofibroblasts also reduced *Mmp2* and *Mmp3* gene expression, while inducing *Mmp9* and *Mmp11* genes (Fig. 19B). An in-depth study of the scleraxis-mediated regulation of MMPs and TIMPs through assessment of protein expression and enzyme activity will provide a clearer understanding of the underlying mechanism of these observed effects. Thus, scleraxis has its effect on genes involved in both ECM synthesis and degradation- thereby affecting ECM turnover in general. These results therefore indicate that scleraxis

exerts broad control of genes regulating ECM homeostasis by cardiac proto-myofibroblasts.

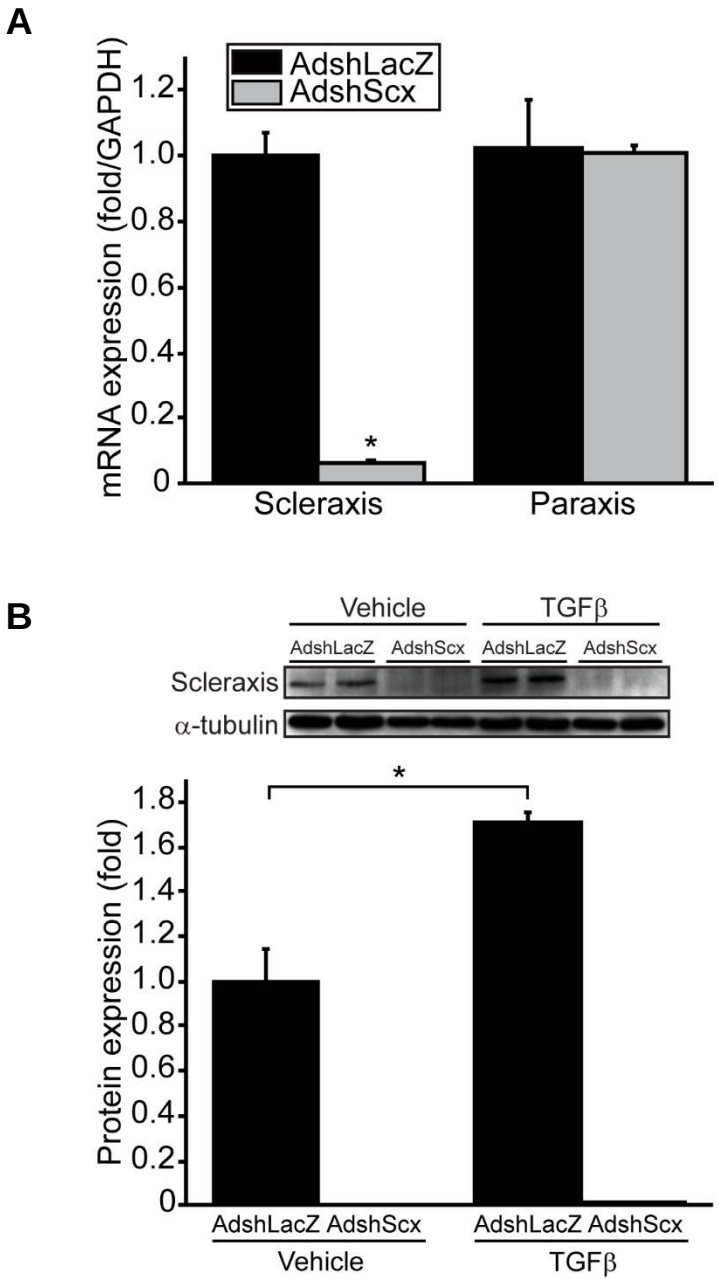

Figure 17: Loss of scleraxis function in cardiac proto-myofibroblasts.

(A) Primary cardiac proto-myofibroblasts were infected with adenovirus encoding shRNA targeting scleraxis (AdshScx) or control shRNA (AdshLacZ) for 72 h and mRNA expression of scleraxis or paraxis assayed by qPCR. Results were normalized to the respective AdshLacZ sample; n=3, *P<0.05 vs AdshLacZ. **(B)** Cells treated as in **(A)**, with or without 10 ng/mL TGF-β or vehicle, were assayed for scleraxis protein expression 72 h after infection. Results were normalized to α-tubulin expression; n=4, *P<0.05 vs AdshLacZ+vehicle.

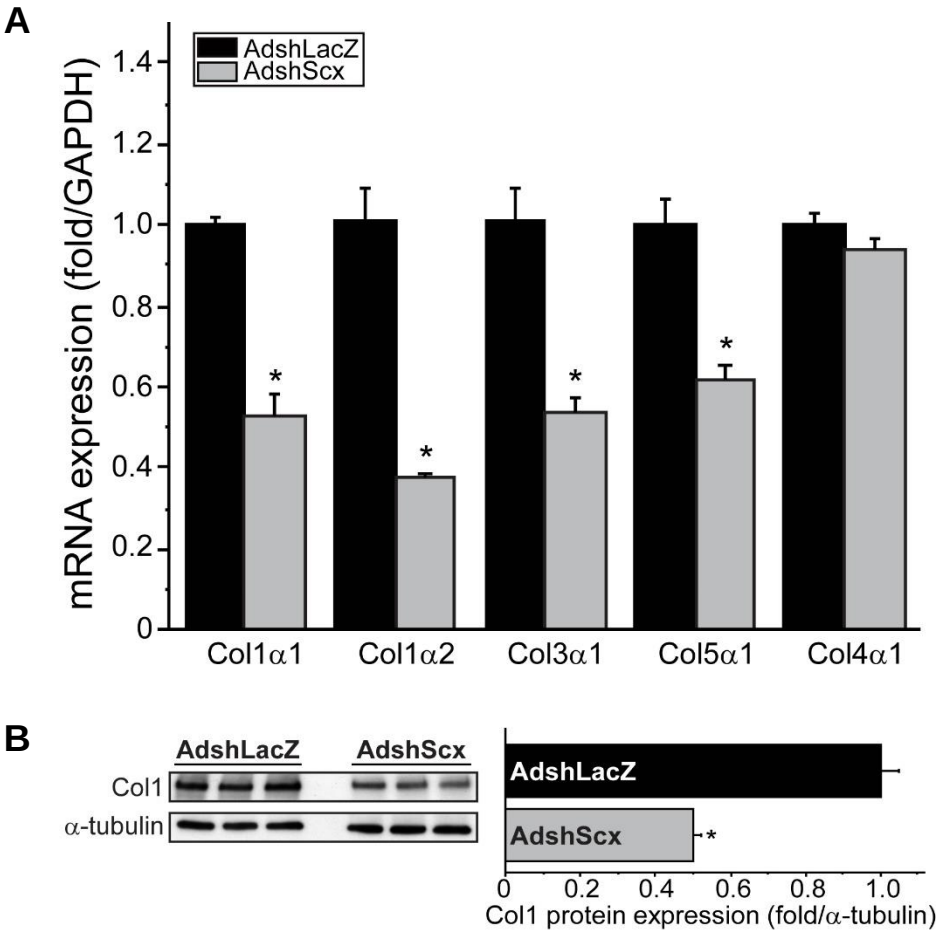

Figure 18: Loss of fibrillar collagen expression in response to scleraxis knockdown.

(A) Collagen mRNA expression was assayed by qPCR with cell treatment and normalization as in Fig.14A; n=3, *P<0.05 vs AdshLacZ. **(B)** Nascent ~150 kDa collagen I protein expression following knockdown of scleraxis in primary cardiac proto-myofibroblasts compared to controls (AdshLacZ) as in Fig.14A; n=3, *P<0.05 vs AdshLacZ.

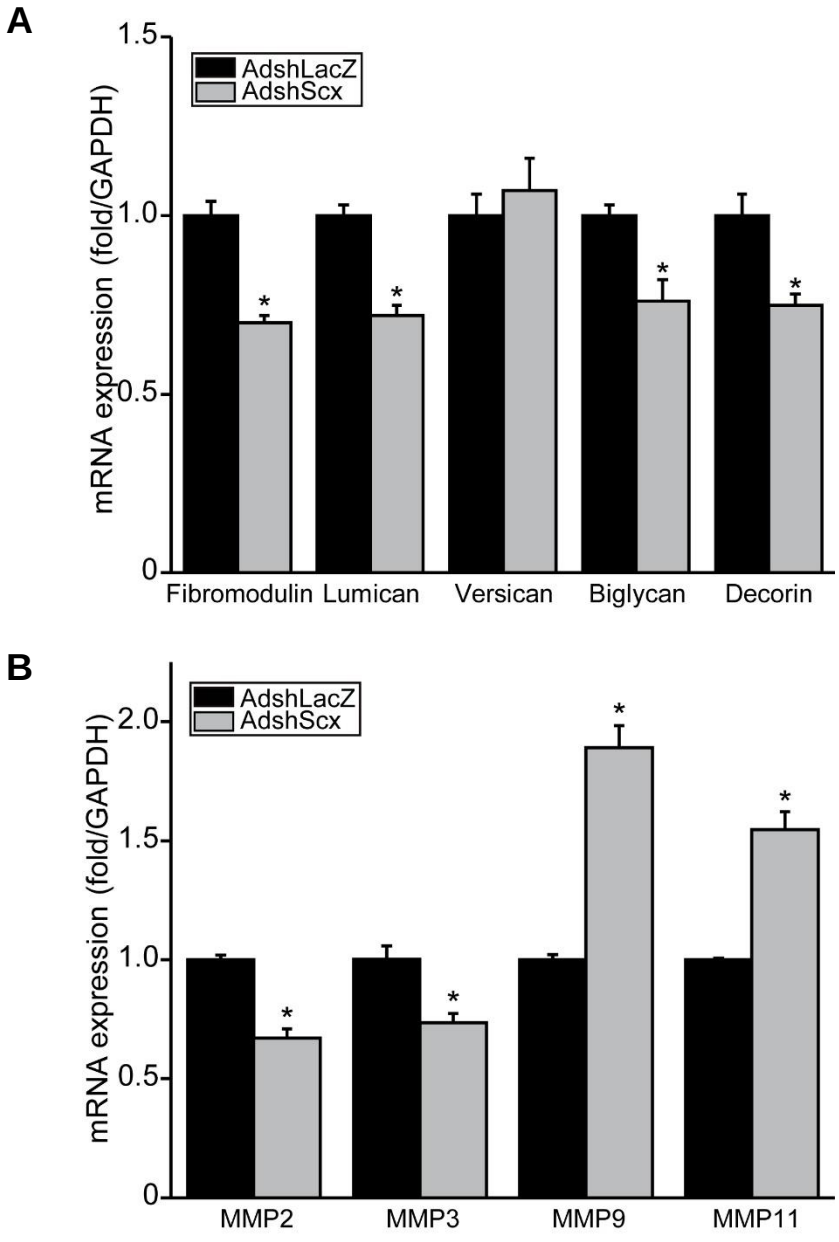

Figure 19: Alteration of proteoglycan and MMP expression following scleraxis knockdown.

Assay of proteoglycan **(A)** and matrix metalloproteinase **(B)** mRNA expression was performed using qPCR following knockdown of scleraxis (AdshScx) in primary rat cardiac proto-myofibroblasts compared to controls (AdshLacZ); n=3, *P<0.05 vs AdshLacZ.

3. Cardiac fibroblast phenotype regulation by scleraxis

3.1: Regulation of fibroblast and myofibroblast marker gene expression by scleraxis

The up-regulation of ECM expression is a hallmark of fibroblast to myofibroblast phenotype conversion. Given the central role of scleraxis in regulating matrix gene expression, we hypothesized that scleraxis may govern cardiac fibroblast phenotype. We assayed a broad panel of fibroblast and myofibroblast markers following gain or loss of scleraxis function. Over-expression of scleraxis in cardiac proto-myofibroblasts increased synthesis of nearly all markers tested (Fig. 20A), including DDR2, EDA-Fn, SMemb, vimentin and periostin, an integrin ligand implicated in cell attachment, fibrosis of various tissues, and cardiac fibroblast specification. In contrast, scleraxis knockdown similarly decreased all markers (Fig. 20B), suggesting reverse transition of these cells away from a myofibroblast phenotype.

We assayed representative human gene promoters for transactivation by scleraxis using luciferase reporters. Both the MMP2 and vimentin promoters were significantly transactivated by scleraxis, supporting direct regulation of these genes by scleraxis (Fig. 21). This is in agreement with our over-expression data as shown in figures 16A and 20A.

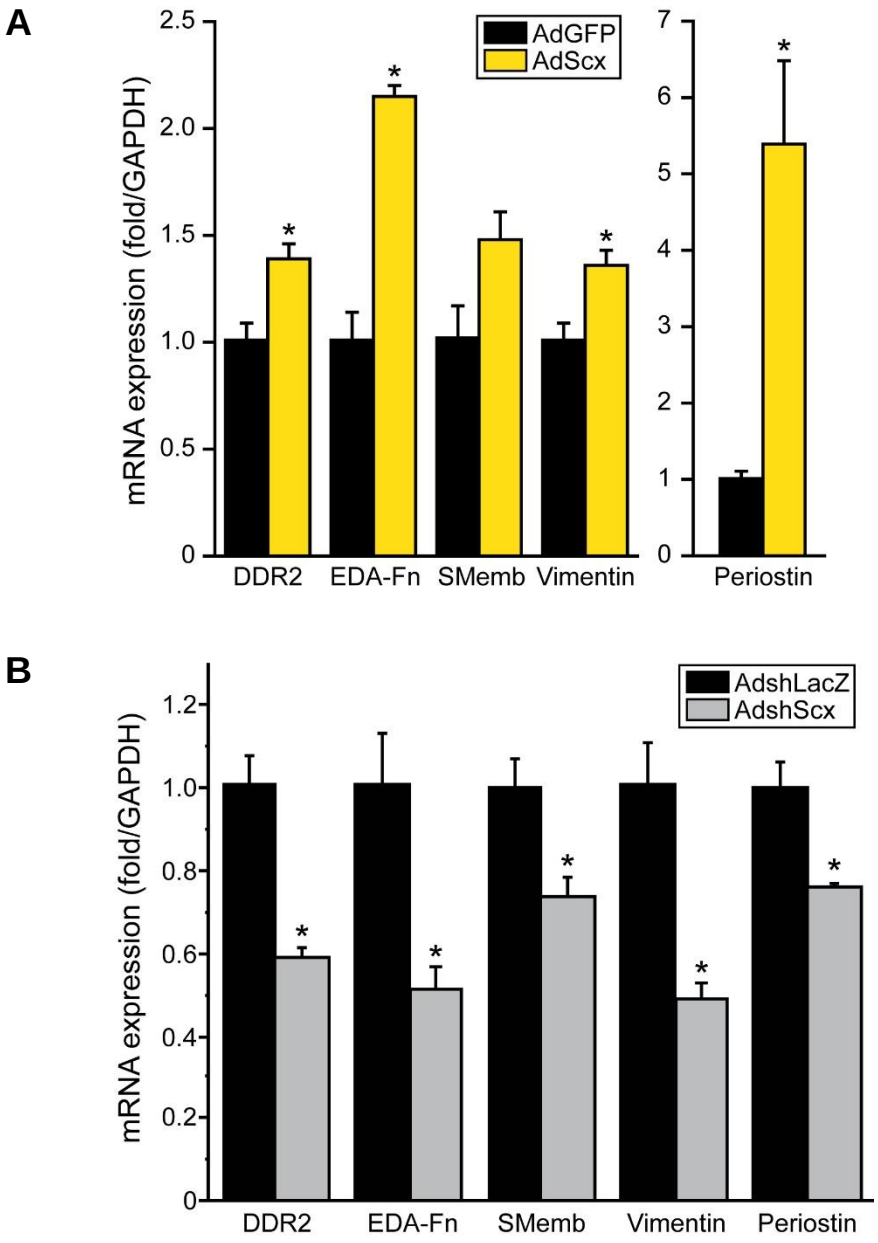

Figure 20: Regulation of fibroblast/myofibroblast markers gene expression by scleraxis.

Fibroblast/myofibroblast marker gene mRNA expression was assayed in primary cardiac proto-myofibroblasts following scleraxis over-expression (AdScx) vs controls (AdGFP) **(A)**, or following knockdown of scleraxis (AdshScx) compared to controls (AdshLacZ) **(B)**; n=3-4, *P<0.05 vs AdGFP **(A)** or vs AdshLacZ **(B)**.

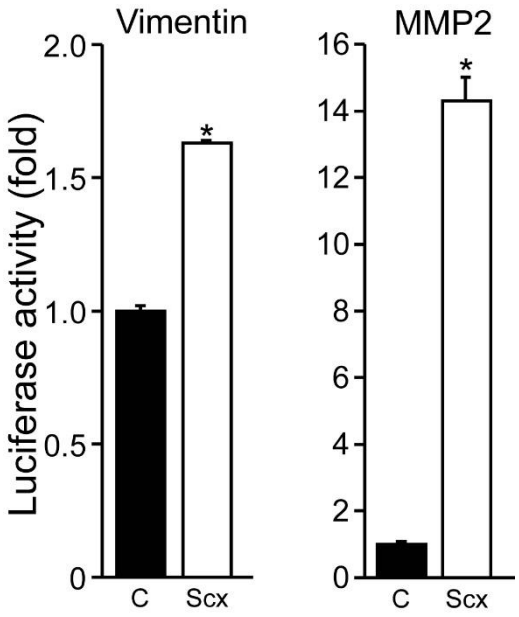

Figure 21: Transactivation of human vimentin and MMP2 gene promoters by scleraxis.

Scleraxis (Scx) transactivation of the human vimentin and MMP2 gene promoters was determined by luciferase reporter assays in NIH-3T3 fibroblasts. Cells transfected with plasmids (Scx:pECE or pECE) were lysed 24h post-transfection and luciferase activity was assayed. n=3-4, *P<0.05 vs control empty vector (C).

3.2: Effect of scleraxis double-deletion mutant (ScxΔΔ) on COL1A2 gene activation and target gene expression

Scleraxis, similar to other bHLH transcription factors, regulates target gene expression via direct interaction with consensus *cis* E boxes within DNA promoter sequences [172, 173]. We previously showed that scleraxis' basic DNA-binding domain and its helix-loop-helix protein-binding domain are functionally critical: deletion of the basic domain resulted in a dominant negative mutant that attenuated myofibroblast type I collagen expression [172, 173]. A scleraxis mutant lacking both domains (ScxΔΔ) did not transactivate a human COL1A2 gene promoter reporter, and failed to attenuate scleraxis-mediated transactivation, suggesting that this double mutant is transcriptionally inactive (Fig. 22). ScxΔΔ was further unable to alter the expression of fibrillar collagens or fibroblast/myofibroblast markers in proto-myofibroblasts, indicating that the transcriptional activity of scleraxis is required for regulating the expression of these genes in agreement with our scleraxis gene knockdown outcomes (Fig. 23).

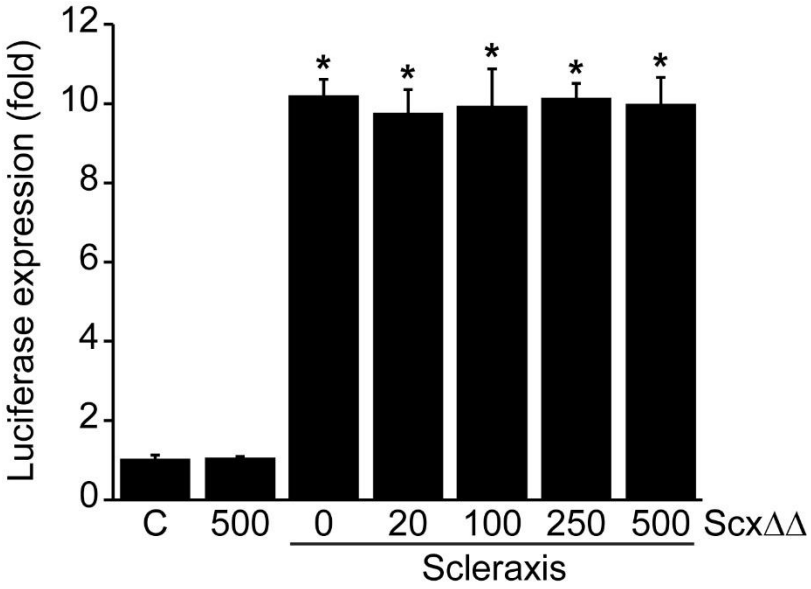

Figure 22: A scleraxis double deletion mutant (ScxΔΔ) has no effect on human COL1A2 promoter activation.

NIH 3T3 fibroblasts were transfected with a human COL1A2 proximal promoter luciferase reporter vector, with or without expression vectors for intact scleraxis (500 ng) or encoding a scleraxis mutant lacking the DNA- and protein-binding domains (ScxΔΔ; 0-500 ng), plus a Renilla luciferase reporter (pRL) for normalization. Twenty-four hours later, cell lysates were collected for luciferase assay. Intact scleraxis transactivated the COL1A2 promoter. In contrast, the ScxΔΔ mutant had no effect either alone or with co-transfected intact scleraxis. Results were normalized to control (C; reporter alone); mean±SEM; n=3; *P<0.05 vs control.

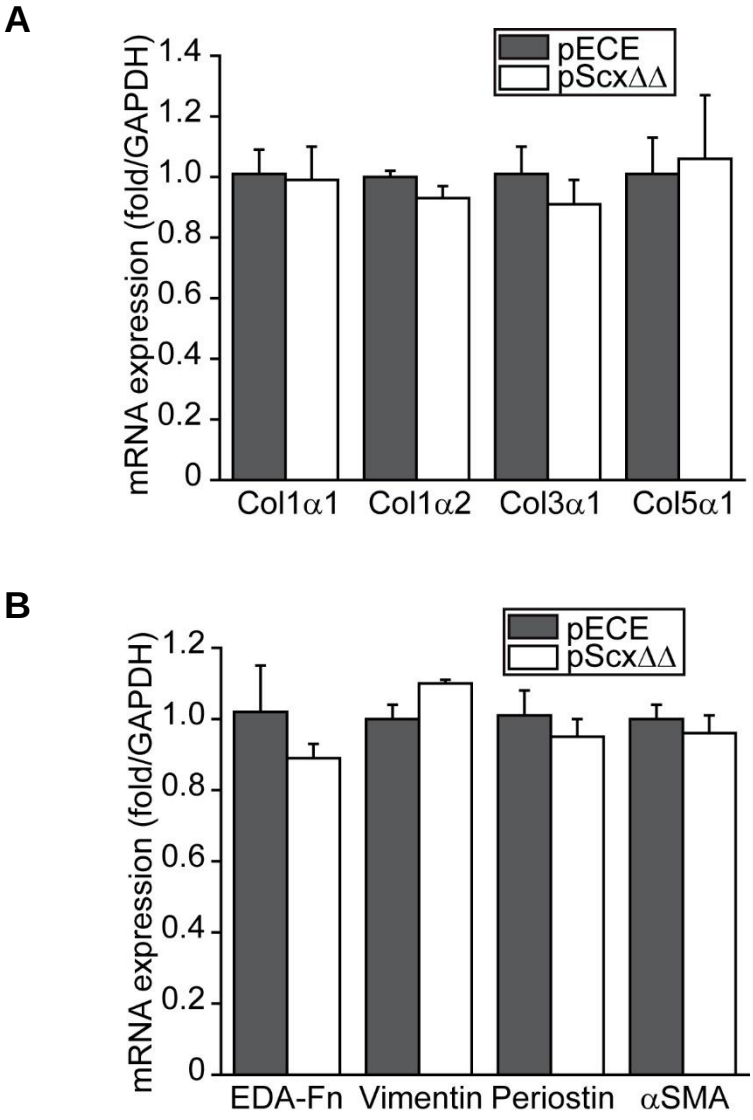

Figure 23: A scleraxis double deletion mutant fails to regulate target gene expression.

Primary cardiac proto-myofibroblasts were transfected by electroporation with an expression vector encoding the scleraxis double mutant (pScxΔΔ) or with control empty vector (pECE). Twenty-four hours later, mRNA expression of fibrillar collagen gene expression **(A)** or (myo)fibroblast markers **(B)** was assayed by qPCR. Results were normalized to the control empty vector and GAPDH expression; mean±SEM; n=3; P>0.05 for all comparisons.

3.3: Effect of scleraxis on cardiac fibroblast α-smooth muscle actin (αSMA) expression

Scleraxis expression and transcriptional activity correlated with both myofibroblast markers and fibrillar collagens in our gain and loss-of-function studies. Hence we then examined the effect of scleraxis on expression of αSMA, a contractile protein that is not typically expressed in cardiac fibroblasts. The expression of this protein is significantly induced during conversion of cardiac fibroblasts to myofibroblasts [100, 173]. Scleraxis overexpression in cardiac proto-myofibroblasts induced the expression of αSMA in these cells (Fig. 24A, B). However, scleraxis knockdown in primary cardiac proto-myofibroblasts reduced αSMA expression (Fig. 24C, D). The *de novo* synthesis of αSMA and its incorporation into stress fibers was also evident in cells where scleraxis was overexpressed (Fig. 25) - this is a distinct characteristic of maturation of fibroblasts to myofibroblasts [103].

3.4: Scleraxis regulates α-SMA expression via direct interaction with E-boxes on its proximal gene promoter

Scleraxis, similar to other bHLH transcription factors, regulates target gene expression via binding to E-boxes in the target gene promoters [172, 173]. Since scleraxis was both sufficient and necessary for αSMA expression, we tested whether αSMA is directly regulated by scleraxis. The rat αSMA proximal gene promoter contains two well-characterized E boxes critical for cis regulation, one of which is perfectly conserved in humans and mice (Fig. 26A) [366, 367]. In agreement with our

overexpression data, scleraxis strongly and significantly transactivated the rat αSMA proximal gene promoter as determined by luciferase gene reporter assays (Fig. 26B). Mutating these E-boxes attenuated the αSMA promoter transactivation mediated by scleraxis (Fig. 26B). This supported our contention of the direct regulation of the αSMA gene by scleraxis.

Electrophoretic mobility shift assay demonstrated that scleraxis forms complexes with both E boxes (Fig. 27A). This interaction is destroyed when the E-boxes are mutated. Chromatin immunoprecipitation (ChIP) assay was performed to confirm this interaction. But due to the close proximity of the two E-boxes with only 32 nucleotides distance between the two putative scleraxis-binding sites, resolution of the individual interactions was not possible. A scleraxis-DNA complex within the region encompassing these E-boxes was detected in primary cardiac fibroblasts (Fig 27B). This interaction was significantly enhanced in mature cardiac myofibroblasts by more than three-fold when compared to fibroblasts (Fig 27B). These findings are consistent with increased scleraxis-mediated αSMA expression during phenotype conversion. In a previous study using mesangial cells, it was demonstrated that scleraxis was capable of binding only to the second E box, resulting in an inhibitory effect on αSMA expression [368]. Although divergent to this report, our results indicate that prediction of scleraxis activity across cell types cannot be readily predicted and requires empirical testing.

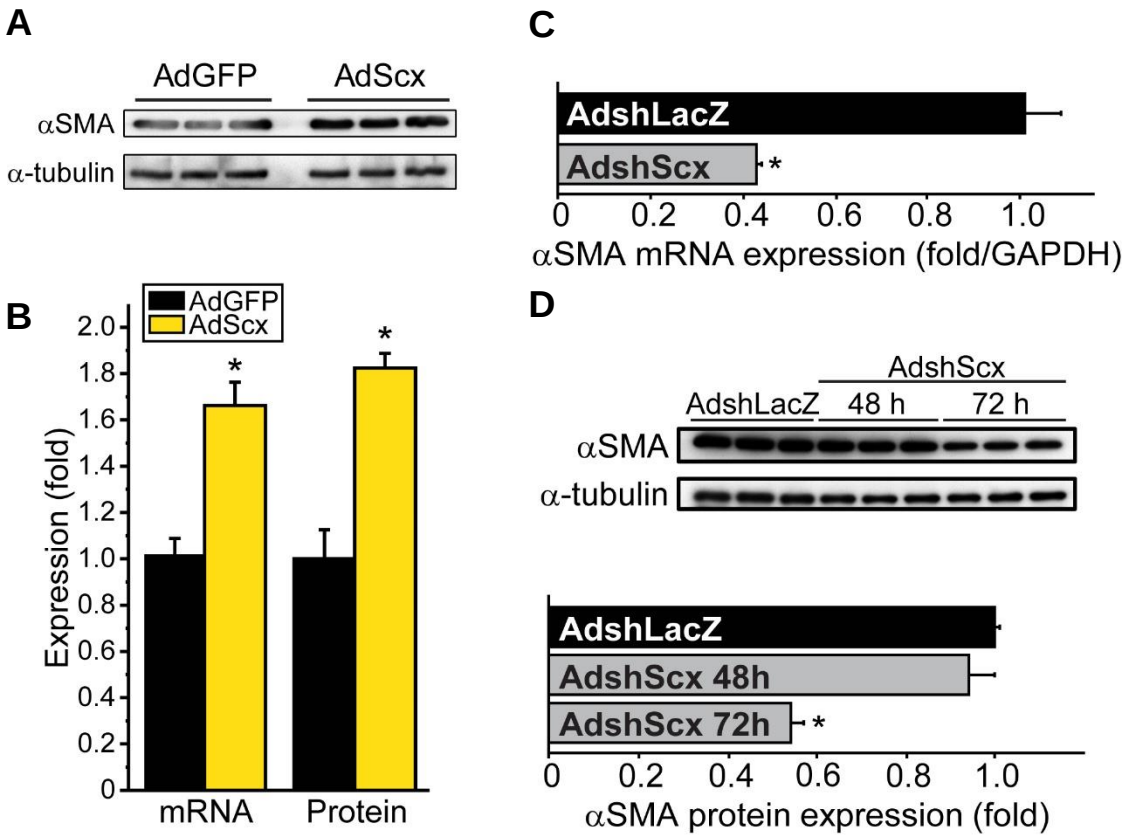

Figure 24: Scleraxis induces cardiac myofibroblast α-smooth muscle actin expression.

(A-B) The effect of scleraxis over-expression (AdScx) on αSMA expression in primary rat cardiac proto-myofibroblasts was determined by mRNA analysis or immunoblotting. n=3, *P<0.05 vs AdGFP. **(C-D)** αSMA mRNA **(C)** and protein **(D)** expression was assayed following knockdown of scleraxis (AdshScx) in primary cardiac proto-myofibroblasts compared to control (AdshLacZ); n=3, *P<0.05 vs AdshLacZ.

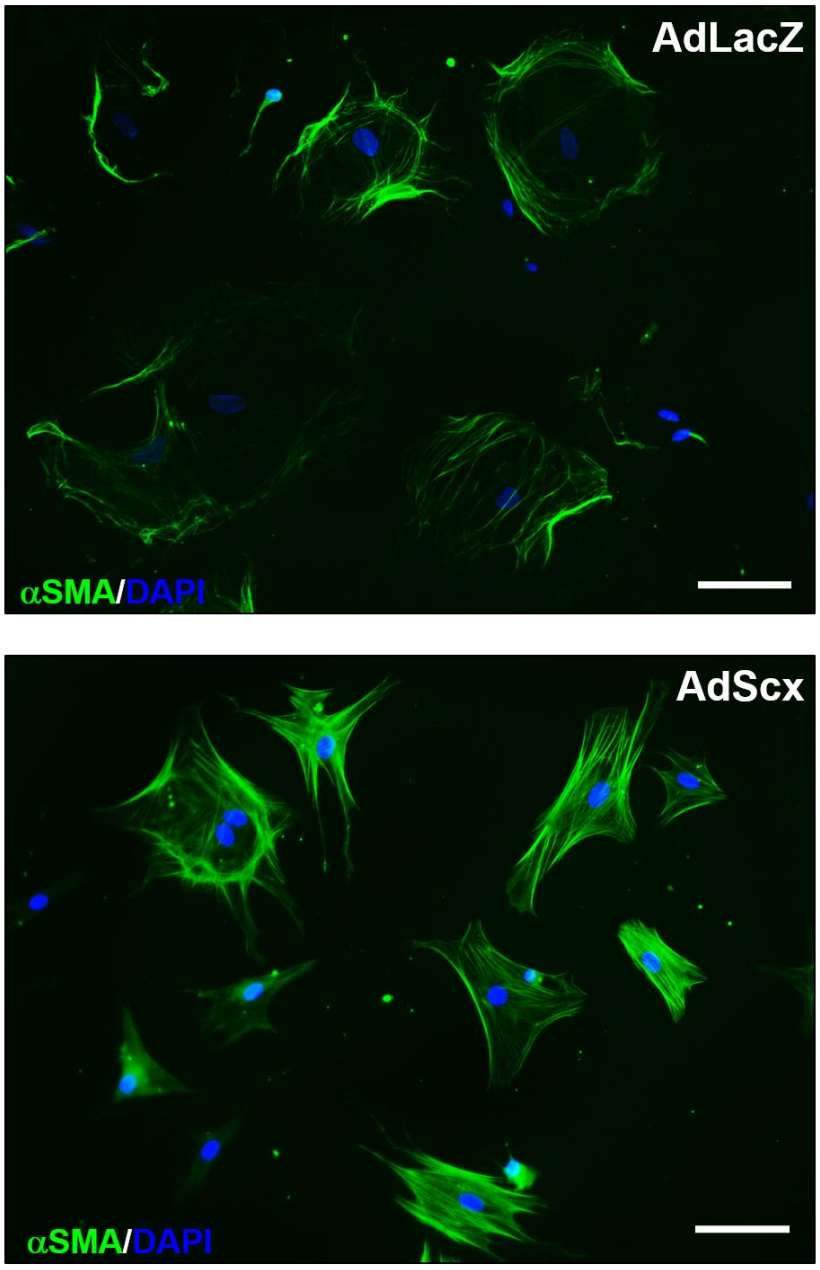

Figure 25: Scleraxis overexpression results in incorporation of αSMA into stress fibers.

The effect of scleraxis overexpression (AdScx) on αSMA expression in primary rat cardiac proto-myofibroblasts was determined by immunocytochemistry. Magnification 20X; scale bar = 70 μm. αSMA^{+} stress fibers are seen in response to scleraxis gene induction.

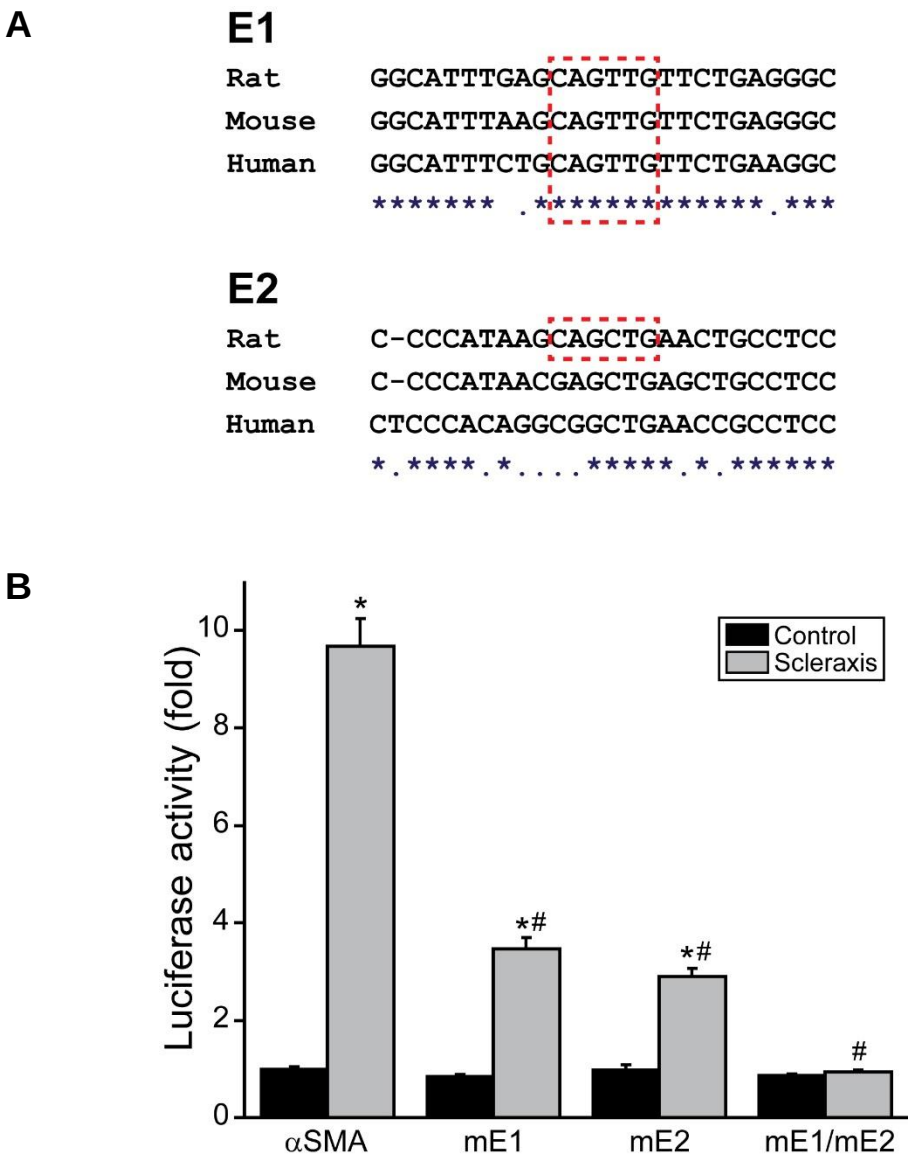

Figure 26: Identification of scleraxis binding sites in the α-smooth muscle actin proximal gene promoter.

(A) Alignment of putative scleraxis-binding E boxes (E1 and E2; dashed lines) in the proximal rat, mouse and human αSMA promoters. Asterisks and periods denote nucleotides conserved across three or two species, respectively. **(B)** Transactivation of the rat αSMA proximal promoter without or with mutation of one or both E boxes (mE1, mE2); n=3, *P<0.05 vs control empty vector; #P<0.05 vs scleraxis + intact promoter.

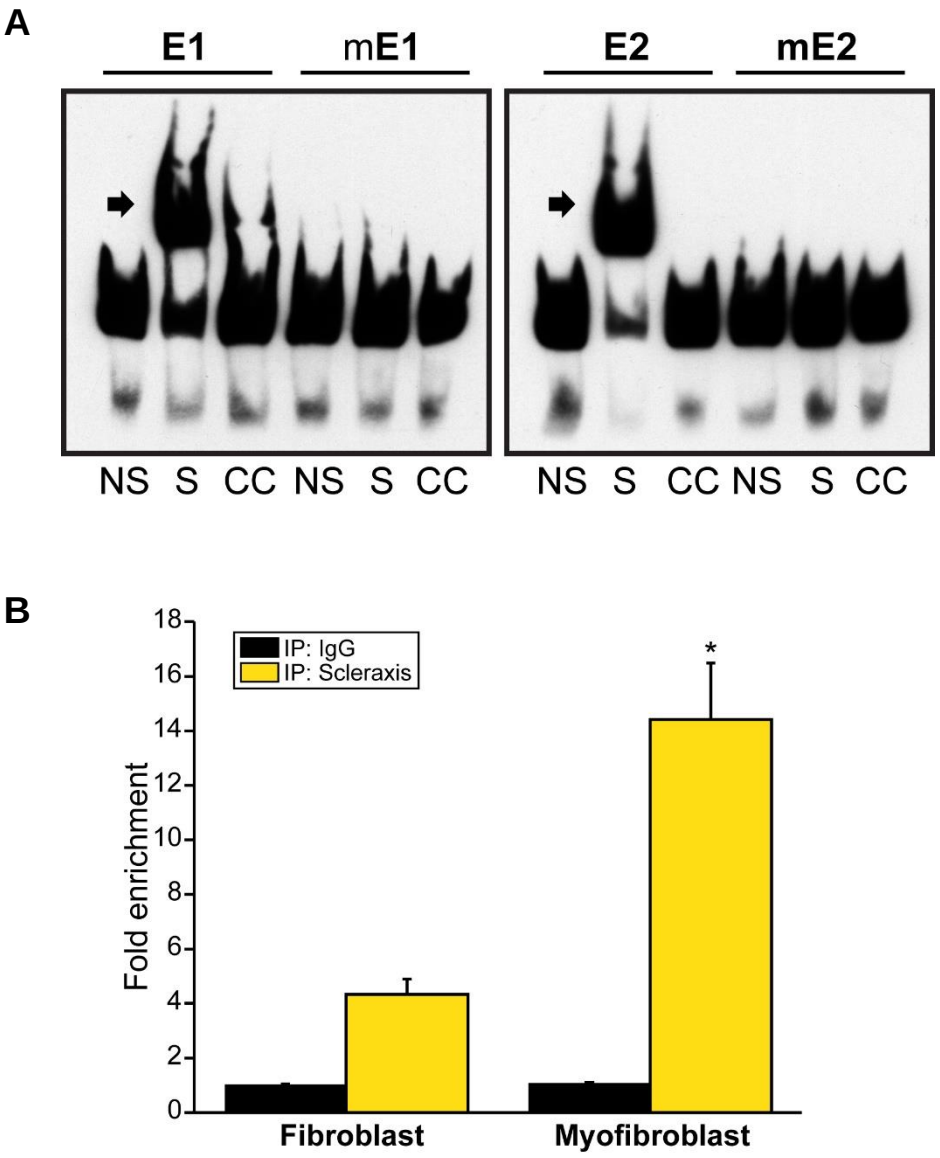

Figure 27: Direct interaction of scleraxis with E-boxes in αSMA proximal gene promoter.

(A) Electrophoretic mobility shift assays were performed for E-boxes E1 and E2 or corresponding mutations mE1 and mE2. NS, non-shifted lane; S, shifted lane; CC, 500x cold competition. Arrow denotes shifted complex. **(B)** Chromatin immunoprecipitation assay of freshly isolated rat cardiac fibroblasts or myofibroblasts was followed by qPCR quantification of scleraxis-bound DNA; n=3, *P<0.05 vs P0.

4. Regulation of cardiac ECM gene expression *in vivo* by scleraxis

4.1: Cardiac phenotype and function in mice with congenital loss of scleraxis

Scleraxis gene deletion was previously reported to induce cardiac structural anomalies including altered valve structure, a rounding of the ventricles and involution of the apex [307]. The pathological ramifications of this in still unclear. In concert with previous reports, we noticed that mating of scleraxis heterozygous mice resulted in under-representation of homozygous null pups at birth [307]. Of 438 pups born, we identified 42 (9.5%) nulls (KO), 261 (59.0%) heterozygotes and 139 (31.4%) wild type (WT) mice. Further, we noted that 10/42 (23.8%) of the null pups died prior to 6 weeks of age. KO mice were significantly runted compared to their WT littermates (Fig. 28A). We also noticed a significant cardiac hypotrophy (~30%) in KO mice compared to WT with heart weights normalized to corresponding tibia lengths (Fig. 28B). Despite this decreased relative size, echocardiographic analysis revealed largely normal systolic and diastolic function (Table 8), in agreement with data from Lincoln's group [307]. Left ventricular end diastolic diameter (LVEDD), normalized to tibia length, was modestly (~10%) but significantly elevated in scleraxis null mice, while endocardial velocity (V_{endo}) trended lower, suggesting the existence of early stage systolic dysfunction, however such modest changes seem unlikely to contribute to the elevated mortality in KO mice, the reasons for which remain unclear.

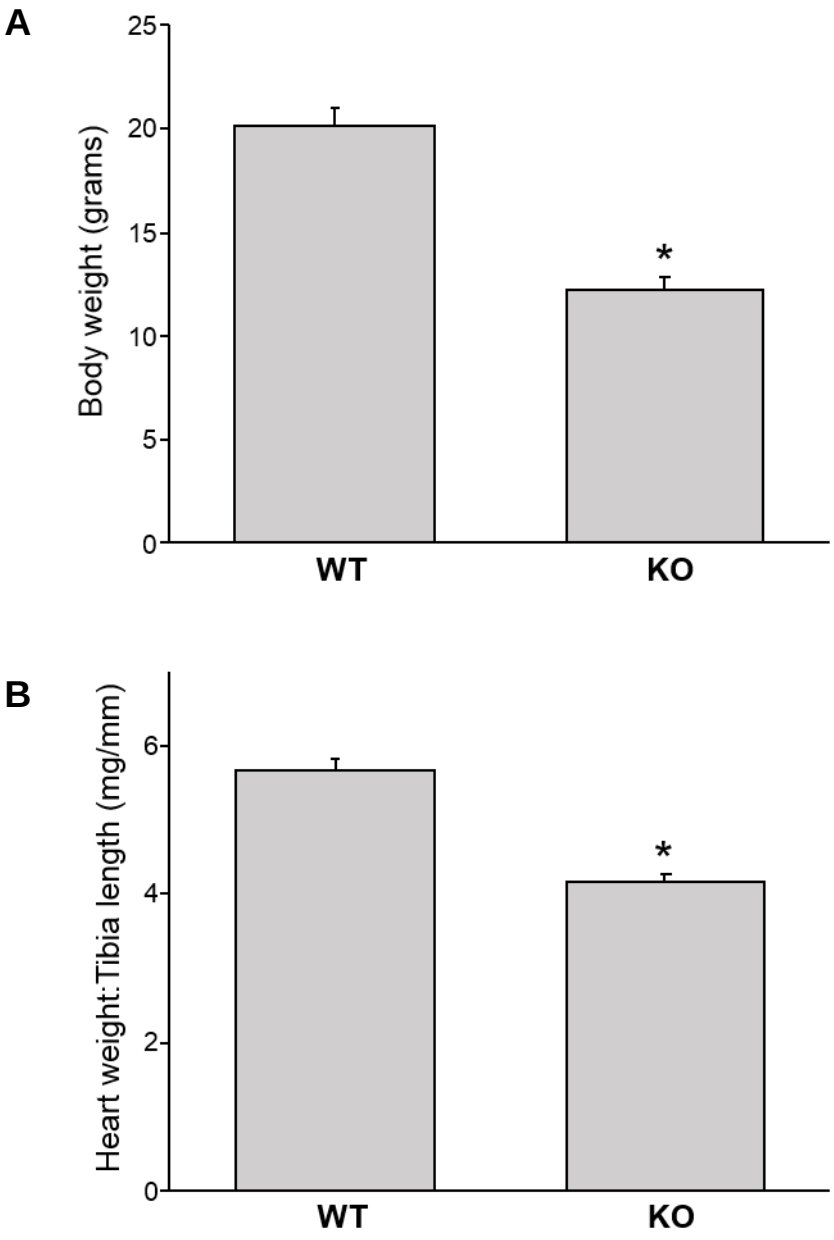

Figure 28: Scleraxis KO mice are runted and exhibit cardiac hypotrophy.

(A) Scleraxis null (KO) mice are runted in size compared to their WT littermates. n=9-12; *P<0.0001. **(B)** KO hearts exhibit significant hypotrophy compared to WT counterparts. Data represents heart weight (mg) normalized to tibia length (mm); n=17-20; *P<0.0001.

Table 8: Echocardiographic parameters of scleraxis KO mice.

Parameter	Wild type (WT)	Scleraxis null (KO)
LVEF (%)	80±1	80±1
HR (bpm)	671±9	679±10
FS (%)	50±1	50±1
LVEDD/TL	0.153±0.003	0.166±0.004*
LVESD/TL	0.077±0.002	0.082±0.003
PWT/TL	0.048±0.001	0.047±0.001
IVS/TL	0.047±0.001	0.045±0.001
V_{endo} (cm/s)	2.2±0.08	2.0±0.06 (P=0.0541)
SR (s^{-1})	18±1	17±1
MV E (m/s)	929±79	882±85
MV A (m/s)	544±35	618±79
E/A	1.71±0.22	1.81±0.27
DT (msec)	27±2	28±5

*P<0.05

LVEF, left ventricular ejection fraction; HR, heart rate; FS, fractional shortening; TL, tibia length; LVEDD, left ventricular end diastolic diameter; LVESD, left ventricular end systolic diameter; PWT, posterior wall thickness; IVS, interventricular septal thickness; Vendo, endocardial velocity; SR, strain rate ; MV E, early diastolic flow velocity; MV A, late diastolic inflow velocity; E/A, ratio of the mitral E to A waves; DT, deceleration time.

4.2: Cardiac ECM gene expression profile as a consequence of congenital loss of scleraxis in mice

We have previously shown that cardiac fibroblast type I collagen gene expression requires intact scleraxis signaling [172, 173]. We thus hypothesized that the cardiac morphological defects in knockout mice may result from alterations in fibrillar collagen and/or extracellular matrix content. To gain a global overview of the gene expression changes resulting from scleraxis knockout, we performed DNA microarray analysis of wild type or knockout mouse hearts. A number of extracellular matrix-associated genes exhibited significant differences between these samples (Table 9). Using the DAVID (Database for Annotation, Visualization and Integrated Discovery) Bioinformatics Resources 6.7, we identified gene ontology pathway terms whose members were enriched in our dataset (1771 genes up- or down-regulated by 2-fold or greater, with $P<0.05$) to a statistically-significantly greater degree than would be expected by chance [369, 370]. Of note, the top five terms included ECM-receptor interaction, focal adhesion and regulation of actin cytoskeleton (Table 10). Other gene ontology terms highlighted by this analysis included cell adhesion molecules (2.0-fold enrichment; $P=0.0012$) and TGF-β signaling pathway (2.2-fold enrichment; $P=0.0064$).

Table 9: Microarray analysis of scleraxis null hearts.

Total cardiac RNA from WT or scleraxis KO mice was analyzed by Affymetrix DNA microarrays. Results for fibrillar collagens and fibroblasts markers are listed for Affymetrix Probe IDs exhibiting at least a 2-fold change in expression between samples.

Probe ID	Gene symbol	Gene name	Fold-change
1456658_at	Acta2	Actin, alpha 2, smooth muscle, aorta	-2.1
1455494_at	Col1a1	Collagen, type I, alpha 1	-2.1
1427884_at	Col3a1	Collagen, type III, alpha 1	-2.2
1441057_at	Myh10	Myosin, heavy polypeptide 10, non-muscle (SM_{emb})	-2.2
1450857_a_at	Col1a2	Collagen, type I, alpha 2	-2.5
1423110_at	Col1a2	Collagen, type I, alpha 2	-3.0
1418122_at	Myh11	Myosin, heavy polypeptide 11, smooth muscle	-4.3

Table 10: Pathway enrichment in hearts of scleraxis null mice.

Genes identified by microarray analysis to be significantly up- or down-regulated (≥2-fold) were analyzed with the DAVID Bioinformatics Resources (http://david.abcc.ncifcrf.gov). A subset of the results is presented in descending order of the calculated Modified Fisher Exact P-Value. Pathway names and their corresponding Kyoto Encyclopedia of Genes and Genomes (KEGG) term identifiers represent gene ontological pathway clusters whose members are significantly over-represented in the microarray dataset compared to the background mouse genome.

Pathway	KEGG Term	Fold-enrichment	P Value
ECM-receptor interaction	mmu04512	4.66	9.31E-13
Focal adhesion	mmu04510	2.67	9.32E-09
Regulation of actin cytoskeleton	mmu04810	2.02	1.12E-04
Cell adhesion molecules	mmu04514	2.01	0.00156
Vascular smooth muscle contraction	mmu04270	2.04	0.00467
TGFβ signaling pathway	mmu04350	2.22	0.00644

4.3: Requirement of scleraxis for normal cardiac ECM gene expression in vivo

Given the gene and pathway changes highlighted by microarray analysis, we examined net fibrillar collagen expression using picrosirius red and Masson's trichrome staining of cardiac tissue sections from wild type or scleraxis knockout mice. Both methods demonstrated a clear diminution in collagen staining, congruent with the microarray analysis results (Fig. 29A, B). Notably, larger diameter collagen fibrils appeared to be diminished in number, and there was considerable reduction of perivascular collagen staining (Fig. 29C). Cardiac ECM dry weight, normalized to cardiac mass or tibia length, was reduced by 36% or 49%, respectively (Fig. 30).

The mRNA expression of various collagens in wild type and knockout hearts was assayed by quantitative real time PCR (qPCR). Intriguingly, the major fibrillar collagen isoforms expressed in the heart (Col1α1, Col1α2 and Col3α1), as well as fibrillar Col5α1, all exhibited a 30-45% reduction in mRNA expression (Fig. 31A). Western blotting confirmed a significant loss of type I and III collagens (Fig. 31B). Conversely, non-fibrillar Col4α1 expression was unaffected by scleraxis gene deletion, suggesting that scleraxis deletion specifically perturbs fibrillar collagen expression, and our results do not represent a general effect on collagen gene expression.

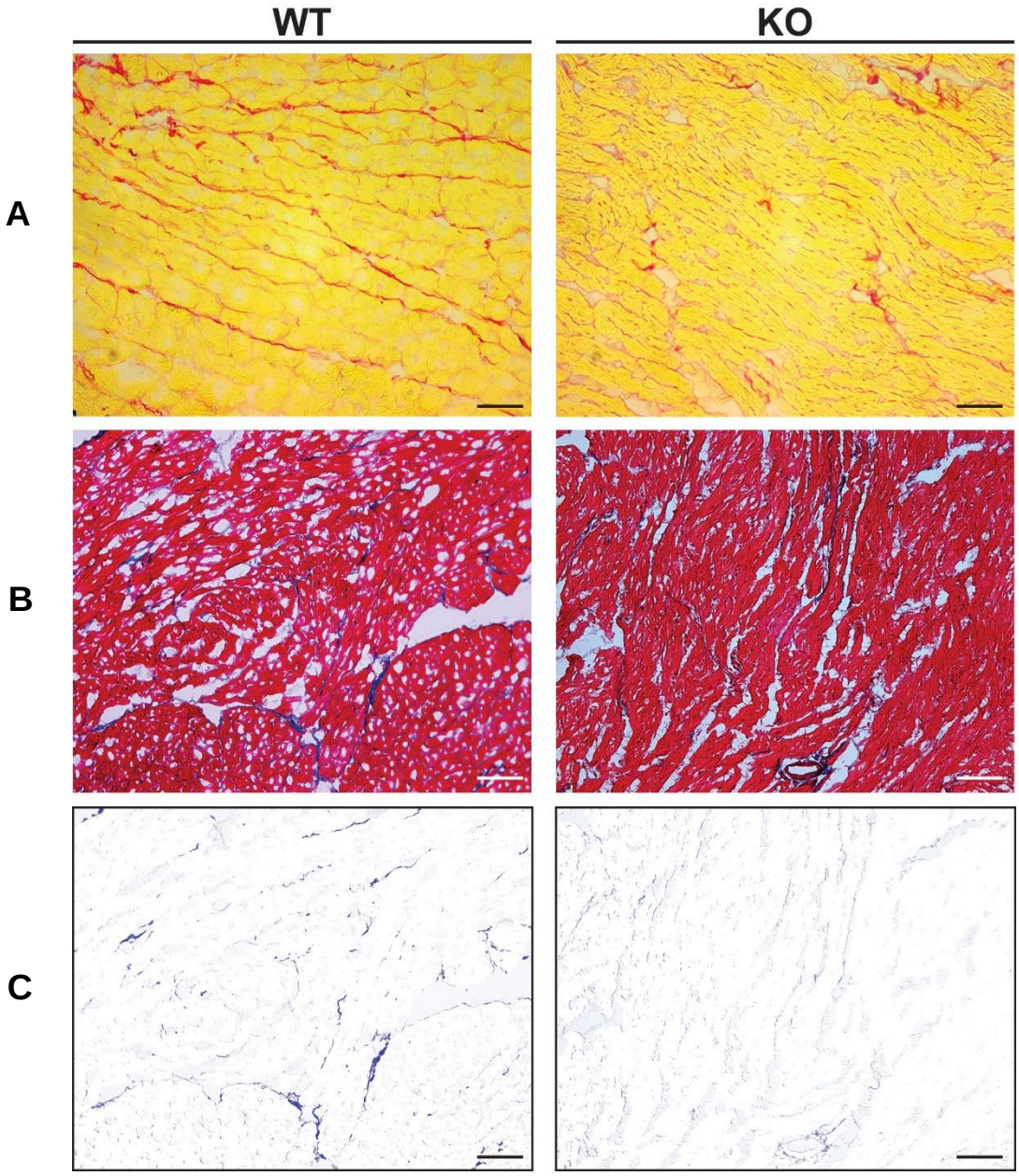

Figure 29: Reduced fibrillar collagen deposition in scleraxis null mice.

Cross sections of hearts from wild type (WT) or scleraxis null (KO) hearts were fixed and stained for fibrillar collagen using picrosirius red **(A)** or Masson's trichrome **(B)**. A generalized decrease in collagen deposition in KO hearts is observed compared to WT (reduced red staining in A; reduced blue staining in B). **(C)** The blue color channel was extracted from the Masson's trichrome sections for improved visualization.

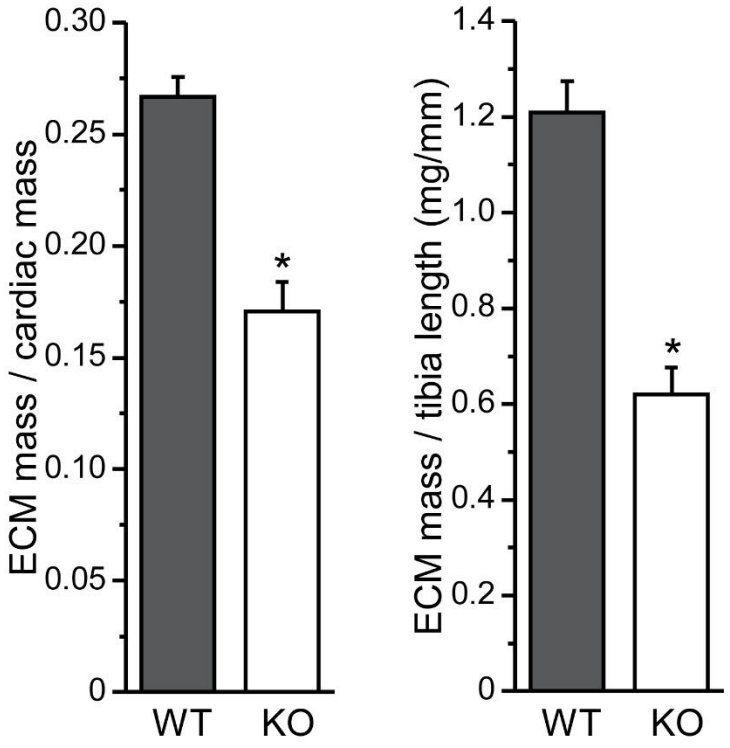

Figure 30: Cardiac ECM dry weight is significantly decreased in scleraxis KO mice.

Decellularized and dehydrated cardiac ECM from WT or KO mice was weighed and the resulting values were normalized to cardiac mass or tibia length; n=7, *P<0.05 vs WT.

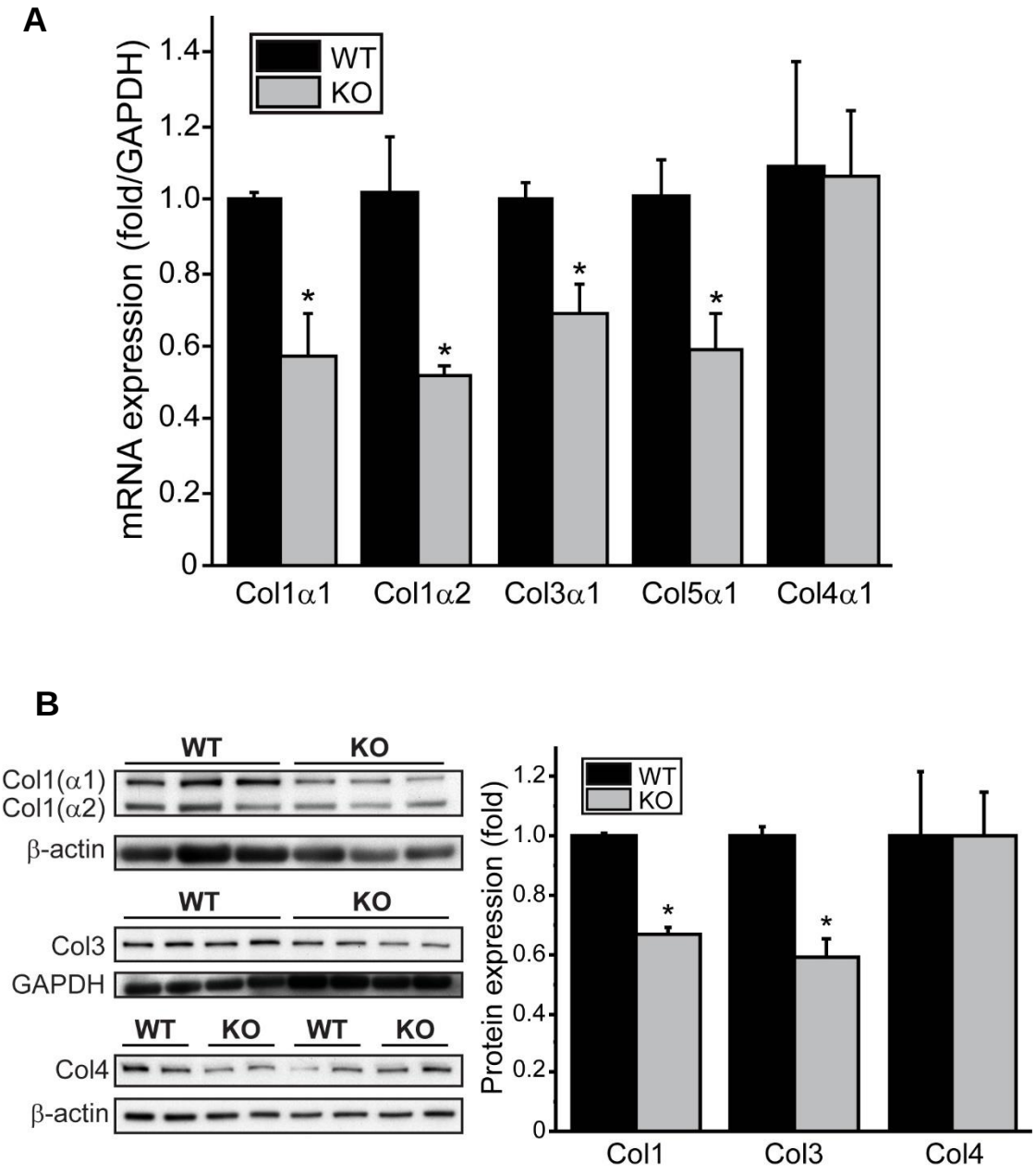

Figure 31: Myocardial fibrillar collagen gene expression is regulated by scleraxis.

(A) Quantification of fibrillar and non-fibrillar (*Col4α1*) collagen gene expression by qPCR in WT or scleraxis KO hearts. Results were normalized to GAPDH and the respective WT sample; n=3, *P<0.05 versus WT. **(B)** Collagen protein expression in WT and KO hearts, with quantification. Collagen 1 expression was determined as the sum of the α1 and α2 isoforms. Results were normalized to β-actin or GAPDH and the respective WT sample; n=3-4, *P<0.05 versus WT.

We examined expression of the other major component of cardiac extracellular matrix, i.e. proteoglycans. We noted a generalized decrease in proteoglycan expression in the hearts of scleraxis null mice compared to wild type, with significant loss of fibromodulin, versican and biglycan (Fig. 32). Lumican exhibited a trend towards reduced expression, although this did not reach statistical significance in our study. Conversely, decorin expression was undisturbed, demonstrating that proteoglycan loss was not universal.

MMPs are well-established regulators of ECM degradation, thus we hypothesized that MMP expression may also be governed by scleraxis. KO hearts exhibited significantly reduced mRNA expression of the gelatinases MMP2 and MMP9, as well as the stromelysin MMP3, while MMP11 was unaffected (Fig. 33A). This down-regulation correlated with a generalized loss of activity of both the mature and latent (pro) forms of MMP2 and MMP9 (Fig. 33B). Together, our data demonstrated that scleraxis gene deletion *in vivo* resulted in altered expression of collagen, proteoglycans and MMPs that closely recapitulated our *in vitro* knockdown data.

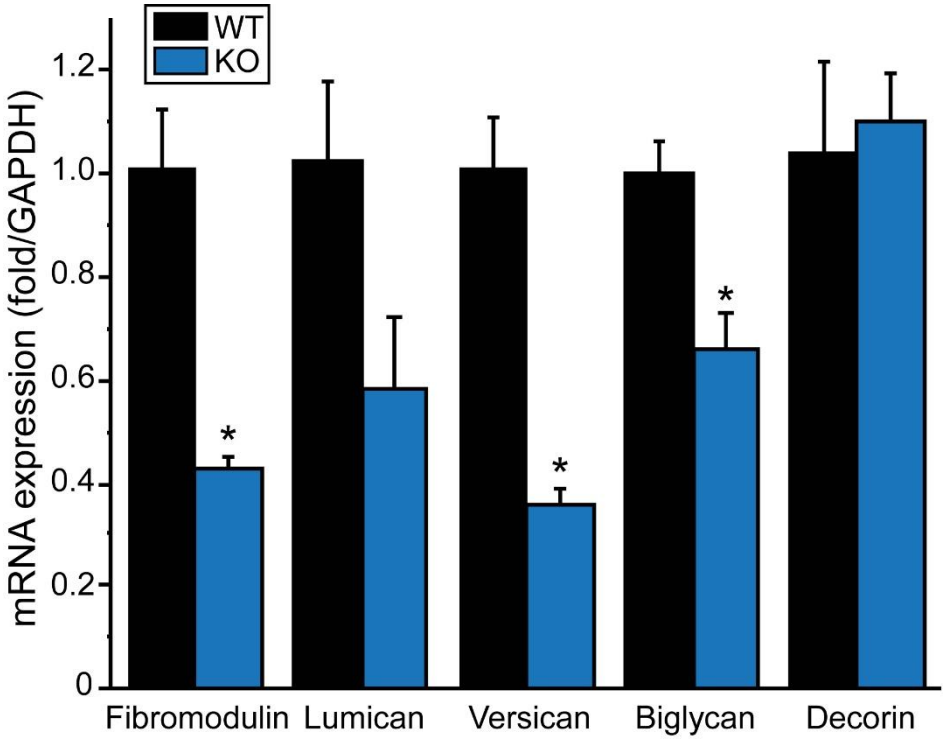

Figure 32: Proteoglycan gene expression is regulated by scleraxis in the myocardium.

Quantification of proteoglycan gene expression was done using qPCR in WT or scleraxis KO hearts. Results were normalized to GAPDH and the respective WT sample; n=3, *P<0.05 versus WT.

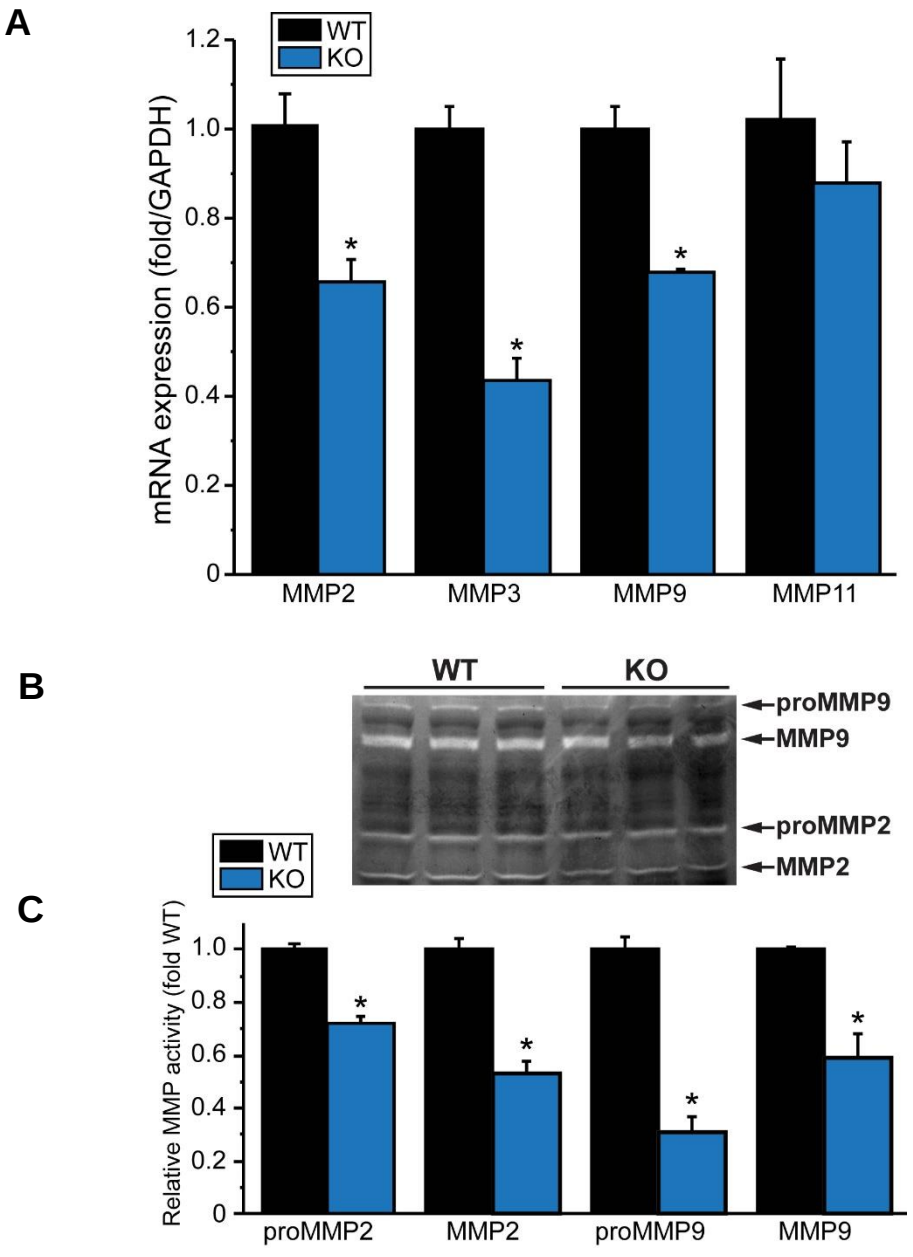

Figure 33: Cardiac MMP gene expression is regulated by scleraxis.

(A) Quantification of MMP gene expression by qPCR in WT or scleraxis KO hearts. Results were normalized to GAPDH and the respective WT sample; n=3, *P<0.05 versus WT. **(B)** Cardiac protein lysates from WT or scleraxis KO animals were assayed by gel zymography to reveal MMP2 and MMP9 activity (latent pro-form and mature). Results are quantified in **(C)**; n=3, *P<0.05 versus WT.

4.4: Assessment of cardiac fibroblast phenotype marker expression in scleraxis null mice

The ability of scleraxis to regulate cardiac fibroblast phenotype is evident from our *in vitro* experiments (Fig. 24-25). Here we assayed the expression of a panel of fibroblast and myofibroblast cell markers in wild type and scleraxis null hearts. All markers tested, including DDR2, EDA-Fn, SM_{emb} and vimentin, were significantly down-regulated following scleraxis deletion, with a >50% decrease in mRNA expression in all markers (Fig. 34). Similar to other markers of fibroblastic cells, we observed a significant loss of αSMA protein expression in scleraxis null hearts (Fig. 34B). This is in agreement with our data demonstrating direct regulation of αSMA expression by scleraxis (Fig. 26-27). This likely reflects changes in the vascular smooth muscle cell population since αSMA is not expressed in cardiac fibroblasts in the healthy heart except in cardiac valves.

4.5: Rescue of target gene expression in scleraxis null proto-myofibroblasts by scleraxis transgene delivery

We tested whether scleraxis was sufficient to rescue gene expression by over-expressing scleraxis in cardiac proto-myofibroblasts from WT and KO mice via adenoviral transgene delivery. As expected, KO cells exhibited virtually no scleraxis expression, but Ad-Scx drove scleraxis to ~6-fold of WT expression (Fig. 35). The significant loss of *Col1a1*, *Col1a2*, *Col3a1*, *vimentin* and *αSMA* observed in these cells was similarly rescued to levels above WT cells (Fig. 35). Thus, loss of expression

of these genes in scleraxis null cells is not due to a generalized defect in the gene expression mechanism, but rather is specific to the loss of scleraxis.

In the previous section, and in [172], we demonstrated the existence of a synergistic interaction between scleraxis and Smad3 in regulating *Col1α2* expression. In fact, deletion of scleraxis binding sites in the *Col1α2* promoter dramatically attenuated Smad3 transactivation of this promoter [172]. Here we examined the impact of scleraxis knockdown on Smad3-mediated collagen gene expression in primary proto-myofibroblasts. Smad3 induced expression of the fibrillar collagens *Col1α1*, *Col1α2* and *Col3α1* as anticipated. This Smad3-mediated effect was significantly blunted following scleraxis gene knockdown (Fig. 36A). Using chromatin immunoprecipitation assay, we observed that Smad3 binding to the Smad Binding Element in the murine *Col1α2* gene proximal promoter was significantly reduced in scleraxis KO hearts compared to WT (Fig. 36B). Together, these results indicate that Smad3 signaling is blunted in the absence of scleraxis, supporting our *in vitro* data [172].

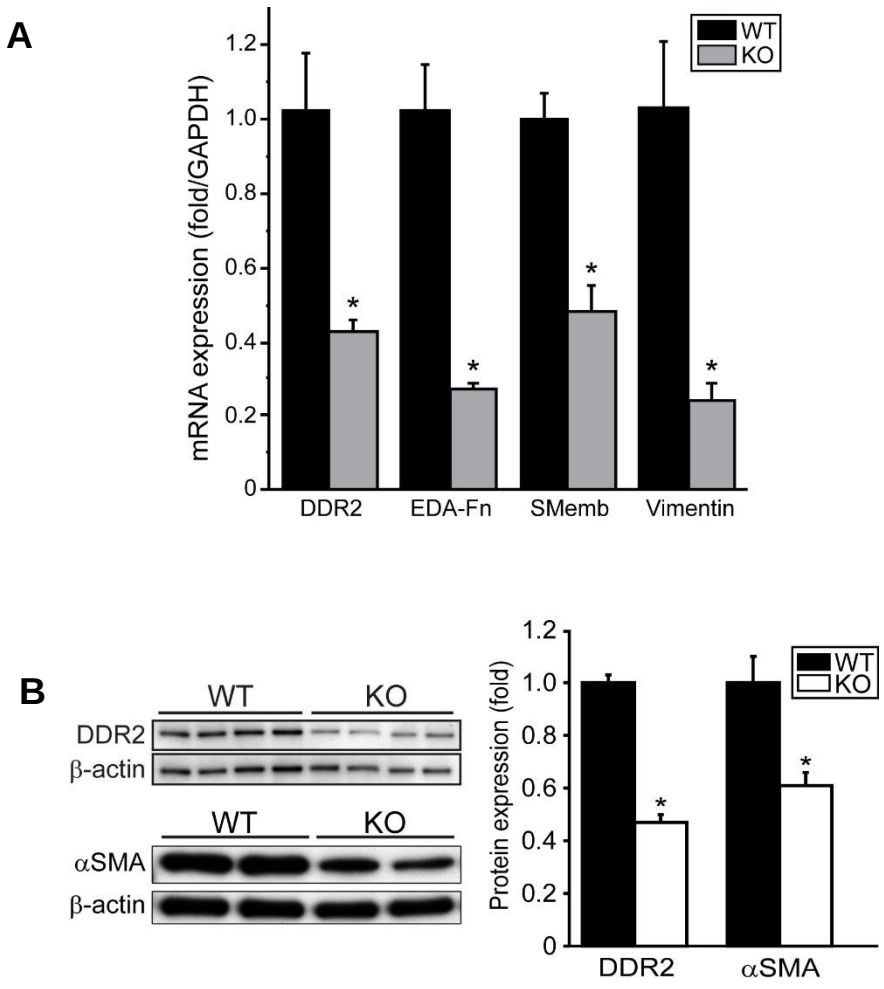

Figure 34: Scleraxis regulates cardiac fibroblast marker gene expression.

Fibroblast/myofibroblast marker gene mRNA **(A)** and protein **(B)** expression was assayed in WT and scleraxis KO mice by qPCR and immunoblotting respectively, normalized to GAPDH or β-actin; n=3-4, *P<0.05 vs WT.

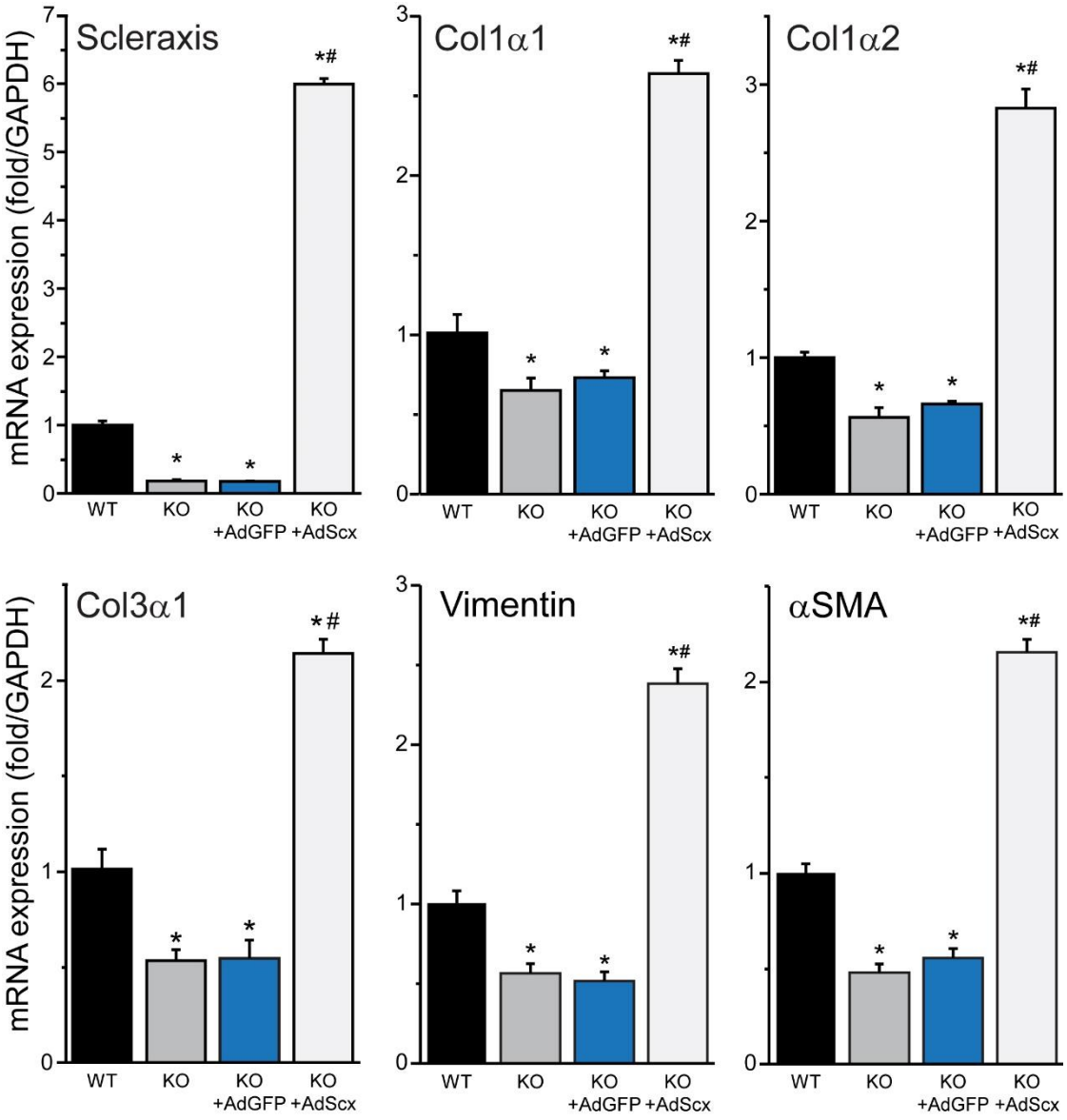

Figure 35: Rescue of putative scleraxis target gene expression in null cardiac proto-myofibroblasts.

Primary rat cardiac proto-myofibroblasts obtained from wild type (WT) or scleraxis null (KO) mice were untreated, or null cells were infected with adenovirus encoding scleraxis (AdScx) or GFP (AdGFP) for 24 h and mRNA expression of scleraxis or fibrillar collagens assayed by qPCR normalized to GAPDH; n=3, *P<0.05 vs WT; #P<0.05 vs KO+AdGFP.

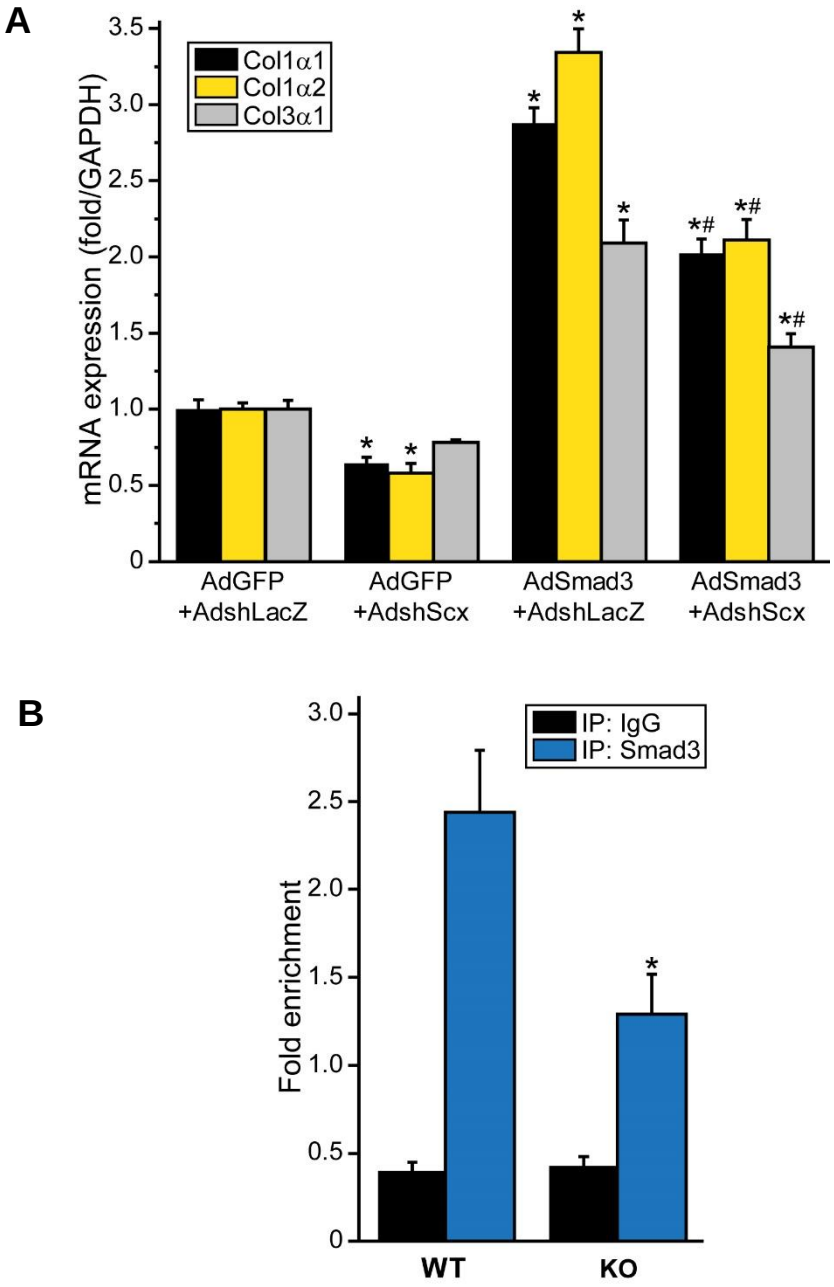

Figure 36: Impairment of Smad3 signaling in scleraxis null hearts.

(A) Up-regulation of fibrillar collagen mRNA expression by Smad3 (assessed by qPCR), is attenuated following scleraxis knockdown (AdshScx) compared to shRNA control in cardiac proto-myofibroblasts (AdshLacZ); n=3. **(B)** Smad3 interaction with the *Col1α2* gene promoter is significantly impaired in cardiac fibroblasts derived from scleraxis KO hearts compared to WT, as assessed by chromatin immunoprecipitation (anti-Smad3 antibody vs non-specific IgG antibody) followed by qPCR, suggesting that scleraxis loss impairs Smad3 signaling; n=3. Data represent mean±SEM; *P<0.05 vs AdGFP+AdshLacZ **(A)** or vs WT (**B**), #P<0.05 vs AdSmad3+AdshLacZ (**A**).

4.6: Loss of cardiac fibroblasts as a consequence of loss of scleraxis

Given the widespread alterations in extracellular matrix composition, it is possible that scleraxis gene deletion adversely affects the net population of cardiac fibroblasts. To examine this possibility, we analyzed cardiac cell identity by flow cytometry using labels for cardiomyocytes (α-myosin heavy chain, αMHC), fibroblasts (discoidin domain receptor 2, DDR2), smooth muscle cells (α-smooth muscle actin, αSMA) and endothelial cells (CD31). We detected a reduction in the number of cells staining positive for αSMA (Fig. 37A). Since αSMA is expressed by other cell types in the heart other than fibroblasts, most notably vascular smooth muscle, we also examined cells stained for DDR2, which is enriched in cardiac fibroblasts [56]. $DDR2^+$ cells were lost to an even greater degree than $\alpha\text{-}SMA^+$ cells in scleraxis null hearts, consistent with a preferential loss of $DDR2^+$ fibroblastic cells (Fig. 37B, C). A similar trend in reduction of $CD31^+$ cells was also observed in KO hearts (Fig. 37C). Normalized to the number of αMHC^+ cardiomyocytes, nearly half of all $DDR2^+$ cells were lost (Fig. 37D). Owing to the reduced number of $\alpha\text{-}SMA^+$ cells, there is a possibility that the cardiac vasculature may be negatively impacted in the scleraxis null mice. A significant ~25% decrease in capillary density in KO hearts further indicated reduced vascularity in these hearts (Fig. 38). Although αMHC^+ cardiomyocyte number appeared unaffected by scleraxis deletion, we observed that cardiomyocyte cross-sectional area significantly decreased (by 29%) in KO mice (Fig. 39). The decrease in cell area is consistent with a decrease in heart weight to a similar extent (~30%) in KO mice. Thus, the net hypotrophy observed in KO hearts appears to

be primarily due to reduced myocyte volume. Nearly half of all $DDR2^{+}$ cells were lost in scleraxis KO hearts (Fig. 37D), and cardiac tissue sections exhibited greatly reduced numbers of DDR2-expressing fibroblasts (Fig. 40). The shRNA-mediated knockdown of scleraxis in cardiac fibroblasts resulted in no change in cell death compared to controls (6.4±2.8% AdshLacZ vs. 4.4±1.0% AdshScx, $P>0.05$; n=3; 789-1660 cells counted/sample; Fig. 41). Although this experiment suggests that scleraxis loss may not cause cell death in isolated rat cardiac fibroblasts, future studies examining the role of scleraxis loss in development of cardiac fibroblasts and maintenance of its population during embryonic and neonatal stages are required to provide a stronger evidence to completely rule out the possible influence of cell death on fibroblast population effected by loss of scleraxis.

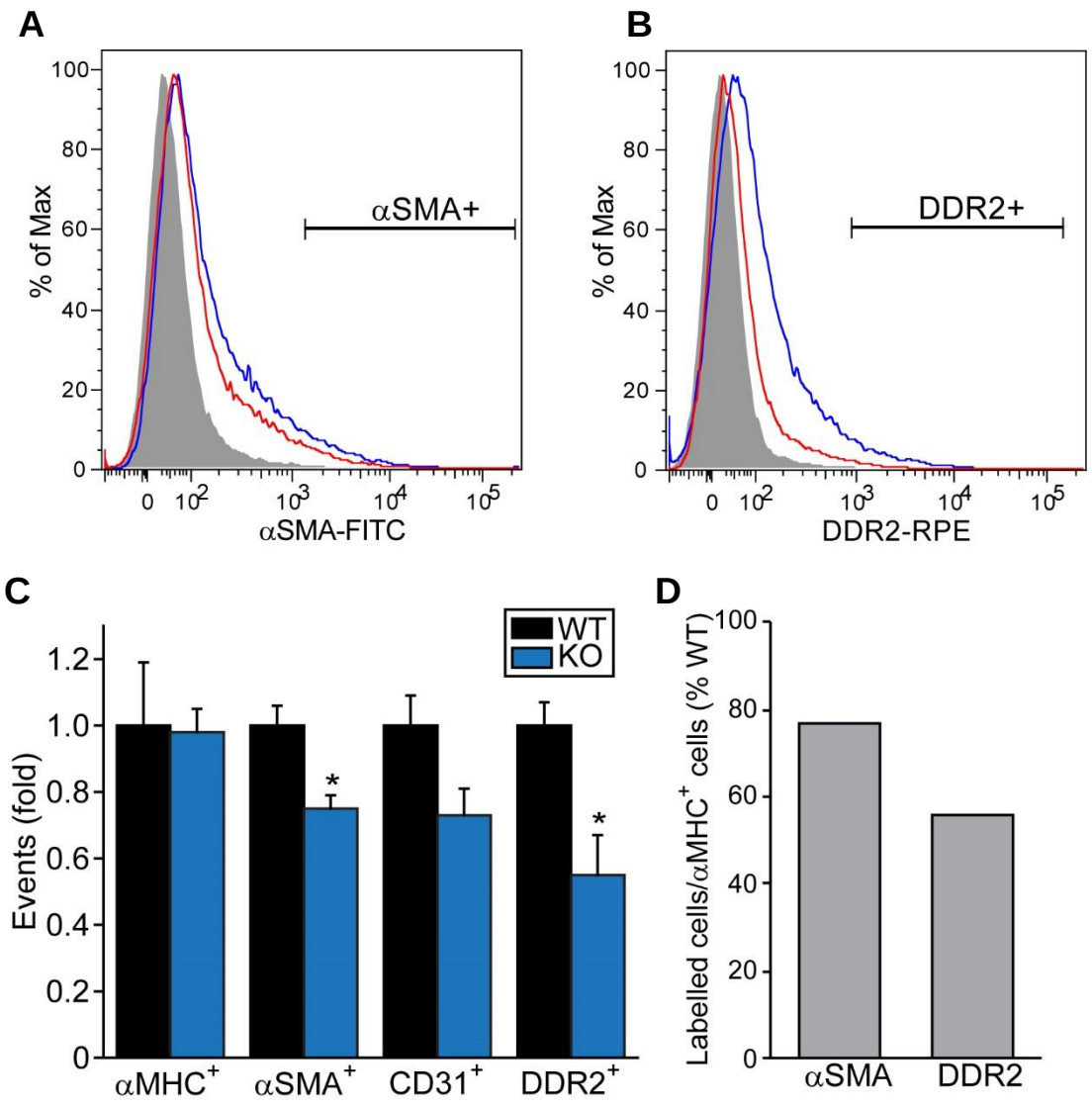

Figure 37: Loss of cardiac fibroblasts following scleraxis deletion in vivo.

Representative flow cytometry histograms of WT and scleraxis KO heart single cell suspensions show cardiac cells stained for αSMA **(A)** or DDR2 **(B)** in WT (blue line) and KO (red line) mice. Unstained cell sample was used as control (shaded histogram). **(C)** Total αMHC^+, αSMA^+, $CD31^+$ or $DDR2^+$ stained events per 50000 events in WT or KO mice normalized to WT counts; n=3-4, *P<0.05 vs WT. **(D)** αSMA^+ or $DDR2^+$ cell counts per αMHC^+ cell count for KO mice normalized to WT mice.

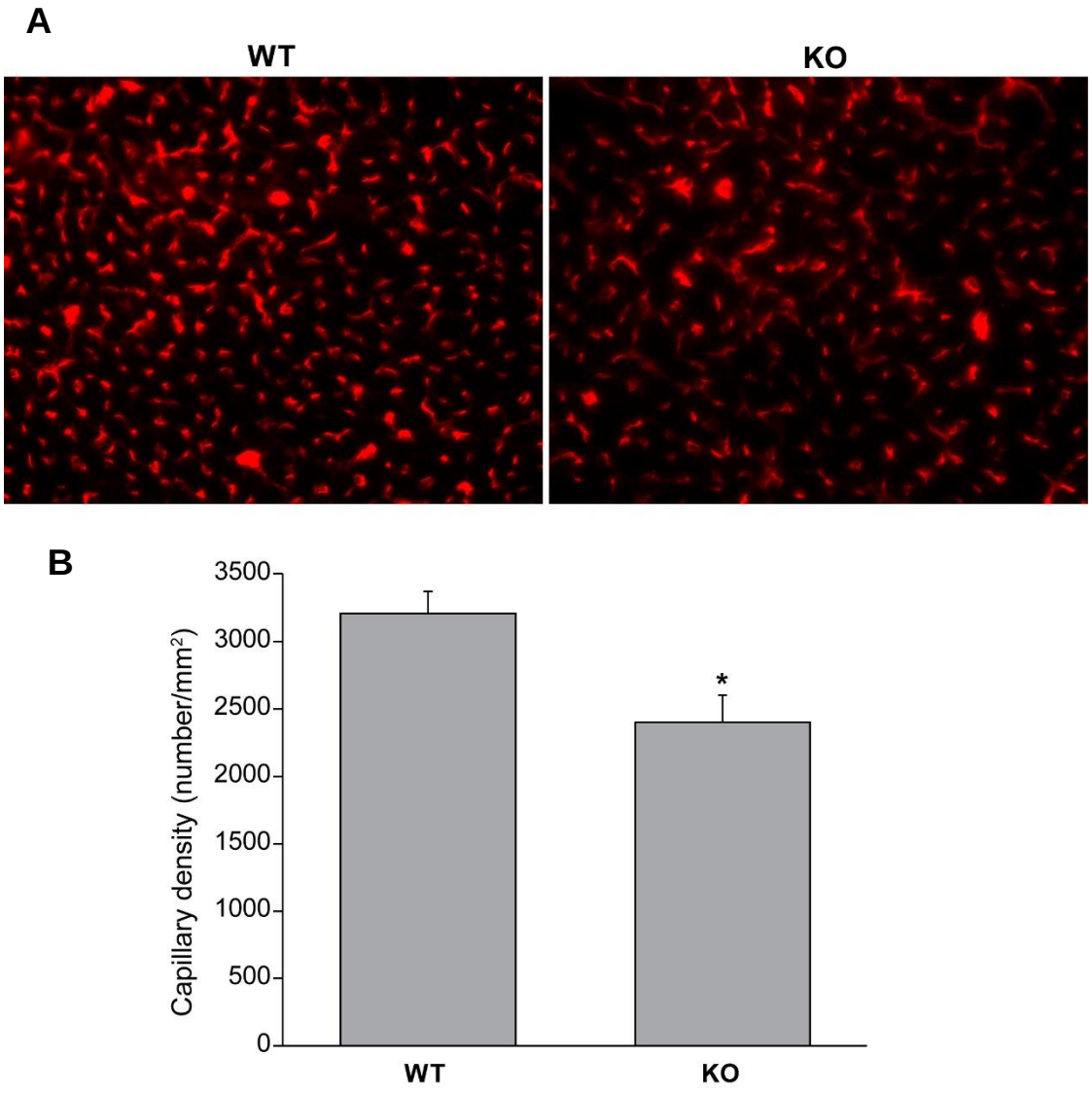

Figure 38: Capillary density analysis of cardiac sections from WT and scleraxis KO mice.

(**A**) Cardiac tissue sections (6 µm) from WT and scleraxis KO mice were stained with Rhodamine-labeled GSL I and capillaries counted to assess density. (**B**) Results represent mean±SEM for n=3 samples per genotype (2 fields/sample); *P<0.05 vs WT.

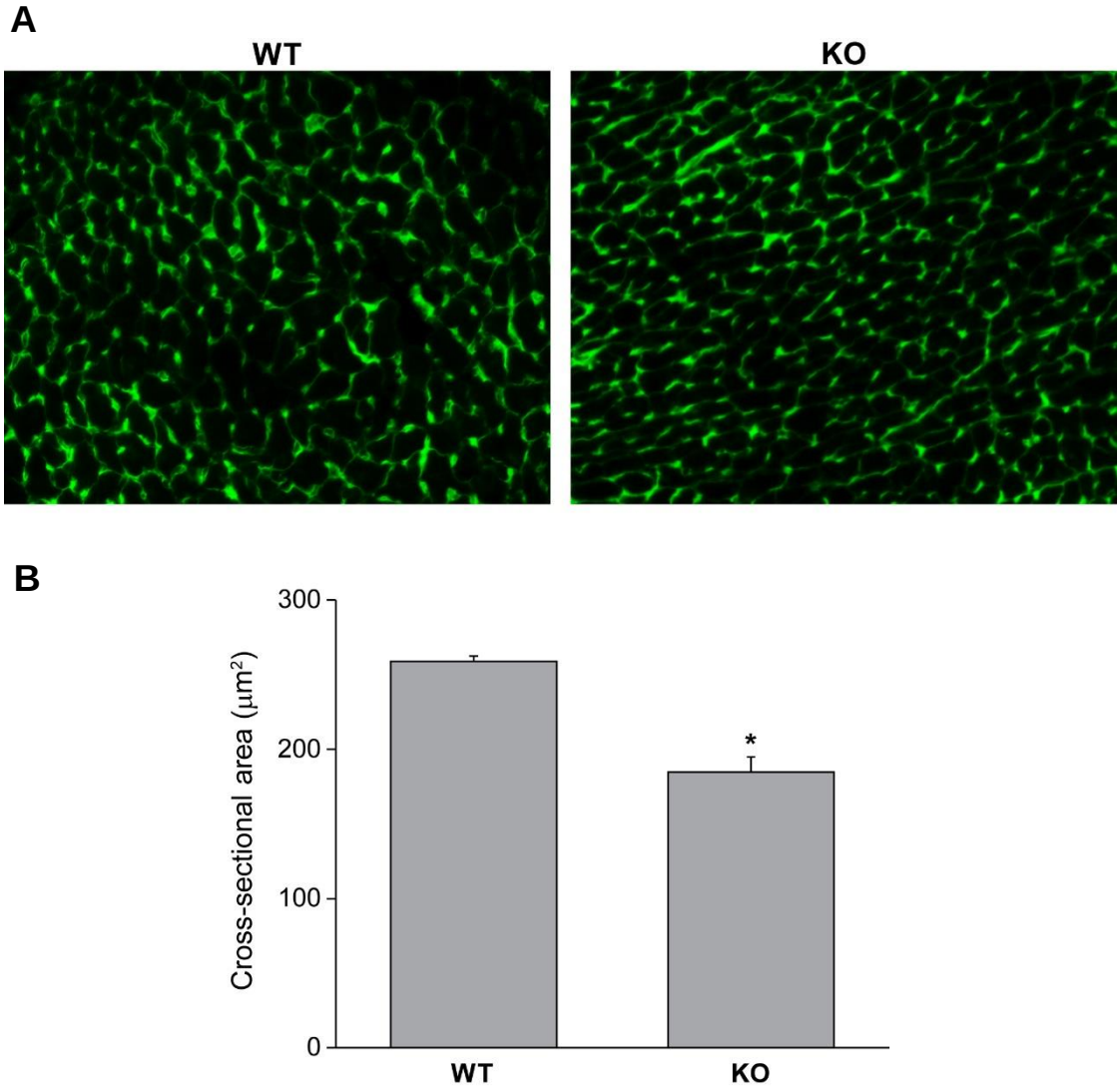

Figure 39: Cardiomyocyte cross-sectional area assessment from WT and scleraxis KO mice.

(A) Cardiac tissue sections (6 μm) from WT and scleraxis KO mice were stained with fluorescein-labelled peanut agglutinin for measurement of cardiomyocyte cross-sectional area. **(B)** Results represent mean±SEM for n=3 samples per genotype (50 cells/sample); *P<0.05 vs WT.

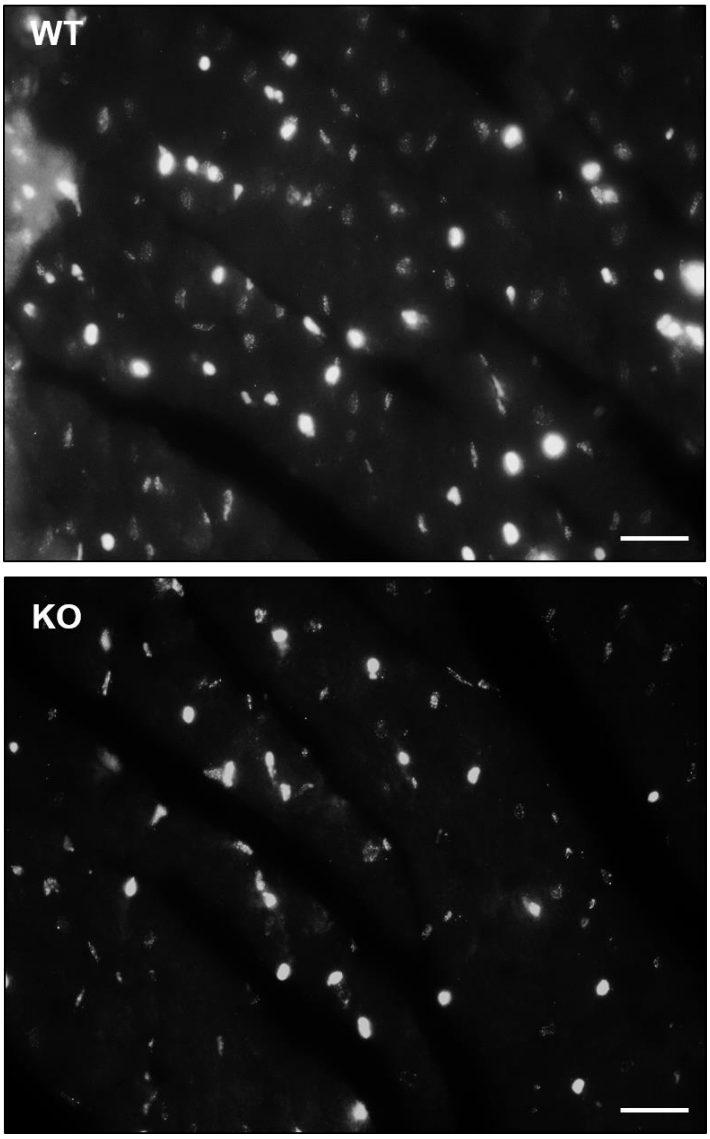

Figure 40: Scleraxis regulates cardiac fibroblast number.

Representative cardiac sections from WT and KO mice immunolabeled for DDR2 confirm the loss of $DDR2^{+}$ cells in the myocardium; 63x magnification; scale bar, 20 μm.

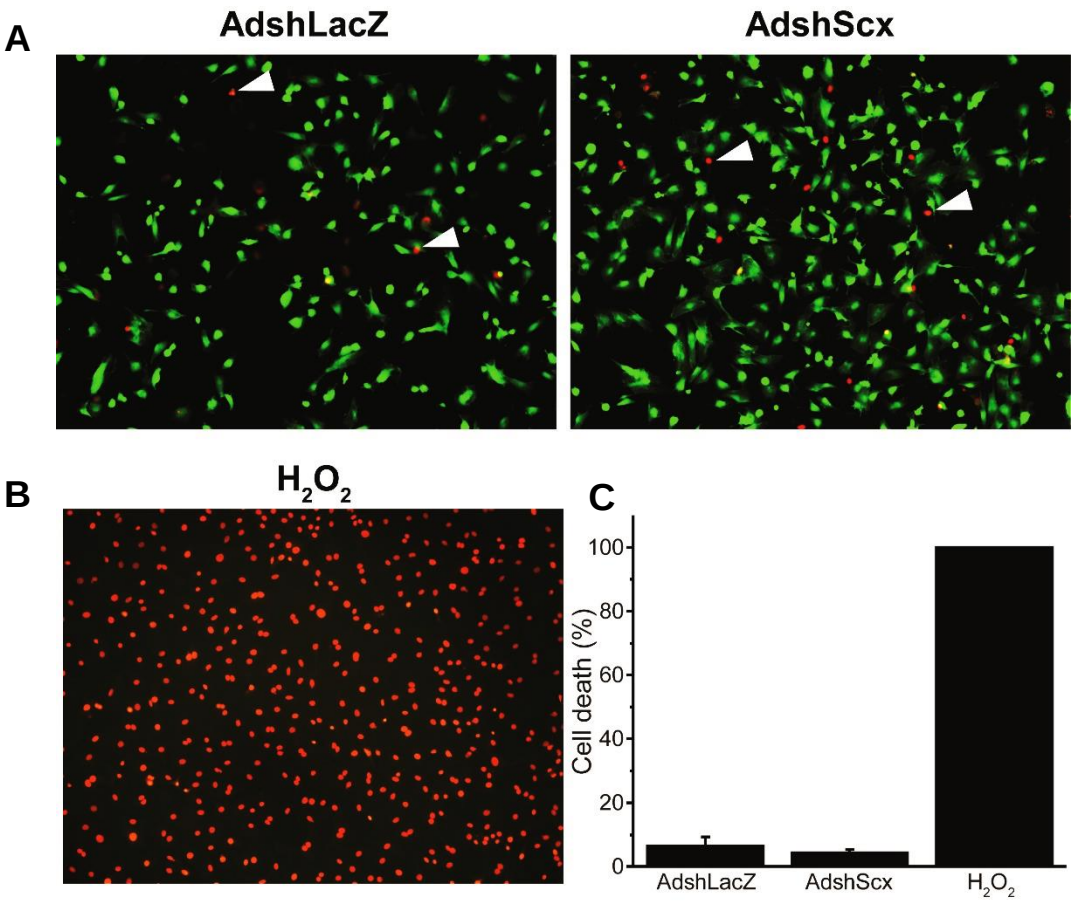

Figure 41: Cell viability of primary cardiac fibroblasts following scleraxis knockdown.

(**A**) Primary adult rat cardiac fibroblasts were assessed for viability by Live/Dead assay following treatment with AdshLacZ or AdshScx for 48 hours. Viable cells are green while dead cells are red (arrowheads). 200 μM H_2O_2 was used as a positive control for cell death (**B**). (**C**) Results from (**A**-**B**) were quantified and reported as percent of dead cells out of total cells (417 to 1660 cells counted per biological replicate; 4-6 fields of cells were assessed for AdshLacZ and AdshScx samples; all cells died following H_2O_2 treatment). Results represent mean±SEM; n=3. $P>0.05$ for AdshLacZ vs AdshScx.

4.7: Impaired epithelial-to-mesenchymal transition (EMT) during cardiac development- a possible mechanism of fibroblast loss in scleraxis null hearts.

Scleraxis knockdown did not impact cell viability in our experiments. The cardiac hypotrophy in KO animals could be explained by reduced myocyte size. Hence, we hypothesized that $DDR2^+$ cell loss in KO hearts may reflect altered cell fate of fibroblast precursors, rather than cell loss. Generation of cardiac fibroblasts from developmental precursors, with further phenotype refinement to myofibroblasts, has been ascribed to epithelial-to-mesenchymal transition (EMT) [371], thus we assayed several EMT markers. TCF21 is a transcription factor that has been recently shown to be required for EMT of cardiac fibroblasts from proepicardial organ precursors [187]. We observed a ~30% loss of mRNA expression of cardiac TCF21 in response to scleraxis deletion (Fig. 42A). Strikingly, all mesenchymal markers tested (*Snail1, Twist1, Zeb1*) were significantly downregulated in KO hearts, while epithelial markers (*desmoplakin, Par3, Claudin1*) increased in expression (Fig. 42B). The reduction in $DDR2^+$ cells in scleraxis KO hearts may thus represent a failure of epithelioid precursors to undergo EMT during development. Gene knockdown of scleraxis in cardiac proto-myofibroblasts significantly reduced the expression of mesenchymal marker genes (Fig. 43A). In a reciprocal experiment with scleraxis over-expression, the opposite effect was observed (Fig. 43B).

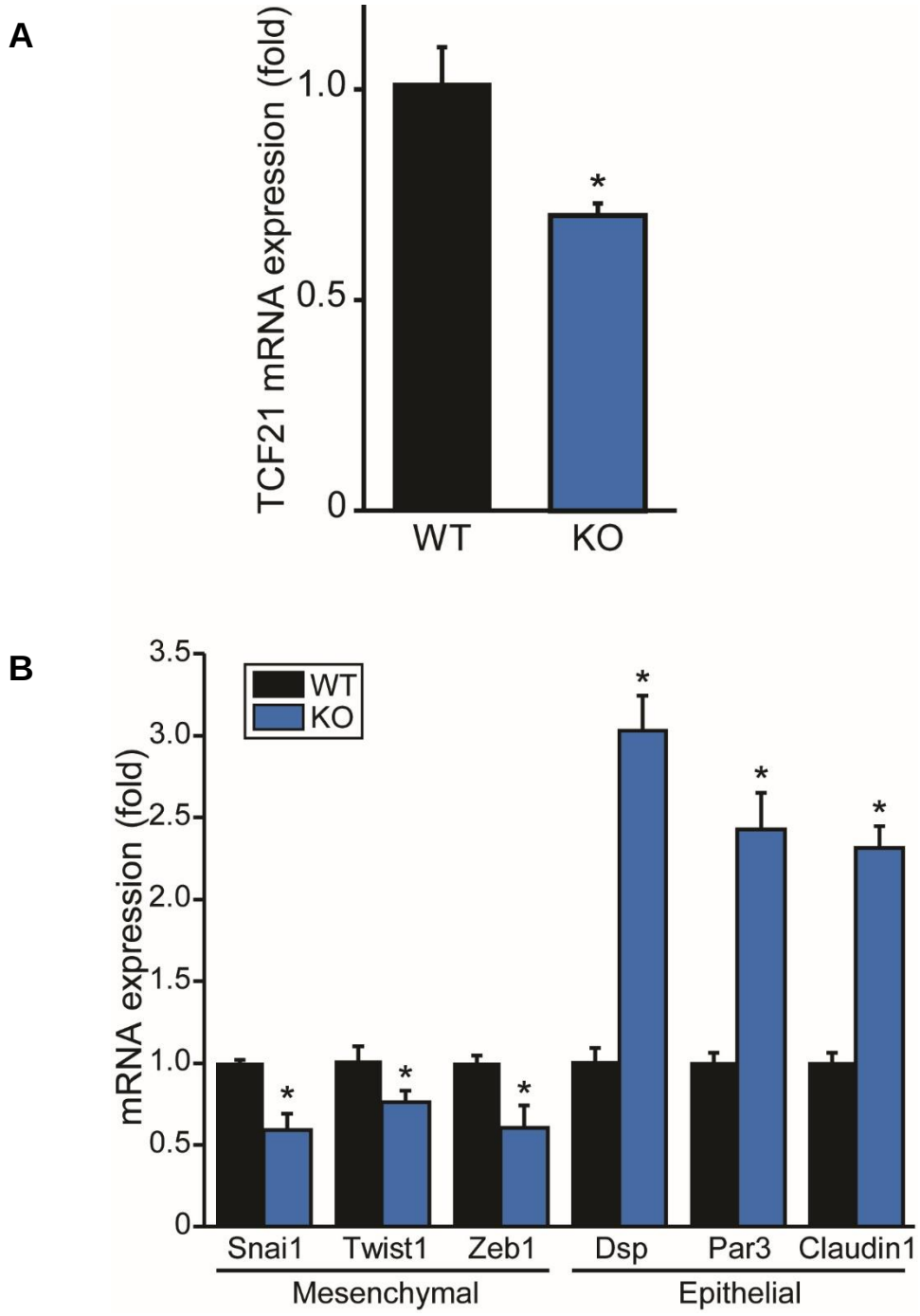

Figure 42: Impaired EMT gene expression in scleraxis null hearts.

Cardiac mRNA from WT and scleraxis KO mice was assayed for expression of (**A**) Tcf21, (**B**) mesenchymal and epithelial marker genes by qPCR, suggesting reduced epithelial-to-mesenchymal transition in KO hearts; n=3-5. Data represent mean±SEM; *P<0.05 vs WT.

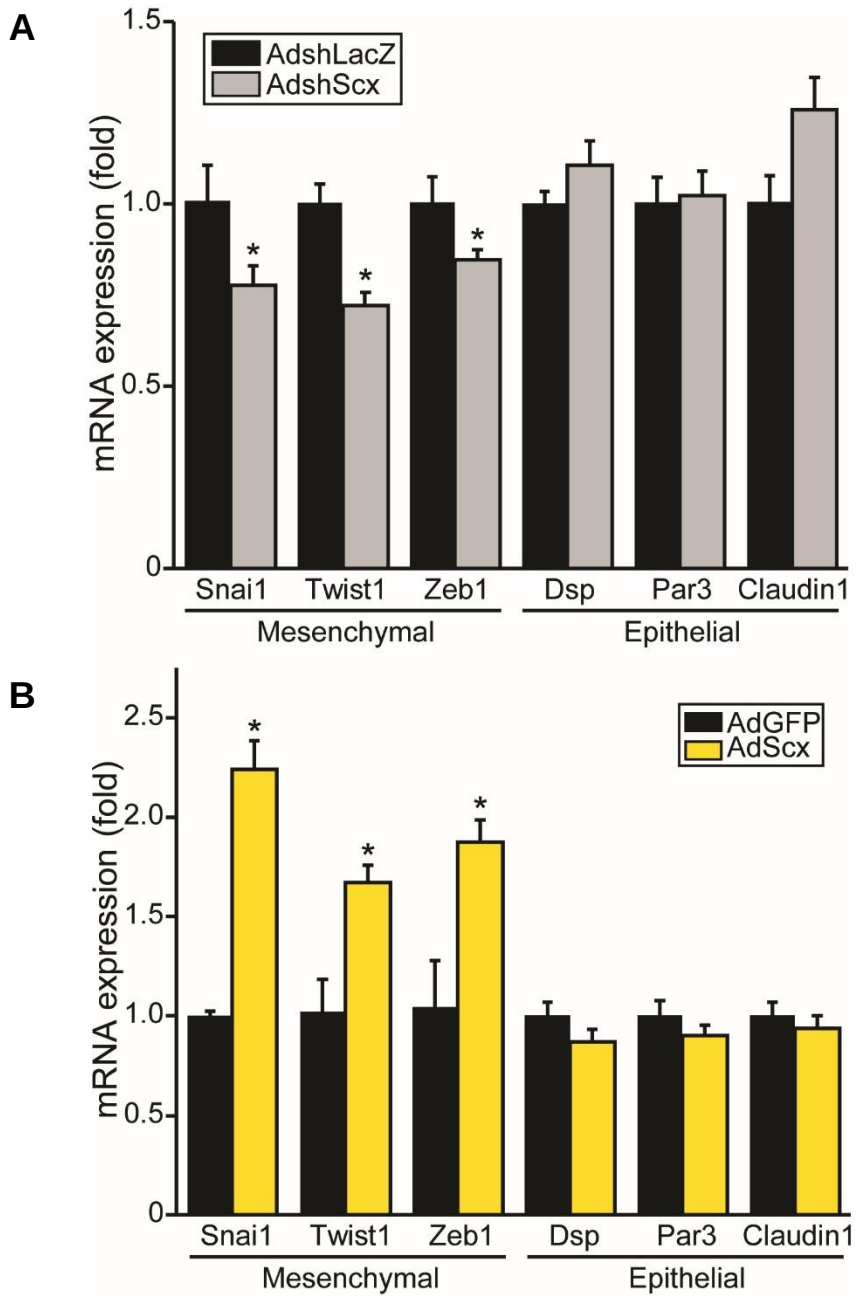

Figure 43: Scleraxis regulates mesenchymal marker gene expression.

Cardiac proto-myofibroblasts were subjected to scleraxis knockdown (**A**) or over-expression (**B**) and EMT markers assessed by qPCR, indicating that scleraxis regulates mesenchymal marker gene expression; n=3-5. Data represent mean±SEM; *P<0.05 vs AdshLacZ (**A**) or vs AdGFP (**B**).

5. Potential role of scleraxis in cardiac fibrosis

5.1: Assessment of cardiac morphometry in response to pressure overload in scleraxis conditional knockout (Scx-cKO) mice

We have previously reported that scleraxis regulates cardiac fibroblast collagen expression. Scleraxis expression is upregulated in the collagen-rich post-infarct scar tissue in a rodent model of myocardial infarction [173]. However, the expression pattern of scleraxis during cardiac fibrosis is unknown. In a preliminary study using a murine model of cardiac hypertrophy and interstitial fibrosis, we observed an almost two-fold induction of scleraxis expression at 8 weeks post-banding (Fig. 45A). This was concomitant with increased fibrosis in the cardiac interstitium and perivascular regions (Fig. 45B). To determine whether scleraxis is required for the induction of collagen expression that occurs during cardiac fibrosis, *in vivo* experiments involving loss-of-scleraxis function were required. Scleraxis knockout (KO) mice exhibited 48% mortality at two months [307]. These mice also exhibited alterations in the morphology and composition of cardiac valves [307]. Thus, employing these mice in a pathological study may confound our experiments. In order to gain a better understanding of the involvement of scleraxis in cardiac pathology, we generated two conditional knockout mouse lines using the Cre-Lox recombination system (see appendix 3). The first line is based on a pan-Cre system where Cre recombinase is expressed in virtually all tissues, but under control of tamoxifen [340]. While Cre is expressed ubiquitously, it cannot translocate to the nucleus to mediate excision of DNA in the absence of tamoxifen. The second line was developed using $TCF21^{iCre}$ mice which have been shown to exhibit fibroblast-specific expression of Cre [339]. By

breeding the Scx^{flox}/Scx^{flox} mice with these lines, we were be able to induce Cre activity and scleraxis gene excision with tamoxifen administered via gavage. Thus, by deletion of scleraxis in adult mice (6 weeks old), we were able to track changes in gene expression occurring due to loss of scleraxis in a pathological setting of cardiac fibrosis. Both these lines responded to surgical aortic banding and exhibited significantly increased heart:body weight (mg/g) and heart weight: tibia length (mg/mm) ratios compared to wild-type (WT) sham control group (Fig. 45). Although both Cre lines were responsive to the stimulus and exhibited hypertrophy, the gene expression profile from the $Scx^{flox/flox}$-$TCF21^{iCre}$ model system is reported here owing to its alignment with the cardiac fibroblast focus of this study.

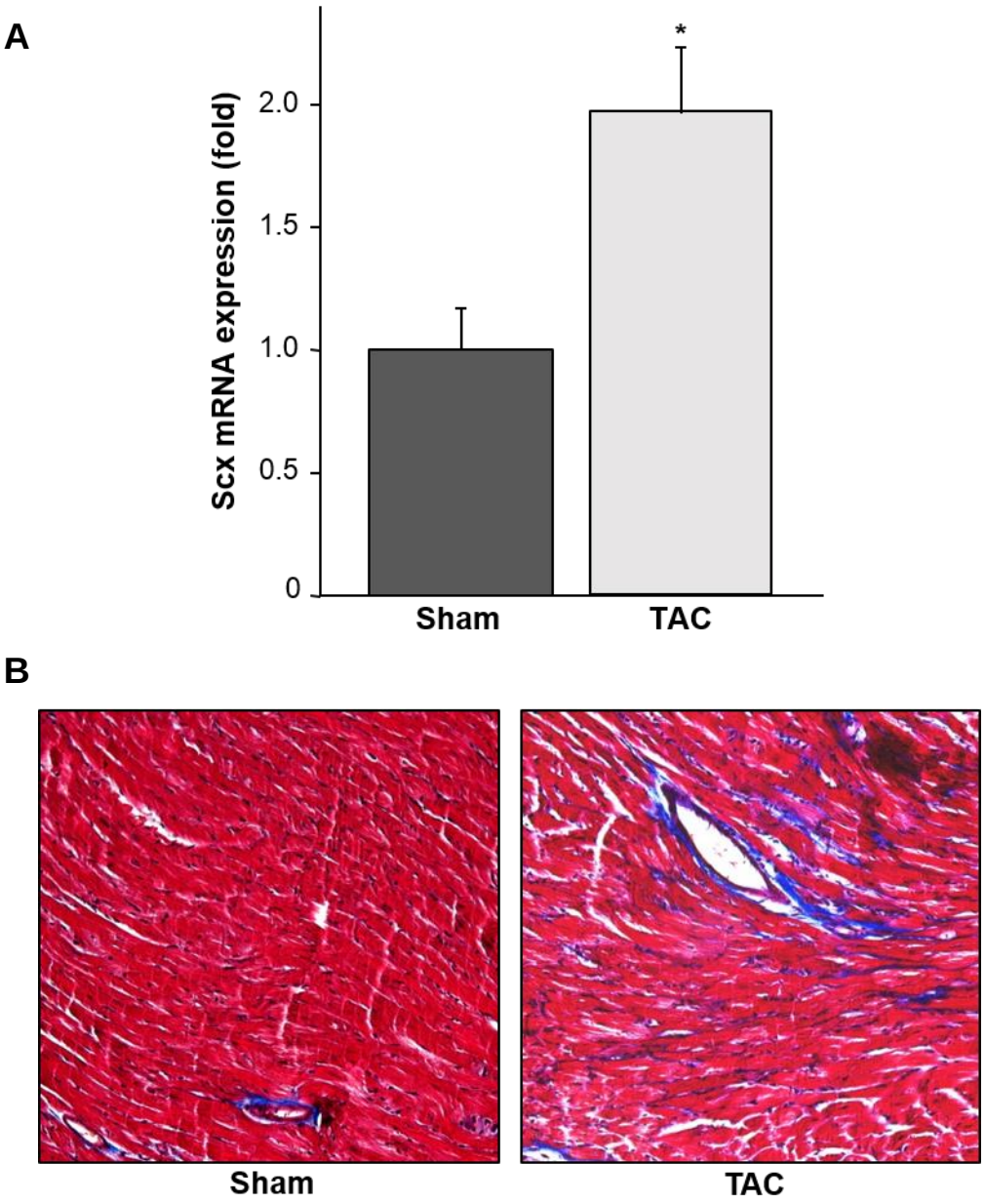

Figure 44: Scleraxis mRNA expression is elevated in pressure- overloaded murine hearts following TAC.

(A) Scx-GFP transgenic mice were subjected to TAC and cardiac tissue was harvested 8 weeks post- TAC and analysed for Scx mRNA expression using qRT-PCR. Sham-operated animals were treated as control group. Scx mRNA abundance was calculated using the $2^{-\Delta\Delta Ct}$ method and was normalized to GAPDH. Results represent three animals per data point, normalized to Sham group, and are reported as mean ± standard error; n=4, *P<0.05 vs. Sham. **(B)** Paraffin-embedded cardiac tissue sections (7μm thick) were processed for Masson's trichrome staining procedure. Blue color represents fibrotic deposits.

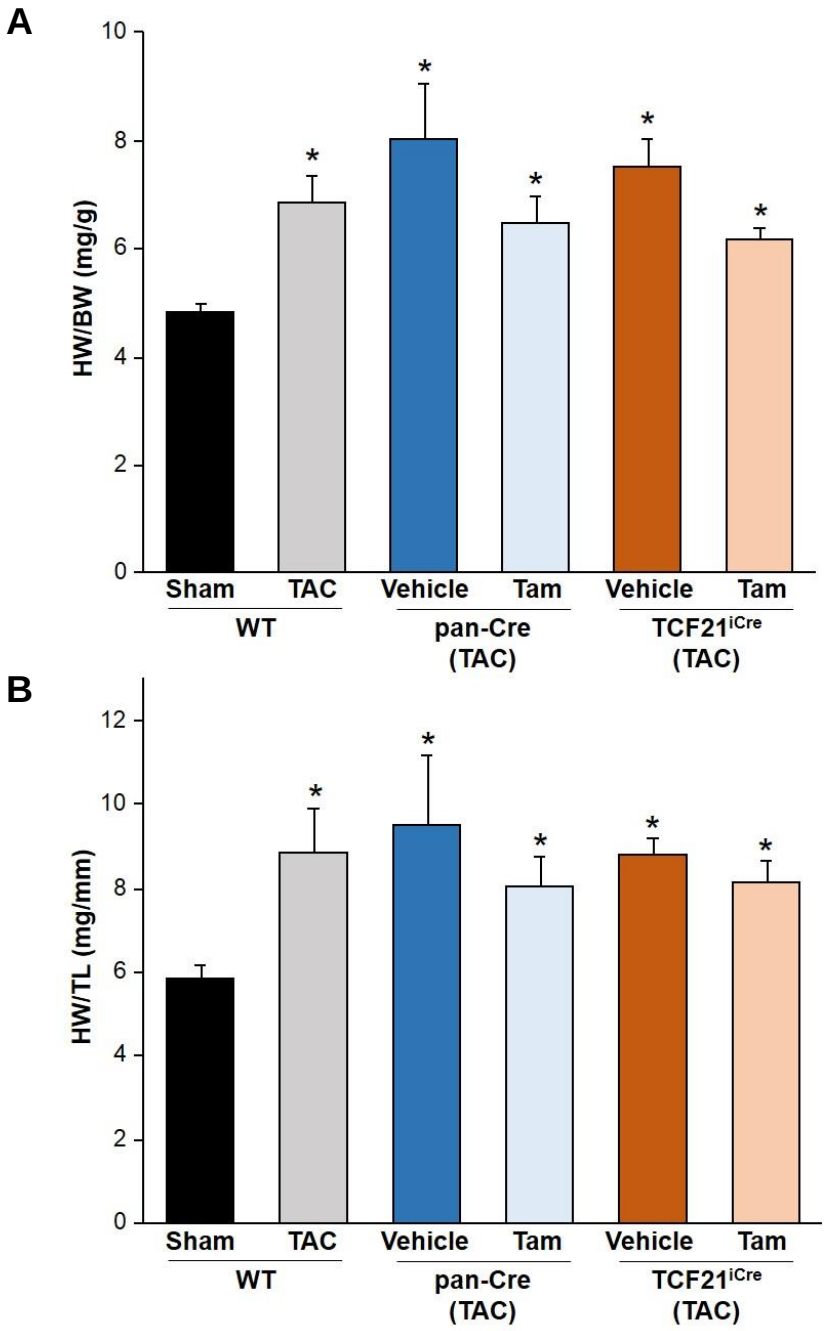

Figure 45: Induction of cardiac hypertrophy.

The ratios of heart weight/body weight (HW/BW; **A**) and heart weight/ tibia length (HW/TL; **B**) were calculated for sham and banded (TAC) animals at the time of tissue harvest 4 weeks post-TAC surgery [following gavage with corn oil (Vehicle) or tamoxifen (Tam)]. The transgenic hearts exhibited hypertrophy similar to the non-transgenic pressure-overloaded hearts. n=3-6, *P<0.05 vs WT Sham group.

5.2: Hypertrophic gene expression in pressure-overloaded conditional knockout (cKO) hearts

In response to thoracic aortic constriction (TAC), the heart undergoes progressive remodeling characterized by left ventricular myocyte hypertrophy and fibrosis. Cardiac hypertrophy is associated with the activation of the fetal gene program- a distinctive feature of pathological hypertrophy. Here we assayed gene expression changes in mice subjected to TAC leading to hypertension. Both atrial natriuretic peptide (ANP) and β-myosin heavy chain (β-MHC) were significantly upregulated in mice subjected to aortic banding (Fig 46). The increase in β-MHC gene expression was more robust than ANP. We also noticed a mild (not significant) decrease in expression of both ANP and β-MHC in Scx^{null}/$TCF21^{iCre}$ mice in comparison to wild-type banded animals. Fibroblasts are known to secrete growth factors that regulate pathological hypertrophy. Although unclear at this time, it is possible that scleraxis plays a role in pro-hypertrophic factor regulation, and hence loss of scleraxis may negatively influence the cardiac hypertrophic gene expression profile. Further investigation needs to be carried out to examine any definitive role of scleraxis in this aspect of cardiac remodeling.

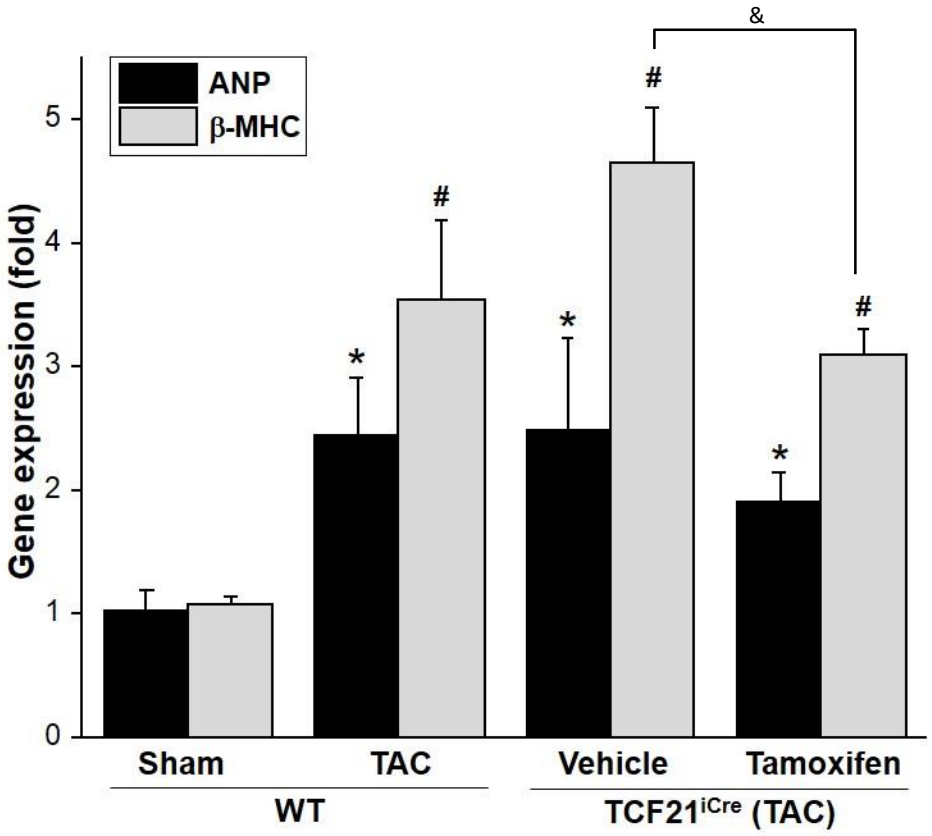

Figure 46: Fetal gene activation in response to pressure overload.

The mRNA expression levels of fetal genes ANP and β-MHC were detected by qRT-PCR using total cardiac RNA from all experimental groups. There was a significant upregulation of these genes in banded animals thereby indicating the activation of the fetal gene program in pathological hypertrophy. Results were normalized to GAPDH; n=3-6; *P<0.05 (ANP) or #P<0.05 (β-MHC) vs WT Sham group; &P<0.05 vs tamoxifen group.

5.3: Cardiac fibrillar collagen gene expression in scleraxis conditional null (cKO) mice post-banding

Scleraxis knockout mice tendons show loss of type I collagen [320].Our data shows that scleraxis regulates the basal expression of collagen genes in the myocardium. The collagen Iα2 promoter is regulated both constitutively and in response to TGF-β_1 activation [360]. It is possible that scleraxis behaves in a similar manner like some other transcription factors that are involved in the regulation of collagen expression in both physiological and pathological settings. Induction of hypertension by aortic constriction led to induction of collagen expression in non-transgenic animals as well as well as those where the scleraxis gene was deleted (Fig. 47). It was quite intriguing to observe a significant blunting of fibrotic collagen expression in tamoxifen-treated scleraxis cKO murine hearts compared to the wild-type group as well as vehicle-treated cKO animals. This trend was apparent in all fibrillar collagen genes that were assayed.

Cardiac myofibroblast collagen I expression induced by pro-fibrotic TGF-β_1 is completely dependent on intact scleraxis signaling [172]. Both Angiotensin II (Ang II) and Connective Tissue Growth Factor (CTGF/CCN2) are also well-known drivers of pro-fibrotic programs in multiple tissues, including the heart [185]. To support our *in vivo* data, we performed scleraxis gene knockdown assay in primary cardiac proto-myofibroblasts and administered various pro-fibrotic agents (TGF-β_1, Ang II, CTGF), and assayed fibrillar collagen expression in these cells. All these agents caused a significant upregulation of type I and III collagen genes as anticipated (Fig. 45). However, loss of scleraxis in these cells blunted the effect of these pro-fibrotic factors

on collagen gene induction (Fig. 48). Thus, it appears that Ang II and CTGF, like TGF-β_1, require intact scleraxis signaling in order to regulate collagen I expression in cardiac proto-myofibroblasts.

Thus, in agreement with our scleraxis knockdown and knockout data, collagen expression is significantly reduced in these animals, suggesting a direct role of scleraxis in regulation of collagen gene expression occurring during cardiac fibrosis.

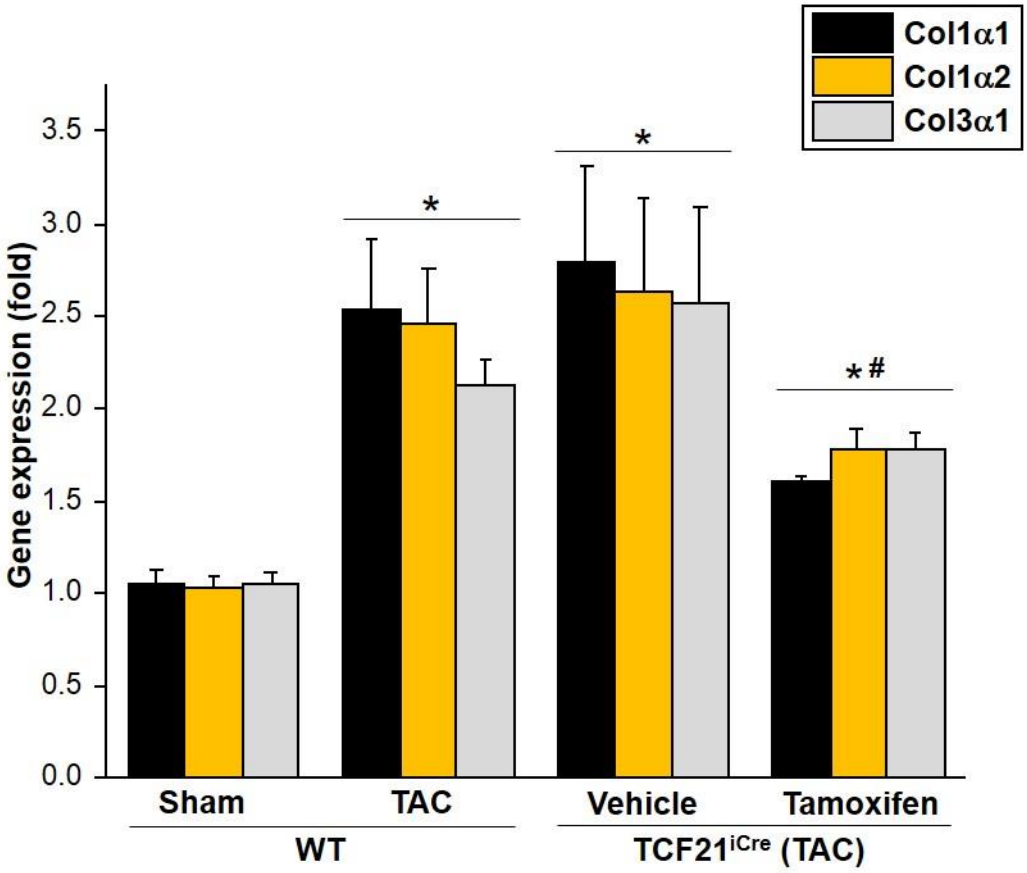

Figure 47: Changes in fibrillar collagen gene expression in scleraxis cKO mice subjected to TAC.

(A) The expression levels of fibrillar collagens (1α1, 1α2, 3α1) in cardiac tissue was detected by qRT-PCR from sham (control) and different experimental groups, and the results were normalized to GAPDH. n=3-6; *P<0.05 vs WT Sham, #P<0.05 vs WT TAC and Vehicle TAC.

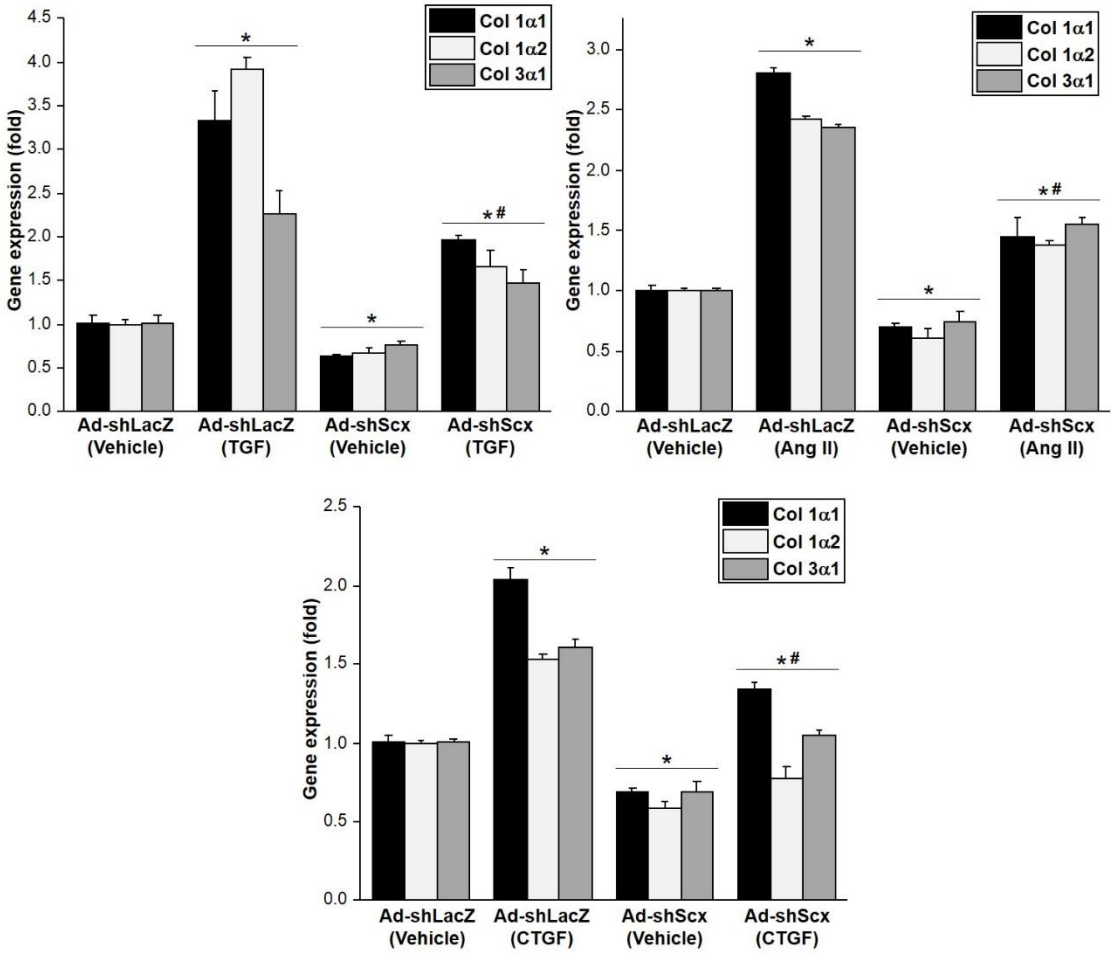

Figure 48: Inhibition of fibrotic collagen expression by scleraxis gene knockdown in cardiac proto-myofibroblasts.

Cardiac proto-myofibroblasts were infected with adenoviral vectors encoding shRNA for scleraxis (Ad-shScx) or LacZ (Ad-shLacZ; control) for 48 hours followed by treatment with pro-fibrotic agents- TGFβ1, angiotensin II (Ang II) or Connective Tissue Growth Factor (CTGF). Total RNA was isolated 24h post-treatment and subjected to qPCR for collagens 1α1, 1α2 and 3αl. mRNA abundance for these genes was normalized to GAPDH. N=3, *P<0.05 vs Ad-shLacZ, #P<0.05 vs Ad-shLacZ+agent.

5.4: Cardiac fibroblast/ myofibroblast marker gene expression profile in scleraxis conditional knockout (cKO) murine tissues in response to pressure overload

Previously we have shown that scleraxis is capable of modulating cardiac fibroblast phenotype. Scleraxis overexpression can induce the phenoconversion of cardiac proto-myofibroblast to myofibroblasts. This is a crucial finding since these myofibroblasts are considered to be the causative cells of cardiac fibrosis. In our murine model of hypertension, we evaluated the expression of distinct cardiac myofibroblast markers. αSMA and vimentin are well-established markers of fibrosis. We observed a significant upregulation of these genes in response to pressure overload in all groups compared to sham controls (Fig. 49). Although there was an increase in the expression of these genes in the scleraxis nulls, there was a significant reduction in their expression when compared to non-transgenic banded hearts. Together with our *in vitro* data, this supports the direct regulation of these genes by scleraxis in the myocardium. Given the observation in pathological fibrosis, scleraxis can thus be deemed a required regulator of fibroblast phenotype in the heart.

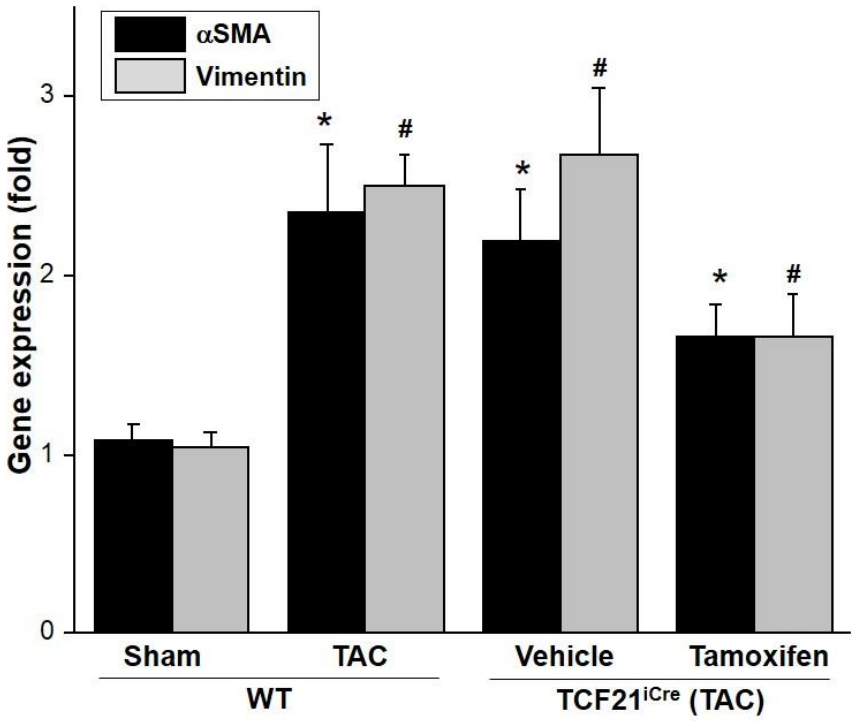

Figure 49: Cardiac (myo)fibroblast gene expression changes in response to pressure overload in cKO mice.

Tamoxifen- gavaged cKO mice exhibited reduced myofibroblast marker gene expression in response to induction of pressure overload. mRNA expression of marker genes (αSMA, Vimetin) was detected with qRT-PCR using specific primers and normalized to GAPDH. n=3-6; *P<0.05 (αSMA) or #P<0.05 (Vimentin) vs WT Sham group.

CHAPTER V: DISCUSSION

Regulation of human COL1A2 gene promoter by Scleraxis and Smads

In response to prolonged stress, the heart undergoes dramatic changes in morphology that impact cardiac function. For example, following myocardial infarction and the subsequent repair process, the ventricles increase in volume and mass, and significant hypertrophy occurs. This is an attempt to improve stroke volume following loss of viable tissue in the infarct scar region. These morphological changes often lead to decompensation over time, which is marked by thinning of the myocardium (dilatation), loss of cardiomyocytes, generalized fibrosis and a devolution of cardiac contractile function into overt heart failure, resulting in significant morbidity and mortality of cardiac patients. To better understand the mechanisms contributing to cardiac fibrosis, the regulation of ECM synthesis in fibroblasts and myofibroblasts, particularly at the transcriptional level, needs to be clarified.

One of the best characterized mechanisms for regulating collagen gene expression involves intracellular signaling proteins called Smads, which are transcriptional regulators of TGF-β_1-activated collagen synthesis and myofibroblast activation [372, 373]. Smads, by themselves, are relatively weak transcriptional activators [374]. Here we elucidate the mechanism by which scleraxis partners with Smad3 to regulate activation of the human COL1A2 gene promoter. We showed that scleraxis binds to E-boxes on this promoter in adult human cardiac fibroblasts- this suggests that scleraxis plays an important role in maintenance of basal collagen synthesis in these cells (Fig. 12B). The data presented here shows that scleraxis alone

is sufficient to regulate collagen 1α2 expression. We also demonstrate that there is extensive cross-talk between scleraxis and the TGF-β1/Smad signaling pathway. In primary rat cardiac fibroblasts, Smad3 overexpression significantly upregulated the expression of scleraxis whereas scleraxis expression was downregulated by inhibitory Smad7 in (Fig. 13). Thus, scleraxis function is downstream of TGF-β_1/Smad signaling. This is also the first instance where we show that scleraxis-mediated collagen 1α2 expression can occur independently of the TGFβ/Smad3 complex in presence of upstream regulators of scleraxis. The distinct increase observed in collagen gene expression mediated by scleraxis, along with the effect on TGFβ and Smad3 on scleraxis expression, is evidence of a novel TGF-β_1-inducible mechanism involved in regulation of collagen synthesis. Our DNA-binding domain scleraxis mutant (ScxΔBD) attenuated basal collagen 1α2 mRNA expression. This mutant also prevented collagen 1α2 gene induction by the pro-fibrotic cytokine TGF-β_1. Thus it is possible that interference with scleraxis function may present a novel approach in fibrotic disease. The results presented in this section support a model of COL1A2 gene expression mediated by the synergistic interaction of scleraxis and Smad3 downstream of TGF-β_1 (Fig.50) [172].

Regulation of cardiac ECM gene expression and fibroblast phenotype by Scleraxis

This study demonstrates for the first time that scleraxis is sufficient to regulate the expression of multiple matrix genes including fibrillar collagens, proteoglycans, and MMPs. Our data supports our contention that scleraxis is required for normal

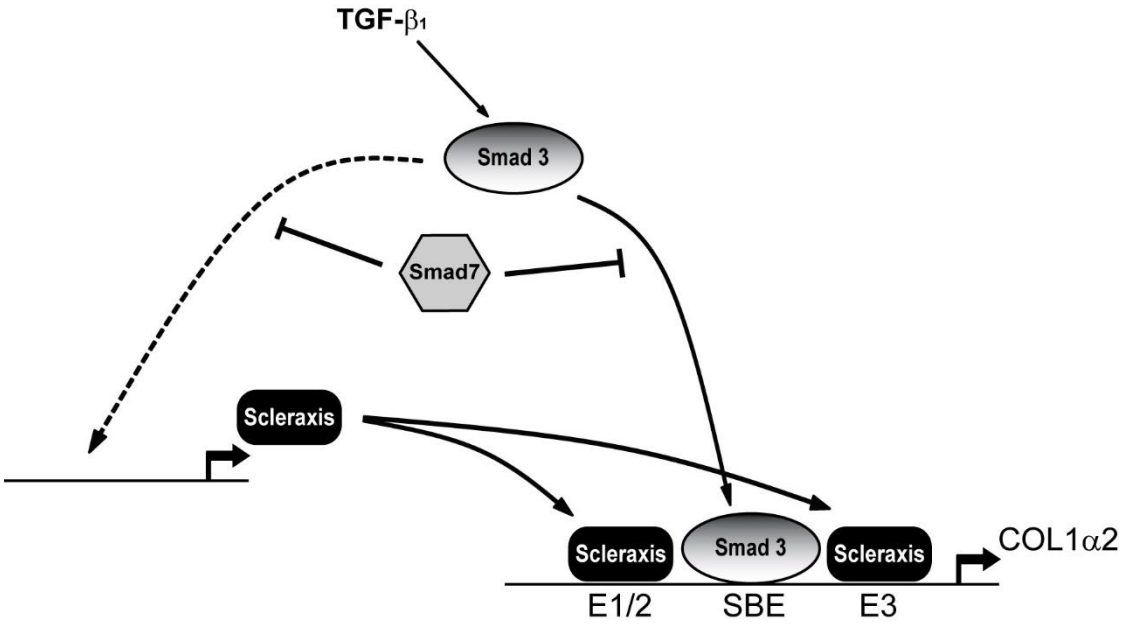

Figure 50: Proposed model for interaction of scleraxis and Smads in the regulation of COL1A2 gene expression.

Pro-fibrotic TGF-β1 binds to its plasma membrane-bound receptor complex to activate Smad3, which in turn regulates the COL1A2 gene via direct binding to the SBE located in the promoter. Our data demonstrates that Smad3 also induces scleraxis expression via an unknown mechanism. Both effects of Smad3 are negatively regulated by inhibitory Smad7. Increased scleraxis expression works synergistically with Smad3 to strongly up-regulate COL1A2 expression via scleraxis binding to E boxes within the proximal promoter. Reprinted from RA Bagchi and MP Czubryt, Synergistic roles of scleraxis and Smads in the regulation of collagen 1α2 gene expression, *Biochimica et Biophysica Acta-Molecular Cell Research*, 1823:1936–1944, © 2012, with permission from ELSEVIER INC. http://www.sciencedirect.com/science/article/pii/S016748891200198X

cardiac ECM production *in vivo*. Data from the present study demonstrate the critical role of scleraxis in regulation of cardiac ECM production and fibroblast phenotype. Scleraxis drives expression of genes that define fibroblast and myofibroblast phenotypes, including type I collagen and αSMA. Loss of scleraxis reduces the expression of these genes. Scleraxis gene ablation also leads to reduction in the fibroblast population of the heart, possibly due to altered fate selection of progenitors.

Cardiac valves and tendons possess a collagen-rich ECM, and scleraxis deletion has been shown to severely affect both these tissues [307, 320]. Congenital deletion of scleraxis causes loss of force-transmitting tendons due to a failure of tendon progenitor differentiation and loss of type I collagen production via an unknown mechanism [320]. Scleraxis over-expression on the other hand has been shown to drive embryonic stem cells to a tenocyte fate and induces the tendon marker tenomodulin [312, 375]. Scleraxis null mice possess thickened cardiac valves with altered collagen expression and fiber organization attributable to reduced valve precursor cell differentiation, [307]. Scleraxis thus plays an important role in regulation of progenitor cell fate and tissue architecture in matrix-rich environments. Interference of scleraxis function results in significant ECM alterations.

The data presented in this study provide the first evidence of a broader role of scleraxis in the matrix-rich cardiac tissue. The wide-spread changes in matrix gene expression in scleraxis null mice (Figs. 31-33) reflects three distinct but closely-related phenomena: direct gene transactivation by scleraxis, maintenance of cardiac fibroblast numbers and phenotype, and a requirement for scleraxis in TGFβ/Smad3 signaling. The expression of all major fibrillar collagens present in the myocardium (I, III, V)

appears to be directly controlled by scleraxis. All these genes have significantly reduced expression with loss of scleraxis, and can be rescued/up-regulated by scleraxis overexpression (Figs. 15, 18, 31, 35). The lack of effect on non-fibrillar collagen IV suggests that scleraxis exerts specific effects on fibrillar collagens in the heart. These alterations are unlikely to be secondary to an indirect effect of scleraxis on an unknown intermediate since rapid changes in target gene expression ocurs within hours of scleraxis knockdown, rescue or over-expression. Our *in vitro* loss of scleraxis expression recapitulated the *in vivo* knockout pattern. We generated a double deletion scleraxis mutant (ScxΔΔ), lacking both the DNA- and protein-binding domains. This mutant had no effect on transactivation of the COL1A2 gene or target gene expression (Fig. 22-23). Our data from gene reporter assays of selected gene promoters (vimentin, MMP2, αSMA; Fig. 21, 27) supports a direct transcriptional role of scleraxis in transactivation of these genes. We elucidated this mechanism for the myofibroblast marker gene, αSMA, by mutation analysis, gel-shift and chromatin immunoprecipitation assays (Fig. 26-27).

MMPs and their inhibitors are required to maintain the equilibrium between ECM synthesis and degradation. MMP2 and MMP9 act on intact fibrillar collagens I, III, and V as their substrates [376]. Alterations in scleraxis expression altered expression of MMP2, 3, 9 and 11 (Figs. 16, 19, 33). MMP2 is a direct scleraxis gene target given the transactivation of its promoter by scleraxis (Fig. 21). The decrease in apparent collagen fiber size in KO mice (Fig. 29) could be due to interference with the fiber maturation process. Further examination of the role of scleraxis in post-translational processing of fibrillar collagens will help elucidate the underlying

mechanism for this anomaly. The expression of proteoglycans was also altered in response to scleraxis loss or overexpression. Fibromodulin and lumican followed the expression pattern of scleraxis. A similar pattern has been recently reported for cardiac valves [364]. Thus, these proteoglycans may be novel direct gene targets of scleraxis.

The present study provides evidence that scleraxis governs the expression of fibroblast and myofibroblast markers including DDR2, EDA-Fn, SM_{emb}, vimentin and αSMA (Figs. 20, 24-26). Scleraxis overexpression in cardiac proto-myofibroblasts led to increased expression of all commonly-employed markers tested (αSMA, EDA-Fn, SM_{emb} and vimentin) (Fig. 20). This indicates that scleraxis is a potential driver of the fibroblast-to- myofibroblast phenotype conversion process. DDR2 was employed in our study as a marker of cardiac fibroblasts [56, 100, 103]. As a consequence of scleraxis loss, all of these markers were significantly downregulated both *in vitro* and *in vivo*. This establishes the role of scleraxis as a novel transcriptional regulator of the fibroblast phenoconversion process. The solid matrix on which these cells were cultured induces αSMA expression in cardiac fibroblasts – however, αSMA is not yet incorporated into stress fibers in proto-myofibroblasts. Scleraxis overexpression resulted in development of robust αSMA-positive stress fibers (Fig. 25). This indicated that scleraxis accelerates the transition of proto-myofibroblasts to a mature myofibroblast phenotype.

Regulation of cell fate by Scleraxis

Our data provides the first evidence for the involvement of scleraxis as a regulator of cardiac fibroblast cell fate, similar to its function in cardiac valve

precursors [307]. It is possible that the apparent loss of matrix components in scleraxis KO animals is due to insufficient fibroblast formation as well as decreased fibroblast ECM synthesis. The knockdown of scleraxis reduced the expression of ECM components (Figs. 18-19). Primary isolated cardiac proto-myofibroblasts from KO mice exhibited decreased expression of *Col1α1*, *Col1α2*, *Col3α1*, vimentin and αSMA- this is indicative of a strong functional deficit in these cells (Fig. 35). Flow cytometry analysis using cardiac single cell suspensions showed a reduction in DDR2 labeling per cell, as well as a ~50% decrease in the total number of $DDR2^+$ cells in scleraxis KO hearts (Fig. 37). This was confirmed by reduced DDR2-immunolabeled fibroblasts in cardiac tissue sections (Fig. 40). Thus there is an apparent loss of fibroblasts along with reduced function in the cells that do arise. Cell loss did not occur following scleraxis knockdown (Fig. 41) which indicates that perhaps the reduction in $DDR2^+$ cells is not occurring due to increased cell death. The cardiac hypotrophy observed in KO mice could be explained fully by the reduction in cardiomyocyte size (Fig. 39) rather than by fibroblast death.

A previous study showed that a significant proportion of scleraxis-positive cells located in the proepicardial organ contributes to the population of future cardiac fibroblasts during development, but it is not known if all fibroblasts derive from this cell population [377]. The fate of these cells in scleraxis null hearts has not been explored to-date. Recently, it was reported that deletion of another bHLH transcription factor, TCF21, results in a complete loss of cardiac fibroblasts due to failure to properly differentiate [187]. TCF21 KO and scleraxis KO hearts are very similar in appearance, including characteristic right side enlargement and rounding and

involution of the apex. TCF21 also regulates scleraxis expression in Sertoli cells [378]. Thus, one cannot rule out the possibility that scleraxis knockout partially phenocopies TCF21 loss in the heart.

Given the importance of EMT in fibroblast generation [379], the downregulation of mesenchymal cell markers, and up-regulation of epithelial markers in scleraxis null hearts (Fig. 42) is consistent with a developmental defect. Alteration of scleraxis expression in cardiac proto-myofibroblasts resulted in equivalent changes in mesenchymal marker expression (Fig. 43). These observations suggest that part of scleraxis acts in part by promotion of a mesenchymal cell fate and the adoption of a myofibroblast phenotype.

There is a lack of information about the role of scleraxis in cardiac fibrosis and pathologic remodeling. The transition of fibroblasts to myofibroblasts in connective tissues of the heart, lungs, liver, kidney, and skin is crucial in matrix remodeling and scar formation [380]. Scleraxis expression is also upregulated in fibrillar collagen-rich keloid scars [335]. Given that scleraxis promotes the myofibroblast cell fate and induces ECM synthesis, it is only fitting that it may play a regulatory role in cardiac fibrosis. A previous report from our laboratory showed that scleraxis expression is increased in the post-infarct healing scar tissue [173]. As mentioned elsewhere, our current data demonstrates that scleraxis works synergistically with the canonical Smad signaling pathway to increase *Col1α2* expression by cardiac fibroblasts and myofibroblasts [172]. Our DNA binding-deficient scleraxis mutant blocks type I collagen synthesis by cardiac myofibroblasts basally as well as in response to TGFβ [172]. This suggests that scleraxis is a critical component of a signaling pathway

directing ECM synthesis during wound healing and/or fibrosis in the heart and other tissues.

Role of Scleraxis in cardiac fibrosis

Our data so far supports the contention for scleraxis to play a pathogenic role. The cardiac developmental defects noted in scleraxis null mice prevents their use in experimental models of cardiac dysfunction such as pressure overload or MI, but conditional gene deletion offers an alternative strategy to address this important question. Scleraxis regulates cardiac fibroblast collagen expression, and its expression increases in the collagen-rich infarct scar in a rodent model of myocardial infarction [172, 173]. For the first time, we show that loss of scleraxis blunts the cardiac fibrillar collagen expression occurring in response to hypertension in a murine model of pressure overload (Fig. 47). Factors like TGFβ, Angiotensin II and CTGF are upregulated during fibrosis and participate in maintenance of the fibrotic response and gene expression. Administration of these pro-fibrotic agents to primary cardiac proto-myofibroblasts where scleraxis gene had been silenced, resulted in dramatic blunting of fibrillar collagen expression occurring under the influence of these potent agents (Fig. 48). Cardiac myofibroblast marker expression was also downregulated in scleraxis nulls generated using the Cre-Lox recombination system (Fig. 49). These results together suggest that scleraxis perhaps plays a direct role in potentiating cardiac fibrosis, and interruption of scleraxis function/ activity presents a novel approach of interfering with the fibrotic pathway. Preliminary studies in our lab demonstrated that scleraxis is expressed in extra cardiac tissues that are prone to fibrosis including

airway smooth muscle cells and lung fibroblasts. Thus, future investigations that target scleraxis in cardiac fibrosis may lead to the development of therapeutics for fibrosis in multiple tissues.

The results presented here demonstrate a novel role for scleraxis in regulating basal and pathological cardiac matrix synthesis via three distinct mechanisms: (1) transcriptional control of ECM genes, (2) modulation of cardiac fibroblast phenotype via regulation of marker gene and αSMA expression, and (3) requirement for TGFβ/Smad signaling (Fig. 51). Future studies that will assess the contributory role of scleraxis to cardiac dysfunction in acute and chronic pathologies, as well as developmental studies to confirm its role in fibroblast differentiation from progenitors, will elucidate the multiple roles of scleraxis. This will also advance the understanding of mechanisms of ECM and cell phenotype regulation in fibrosis, thus permitting the development of drugs to target scleraxis directly in cardiac fibrosis.

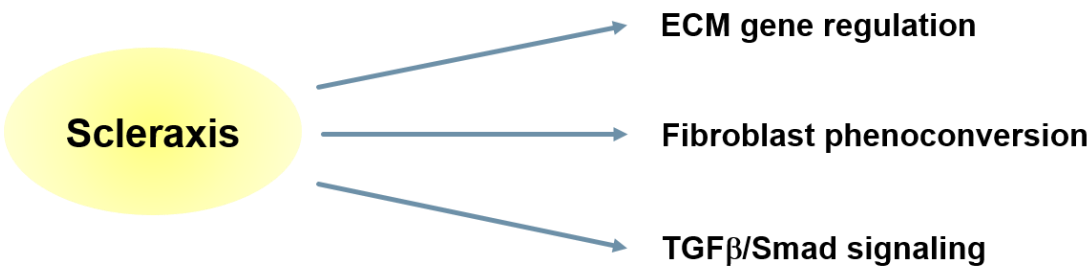

Figure 51: Role of scleraxis in the myocardium.

This schematic summarizes the various functions of scleraxis under basal and pathological conditions. The data presented here overall points to the multiple roles of scleraxis- maintenance of cardiac ECM homeostasis by regulating ECM gene expression, phenotype transition of fibroblasts to myofibroblasts via direct action on phenotype regulatory genes, and its critical role in TGFβ/Smad signaling pathway via cooperativity with Smad proteins.

CHAPTER VI: CONCLUSIONS

Based on our data in the present study, we conclude that:

1. Scleraxis interacts with Smads resulting in a synergistic regulation of the human COL1A2 gene.
2. Scleraxis is a required regulator of cardiac fibroblast ECM gene expression.
3. The transition of fibroblast to myofibroblast phenotype requires the presence of scleraxis.
4. Congenital loss of scleraxis causes alterations in ECM composition at the basal level.
5. Scleraxis loss leads to significant loss of the fibroblast population in the murine myocardium, which is likely due to impaired EMT.
6. Scleraxis is involved in potentiation of cardiac fibrosis in a murine model of pressure overload (hypertension).

CHAPTER VII: STUDY LIMITATIONS AND FUTURE DIRECTIONS

The present study provides an insight in to the role of scleraxis as a novel regulator of multiple cellular processes- fibroblast ECM synthesis, fibroblast-myofibroblast phenoconversion, determination of cell fate via EMT, and cardiac fibrosis consequent to pressure overload. Although a concrete study in itself with substantial evidence supporting our hypothesis, there are a few caveats that can be addressed through future investigations.

Our data shows that the dominant negative scleraxis mutant (Ad-ScxΔBD) abrogates the effect of TGFβ on collagen expression in primary cardiac myofibroblasts. However, the *in vivo* implication of this finding is far from understood. The potential of this mutant can be assessed in one or many pathological models of cardiac fibrosis such as those induced by pressure overload or MI. Tail-vein or direct myocardial delivery of this mutant subsequent to TAC or MI will provide a better understanding of the mechanism of scleraxis function and effects of its interruption on cardiac pathology. The interaction of scleraxis and Smads has been elucidated in this study. But, being a bHLH transcription factor, it is possible that scleraxis interacts with other partner proteins in regulation of target gene expression. Identification of these partners should be carried out by scleraxis pulldown assays followed by mass spectrometry for recognition of the bound proteins.

Concerning the broader role of scleraxis in the transcriptional regulation of multiple ECM genes, the current study relied on the use of real-time RT-PCR to a major extent to measure changes in gene expression levels. Although this is a reliable

method of detecting alterations in gene expression, it may not strictly translate to similar trends in protein expression, especially for collagens and MMPs- this can be achieved using immunoblotting for detection of these proteins.

Although this study focuses on collagens in the ECM, the expression of proteoglycans at the protein level needs to be examined using immunoblotting. Perhaps, this should be incorporated in a future study designed to examine the mechanism of scleraxis-mediated regulation of selected proteoglycan gene targets such as fibromodulin and lumican. Both these ECM components have been implicated in heart failure patients [381]. Studies in mice have shown a significant alteration of expression of these proteoglycans in heart failure, and an effect on collagen fibril assembly [382, 383]. Thus, an in-depth investigation of the regulation of these ECM constituents may identify scleraxis as a direct regulator of these matrix entities.

The expression of TIMPs also needs to be examined - this will provide a better understanding of the regulation of MMPs at the cellular and tissue levels. Putative scleraxis-binding sites on the MMP2 gene promoter need to be validated using promoter analysis tools- mutagenesis of E boxes, chromatin immunoprecipitation and gel-shift assays. RNA- and ChIP-sequencing procedures will help identify other target genes that are directly regulated by scleraxis.

Our analysis of fibroblast phenotype and αSMA expression was carried out using rigid tissue culture plastic dishes. The stiffness of the substrate and force generated affects the expression of myofibroblast markers and αSMA dynamics- a phenomenon that is recapitulated *in vivo* [139, 384]. Soft-substrate polymer coated

tissue culture plates will provide a better assessment tool for examining fibroblast phenotype modulation by scleraxis. If scleraxis is a true inducer of the myofibroblast phenotype, overexpression of this gene in primary fibroblasts growing on these specialized plates should direct them to a myofibroblast phenotype. This will also elucidate the role of scleraxis in force transduction and ECM mechanics in these cells.

Our $Scx^{flox/flox}$-$TCF21^{iCre}$ mice that were gavaged with tamoxifen leading to scleraxis gene excision, exhibited significant blunting of fibrillar collagen expression in a model of pressure overload (TAC). Although these alterations provide evidence for the involvement of scleraxis in cardiac fibrosis, the question that still remains to be addressed is whether scleraxis expression precedes the induction of fibrillar collagen genes. Early stages of assessment (1 day and 1 week post-TAC) of scleraxis and matrix gene expression should be considered in future studies to answer this question. Due to the typically long half-life of ECM components, analysis of these mice at 6 months and 12 months post-tamoxifen gavage should be performed. Long-term deletion of scleraxis without or without induction of pathology may lead to cardiac dysfunction due to underlying alteration in ECM- this will strengthen the role of scleraxis as a potent regulator of cardiac ECM homeostasis. The $Scx^{fl/fl}$- panCre system provides an efficient tool to assess effects of scleraxis loss not just in multiple cells of the heart, but also in extra cardiac tissues that are prone to fibrosis including lungs and skin. Studies should be carried out in pre-clinical models of fibrosis to evaluate the effects of interference of scleraxis function using small molecule inhibitors or stable peptides. These studies would help determine the possible modes of scleraxis inhibition in a clinical setting.

Thus, the future studies outlined above would complement our findings in this report and help advance the understanding of the multi-functional role of scleraxis in health and disease.

CHAPTER VIII: REFERENCES

1. *Cardiovascular diseases (CVDs) Fact sheet N°317*. 2015, World Health Organization.
2. *Cardiovascular disease* 2015, World Health Organization.
3. CANSIM, *Table 102-0561 - Leading causes of death, total population, by age group and sex, Canada, annual,*. 2015, Statistics Canada.
4. *The Canadian Heart Health Strategy: Risk Factors and Future Cost Implications Report*. 2010, Conference Board of Canada.
5. Roger, V.L., et al., *Heart disease and stroke statistics--2011 update: a report from the American Heart Association.* Circulation, 2011. **123**(4): p. e18-e209.
6. Colucci, W.S. and E. Barunwald, *Pathophysiology of Heart Failure*, in *Heart Disease*, E. Barauwald, Editor. 1997, W.B. Saunders Company: Philadelphia. p. 394-420.
7. Barry, S.P., S.M. Davidson, and P.A. Townsend, *Molecular regulation of cardiac hypertrophy.* Int J Biochem Cell Biol, 2008. **40**(10): p. 2023-39.
8. Allard, M.F., et al., *Contribution of oxidative metabolism and glycolysis to ATP production in hypertrophied hearts.* Am J Physiol, 1994. **267**(2 Pt 2): p. H742-50.
9. Davila-Roman, V.G., et al., *Altered myocardial fatty acid and glucose metabolism in idiopathic dilated cardiomyopathy.* J Am Coll Cardiol, 2002. **40**(2): p. 271-7.

10. van Bilsen, M., F.A. van Nieuwenhoven, and G.J. van der Vusse, *Metabolic remodelling of the failing heart: beneficial or detrimental?* Cardiovasc Res, 2009. **81**(3): p. 420-8.

11. Bernardo, B.C., et al., *Molecular distinction between physiological and pathological cardiac hypertrophy: experimental findings and therapeutic strategies.* Pharmacol Ther, 2010. **128**(1): p. 191-227.

12. Izumo, S., et al., *Myosin heavy chain messenger RNA and protein isoform transitions during cardiac hypertrophy. Interaction between hemodynamic and thyroid hormone-induced signals.* J Clin Invest, 1987. **79**(3): p. 970-7.

13. Mahdavi, V., et al., *Cardiac myosin heavy chain isozymic transitions during development and under pathological conditions are regulated at the level of mRNA availability.* Eur Heart J, 1984. **5 Suppl F**: p. 181-91.

14. Gardner, D.G., *Natriuretic peptides: markers or modulators of cardiac hypertrophy?* Trends Endocrinol Metab, 2003. **14**(9): p. 411-6.

15. Gardner, D.G., et al., *Molecular biology of the natriuretic peptide system: implications for physiology and hypertension.* Hypertension, 2007. **49**(3): p. 419-26.

16. Sadoshima, J. and S. Izumo, *The cellular and molecular response of cardiac myocytes to mechanical stress.* Annu Rev Physiol, 1997. **59**: p. 551-71.

17. Akazawa, H. and I. Komuro, *Roles of cardiac transcription factors in cardiac hypertrophy.* Circ Res, 2003. **92**(10): p. 1079-88.

18. Kogler, H., et al., *Relevance of brain natriuretic peptide in preload-dependent regulation of cardiac sarcoplasmic reticulum Ca2+ ATPase expression.* Circulation, 2006. **113**(23): p. 2724-32.

19. McMullen, J.R. and G.L. Jennings, *Differences between pathological and physiological cardiac hypertrophy: novel therapeutic strategies to treat heart failure.* Clin Exp Pharmacol Physiol, 2007. **34**(4): p. 255-62.

20. Weeks, K.L. and J.R. McMullen, *The athlete's heart vs. the failing heart: can signaling explain the two distinct outcomes?* Physiology (Bethesda), 2011. **26**(2): p. 97-105.

21. Romano, C., et al., *Reduced hemodynamic load and cardiac hypotrophy in patients with anorexia nervosa.* Am J Clin Nutr, 2003. **77**(2): p. 308-12.

22. Lee, S., et al., *Total beta-adrenoceptor deficiency results in cardiac hypotrophy and negative inotropy.* Physiol Res, 2010. **59**(5): p. 679-89.

23. Czubryt, M.P., *Common threads in cardiac fibrosis, infarct scar formation, and wound healing.* Fibrogenesis Tissue Repair, 2012. **5**(1): p. 19.

24. Liehn, E.A., et al., *Repair after myocardial infarction, between fantasy and reality: the role of chemokines.* J Am Coll Cardiol, 2011. **58**(23): p. 2357-62.

25. Vanhoutte, D., et al., *Relevance of matrix metalloproteinases and their inhibitors after myocardial infarction: a temporal and spatial window.* Cardiovasc Res, 2006. **69**(3): p. 604-13.

26. Weber, K.T. and C.G. Brilla, *Pathological hypertrophy and cardiac interstitium. Fibrosis and renin-angiotensin-aldosterone system.* Circulation, 1991. **83**(6): p. 1849-65.

27. Tanaka, M., et al., *Quantitative analysis of myocardial fibrosis in normals, hypertensive hearts, and hypertrophic cardiomyopathy.* Br Heart J, 1986. **55**(6): p. 575-81.

28. Boudina, S. and E.D. Abel, *Diabetic cardiomyopathy revisited.* Circulation, 2007. **115**(25): p. 3213-23.

29. Weber, K.T., et al., *Collagen remodeling of the pressure-overloaded, hypertrophied nonhuman primate myocardium.* Circ Res, 1988. **62**(4): p. 757-65.

30. Schwarz, F., et al., *Myocardial structure and function in patients with aortic valve disease and their relation to postoperative results.* Am J Cardiol, 1978. **41**(4): p. 661-9.

31. Weidemann, F., et al., *Impact of myocardial fibrosis in patients with symptomatic severe aortic stenosis.* Circulation, 2009. **120**(7): p. 577-84.

32. Marijianowski, M.M., P. Teeling, and A.E. Becker, *Remodeling after myocardial infarction in humans is not associated with interstitial fibrosis of noninfarcted myocardium.* J Am Coll Cardiol, 1997. **30**(1): p. 76-82.

33. Sutton, M.G. and N. Sharpe, *Left ventricular remodeling after myocardial infarction: pathophysiology and therapy.* Circulation, 2000. **101**(25): p. 2981-8.

34. Karamitsos, T.D., et al., *The role of cardiovascular magnetic resonance imaging in heart failure.* J Am Coll Cardiol, 2009. **54**(15): p. 1407-24.

35. Bohl, S., et al., *Delayed enhancement cardiac magnetic resonance imaging reveals typical patterns of myocardial injury in patients with various forms of non-ischemic heart disease.* Int J Cardiovasc Imaging, 2008. **24**(6): p. 597-607.

36. Shah, K.B., Y. Inoue, and M.R. Mehra, *Amyloidosis and the heart: a comprehensive review.* Arch Intern Med, 2006. **166**(17): p. 1805-13.

37. Zarate, Y.A. and R.J. Hopkin, *Fabry's disease.* Lancet, 2008. **372**(9647): p. 1427-35.

38. Bataller, R. and D.A. Brenner, *Liver fibrosis.* J Clin Invest, 2005. **115**(2): p. 209-18.

39. Noble, P.W., *Idiopathic pulmonary fibrosis: natural history and prognosis.* Clin Chest Med, 2006. **27**(1 Suppl 1): p. S11-6, v.

40. Krenning, G., E.M. Zeisberg, and R. Kalluri, *The origin of fibroblasts and mechanism of cardiac fibrosis.* J Cell Physiol, 2010. **225**(3): p. 631-7.

41. Schnaper, H.W. and J.B. Kopp, *Renal fibrosis.* Front Biosci, 2003. **8**: p. e68-86.

42. Chaturvedi, R.R., et al., *Passive stiffness of myocardium from congenital heart disease and implications for diastole.* Circulation, 2010. **121**(8): p. 979-88.

43. Stuckey, D.J., et al., *T(1) mapping detects pharmacological retardation of diffuse cardiac fibrosis in mouse pressure-overload hypertrophy.* Circ Cardiovasc Imaging, 2014. **7**(2): p. 240-9.

44. Won, S., et al., *Noninvasive imaging of myocardial extracellular matrix for assessment of fibrosis.* Curr Opin Cardiol, 2013. **28**(3): p. 282-9.

45. Vohringer, M., et al., *Significance of late gadolinium enhancement in cardiovascular magnetic resonance imaging (CMR).* Herz, 2007. **32**(2): p. 129-37.

46. Ghann, W.E., et al., *Syntheses and characterization of lisinopril-coated gold nanoparticles as highly stable targeted CT contrast agents in cardiovascular diseases.* Langmuir, 2012. **28**(28): p. 10398-408.

47. Femia, F.J., et al., *Synthesis and evaluation of a series of 99mTc(CO)3+ lisinopril complexes for in vivo imaging of angiotensin-converting enzyme expression.* J Nucl Med, 2008. **49**(6): p. 970-7.

48. Brilla, C.G., R.C. Funck, and H. Rupp, *Lisinopril-mediated regression of myocardial fibrosis in patients with hypertensive heart disease.* Circulation, 2000. **102**(12): p. 1388-93.

49. Ciulla, M.M., et al., *Effects of antihypertensive treatment on ultrasound measures of myocardial fibrosis in hypertensive patients with left ventricular hypertrophy: results of a randomized trial comparing the angiotensin receptor antagonist, candesartan and the angiotensin-converting enzyme inhibitor, enalapril.* J Hypertens, 2009. **27**(3): p. 626-32.

50. Roche, P.L. and M.P. Czubryt, *Current and Future Strategies for the Diagnosis and Treatment of Cardiac Fibrosis*, in *Cardiac Fibrosis and Heart Failure: Cause or Effect?*, I.M. Dixon and J.T. Wigle, Editors. 2015, Springer International Publishing: Switzerland.

51. Diez, J., et al., *Losartan-dependent regression of myocardial fibrosis is associated with reduction of left ventricular chamber stiffness in hypertensive patients.* Circulation, 2002. **105**(21): p. 2512-7.

52. Hayashi, M., et al., *Immediate administration of mineralocorticoid receptor antagonist spironolactone prevents post-infarct left ventricular remodeling associated with suppression of a marker of myocardial collagen synthesis in patients with first anterior acute myocardial infarction.* Circulation, 2003. **107**(20): p. 2559-65.

53. Cicoira, M., et al., *Long-term, dose-dependent effects of spironolactone on left ventricular function and exercise tolerance in patients with chronic heart failure.* J Am Coll Cardiol, 2002. **40**(2): p. 304-10.

54. Kveiborg, B., et al., *Carvedilol in the treatment of chronic heart failure: lessons from the Carvedilol Or Metoprolol European Trial.* Vasc Health Risk Manag, 2007. **3**(1): p. 31-7.

55. Souders, C.A., S.L. Bowers, and T.A. Baudino, *Cardiac fibroblast: the renaissance cell.* Circ Res, 2009. **105**(12): p. 1164-76.

56. Camelliti, P., T.K. Borg, and P. Kohl, *Structural and functional characterisation of cardiac fibroblasts.* Cardiovasc Res, 2005. **65**(1): p. 40-51.

57. Fries, K.M., et al., *Evidence of fibroblast heterogeneity and the role of fibroblast subpopulations in fibrosis.* Clin Immunol Immunopathol, 1994. **72**(3): p. 283-92.

58. Norris, R.A., et al., *Neonatal and adult cardiovascular pathophysiological remodeling and repair: developmental role of periostin.* Ann N Y Acad Sci, 2008. **1123**: p. 30-40.

59. Lie-Venema, H., et al., *Origin, fate, and function of epicardium-derived cells (EPDCs) in normal and abnormal cardiac development.* ScientificWorldJournal, 2007. **7**: p. 1777-98.

60. Gittenberger-de Groot, A.C., et al., *Epicardium-derived cells contribute a novel population to the myocardial wall and the atrioventricular cushions.* Circ Res, 1998. **82**(10): p. 1043-52.

61. Munoz-Chapuli, R., et al., *The epicardium as a source of mesenchyme for the developing heart.* Ital J Anat Embryol, 2001. **106**(2 Suppl 1): p. 187-96.

62. Kolditz, D.P., et al., *Epicardium-derived cells in development of annulus fibrosis and persistence of accessory pathways.* Circulation, 2008. **117**(12): p. 1508-17.

63. de Lange, F.J., et al., *Lineage and morphogenetic analysis of the cardiac valves.* Circ Res, 2004. **95**(6): p. 645-54.

64. Lucas, J.A., et al., *Inhibition of transforming growth factor-beta signaling induces left ventricular dilation and dysfunction in the pressure-overloaded heart.* Am J Physiol Heart Circ Physiol, 2010. **298**(2): p. H424-32.

65. Mandache, E., et al., *The proliferative activity of the heart tissues in various forms of experimental cardiac hypertrophy studied by electron microscope autoradiography.* Virchows Arch B Cell Pathol, 1973. **12**(2): p. 112-22.

66. Ljungqvist, A. and G. Unge, *The proliferative activity of the myocardial tissue in various forms of experimental cardiac hypertrophy.* Acta Pathol Microbiol Scand A, 1973. **81**(3): p. 233-40.

67. Humphreys, B.D., et al., *Fate tracing reveals the pericyte and not epithelial origin of myofibroblasts in kidney fibrosis.* Am J Pathol, 2010. **176**(1): p. 85-97.

68. Covas, D.T., et al., *Multipotent mesenchymal stromal cells obtained from diverse human tissues share functional properties and gene-expression profile with CD146+ perivascular cells and fibroblasts.* Exp Hematol, 2008. **36**(5): p. 642-54.

69. Sundberg, C., et al., *Pericytes as collagen-producing cells in excessive dermal scarring.* Lab Invest, 1996. **74**(2): p. 452-66.

70. van Amerongen, M.J., et al., *Bone marrow-derived myofibroblasts contribute functionally to scar formation after myocardial infarction.* J Pathol, 2008. **214**(3): p. 377-86.

71. Kania, G., et al., *Heart-infiltrating prominin-1+/CD133+ progenitor cells represent the cellular source of transforming growth factor beta-mediated cardiac fibrosis in experimental autoimmune myocarditis.* Circ Res, 2009. **105**(5): p. 462-70.

72. Zeisberg, E.M., et al., *Endothelial-to-mesenchymal transition contributes to cardiac fibrosis.* Nat Med, 2007. **13**(8): p. 952-61.

73. Haudek, S.B., et al., *Bone marrow-derived fibroblast precursors mediate ischemic cardiomyopathy in mice.* Proc Natl Acad Sci U S A, 2006. **103**(48): p. 18284-9.

74. van Amerongen, M.J., et al., *Macrophage depletion impairs wound healing and increases left ventricular remodeling after myocardial injury in mice.* Am J Pathol, 2007. **170**(3): p. 818-29.

75. Abe, R., et al., *Peripheral blood fibrocytes: differentiation pathway and migration to wound sites.* J Immunol, 2001. **166**(12): p. 7556-62.

76. Strieter, R.M., et al., *The role of circulating mesenchymal progenitor cells, fibrocytes, in promoting pulmonary fibrosis.* Trans Am Clin Climatol Assoc, 2009. **120**: p. 49-59.

77. Moonen, J.R., et al., *Endothelial progenitor cells give rise to pro-angiogenic smooth muscle-like progeny.* Cardiovasc Res, 2010. **86**(3): p. 506-15.

78. Krenning, G., et al., *Vascular smooth muscle cells for use in vascular tissue engineering obtained by endothelial-to-mesenchymal transdifferentiation (EnMT) on collagen matrices.* Biomaterials, 2008. **29**(27): p. 3703-11.

79. Garcia, J., et al., *Tie1 deficiency induces endothelial-mesenchymal transition.* EMBO Rep, 2012. **13**(5): p. 431-9.

80. Bosman, F.T. and I. Stamenkovic, *Functional structure and composition of the extracellular matrix.* J Pathol, 2003. **200**(4): p. 423-8.

81. Butt, R.P., G.J. Laurent, and J.E. Bishop, *Collagen production and replication by cardiac fibroblasts is enhanced in response to diverse classes of growth factors.* Eur J Cell Biol, 1995. **68**(3): p. 330-5.

82. Tsuruda, T., L.C. Costello-Boerrigter, and J.C. Burnett, Jr., *Matrix metalloproteinases: pathways of induction by bioactive molecules.* Heart Fail Rev, 2004. **9**(1): p. 53-61.

83. Moore, L., et al., *Tissue inhibitor of metalloproteinases (TIMPs) in heart failure.* Heart Fail Rev, 2012. **17**(4-5): p. 693-706.

84. Villaschi, S. and R.F. Nicosia, *Paracrine interactions between fibroblasts and endothelial cells in a serum-free coculture model. Modulation of angiogenesis and collagen gel contraction.* Lab Invest, 1994. **71**(2): p. 291-9.

85. Zhao, L. and M. Eghbali-Webb, *Release of pro- and anti-angiogenic factors by human cardiac fibroblasts: effects on DNA synthesis and protection under hypoxia in human endothelial cells.* Biochim Biophys Acta, 2001. **1538**(2-3): p. 273-82.

86. Chintalgattu, V., D.M. Nair, and L.C. Katwa, *Cardiac myofibroblasts: a novel source of vascular endothelial growth factor (VEGF) and its receptors Flt-1 and KDR.* J Mol Cell Cardiol, 2003. **35**(3): p. 277-86.

87. Rychli, K., K. Huber, and J. Wojta, *Pigment epithelium-derived factor (PEDF) as a therapeutic target in cardiovascular disease.* Expert Opin Ther Targets, 2009. **13**(11): p. 1295-302.

88. Engel, F.B., et al., *p38 MAP kinase inhibition enables proliferation of adult mammalian cardiomyocytes.* Genes Dev, 2005. **19**(10): p. 1175-87.

89. Kuhn, B., et al., *Periostin induces proliferation of differentiated cardiomyocytes and promotes cardiac repair.* Nat Med, 2007. **13**(8): p. 962-9.

90. Porter, K.E. and N.A. Turner, *Cardiac fibroblasts: at the heart of myocardial remodeling.* Pharmacol Ther, 2009. **123**(2): p. 255-78.

91. Kohl, P., *Heterogeneous cell coupling in the heart: an electrophysiological role for fibroblasts.* Circ Res, 2003. **93**(5): p. 381-3.

92. Chilton, L., W.R. Giles, and G.L. Smith, *Evidence of intercellular coupling between co-cultured adult rabbit ventricular myocytes and myofibroblasts.* J Physiol, 2007. **583**(Pt 1): p. 225-36.

93. Gaudesius, G., et al., *Coupling of cardiac electrical activity over extended distances by fibroblasts of cardiac origin.* Circ Res, 2003. **93**(5): p. 421-8.

94. Miragoli, M., G. Gaudesius, and S. Rohr, *Electrotonic modulation of cardiac impulse conduction by myofibroblasts.* Circ Res, 2006. **98**(6): p. 801-10.

95. Rohr, S., *Role of gap junctions in the propagation of the cardiac action potential.* Cardiovasc Res, 2004. **62**(2): p. 309-22.

96. Zhou, B., et al., *Genetic fate mapping demonstrates contribution of epicardium-derived cells to the annulus fibrosis of the mammalian heart.* Dev Biol, 2010. **338**(2): p. 251-61.

97. Li, G.R., et al., *Characterization of multiple ion channels in cultured human cardiac fibroblasts.* PLoS One, 2009. **4**(10): p. e7307.

98. Kamkin, A., et al., *Cardiac fibroblasts and the mechano-electric feedback mechanism in healthy and diseased hearts.* Prog Biophys Mol Biol, 2003. **82**(1-3): p. 111-20.

99. Camelliti, P., et al., *Fibroblast network in rabbit sinoatrial node: structural and functional identification of homogeneous and heterogeneous cell coupling.* Circ Res, 2004. **94**(6): p. 828-35.

100. Santiago, J.J., et al., *Cardiac fibroblast to myofibroblast differentiation in vivo and in vitro: expression of focal adhesion components in neonatal and adult rat ventricular myofibroblasts.* Dev Dyn, 2010. **239**(6): p. 1573-84.

101. Driesen, R.B., et al., *Reversible and irreversible differentiation of cardiac fibroblasts.* Cardiovasc Res, 2014. **101**(3): p. 411-22.

102. Hinz, B., et al., *The myofibroblast: one function, multiple origins.* Am J Pathol, 2007. **170**(6): p. 1807-16.

103. Tomasek, J.J., et al., *Myofibroblasts and mechano-regulation of connective tissue remodelling.* Nat Rev Mol Cell Biol, 2002. **3**(5): p. 349-63.

104. Darby, I., O. Skalli, and G. Gabbiani, *Alpha-smooth muscle actin is transiently expressed by myofibroblasts during experimental wound healing.* Lab Invest, 1990. **63**(1): p. 21-9.

105. Dugina, V., et al., *Focal adhesion features during myofibroblastic differentiation are controlled by intracellular and extracellular factors.* J Cell Sci, 2001. **114**(Pt 18): p. 3285-96.

106. Ronnov-Jessen, L. and O.W. Petersen, *Induction of alpha-smooth muscle actin by transforming growth factor-beta 1 in quiescent human breast gland fibroblasts. Implications for myofibroblast generation in breast neoplasia.* Lab Invest, 1993. **68**(6): p. 696-707.

107. Serini, G., et al., *The fibronectin domain ED-A is crucial for myofibroblastic phenotype induction by transforming growth factor-beta1*. J Cell Biol, 1998. **142**(3): p. 873-81.

108. Stocks, S.Z., S.M. Taylor, and I.A. Shiels, *Transforming growth factor-beta1 induces alpha-smooth muscle actin expression and fibronectin synthesis in cultured human retinal pigment epithelial cells.* Clin Experiment Ophthalmol, 2001. **29**(1): p. 33-7.

109. Hinz, B., *The myofibroblast: paradigm for a mechanically active cell.* J Biomech, 2010. **43**(1): p. 146-55.

110. Desmouliere, A., et al., *Transforming growth factor-beta 1 induces alpha-smooth muscle actin expression in granulation tissue myofibroblasts and in quiescent and growing cultured fibroblasts.* J Cell Biol, 1993. **122**(1): p. 103-11.

111. Petrov, V.V., R.H. Fagard, and P.J. Lijnen, *Stimulation of collagen production by transforming growth factor-beta1 during differentiation of cardiac fibroblasts to myofibroblasts.* Hypertension, 2002. **39**(2): p. 258-63.

112. Evans, R.A., et al., *TGF-beta1-mediated fibroblast-myofibroblast terminal differentiation-the role of Smad proteins.* Exp Cell Res, 2003. **282**(2): p. 90-100.

113. Petrov, V.V., R.H. Fagard, and P.J. Lijnen, *Transforming growth factor-beta(1) induces angiotensin-converting enzyme synthesis in rat cardiac fibroblasts during their differentiation to myofibroblasts.* J Renin Angiotensin Aldosterone Syst, 2000. **1**(4): p. 342-52.

114. Dixon, I.M., et al., *Effect of chronic AT(1) receptor blockade on cardiac Smad overexpression in hereditary cardiomyopathic hamsters.* Cardiovasc Res, 2000. **46**(2): p. 286-97.

115. Olson, E.R., et al., *Inhibition of cardiac fibroblast proliferation and myofibroblast differentiation by resveratrol.* Am J Physiol Heart Circ Physiol, 2005. **288**(3): p. H1131-8.

116. Campbell, S.E. and L.C. Katwa, *Angiotensin II stimulated expression of transforming growth factor-beta1 in cardiac fibroblasts and myofibroblasts.* J Mol Cell Cardiol, 1997. **29**(7): p. 1947-58.

117. Lee, A.A., et al., *Angiotensin II stimulates the autocrine production of transforming growth factor-beta 1 in adult rat cardiac fibroblasts.* J Mol Cell Cardiol, 1995. **27**(10): p. 2347-57.

118. Annes, J.P., J.S. Munger, and D.B. Rifkin, *Making sense of latent TGFbeta activation.* J Cell Sci, 2003. **116**(Pt 2): p. 217-24.

119. Saharinen, J. and J. Keski-Oja, *Specific sequence motif of 8-Cys repeats of TGF-beta binding proteins, LTBPs, creates a hydrophobic interaction surface for binding of small latent TGF-beta.* Mol Biol Cell, 2000. **11**(8): p. 2691-704.

120. Schoppet, M., et al., *Molecular interactions and functional interference between vitronectin and transforming growth factor-beta.* Lab Invest, 2002. **82**(1): p. 37-46.

121. Taipale, J., et al., *Latent transforming growth factor-beta 1 associates to fibroblast extracellular matrix via latent TGF-beta binding protein.* J Cell Biol, 1994. **124**(1-2): p. 171-81.

122. ten Dijke, P. and H.M. Arthur, *Extracellular control of TGFbeta signalling in vascular development and disease.* Nat Rev Mol Cell Biol, 2007. **8**(11): p. 857-69.

123. D'Angelo, M., et al., *Authentic matrix vesicles contain active metalloproteases (MMP). a role for matrix vesicle-associated MMP-13 in activation of transforming growth factor-beta.* J Biol Chem, 2001. **276**(14): p. 11347-53.

124. Maeda, S., et al., *The first stage of transforming growth factor beta1 activation is release of the large latent complex from the extracellular matrix of growth plate chondrocytes by matrix vesicle stromelysin-1 (MMP-3).* Calcif Tissue Int, 2002. **70**(1): p. 54-65.

125. Yu, Q. and I. Stamenkovic, *Cell surface-localized matrix metalloproteinase-9 proteolytically activates TGF-beta and promotes tumor invasion and angiogenesis.* Genes Dev, 2000. **14**(2): p. 163-76.

126. Miyazono, K. and C.H. Heldin, *Role for carbohydrate structures in TGF-beta 1 latency.* Nature, 1989. **338**(6211): p. 158-60.

127. Murphy-Ullrich, J.E. and M. Poczatek, *Activation of latent TGF-beta by thrombospondin-1: mechanisms and physiology.* Cytokine Growth Factor Rev, 2000. **11**(1-2): p. 59-69.

128. Assoian, R.K., et al., *Expression and secretion of type beta transforming growth factor by activated human macrophages.* Proc Natl Acad Sci U S A, 1987. **84**(17): p. 6020-4.

129. Fisher, S.A. and M. Absher, *Norepinephrine and ANG II stimulate secretion of TGF-beta by neonatal rat cardiac fibroblasts in vitro.* Am J Physiol, 1995. **268**(4 Pt 1): p. C910-7.

130. Inoue, A., et al., *The human endothelin family: three structurally and pharmacologically distinct isopeptides predicted by three separate genes.* Proc Natl Acad Sci U S A, 1989. **86**(8): p. 2863-7.

131. Inoue, A., et al., *The human preproendothelin-1 gene. Complete nucleotide sequence and regulation of expression.* J Biol Chem, 1989. **264**(25): p. 14954-9.

132. Agapitov, A.V. and W.G. Haynes, *Role of endothelin in cardiovascular disease.* J Renin Angiotensin Aldosterone Syst, 2002. **3**(1): p. 1-15.

133. Nishida, M., et al., *Galpha12/13-mediated up-regulation of TRPC6 negatively regulates endothelin-1-induced cardiac myofibroblast formation and collagen synthesis through nuclear factor of activated T cells activation.* J Biol Chem, 2007. **282**(32): p. 23117-28.

134. Kuwahara, K., et al., *TRPC6 fulfills a calcineurin signaling circuit during pathologic cardiac remodeling.* J Clin Invest, 2006. **116**(12): p. 3114-26.

135. Davis, J., et al., *A TRPC6-dependent pathway for myofibroblast transdifferentiation and wound healing in vivo.* Dev Cell, 2012. **23**(4): p. 705-15.

136. Kapur, N.K., et al., *Reducing Endoglin Activity Limits Calcineurin and TRPC-6 Expression and Improves Survival in a Mouse Model of Right Ventricular Pressure Overload.* J Am Heart Assoc, 2014. **3**(4).

137. Thodeti, C.K., S. Paruchuri, and J.G. Meszaros, *A TRP to cardiac fibroblast differentiation.* Channels (Austin), 2013. **7**(3): p. 211-4.

138. Yue, L., J. Xie, and S. Nattel, *Molecular determinants of cardiac fibroblast electrical function and therapeutic implications for atrial fibrillation.* Cardiovasc Res, 2011. **89**(4): p. 744-53.

139. Zhao, X.H., et al., *Force activates smooth muscle alpha-actin promoter activity through the Rho signaling pathway.* J Cell Sci, 2007. **120**(Pt 10): p. 1801-9.

140. Bauersachs, J. and T. Thum, *Biogenesis and regulation of cardiovascular microRNAs.* Circ Res, 2011. **109**(3): p. 334-47.

141. Brodersen, P. and O. Voinnet, *Revisiting the principles of microRNA target recognition and mode of action.* Nat Rev Mol Cell Biol, 2009. **10**(2): p. 141-8.

142. Wang, Y.S., et al., *Role of miR-145 in cardiac myofibroblast differentiation.* J Mol Cell Cardiol, 2014. **66**: p. 94-105.

143. Cheng, Y., et al., *MicroRNA-145, a novel smooth muscle cell phenotypic marker and modulator, controls vascular neointimal lesion formation.* Circ Res, 2009. **105**(2): p. 158-66.

144. Small, E.M., et al., *Myocardin-related transcription factor-a controls myofibroblast activation and fibrosis in response to myocardial infarction.* Circ Res, 2010. **107**(2): p. 294-304.

145. Pipes, G.C., E.E. Creemers, and E.N. Olson, *The myocardin family of transcriptional coactivators: versatile regulators of cell growth, migration, and myogenesis.* Genes Dev, 2006. **20**(12): p. 1545-56.

146. Wang, D., et al., *Activation of cardiac gene expression by myocardin, a transcriptional cofactor for serum response factor.* Cell, 2001. **105**(7): p. 851-62.

147. Kuwahara, K., et al., *Muscle-specific signaling mechanism that links actin dynamics to serum response factor.* Mol Cell Biol, 2005. **25**(8): p. 3173-81.

148. Mack, C.P., et al., *Smooth muscle differentiation marker gene expression is regulated by RhoA-mediated actin polymerization.* J Biol Chem, 2001. **276**(1): p. 341-7.

149. Miralles, F., et al., *Actin dynamics control SRF activity by regulation of its coactivator MAL.* Cell, 2003. **113**(3): p. 329-42.

150. Kavsak, P., et al., *Smad7 binds to Smurf2 to form an E3 ubiquitin ligase that targets the TGF beta receptor for degradation.* Mol Cell, 2000. **6**(6): p. 1365-75.

151. Cunnington, R.H., et al., *Antifibrotic properties of c-Ski and its regulation of cardiac myofibroblast phenotype and contractility.* Am J Physiol Cell Physiol, 2011. **300**(1): p. C176-86.

152. Suzuki, H., et al., *c-Ski inhibits the TGF-beta signaling pathway through stabilization of inactive Smad complexes on Smad-binding elements.* Oncogene, 2004. **23**(29): p. 5068-76.

153. Cunnington, R.H., et al., *The Ski-Zeb2-Meox2 pathway provides a novel mechanism for regulation of the cardiac myofibroblast phenotype.* J Cell Sci, 2014. **127**(Pt 1): p. 40-9.

154. Chen, Y., et al., *Regulation of the expression and activity of the antiangiogenic homeobox gene GAX/MEOX2 by ZEB2 and microRNA-221.* Mol Cell Biol, 2010. **30**(15): p. 3902-13.

155. Li, P., et al., *Atrial natriuretic peptide inhibits transforming growth factor beta-induced Smad signaling and myofibroblast transformation in mouse cardiac fibroblasts.* Circ Res, 2008. **102**(2): p. 185-92.

156. Redondo, J., J.E. Bishop, and M.R. Wilkins, *Effect of atrial natriuretic peptide and cyclic GMP phosphodiesterase inhibition on collagen synthesis by adult cardiac fibroblasts.* Br J Pharmacol, 1998. **124**(7): p. 1455-62.

157. Leask, A. and D.J. Abraham, *TGF-beta signaling and the fibrotic response.* FASEB J, 2004. **18**(7): p. 816-27.

158. Rosenkranz, A.C., et al., *Antihypertrophic actions of the natriuretic peptides in adult rat cardiomyocytes: importance of cyclic GMP.* Cardiovasc Res, 2003. **57**(2): p. 515-22.

159. Kinoshita, T., et al., *Antifibrotic response of cardiac fibroblasts in hypertensive hearts through enhanced TIMP-1 expression by basic fibroblast growth factor.* Cardiovasc Pathol, 2014. **23**(2): p. 92-100.

160. Santiago, J.J., et al., *Preferential accumulation and export of high molecular weight FGF-2 by rat cardiac non-myocytes.* Cardiovasc Res, 2011. **89**(1): p. 139-47.

161. Santiago, J.J., et al., *High molecular weight fibroblast growth factor-2 in the human heart is a potential target for prevention of cardiac remodeling.* PLoS One, 2014. **9**(5): p. e97281.

162. Sun, Y. and K.T. Weber, *Infarct scar: a dynamic tissue.* Cardiovasc Res, 2000. **46**(2): p. 250-6.

163. Desmouliere, A. and G. Gabbiani, *Modulation of fibroblastic cytoskeletal features during pathological situations: the role of extracellular matrix and cytokines.* Cell Motil Cytoskeleton, 1994. **29**(3): p. 195-203.

164. Lazard, D., et al., *Expression of smooth muscle-specific proteins in myoepithelium and stromal myofibroblasts of normal and malignant human breast tissue.* Proc Natl Acad Sci U S A, 1993. **90**(3): p. 999-1003.

165. Qiu, P., X.H. Feng, and L. Li, *Interaction of Smad3 and SRF-associated complex mediates TGF-beta1 signals to regulate SM22 transcription during myofibroblast differentiation.* J Mol Cell Cardiol, 2003. **35**(12): p. 1407-20.

166. Sappino, A.P., W. Schurch, and G. Gabbiani, *Differentiation repertoire of fibroblastic cells: expression of cytoskeletal proteins as marker of phenotypic modulations.* Lab Invest, 1990. **63**(2): p. 144-61.

167. Walker, G.A., et al., *Valvular myofibroblast activation by transforming growth factor-beta: implications for pathological extracellular matrix remodeling in heart valve disease.* Circ Res, 2004. **95**(3): p. 253-60.

168. Leask, A., *TGFbeta, cardiac fibroblasts, and the fibrotic response.* Cardiovasc Res, 2007. **74**(2): p. 207-12.

169. Hinz, B., *Formation and function of the myofibroblast during tissue repair.* J Invest Dermatol, 2007. **127**(3): p. 526-37.

170. Phan, S.H., *Biology of fibroblasts and myofibroblasts.* Proc Am Thorac Soc, 2008. **5**(3): p. 334-7.

171. Zhang, H.Y., et al., *Lung fibroblast alpha-smooth muscle actin expression and contractile phenotype in bleomycin-induced pulmonary fibrosis.* Am J Pathol, 1996. **148**(2): p. 527-37.

172. Bagchi, R.A. and M.P. Czubryt, *Synergistic roles of scleraxis and Smads in the regulation of collagen 1alpha2 gene expression.* Biochim Biophys Acta, 2012. **1823**(10): p. 1936-44.

173. Espira, L., et al., *The basic helix-loop-helix transcription factor scleraxis regulates fibroblast collagen synthesis.* J Mol Cell Cardiol, 2009. **47**(2): p. 188-95.

174. Verrecchia, F., M.L. Chu, and A. Mauviel, *Identification of novel TGF-beta /Smad gene targets in dermal fibroblasts using a combined cDNA microarray/promoter transactivation approach.* J Biol Chem, 2001. **276**(20): p. 17058-62.

175. Dobaczewski, M., et al., *Smad3 signaling critically regulates fibroblast phenotype and function in healing myocardial infarction.* Circ Res, 2010. **107**(3): p. 418-28.

176. Davis, J. and J.D. Molkentin, *Myofibroblasts: trust your heart and let fate decide.* J Mol Cell Cardiol, 2014. **70**: p. 9-18.

177. Koitabashi, N., et al., *Pivotal role of cardiomyocyte TGF-beta signaling in the murine pathological response to sustained pressure overload.* J Clin Invest, 2011. **121**(6): p. 2301-12.

178. Haudek, S.B., et al., *Monocytic fibroblast precursors mediate fibrosis in angiotensin-II-induced cardiac hypertrophy.* J Mol Cell Cardiol, 2010. **49**(3): p. 499-507.

179. Holtz, J., *Pathophysiology of heart failure and the renin-angiotensin-system.* Basic Res Cardiol, 1993. **88 Suppl 1**: p. 183-201.

180. Gao, X., et al., *Angiotensin II increases collagen I expression via transforming growth factor-beta1 and extracellular signal-regulated kinase in cardiac fibroblasts.* Eur J Pharmacol, 2009. **606**(1-3): p. 115-20.

181. Yang, F., et al., *Angiotensin II induces connective tissue growth factor and collagen I expression via transforming growth factor-beta-dependent and -independent Smad pathways: the role of Smad3.* Hypertension, 2009. **54**(4): p. 877-84.

182. Leask, A., *Targeting the TGFbeta, endothelin-1 and CCN2 axis to combat fibrosis in scleroderma.* Cell Signal, 2008. **20**(8): p. 1409-14.

183. Cheng, T.H., et al., *Involvement of reactive oxygen species in angiotensin II-induced endothelin-1 gene expression in rat cardiac fibroblasts.* J Am Coll Cardiol, 2003. **42**(10): p. 1845-54.

184. Shi-wen, X., et al., *Endothelin is a downstream mediator of profibrotic responses to transforming growth factor beta in human lung fibroblasts.* Arthritis Rheum, 2007. **56**(12): p. 4189-94.

185. Leask, A., *Potential therapeutic targets for cardiac fibrosis: TGFbeta, angiotensin, endothelin, CCN2, and PDGF, partners in fibroblast activation.* Circ Res, 2010. **106**(11): p. 1675-80.

186. Pramod, S. and K. Shivakumar, *Mechanisms in cardiac fibroblast growth: an obligate role for Skp2 and FOXO3a in ERK1/2 MAPK-dependent regulation of p27kip1.* Am J Physiol Heart Circ Physiol, 2014. **306**(6): p. H844-55.

187. Acharya, A., et al., *The bHLH transcription factor Tcf21 is required for lineage-specific EMT of cardiac fibroblast progenitors.* Development, 2012. **139**(12): p. 2139-49.

188. Chang, H.Y., et al., *Diversity, topographic differentiation, and positional memory in human fibroblasts.* Proc Natl Acad Sci U S A, 2002. **99**(20): p. 12877-82.

189. Burstein, B., et al., *Differential behaviors of atrial versus ventricular fibroblasts: a potential role for platelet-derived growth factor in atrial-ventricular remodeling differences.* Circulation, 2008. **117**(13): p. 1630-41.

190. Pillai, M.S., S. Sapna, and K. Shivakumar, *p38 MAPK regulates G1-S transition in hypoxic cardiac fibroblasts.* Int J Biochem Cell Biol, 2011. **43**(6): p. 919-27.

191. Corda, S., J.L. Samuel, and L. Rappaport, *Extracellular matrix and growth factors during heart growth.* Heart Fail Rev, 2000. **5**(2): p. 119-30.

192. Eghbali, M. and K.T. Weber, *Collagen and the myocardium: fibrillar structure, biosynthesis and degradation in relation to hypertrophy and its regression.* Mol Cell Biochem, 1990. **96**(1): p. 1-14.

193. Holmes, J.W., T.K. Borg, and J.W. Covell, *Structure and mechanics of healing myocardial infarcts.* Annu Rev Biomed Eng, 2005. **7**: p. 223-53.

194. Eghbali, M., *Cardiac fibroblasts: function, regulation of gene expression, and phenotypic modulation.* Basic Res Cardiol, 1992. **87 Suppl 2**: p. 183-9.

195. Bashey, R.I., A. Martinez-Hernandez, and S.A. Jimenez, *Isolation, characterization, and localization of cardiac collagen type VI. Associations with other extracellular matrix components.* Circ Res, 1992. **70**(5): p. 1006-17.

196. de Souza, R.R., *Aging of myocardial collagen.* Biogerontology, 2002. **3**(6): p. 325-35.

197. Bishop, J.E. and G.J. Laurent, *Collagen turnover and its regulation in the normal and hypertrophying heart.* Eur Heart J, 1995. **16 Suppl C**: p. 38-44.

198. McClain, P.E., *Characterization of cardiac muscle collagen. Molecular heterogeneity.* J Biol Chem, 1974. **249**(7): p. 2303-11.

199. Shamhart, P.E. and J.G. Meszaros, *Non-fibrillar collagens: key mediators of post-infarction cardiac remodeling?* J Mol Cell Cardiol, 2010. **48**(3): p. 530-7.

200. Colige, A., et al., *Cloning and characterization of ADAMTS-14, a novel ADAMTS displaying high homology with ADAMTS-2 and ADAMTS-3.* J Biol Chem, 2002. **277**(8): p. 5756-66.

201. Kessler, E., et al., *Bone morphogenetic protein-1: the type I procollagen C-proteinase.* Science, 1996. **271**(5247): p. 360-2.

202. Weber, K.T., *Monitoring tissue repair and fibrosis from a distance.* Circulation, 1997. **96**(8): p. 2488-92.

203. Martos, R., et al., *Diastolic heart failure: evidence of increased myocardial collagen turnover linked to diastolic dysfunction.* Circulation, 2007. **115**(7): p. 888-95.

204. Cicoira, M., et al., *Independent and additional prognostic value of aminoterminal propeptide of type III procollagen circulating levels in patients with chronic heart failure.* J Card Fail, 2004. **10**(5): p. 403-11.

205. Sato, Y., et al., *Measuring serum aminoterminal type III procollagen peptide, 7S domain of type IV collagen, and cardiac troponin T in patients with idiopathic dilated cardiomyopathy and secondary cardiomyopathy.* Heart, 1997. **78**(5): p. 505-8.

206. Bing, O.H., et al., *Localization of alpha1(I) collagen mRNA in myocardium from the spontaneously hypertensive rat during the transition from compensated hypertrophy to failure.* J Mol Cell Cardiol, 1997. **29**(9): p. 2335-44.

207. Chen, Y.G., F. Liu, and J. Massague, *Mechanism of TGFbeta receptor inhibition by FKBP12.* EMBO J, 1997. **16**(13): p. 3866-76.

208. Heldin, C.H., K. Miyazono, and P. ten Dijke, *TGF-beta signalling from cell membrane to nucleus through SMAD proteins.* Nature, 1997. **390**(6659): p. 465-71.

209. Bujak, M. and N.G. Frangogiannis, *The role of TGF-beta signaling in myocardial infarction and cardiac remodeling.* Cardiovasc Res, 2007. **74**(2): p. 184-95.

210. Nakao, A., et al., *TGF-beta receptor-mediated signalling through Smad2, Smad3 and Smad4.* EMBO J, 1997. **16**(17): p. 5353-62.

211. Wrana, J.L., *The secret life of Smad4.* Cell, 2009. **136**(1): p. 13-4.

212. Chen, S.J., et al., *Interaction of smad3 with a proximal smad-binding element of the human alpha2(I) procollagen gene promoter required for transcriptional activation by TGF-beta.* J Cell Physiol, 2000. **183**(3): p. 381-92.

213. Nakao, A., et al., *Identification of Smad7, a TGFbeta-inducible antagonist of TGF-beta signalling.* Nature, 1997. **389**(6651): p. 631-5.

214. Ogunjimi, A.A., et al., *Regulation of Smurf2 ubiquitin ligase activity by anchoring the E2 to the HECT domain.* Mol Cell, 2005. **19**(3): p. 297-308.

215. Buja, L.M., *Modulation of the myocardial response to ischemia.* Lab Invest, 1998. **78**(11): p. 1345-73.

216. Frey, R.S. and K.M. Mulder, *Involvement of extracellular signal-regulated kinase 2 and stress-activated protein kinase/Jun N-terminal kinase activation by transforming growth factor beta in the negative growth control of breast cancer cells.* Cancer Res, 1997. **57**(4): p. 628-33.

217. Frey, R.S. and K.M. Mulder, *TGFbeta regulation of mitogen-activated protein kinases in human breast cancer cells.* Cancer Lett, 1997. **117**(1): p. 41-50.

218. Mulder, K.M. and S.L. Morris, *Activation of p21ras by transforming growth factor beta in epithelial cells.* J Biol Chem, 1992. **267**(8): p. 5029-31.

219. Liu, S., et al., *FAK is required for TGFbeta-induced JNK phosphorylation in fibroblasts: implications for acquisition of a matrix-remodeling phenotype.* Mol Biol Cell, 2007. **18**(6): p. 2169-78.

220. Shi-wen, X., et al., *Requirement of transforming growth factor beta-activated kinase 1 for transforming growth factor beta-induced alpha-smooth muscle*

actin expression and extracellular matrix contraction in fibroblasts. Arthritis Rheum, 2009. **60**(1): p. 234-41.

221. Chen, Y., et al., *Matrix contraction by dermal fibroblasts requires transforming growth factor-beta/activin-linked kinase 5, heparan sulfate-containing proteoglycans, and MEK/ERK: insights into pathological scarring in chronic fibrotic disease.* Am J Pathol, 2005. **167**(6): p. 1699-711.

222. Leask, A., et al., *Connective tissue growth factor gene regulation. Requirements for its induction by transforming growth factor-beta 2 in fibroblasts.* J Biol Chem, 2003. **278**(15): p. 13008-15.

223. Liu, X., et al., *cAMP inhibits transforming growth factor-beta-stimulated collagen synthesis via inhibition of extracellular signal-regulated kinase 1/2 and Smad signaling in cardiac fibroblasts.* Mol Pharmacol, 2006. **70**(6): p. 1992-2003.

224. Yu, L., M.C. Hebert, and Y.E. Zhang, *TGF-beta receptor-activated p38 MAP kinase mediates Smad-independent TGF-beta responses.* EMBO J, 2002. **21**(14): p. 3749-59.

225. Esparza-Lopez, J., et al., *Ligand binding and functional properties of betaglycan, a co-receptor of the transforming growth factor-beta superfamily. Specialized binding regions for transforming growth factor-beta and inhibin A.* J Biol Chem, 2001. **276**(18): p. 14588-96.

226. Lopez-Casillas, F., J.L. Wrana, and J. Massague, *Betaglycan presents ligand to the TGF beta signaling receptor.* Cell, 1993. **73**(7): p. 1435-44.

227. Santander, C. and E. Brandan, *Betaglycan induces TGF-beta signaling in a ligand-independent manner, through activation of the p38 pathway.* Cell Signal, 2006. **18**(9): p. 1482-91.

228. Brilla, C.G., et al., *Collagen metabolism in cultured adult rat cardiac fibroblasts: response to angiotensin II and aldosterone.* J Mol Cell Cardiol, 1994. **26**(7): p. 809-20.

229. Dinh, D.T., et al., *Angiotensin receptors: distribution, signalling and function.* Clin Sci (Lond), 2001. **100**(5): p. 481-92.

230. Manabe, I., T. Shindo, and R. Nagai, *Gene expression in fibroblasts and fibrosis: involvement in cardiac hypertrophy.* Circ Res, 2002. **91**(12): p. 1103-13.

231. Zou, Y., et al., *Cell type-specific angiotensin II-evoked signal transduction pathways: critical roles of Gbetagamma subunit, Src family, and Ras in cardiac fibroblasts.* Circ Res, 1998. **82**(3): p. 337-45.

232. Rodriguez-Vita, J., et al., *Angiotensin II activates the Smad pathway in vascular smooth muscle cells by a transforming growth factor-beta-independent mechanism.* Circulation, 2005. **111**(19): p. 2509-17.

233. Martin, M.M., et al., *TGF-beta1 stimulates human AT1 receptor expression in lung fibroblasts by cross talk between the Smad, p38 MAPK, JNK, and PI3K signaling pathways.* Am J Physiol Lung Cell Mol Physiol, 2007. **293**(3): p. L790-9.

234. Trombetta-eSilva, J., et al., *The effects of age and the expression of SPARC on extracellular matrix production by cardiac fibroblasts in 3-D cultures.* PLoS One, 2013. **8**(11): p. e79715.

235. Borg, T.K., et al., *Recognition of extracellular matrix components by neonatal and adult cardiac myocytes.* Dev Biol, 1984. **104**(1): p. 86-96.

236. Manabe, R., et al., *Modulation of cell-adhesive activity of fibronectin by the alternatively spliced EDA segment.* J Cell Biol, 1997. **139**(1): p. 295-307.

237. Liao, Y.F., et al., *The EIIIA segment of fibronectin is a ligand for integrins alpha 9beta 1 and alpha 4beta 1 providing a novel mechanism for regulating cell adhesion by alternative splicing.* J Biol Chem, 2002. **277**(17): p. 14467-74.

238. Sottile, J. and D.C. Hocking, *Fibronectin polymerization regulates the composition and stability of extracellular matrix fibrils and cell-matrix adhesions.* Mol Biol Cell, 2002. **13**(10): p. 3546-59.

239. Arslan, F., et al., *Lack of fibronectin-EDA promotes survival and prevents adverse remodeling and heart function deterioration after myocardial infarction.* Circ Res, 2011. **108**(5): p. 582-92.

240. Gondokaryono, S.P., et al., *The extra domain A of fibronectin stimulates murine mast cells via toll-like receptor 4.* J Leukoc Biol, 2007. **82**(3): p. 657-65.

241. Ma, Y., et al., *Toll-like receptor (TLR) 2 and TLR4 differentially regulate doxorubicin induced cardiomyopathy in mice.* PLoS One, 2012. **7**(7): p. e40763.

242. Zamilpa, R., et al., *Proteomic analysis identifies in vivo candidate matrix metalloproteinase-9 substrates in the left ventricle post-myocardial infarction.* Proteomics, 2010. **10**(11): p. 2214-23.

243. Toole, B.P., *Hyaluronan is not just a goo!* J Clin Invest, 2000. **106**(3): p. 335-6.

244. Bernanke, D.H. and R.R. Markwald, *Effects of hyaluronic acid on cardiac cushion tissue cells in collagen matrix cultures.* Tex Rep Biol Med, 1979. **39**: p. 271-85.

245. Camenisch, T.D., et al., *Disruption of hyaluronan synthase-2 abrogates normal cardiac morphogenesis and hyaluronan-mediated transformation of epithelium to mesenchyme.* J Clin Invest, 2000. **106**(3): p. 349-60.

246. Meran, S., et al., *Involvement of hyaluronan in regulation of fibroblast phenotype.* J Biol Chem, 2007. **282**(35): p. 25687-97.

247. Webber, J., et al., *Hyaluronan orchestrates transforming growth factor-beta1-dependent maintenance of myofibroblast phenotype.* J Biol Chem, 2009. **284**(14): p. 9083-92.

248. Webber, J., et al., *Modulation of TGFbeta1-dependent myofibroblast differentiation by hyaluronan.* Am J Pathol, 2009. **175**(1): p. 148-60.

249. Fitzgerald, K.A., et al., *Ras, protein kinase C zeta, and I kappa B kinases 1 and 2 are downstream effectors of CD44 during the activation of NF-kappa B by hyaluronic acid fragments in T-24 carcinoma cells.* J Immunol, 2000. **164**(4): p. 2053-63.

250. Kamikura, D.M., et al., *Enhanced transformation by a plasma membrane-associated met oncoprotein: activation of a phosphoinositide 3'-kinase-dependent autocrine loop involving hyaluronic acid and CD44.* Mol Cell Biol, 2000. **20**(10): p. 3482-96.

251. Oliferenko, S., et al., *Hyaluronic acid (HA) binding to CD44 activates Rac1 and induces lamellipodia outgrowth.* J Cell Biol, 2000. **148**(6): p. 1159-64.

252. Lindsey, M.L., *MMP induction and inhibition in myocardial infarction.* Heart Fail Rev, 2004. **9**(1): p. 7-19.

253. Raffetto, J.D. and R.A. Khalil, *Matrix metalloproteinases and their inhibitors in vascular remodeling and vascular disease.* Biochem Pharmacol, 2008. **75**(2): p. 346-59.

254. Visse, R. and H. Nagase, *Matrix metalloproteinases and tissue inhibitors of metalloproteinases: structure, function, and biochemistry.* Circ Res, 2003. **92**(8): p. 827-39.

255. Kelly, D., et al., *Circulating stromelysin-1 (MMP-3): a novel predictor of LV dysfunction, remodelling and all-cause mortality after acute myocardial infarction.* Eur J Heart Fail, 2008. **10**(2): p. 133-9.

256. Ma, Y., et al., *Matrix metalloproteinase-28 deletion amplifies inflammatory and extracellular matrix responses to cardiac aging.* Microsc Microanal, 2012. **18**(1): p. 81-90.

257. Mann, D.L. and F.G. Spinale, *Activation of matrix metalloproteinases in the failing human heart: breaking the tie that binds.* Circulation, 1998. **98**(17): p. 1699-702.

258. Spinale, F.G., *Myocardial matrix remodeling and the matrix metalloproteinases: influence on cardiac form and function.* Physiol Rev, 2007. **87**(4): p. 1285-342.

259. Steffensen, B., U.M. Wallon, and C.M. Overall, *Extracellular matrix binding properties of recombinant fibronectin type II-like modules of human 72-kDa gelatinase/type IV collagenase. High affinity binding to native type I collagen but not native type IV collagen.* J Biol Chem, 1995. **270**(19): p. 11555-66.

260. Bergman, M.R., et al., *A functional activating protein 1 (AP-1) site regulates matrix metalloproteinase 2 (MMP-2) transcription by cardiac cells through interactions with JunB-Fra1 and JunB-FosB heterodimers.* Biochem J, 2003. **369**(Pt 3): p. 485-96.

261. Brown, R.D., et al., *Cytokines regulate matrix metalloproteinases and migration in cardiac fibroblasts.* Biochem Biophys Res Commun, 2007. **362**(1): p. 200-5.

262. Guo, X.G., et al., *Imidaprilat inhibits matrix metalloproteinase-2 activity in human cardiac fibroblasts induced by interleukin-1beta via NO-dependent pathway.* Int J Cardiol, 2008. **126**(3): p. 414-20.

263. Husse, B., et al., *Cyclical mechanical stretch modulates expression of collagen I and collagen III by PKC and tyrosine kinase in cardiac fibroblasts.* Am J Physiol Regul Integr Comp Physiol, 2007. **293**(5): p. R1898-907.

264. Makino, N., et al., *Peroxisome proliferator-activated receptor-gamma ligands attenuate brain natriuretic peptide production and affect remodeling in*

cardiac fibroblasts in reoxygenation after hypoxia. Cell Biochem Biophys, 2006. **44**(1): p. 65-71.

265. Mookerjee, I., et al., *Relaxin modulates fibroblast function, collagen production, and matrix metalloproteinase-2 expression by cardiac fibroblasts.* Ann N Y Acad Sci, 2005. **1041**: p. 190-3.

266. Siwik, D.A., D.L. Chang, and W.S. Colucci, *Interleukin-1beta and tumor necrosis factor-alpha decrease collagen synthesis and increase matrix metalloproteinase activity in cardiac fibroblasts in vitro.* Circ Res, 2000. **86**(12): p. 1259-65.

267. Siwik, D.A., P.J. Pagano, and W.S. Colucci, *Oxidative stress regulates collagen synthesis and matrix metalloproteinase activity in cardiac fibroblasts.* Am J Physiol Cell Physiol, 2001. **280**(1): p. C53-60.

268. Stawowy, P., et al., *Regulation of matrix metalloproteinase MT1-MMP/MMP-2 in cardiac fibroblasts by TGF-beta1 involves furin-convertase.* Cardiovasc Res, 2004. **63**(1): p. 87-97.

269. Tsuruda, T., et al., *Brain natriuretic Peptide is produced in cardiac fibroblasts and induces matrix metalloproteinases.* Circ Res, 2002. **91**(12): p. 1127-34.

270. Porter, K.E., et al., *Tumor necrosis factor alpha induces human atrial myofibroblast proliferation, invasion and MMP-9 secretion: inhibition by simvastatin.* Cardiovasc Res, 2004. **64**(3): p. 507-15.

271. Stacy, L.B., et al., *Effect of angiotensin II on primary cardiac fibroblast matrix metalloproteinase activities.* Perfusion, 2007. **22**(1): p. 51-5.

272. Pan, C.H., C.H. Wen, and C.S. Lin, *Interplay of angiotensin II and angiotensin(1-7) in the regulation of matrix metalloproteinases of human cardiocytes.* Exp Physiol, 2008. **93**(5): p. 599-612.

273. Shen, X.M., et al., *Interaction of MT1-MMP and laminin-5gamma2 chain correlates with metastasis and invasiveness in human esophageal squamous cell carcinoma.* Clin Exp Metastasis, 2007. **24**(7): p. 541-50.

274. Manso, A.M., et al., *Integrins, membrane-type matrix metalloproteinases and ADAMs: potential implications for cardiac remodeling.* Cardiovasc Res, 2006. **69**(3): p. 574-84.

275. Barbolina, M.V. and M.S. Stack, *Membrane type 1-matrix metalloproteinase: substrate diversity in pericellular proteolysis.* Semin Cell Dev Biol, 2008. **19**(1): p. 24-33.

276. Tyagi, S.C., S. Kumar, and G. Glover, *Induction of tissue inhibitor and matrix metalloproteinase by serum in human heart-derived fibroblast and endomyocardial endothelial cells.* J Cell Biochem, 1995. **58**(3): p. 360-71.

277. Heymans, S., et al., *Increased cardiac expression of tissue inhibitor of metalloproteinase-1 and tissue inhibitor of metalloproteinase-2 is related to cardiac fibrosis and dysfunction in the chronic pressure-overloaded human heart.* Circulation, 2005. **112**(8): p. 1136-44.

278. Kandalam, V., et al., *TIMP2 deficiency accelerates adverse post-myocardial infarction remodeling because of enhanced MT1-MMP activity despite lack of MMP2 activation.* Circ Res, 2010. **106**(4): p. 796-808.

279. Li, Y.Y., et al., *Downregulation of matrix metalloproteinases and reduction in collagen damage in the failing human heart after support with left ventricular assist devices.* Circulation, 2001. **104**(10): p. 1147-52.

280. Deschamps, A.M. and F.G. Spinale, *Pathways of matrix metalloproteinase induction in heart failure: bioactive molecules and transcriptional regulation.* Cardiovasc Res, 2006. **69**(3): p. 666-76.

281. Tyagi, S.C., et al., *Co-expression of tissue inhibitor and matrix metalloproteinase in myocardium.* J Mol Cell Cardiol, 1995. **27**(10): p. 2177-89.

282. Spinale, F.G., et al., *A matrix metalloproteinase induction/activation system exists in the human left ventricular myocardium and is upregulated in heart failure.* Circulation, 2000. **102**(16): p. 1944-9.

283. Li, Y.Y., et al., *Differential expression of tissue inhibitors of metalloproteinases in the failing human heart.* Circulation, 1998. **98**(17): p. 1728-34.

284. Thomas, C.V., et al., *Increased matrix metalloproteinase activity and selective upregulation in LV myocardium from patients with end-stage dilated cardiomyopathy.* Circulation, 1998. **97**(17): p. 1708-15.

285. Tyagi, S.C., et al., *Matrix metalloproteinase activity expression in infarcted, noninfarcted and dilated cardiomyopathic human hearts.* Mol Cell Biochem, 1996. **155**(1): p. 13-21.

286. Schweitzer, R., et al., *Analysis of the tendon cell fate using Scleraxis, a specific marker for tendons and ligaments.* Development, 2001. **128**(19): p. 3855-66.

287. Brent, A.E., R. Schweitzer, and C.J. Tabin, *A somitic compartment of tendon progenitors.* Cell, 2003. **113**(2): p. 235-48.

288. Cserjesi, P., et al., *Scleraxis: a basic helix-loop-helix protein that prefigures skeletal formation during mouse embryogenesis.* Development, 1995. **121**(4): p. 1099-110.

289. Kadesch, T., *Consequences of heteromeric interactions among helix-loop-helix proteins.* Cell Growth Differ, 1993. **4**(1): p. 49-55.

290. Jan, Y.N. and L.Y. Jan, *Functional gene cassettes in development.* Proc Natl Acad Sci U S A, 1993. **90**(18): p. 8305-7.

291. Olson, E.N. and W.H. Klein, *bHLH factors in muscle development: dead lines and commitments, what to leave in and what to leave out.* Genes Dev, 1994. **8**(1): p. 1-8.

292. Goldfarb, A.N. and K. Lewandowska, *Nuclear redirection of a cytoplasmic helix-loop-helix protein via heterodimerization with a nuclear localizing partner.* Exp Cell Res, 1994. **214**(2): p. 481-5.

293. Littlewood, T.D. and G.I. Evan, *Helix-loop-helix transcription factors*. 3 ed. 1998, U.S.A.: Oxford University Press.

294. Chaudhary, J. and M.K. Skinner, *Basic helix-loop-helix proteins can act at the E-box within the serum response element of the c-fos promoter to influence hormone-induced promoter activation in Sertoli cells.* Mol Endocrinol, 1999. **13**(5): p. 774-86.

295. Ephrussi, A., et al., *B lineage--specific interactions of an immunoglobulin enhancer with cellular factors in vivo.* Science, 1985. **227**(4683): p. 134-40.

296. Molkentin, J.D. and E.N. Olson, *Combinatorial control of muscle development by basic helix-loop-helix and MADS-box transcription factors.* Proc Natl Acad Sci U S A, 1996. **93**(18): p. 9366-73.

297. Murre, C., et al., *Interactions between heterologous helix-loop-helix proteins generate complexes that bind specifically to a common DNA sequence.* Cell, 1989. **58**(3): p. 537-44.

298. Carlberg, A.L., R.S. Tuan, and D.J. Hall, *Regulation of scleraxis function by interaction with the bHLH protein E47.* Mol Cell Biol Res Commun, 2000. **3**(2): p. 82-6.

299. Liu, Y., et al., *Overexpression of a single helix-loop-helix-type transcription factor, scleraxis, enhances aggrecan gene expression in osteoblastic osteosarcoma ROS17/2.8 cells.* J Biol Chem, 1997. **272**(47): p. 29880-5.

300. Muir, T., et al., *Integration of CREB and bHLH transcriptional signaling pathways through direct heterodimerization of the proteins: role in muscle and testis development.* Mol Reprod Dev, 2008. **75**(11): p. 1637-52.

301. Liu, Y., et al., *Sclerotome-related helix-loop-helix type transcription factor (scleraxis) mRNA is expressed in osteoblasts and its level is enhanced by type-beta transforming growth factor.* J Endocrinol, 1996. **151**(3): p. 491-9.

302. Muir, T., I. Sadler-Riggleman, and M.K. Skinner, *Role of the basic helix-loop-helix transcription factor, scleraxis, in the regulation of Sertoli cell function and differentiation.* Mol Endocrinol, 2005. **19**(8): p. 2164-74.

303. Smith, T.G., et al., *Feedback interactions between MKP3 and ERK MAP kinase control scleraxis expression and the specification of rib progenitors in the developing chick somite.* Development, 2005. **132**(6): p. 1305-14.

304. Brent, A.E. and C.J. Tabin, *FGF acts directly on the somitic tendon progenitors through the Ets transcription factors Pea3 and Erm to regulate scleraxis expression.* Development, 2004. **131**(16): p. 3885-96.

305. Zhao, B., et al., *BMP and FGF regulatory pathways in semilunar valve precursor cells.* Dev Dyn, 2007. **236**(4): p. 971-80.

306. Edom-Vovard, F., et al., *Fgf4 positively regulates scleraxis and tenascin expression in chick limb tendons.* Dev Biol, 2002. **247**(2): p. 351-66.

307. Levay, A.K., et al., *Scleraxis is required for cell lineage differentiation and extracellular matrix remodeling during murine heart valve formation in vivo.* Circ Res, 2008. **103**(9): p. 948-56.

308. Brown, D., et al., *Dual role of the basic helix-loop-helix transcription factor scleraxis in mesoderm formation and chondrogenesis during mouse embryogenesis.* Development, 1999. **126**(19): p. 4317-29.

309. Lincoln, J., C.M. Alfieri, and K.E. Yutzey, *Development of heart valve leaflets and supporting apparatus in chicken and mouse embryos.* Dev Dyn, 2004. **230**(2): p. 239-50.

310. Dubrulle, J. and O. Pourquie, *Welcome to syndetome: a new somitic compartment.* Dev Cell, 2003. **4**(5): p. 611-2.

311. Asou, Y., et al., *Coordinated expression of scleraxis and Sox9 genes during embryonic development of tendons and cartilage.* J Orthop Res, 2002. **20**(4): p. 827-33.

312. Shukunami, C., et al., *Scleraxis positively regulates the expression of tenomodulin, a differentiation marker of tenocytes.* Dev Biol, 2006. **298**(1): p. 234-47.

313. zur Nieden, N.I., et al., *Induction of chondro-, osteo- and adipogenesis in embryonic stem cells by bone morphogenetic protein-2: effect of cofactors on differentiating lineages.* BMC Dev Biol, 2005. **5**: p. 1.

314. Furumatsu, T., et al., *Scleraxis and E47 cooperatively regulate the Sox9-dependent transcription.* Int J Biochem Cell Biol, 2010. **42**(1): p. 148-56.

315. Mendias, C.L., K.I. Bakhurin, and J.A. Faulkner, *Tendons of myostatin-deficient mice are small, brittle, and hypocellular.* Proc Natl Acad Sci U S A, 2008. **105**(1): p. 388-93.

316. Watanabe, H., et al., *Mouse cartilage matrix deficiency (cmd) caused by a 7 bp deletion in the aggrecan gene.* Nat Genet, 1994. **7**(2): p. 154-7.

317. Salingcarnboriboon, R., et al., *Establishment of tendon-derived cell lines exhibiting pluripotent mesenchymal stem cell-like property.* Exp Cell Res, 2003. **287**(2): p. 289-300.

318. Lejard, V., et al., *Scleraxis and NFATc regulate the expression of the pro-alpha1(I) collagen gene in tendon fibroblasts.* J Biol Chem, 2007. **282**(24): p. 17665-75.

319. Strezoska, Z., D.G. Pestov, and L.F. Lau, *Functional inactivation of the mouse nucleolar protein Bop1 inhibits multiple steps in pre-rRNA processing and blocks cell cycle progression.* J Biol Chem, 2002. **277**(33): p. 29617-25.

320. Murchison, N.D., et al., *Regulation of tendon differentiation by scleraxis distinguishes force-transmitting tendons from muscle-anchoring tendons.* Development, 2007. **134**(14): p. 2697-708.

321. Kannus, P., *Structure of the tendon connective tissue.* Scand J Med Sci Sports, 2000. **10**(6): p. 312-20.

322. Liu, Q., et al., *[Expression of Scleraxis in human periodontal ligament cells and gingival fibroblasts]*. Zhonghua Kou Qiang Yi Xue Za Zhi, 2006. **41**(9): p. 556-8.

323. Shi, S., et al., *The efficacy of mesenchymal stem cells to regenerate and repair dental structures.* Orthod Craniofac Res, 2005. **8**(3): p. 191-9.

324. Tomokiyo, A., et al., *Development of a multipotent clonal human periodontal ligament cell line.* Differentiation, 2008. **76**(4): p. 337-47.

325. Yokoi, T., et al., *Establishment of immortalized dental follicle cells for generating periodontal ligament in vivo.* Cell Tissue Res, 2007. **327**(2): p. 301-11.

326. Fujii, S., et al., *Investigating a clonal human periodontal ligament progenitor/stem cell line in vitro and in vivo.* J Cell Physiol, 2008. **215**(3): p. 743-9.

327. Yuan, Y.D., S. Miao, and H. Xie, *[Effect of high glucose on the expression of transcription factor Scleraxis in periodontal ligament cells in vitro]*. Zhonghua Kou Qiang Yi Xue Za Zhi, 2008. **43**(11): p. 668-70.

328. Itaya, T., et al., *Characteristic changes of periodontal ligament-derived cells during passage.* J Periodontal Res, 2009. **44**(4): p. 425-33.

329. Callewaert, B., et al., *Ehlers-Danlos syndromes and Marfan syndrome.* Best Pract Res Clin Rheumatol, 2008. **22**(1): p. 165-89.

330. Yeghiazaryan, K., et al., *Downregulation of the transcription factor scleraxis in brain of patients with Down syndrome.* J Neural Transm Suppl, 1999. **57**: p. 305-14.

331. Scott, A., et al., *Scleraxis expression is coordinately regulated in a murine model of patellar tendon injury.* J Orthop Res, 2011. **29**(2): p. 289-96.

332. Yeh, L.C., A.D. Tsai, and J.C. Lee, *Bone morphogenetic protein-7 regulates differentially the mRNA expression of bone morphogenetic proteins and their receptors in rat achilles and patellar tendon cell cultures.* J Cell Biochem, 2008. **104**(6): p. 2107-22.

333. Espira, L. and M.P. Czubryt, *Emerging concepts in cardiac matrix biology.* Can J Physiol Pharmacol, 2009. **87**(12): p. 996-1008.

334. Czubryt, M.P., et al., *Regulation of peroxisome proliferator-activated receptor gamma coactivator 1 alpha (PGC-1 alpha) and mitochondrial function by MEF2 and HDAC5.* Proc Natl Acad Sci U S A, 2003. **100**(4): p. 1711-6.

335. Naitoh, M., et al., *Gene expression in human keloids is altered from dermal to chondrocytic and osteogenic lineage.* Genes Cells, 2005. **10**(11): p. 1081-91.

336. Pick, R., et al., *The fibrillar nature and structure of isoproterenol-induced myocardial fibrosis in the rat.* Am J Pathol, 1989. **134**(2): p. 365-71.

337. Raizman, J.E., et al., *The participation of the Na+-Ca2+ exchanger in primary cardiac myofibroblast migration, contraction, and proliferation.* J Cell Physiol, 2007. **213**(2): p. 540-51.

338. Ju, H., et al., *Antiproliferative and antifibrotic effects of mimosine on adult cardiac fibroblasts.* Biochim Biophys Acta, 1998. **1448**(1): p. 51-60.

339. Acharya, A., et al., *Efficient inducible Cre-mediated recombination in Tcf21 cell lineages in the heart and kidney.* Genesis, 2011. **49**(11): p. 870-7.

340. Hayashi, S. and A.P. McMahon, *Efficient recombination in diverse tissues by a tamoxifen-inducible form of Cre: a tool for temporally regulated gene activation/inactivation in the mouse.* Dev Biol, 2002. **244**(2): p. 305-18.

341. Rothermel, B.A., et al., *Differential activation of stress-response signaling in load-induced cardiac hypertrophy and failure.* Physiol Genomics, 2005. **23**(1): p. 18-27.

342. Jassal, D.S., et al., *Utility of tissue Doppler and strain rate imaging in the early detection of trastuzumab and anthracycline mediated cardiomyopathy.* J Am Soc Echocardiogr, 2009. **22**(4): p. 418-24.

343. Walker, J.R., et al., *The cardioprotective role of probucol against anthracycline and trastuzumab-mediated cardiotoxicity.* J Am Soc Echocardiogr, 2011. **24**(6): p. 699-705.

344. Rossi, M.A., *Fibrosis and inflammatory cells in human chronic chagasic myocarditis: scanning electron microscopy and immunohistochemical observations.* Int J Cardiol, 1998. **66**(2): p. 183-94.

345. Rossi, M.A., M.A. Abreu, and L.B. Santoro, *Images in cardiovascular medicine. Connective tissue skeleton of the human heart: a demonstration by cell-maceration scanning electron microscope method.* Circulation, 1998. **97**(9): p. 934-5.

346. Abrenica, B., M. AlShaaban, and M.P. Czubryt, *The A-kinase anchor protein AKAP121 is a negative regulator of cardiomyocyte hypertrophy.* J Mol Cell Cardiol, 2009. **46**(5): p. 674-81.

347. Toth, M., A. Sohail, and R. Fridman, *Assessment of gelatinases (MMP-2 and MMP-9) by gelatin zymography.* Methods Mol Biol, 2012. **878**: p. 121-35.

348. Hu, X. and C. Beeton, *Detection of functional matrix metalloproteinases by zymography.* J Vis Exp, 2010(45).

349. Banerjee, I., et al., *Determination of cell types and numbers during cardiac development in the neonatal and adult rat and mouse.* Am J Physiol Heart Circ Physiol, 2007. **293**(3): p. H1883-91.

350. Hu, B., Z. Wu, and S.H. Phan, *Smad3 mediates transforming growth factor-beta-induced alpha-smooth muscle actin expression.* Am J Respir Cell Mol Biol, 2003. **29**(3 Pt 1): p. 397-404.

351. Qin, H., Y. Sun, and E.N. Benveniste, *The transcription factors Sp1, Sp3, and AP-2 are required for constitutive matrix metalloproteinase-2 gene expression in astroglioma cells.* J Biol Chem, 1999. **274**(41): p. 29130-7.

352. Gilles, C., et al., *Transactivation of vimentin by beta-catenin in human breast cancer cells.* Cancer Res, 2003. **63**(10): p. 2658-64.

353. Bindels, S., et al., *Regulation of vimentin by SIP1 in human epithelial breast tumor cells.* Oncogene, 2006. **25**(36): p. 4975-85.

354. Kalita, K., et al., *Role of megakaryoblastic acute leukemia-1 in ERK1/2-dependent stimulation of serum response factor-driven transcription by BDNF or increased synaptic activity.* J Neurosci, 2006. **26**(39): p. 10020-32.

355. Liu, Y.H., et al., *Effect of ACE inhibitors and angiotensin II type 1 receptor antagonists on endothelial NO synthase knockout mice with heart failure.* Hypertension, 2002. **39**(2 Pt 2): p. 375-81.

356. Spiltoir, J.I., et al., *BET acetyl-lysine binding proteins control pathological cardiac hypertrophy.* J Mol Cell Cardiol, 2013. **63**: p. 175-9.

357. Harding, P., et al., *Lack of microsomal prostaglandin E synthase-1 reduces cardiac function following angiotensin II infusion.* Am J Physiol Heart Circ Physiol, 2011. **300**(3): p. H1053-61.

358. Izumiya, Y., et al., *Vascular endothelial growth factor blockade promotes the transition from compensatory cardiac hypertrophy to failure in response to pressure overload.* Hypertension, 2006. **47**(5): p. 887-93.

359. Boast, S., et al., *Functional analysis of cis-acting DNA sequences controlling transcription of the human type I collagen genes.* J Biol Chem, 1990. **265**(22): p. 13351-6.

360. Ramirez, F., S. Tanaka, and G. Bou-Gharios, *Transcriptional regulation of the human alpha2(I) collagen gene (COL1A2), an informative model system to study fibrotic diseases.* Matrix Biol, 2006. **25**(6): p. 365-72.

361. Higashi, K., et al., *A proximal element within the human alpha 2(I) collagen (COL1A2) promoter, distinct from the tumor necrosis factor-alpha response element, mediates transcriptional repression by interferon-gamma.* Matrix Biol, 1998. **16**(8): p. 447-56.

362. Nagarajan, R.P. and Y. Chen, *Structural basis for the functional difference between Smad2 and Smad3 in FAST-2 (forkhead activin signal transducer-2)-mediated transcription.* Biochem J, 2000. **350 Pt 1**: p. 253-9.

363. Langlands, K., et al., *Differential interactions of Id proteins with basic-helix-loop-helix transcription factors.* J Biol Chem, 1997. **272**(32): p. 19785-93.

364. Barnette, D.N., et al., *Tgfbeta-Smad and MAPK signaling mediate scleraxis and proteoglycan expression in heart valves.* J Mol Cell Cardiol, 2013. **65**: p. 137-46.

365. Burgess, R., et al., *Paraxis: a basic helix-loop-helix protein expressed in paraxial mesoderm and developing somites.* Dev Biol, 1995. **168**(2): p. 296-306.

366. Blank, R.S., et al., *Elements of the smooth muscle alpha-actin promoter required in cis for transcriptional activation in smooth muscle. Evidence for cell type-specific regulation.* J Biol Chem, 1992. **267**(2): p. 984-9.

367. Jung, F., et al., *Characterization of an E-box-dependent cis element in the smooth muscle alpha-actin promoter.* Arterioscler Thromb Vasc Biol, 1999. **19**(11): p. 2591-9.

368. Abe, H., et al., *Scleraxis modulates bone morphogenetic protein 4 (BMP4)-Smad1 protein-smooth muscle alpha-actin (SMA) signal transduction in diabetic nephropathy.* J Biol Chem, 2012. **287**(24): p. 20430-42.

369. Huang da, W., B.T. Sherman, and R.A. Lempicki, *Systematic and integrative analysis of large gene lists using DAVID bioinformatics resources.* Nat Protoc, 2009. **4**(1): p. 44-57.

370. Huang da, W., B.T. Sherman, and R.A. Lempicki, *Bioinformatics enrichment tools: paths toward the comprehensive functional analysis of large gene lists.* Nucleic Acids Res, 2009. **37**(1): p. 1-13.

371. Kalluri, R. and E.G. Neilson, *Epithelial-mesenchymal transition and its implications for fibrosis.* J Clin Invest, 2003. **112**(12): p. 1776-84.

372. Wang, B., et al., *Decreased Smad 7 expression contributes to cardiac fibrosis in the infarcted rat heart.* Am J Physiol Heart Circ Physiol, 2002. **282**(5): p. H1685-96.

373. Schiller, M., D. Javelaud, and A. Mauviel, *TGF-beta-induced SMAD signaling and gene regulation: consequences for extracellular matrix remodeling and wound healing.* J Dermatol Sci, 2004. **35**(2): p. 83-92.

374. Derynck, R., Y. Zhang, and X.H. Feng, *Smads: transcriptional activators of TGF-beta responses.* Cell, 1998. **95**(6): p. 737-40.

375. Chen, X., et al., *Force and scleraxis synergistically promote the commitment of human ES cells derived MSCs to tenocytes.* Sci Rep, 2012. **2**: p. 977.

376. Lindsey, M.L. and R. Zamilpa, *Temporal and spatial expression of matrix metalloproteinases and tissue inhibitors of metalloproteinases following myocardial infarction.* Cardiovasc Ther, 2012. **30**(1): p. 31-41.

377. Katz, T.C., et al., *Distinct compartments of the proepicardial organ give rise to coronary vascular endothelial cells.* Dev Cell, 2012. **22**(3): p. 639-50.

378. Bhandari, R.K., et al., *SRY Induced TCF21 Genome-Wide Targets and Cascade of bHLH Factors During Sertoli Cell Differentiation and Male Sex Determination in Rats.* Biol Reprod, 2012. **87**(6): p. 131.

379. Kalluri, R. and R.A. Weinberg, *The basics of epithelial-mesenchymal transition.* J Clin Invest, 2009. **119**(6): p. 1420-8.

380. Klingberg, F., B. Hinz, and E.S. White, *The myofibroblast matrix: implications for tissue repair and fibrosis.* J Pathol, 2013. **229**(2): p. 298-309.

381. Tan, F.L., et al., *The gene expression fingerprint of human heart failure.* Proc Natl Acad Sci U S A, 2002. **99**(17): p. 11387-92.

382. Svensson, L., et al., *Fibromodulin-null mice have abnormal collagen fibrils, tissue organization, and altered lumican deposition in tendon.* J Biol Chem, 1999. **274**(14): p. 9636-47.

383. Waehre, A., et al., *Lack of chemokine signaling through CXCR5 causes increased mortality, ventricular dilatation and deranged matrix during cardiac pressure overload.* PLoS One, 2011. **6**(4): p. e18668.

384. Hinz, B., *Tissue stiffness, latent TGF-beta1 activation, and mechanical signal transduction: implications for the pathogenesis and treatment of fibrosis.* Curr Rheumatol Rep, 2009. **11**(2): p. 120-6.

List of Publications arising during PhD program

1. **RA Bagchi**, V Mozolevska, B Abrenica, MP Czubryt. Development of a high-throughput luciferase reporter gene system for screening activators and repressors of human collagen Iα2 gene expression, *Canadian Journal of Physiology and Pharmacology*, 2015. (Invited; *In Press*)
2. P Roche, K Filomeno, **RA Bagchi**, MP Czubryt. Intracellular signaling of cardiac fibroblasts, *Comprehensive Physiology*, 5(2): 721-760, 2015.
3. Ramjiawan A*, **Bagchi RA***, Blant A, Albak L, Cavasin MA, Horn TR, McKinsey TA, Czubryt MP.: Roles of Histone Deacetylation and AMP Kinase in regulation of cardiomyocyte PGC-1 gene expression in hypoxia. *American Journal of Physiology: Cell Physiology* 304(11): C1064-C1072, 2013. ***Co-first authors.***
4. Rydell-Tormanen K, Risse PA, Kanabar V, **Bagchi RA**, Czubryt MP, Johnson JR.: Smooth muscle in tissue remodeling and hyperreactivity: airways and arteries. *Pulmonary Pharmacology and Therapeutics* 16(1): 13-23, 2013. (Invited)
5. Wright DB, Trian T, Siddiqui S, Pascoe CD, Johnson JR, Dekkers BG, Dakshinamurti S, **Bagchi R**, Burgess JK, Kanabar V, Ojo OO.: Phenotype modulation of airway smooth muscle in asthma. *Pulmonary Pharmacology and Therapeutics* 16(1): 42-49, 2013. (Invited)
6. Yeganeh B, Mukherjee S, Moir LM, Kumawat K, Kashani HH, **Bagchi RA**, Baarsma HA, Gosens R, Ghavami S.: Novel non-canonical TGF- signaling networks: Emerging roles in airway smooth muscle phenotype and function. *Pulmonary Pharmacology and Therapeutics* 16(1): 50-63, 2013. (Invited)
7. Wright DB, Trian T, Siddiqui S, Pascoe CD, Ojo OO Johnson JR, Dekkers BG, Dakshinamurti S, **Bagchi R**, Burgess JK, Kanabar V.: Functional phenotype of airway myocytes from asthmatic airways. *Pulmonary Pharmacology and Therapeutics* 16(1): 95-104, 2013. (Invited)
8. Ramjiawan A, **Bagchi RA**, Albak L, Czubryt MP: Mechanism of cardiomyocyte PGC-1α gene regulation by ERRα. *Biochemistry and Cell Biology* 91(3): 148-154, 2013.
9. **RA Bagchi** and MP Czubryt. Synergistic roles of scleraxis and Smads in the regulation of collagen 1α2 gene expression, *Biochimica et Biophysica Acta-Molecular Cell Research*, 1823: 1936-1944, 2012.
10. **RA Bagchi** and MP Czubryt. Scleraxis: A new regulator of extracellular matrix formation, In: *Genes and Cardiovascular Function*, *57-65,* Springer, 2011.

Selected published abstracts:

1. **Bagchi RA**, Roche P, Schweitzer R, Czubryt MP. Scleraxis: A novel transcriptional regulator of cardiac fibroblast function and phenotype. *FASEB J* April 2015 29:556.2.
2. **Bagchi RA**, Roche P, Schweitzer R, Czubryt MP. Regulation of cardiac fibroblast phenotype by scleraxis. *Circulation*. 2014; 130:A12519.
3. **Bagchi RA**, Schweitzer R, Czubryt MP. Scleraxis is a critical regulator of cardiac extracellular matrix synthesis. 2nd Cardiovascular Forum for Promoting Centers of Excellence and Young Investigators, *Curr Res Cardiol* 1 (1) p.34, 2014.
4. **Bagchi RA**, Roche P, Aroutiounova N, et al. Scleraxis regulates cardiac extracellular matrix composition and fibroblast phenotype. XXXIV Annual Meeting of the International Society for Heart Research- North American Section, *JMCC* 74 (2014) S1–S33.
5. **Bagchi RA**, Roche P, Aroutiounova N, Schweitzer R, Czubryt MP. Scleraxis regulates myocardial extracellular matrix synthesis and homeostasis. *FASEB J* 28:1152.14, 2014.
6. **Bagchi RA**, Roche P, Aroutiounova N, Schweitzer R, Czubryt MP. Regulation of cardiac fibroblast population and cell fate by Scleraxis. *FASEB J* 28:15.2, 2014.
7. **Bagchi RA**, Roche P, Schweitzer R, Czubryt MP. Scleraxis: A novel regulator of extracellular matrix synthesis and fibrotic gene expression in the heart. XXI World Congress of the International Society for Heart Research, *JMCC* 65 (2013) S1–S162.
8. **Bagchi RA**, Roche P, Schweitzer R, Czubryt MP. Identification of novel scleraxis gene targets in cardiac myofibroblasts. *FASEB J* 27:1129.13, 2013.
9. Czubryt MP*, **Bagchi RA***. Scleraxis is a general regulator of ECM gene expression in cardiac myofibroblasts. *Glycobiology* 22(11): 1624, 2012. **equal contribution*
10. **Bagchi RA**, Czubryt MP. Scleraxis works synergistically with Smads to regulate collagen gene expression. *FASEB J* 26: 1059.2, 2012.
11. **Bagchi RA**, Dixon IMC, Czubryt MP. Interaction of scleraxis and Smad-dependent cardiac collagen expression. *FASEB J* 25: 1032.5, 2011.
12. Czubryt MP*, **Bagchi R***, Chahine M, Pierce GN, Halayko A. Scleraxis gene expression is regulated by stretch and cell type. *J Mol Cell Cardiol* 48 (Suppl 1):S77, 2010. **Co-first author*

APPENDICES

Appendix 1: Optimization of MOI for AdshScx in primary cardiac proto-myofibroblasts.

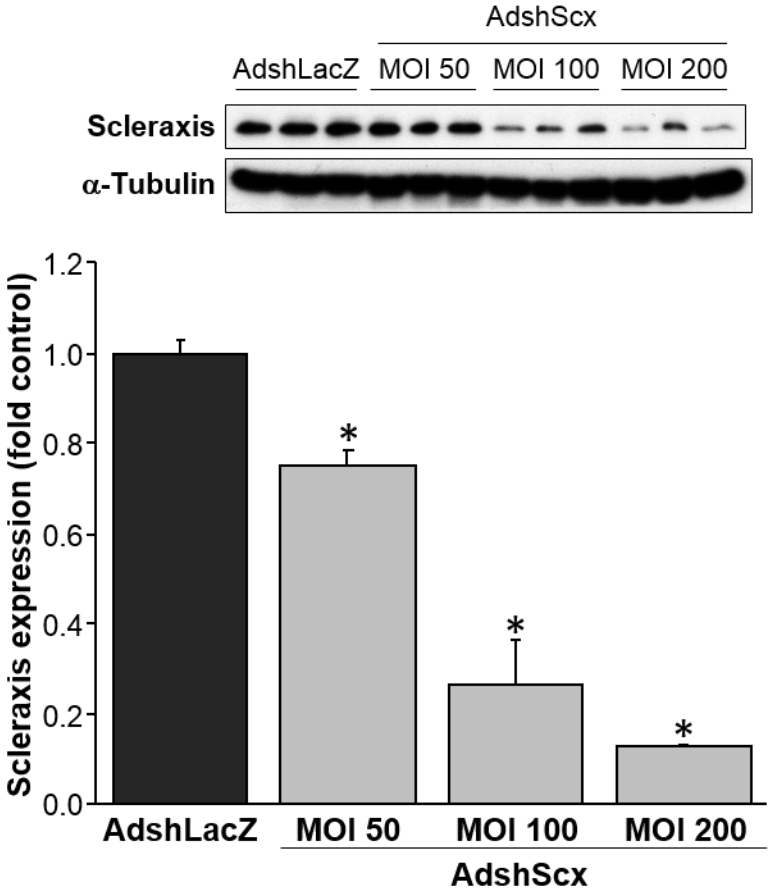

Primary rat cardiac proto-myofibroblasts (P1) were infected with adenovirus encoding shRNA for scleraxis (AdshScx) or LacZ (AdshLacZ; control) for 48 hours. Total protein was isolated and subjected to SDS-PAGE followed by immunoblotting with anti-scleraxis antibody [172, 173]. MOI 200 was used for all gene knockdown experiments.

Appendix 2: Flow cytometry analysis of cardiac cells from WT and scleraxis KO mice.

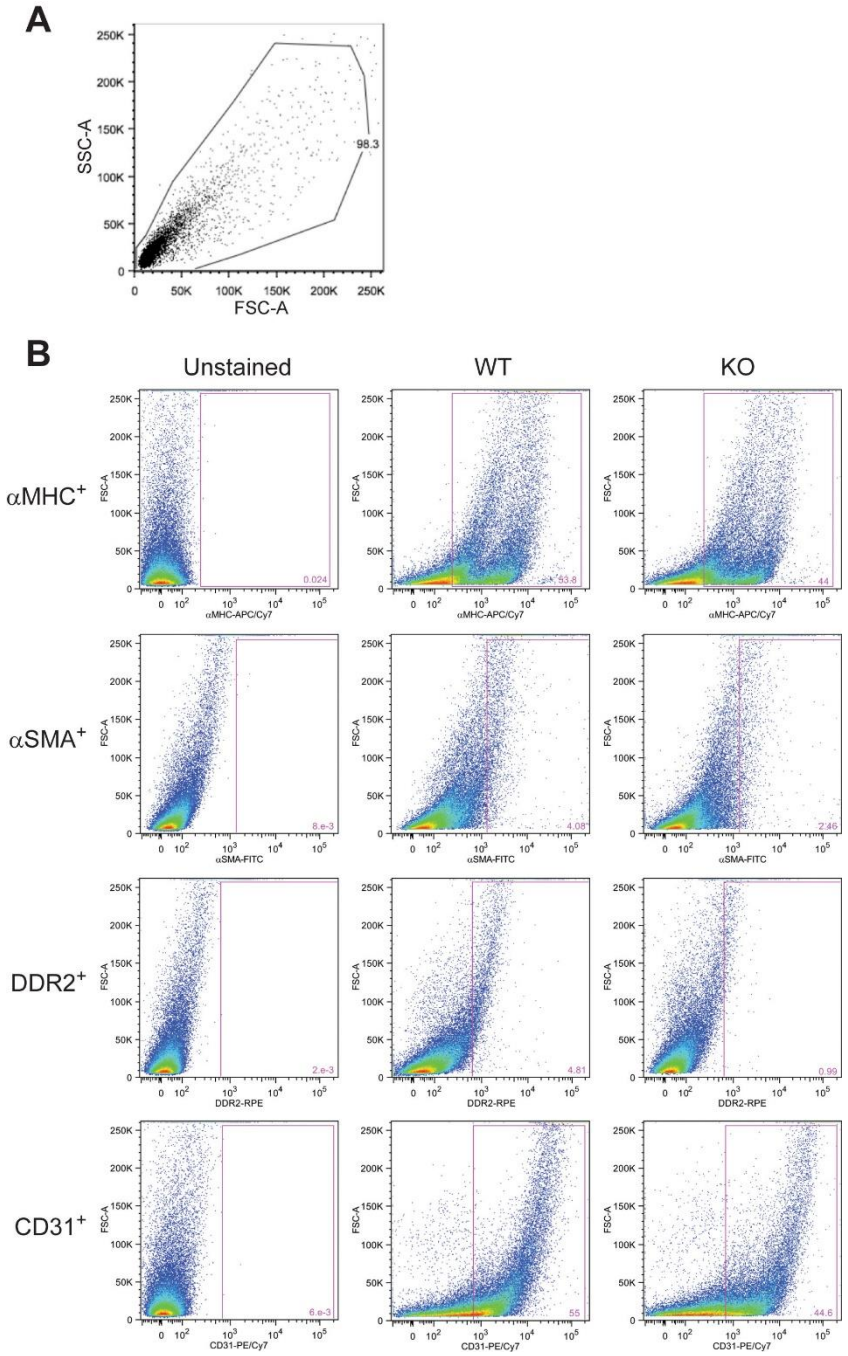

(A) Scatter profile shows cellular aggregates and tissue debris being gated out using side-scatter area (SSC-A) and forward-scatter area (FSC-A). **(B)** Forward-scatter plots for 50,000 events labeled for αMHC, αSMA, DDR2 or CD31; left column, unstained cells; center column, stained cells from WT tissue; right column, stained cells from scleraxis KO tissue. Results are representative of n=3 independent assessments. Purple outline denotes labeled cells, and is derived from unstained plots.

Appendix 3: Generation of the scleraxis conditional knockout (cKO) mice.

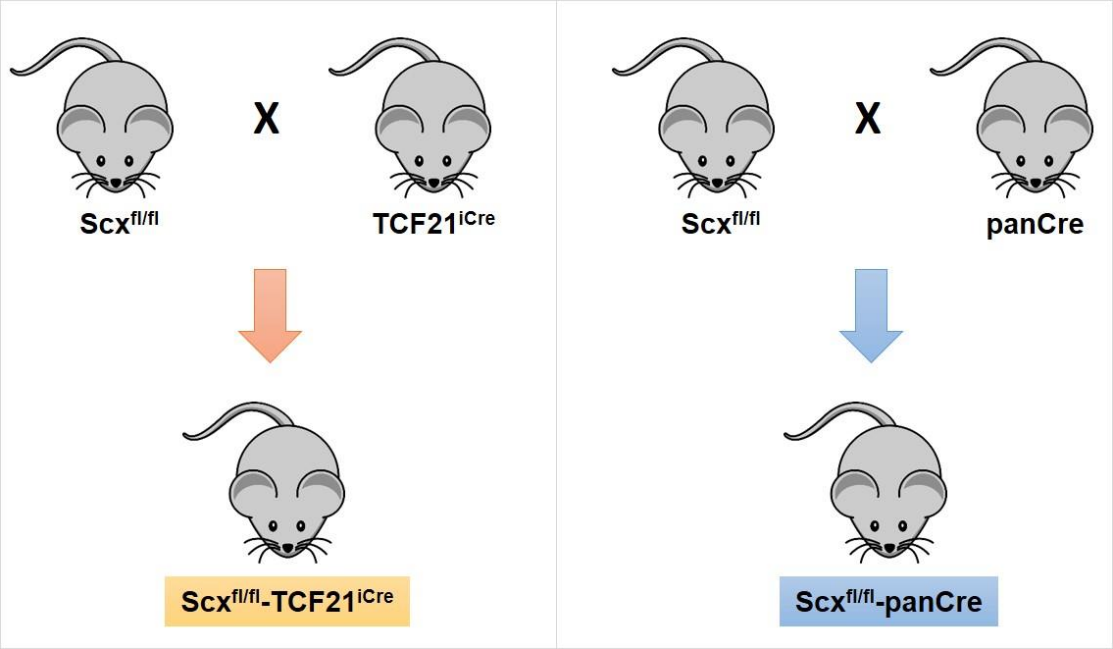

Scleraxis floxed mice were bred to TCF21^{iCre} or B6.Cg-Tg(CAG-cre/Esr1*)5Amc/J mice to generate Scx$^{flox/flox}$-TCF21^{iCre} and Scx$^{flox/flox}$-panCre lines respectively.